Monocyte dimethylarginine dimethylaminohydrolase 2 is regulated by pathological stress and plays a critical role in the immune response to sepsis

A thesis presented for the degree of Doctor of Philosophy

by

Dr Simon Lambden

Imperial College London, Institute of Clinical Sciences

Declaration

I, Dr Simon Lambden, confirm that the work presented within this thesis is entirely my own work. Where data has been collected experimentally or analysed by a third party, this is acknowledged in the text.

Abstract

Background: Asymmetric dimethylarginine (ADMA) is an endogenous competitive inhibitor of nitric oxide synthase (NOS) and regulates the synthesis of nitric oxide (NO) *in vivo*. ADMA is metabolised by the enzymes dimethylarginine dimethylaminohydrolase 1 and 2 (DDAH 1 and 2), which have differing tissue distributions, with DDAH2 the only isoform found in immune cells. These studies tested the hypothesis that DDAH2 plays an important role in regulating the immune response to infection by modulating ADMA concentrations.

Methods: In order to test this hypothesis, a series of experiments explored the regulation of murine and human monocyte DDAH2 in response to pathophysiological stressors. The impact of global and macrophage-specific DDAH2 knockout on the haemodynamic and immune response to sepsis and the resulting association with mortality was determined using transgenic animal models. Finally, the role of DDAH2 in human septic shock was determined by analysing plasma and DNA from patients enrolled in a randomised controlled trial of vasopressor therapy.

Results: In isolated monocytes, DDAH2 was found to be regulated by both Interferon-γ and hypoxia, leading to reduced intracellular ADMA concentrations and exaggerated NO synthesis by immune cells. Both global and macrophage-specific knockout of DDAH2 led to significant impairment of immune cell function and increased mortality following caecal ligation and puncture in animal models. Increased plasma ADMA and SDMA levels were shown to be associated with risk of death in 215 patients with septic shock. However, when data were corrected for methylarginine clearance, ADMA was also found to play a protective role. In this population, the DDAH2 single nucleotide polymorphism rs805305 was associated with improved survival and increased ADMA:SDMA ratio.

Conclusions: Considered as a whole, these data demonstrate that DDAH2 plays an important role in regulating the immune response to sepsis and the risk of death in human septic shock.

Acknowledgements

Thanks must first go to Dr James Leiper for his faith in this project and tireless support throughout. To my second supervisor Prof Mervyn Singer, I would like to offer my thanks for the insight and wise counsel.

The members of my group who have supported me so generously with both their time and expertise over the course of the last three years are also due my sincere gratitude. It would have been impossible to get to this point without them.

I would like to thank my parents for their continual support throughout my research, without whom I would not have been able to reach the end of this process. Last but by no means least, to Jen, who has been a voice of encouragement, sounding board and counsellor throughout my time in the lab. Words cannot express how grateful I am for your help and support.

Table of Contents

List of figures

List of tables

Publications, Presentations and Prizes

Publications

- S Lambden, D Martin, K Vanezis, B Lee, James Tomlinson, S Piper, O Boruc, M Mythen, J Leiper. Hypoxia causes increased monocyte nitric oxide synthesis which is mediated by changes in Dimethylarginine Dimethylaminohydrolase 2 expression in animal and human models of normobaric hypoxia. *Clin Sci* (in revision)
- S Lambden, P Kelly, Z Wang, B Ahmetaj, M Nandi, B Torondel, M Delahaye, L Dowsett, J Tomlinson, B Caplin, O Boruc, A Slaviero, S Khadayate, B Lee, J Leiper. Dimethylarginine Dimethylaminohydrolase 2 regulates Nitric Oxide production, haemodynamics and vascular responsiveness under basal conditions and outcome in polymicrobial sepsis. *Arterioscler Thromb Vasc Biol*. 2015; 35:1382-1392 DOI: 10.1161/ATVBAHA.115.305278
- Z Wang, S Lambden, V Taylor, E Sujkovic, M Nandi, J Tomlinson, A Dyson, N McDonald, S Caddick, M Singer, J Leiper. Pharmacological inhibition of DDAH1 improves survival, hemodynamics and organ function in experimental septic shock. *Biochem J*. 2014; 460:309-316 DOI: 10.1042/BJ20131666

Published Abstracts

- S Lambden, D Martin, K Vanezis, J Tomlinson, O Boruc, M Mythen, J Leiper. Dimethylarginine Dimethylaminohydrolase 2(DDAH2) regulates nitric oxide synthesis in animal and observational human models of normobaric hypoxia. *The Lancet (in press)*
- P Kelly, Z Wang, B Ahmetaj, S Lambden, M Nandi, B Torondel, M Delahaye, L Dowsett, J Tomlinson, B Caplin, O Boruc, A Slaveiro, S Khadayate, B Lee, J Leiper. Dimethylarginine dimethylaminohydrolase 2 (DDAH2) regulates nitric oxide production, haemodynamics and vascular responsiveness under basal conditions and outcome in polymicrobial sepsis. *Nitric Oxide*. 2014; 42:130 DOI: 10.1016/j.niox.2014.09.094
- Z Wang, S Lambden, V Taylor, E Sujkovic, M Nandi, J Tomlinson, A Dyson, N McDonald, S Caddick, M Singer and J Leiper. A novel dimethylarginine dimethylaminohydrolase (DDAH-1) inhibitor improves survival, hemodynamics and organ function in rodent sepsis. *Nitric Oxide*. 2014; 42:100 DOI: 10.1016/j.niox.2014.09.010

Presentations

- S Lambden, S Piper, K Vanezis, J Tomlinson, L Doswett, M Singer, J Leiper. Dimethylarginine Dimethylaminohydrolase 2 (DDAH2) is upregulated by interferon-γ which alters methylarginine metabolism and mediates nitric oxide synthesis by monocytes in *ex vivo* and *in vivo* models. **The Intensive Care Society state of the art meeting 2015**
- S Lambden, D Martin, K Vanezis, J Tomlinson, O Boruc, M Mythen, J Leiper. Dimethylarginine Dimethylaminohydrolase 2(DDAH2) regulates nitric oxide synthesis in animal and observational human models of normobaric hypoxia. **The Academy of Medical Sciences Spring meeting 2016**
- S Lambden, J Leiper, A Gordon. Plasma asymmetric dimethylarginine (ADMA) association with risk of death in septic shock – subgroup analysis of patients from the VANISH trial. **The American Thoracic Society Annual Conference 2016 (pending review)**

Prizes

- Oral presentation prize, **London Perioperative Research Forum**, Royal College of Anaesthetists 2014

List of Abbreviations

ADMA	asymmetric dimethylarginine
AGXT2	alanine-glycoxylate 2
AKI	Acute kidney injury
AMPK	AMP-activated protein kinase
AMPK	5' AMP-activated protein kinase
AMPs	antimicrobial peptides
ANOVA	Analysis of Variance
APC	activated protein C
BH4	Tetrahydrobiopterin
CAP	Community acquired pneumonia
CARS	compensatory anti-inflammatory response syndrome
cGMP	cyclic guanosine monophosphate
cGMP	cyclic guanosine monophosphate
CLRs	C-type lectins
DAMPs	danger associated molecular patterns
DDAH	dimethylarginine dimethylaminohydrolase
DDAH1	Dimethylarginine Dimethylaminohydrolase 1 protein
Ddah2	Dimethylarginine Dimethylaminohydrolase 2 gene
DDAH2	Dimethylarginine Dimethylaminohydrolase 2 protein
Ddah2-/-	Ddah2 global knockout mouse
$Ddah2^{+/+}$	Ddah2 wild type mouse
$Ddah2^{flox/flox}$	LoxP positive Cre negative litter mate controls
$Ddah2^{M\Phi-}$	Ddah2flox/flox LysM-cre Monocyte specific DDAH2 knockout animals
DIC	Disseminated intravascular coagulopathy
DNA	Deoxyribonucleic acid
EDTA	Ethylenediaminetetraacetic acid
ELISA	Enzyme Linked Immunosorbent Assay
eNOS	endothelial nitric oxide synthase
FAD	Flavin adenine dinucleotide
FiO_2	Fraction of inspired oxygen

FMN	Flavin mononucleotide
FP	Faecal Peritonitis
GAinS	Genome wide Association in Sepsis
GAS	Gamma Activated Site
GenOSept	Genetics Of sepsis and Septic shock in Europe
GM-CSF	Granulocyte Macrophage colony stimulating factor
GTP	guanosine triphosphate
GTP	guanosine triphosphate
HIF-1	hypoxia inducible factor 1
HMGB-1	high-mobility group box-1 protein
HSP	heat shock protein
HSP	Heat Shock Proteins
ICU	intensive care unit
IFNAR	interferon alpha response element
IFNGR	interferon gamma response element
IFN-γ	Interferon γ
IL-10	Interleukin 10
IL-1β	interleukin 1β
IL-6	Interleukin 6
iNOS	inducible nitric oxide synthase
INR	international normalized ratio
IQR	Interquartile range
IRF-3	Interferon regulatory factor 3
IRF-7	Interferon regulatory factor 7
ISRE	interferon sensitive response elements
JAK	Janus tyrosine Kinase
JNK	c-Jun N-terminal kinases
Kca	cytosolic calcium sensitive potassium channels
LC-MS/MS	liquid chromatographic assay with tandem mass spectrometric detection
LD	linkage disequilibrium
L-NMMA	monomethyl-L-arginine
LPS	lipopolysaccharide

MA	methylarginines
MAPK	membrane associated protein kinase
MHC	major histocompatibility complex
MHC	major histocompatibility complex
mRNA	Messenger RNA
MTOR	mammalian target of rapamycin
MTOR	mammalian target of rapamycin
MyD88	myeloid differentiation primary-response protein 88
NADPH	Nicotinamide-adenine-dinucleotide phosphate
NF-κB	Nuclear Factor Kappa B
NLR	Nod Like receptor
NLRs	Nod-like receptors
NO	Nitric Oxide
NOS	nitric oxide synthase
NOx	Nitrate + Nitrite
NOX	NADPH oxidase
PAMPs	pathogen associated molecular patterns
PaO_2	partial pressure of arterial oxygen
PBMC	peripheral blood mononuclear cells
PBS	Phosphate Buffered Saline
PCR	Polymerase chain reaction
PD-1	programmed cell death protein 1
PH	Pulmonary hypertension
Poly I:C	Polyinosinic polycytidylic acid
PRMT	Protein arginine methyltransferases
PRMT	protein arginine methyltransferases
PRR	Pattern recognition receptors
qPCR	Quantitative reverse-transcription PCR
RIRs	RIG-I-Like receptors
RNS	reactive nitrogen species
ROC	Receiver operator characteristic
ROS	reactive oxygen species
SD	Standard deviation

SDMA	symmetric dimethylarginine
sGC	soluble guanylate cyclase
sGC	soluble guanylate cyclase
siRNA	Short interfering RNA
SIRS	Systemic inflammatory response syndrome
SNP	Single nucleotide polymorphism
SOFA	Sequential Organ Failure Assessment
STAT	Signal Transducer and Activator of Transcription
TF	Tissue factor
TLR	Toll Like receptor
TNF-α	Tumour necrosis factor α
Treg	T regulatory
TRIF	TIR domain-containing adaptor protein-inducing IFN-β
VANISH	VAsopressin versus Noradrenaline as Initial therapy in Septic sHock
y+ CAT	y+ cationic amino acid transporter
95% CI	95% Confidence interval

1 Introduction

This introductory chapter will describe the background surrounding this study and discuss the clinical context for which this work is relevant. The synthesis and regulation of nitric oxide (NO) will first be described with particular emphasis on the role of endogenous inhibitors of NO synthesis in human health and disease. This will be followed by a discussion on the clinical relevance of sepsis and on how key features of the innate immune response may contribute towards disease pathophysiology. Finally, this chapter will describe the existing literature which suggests a relationship between endogenous inhibitors of NO synthesis and septic syndrome.

1.1 Nitric Oxide Signalling, Synthesis and Regulation

NO is a protean molecule with diverse physiological roles across numerous tissue types. Whilst only formally identified in 1987[1], its actions have been recognised and exploited therapeutically for over a century. Following the identification of the canonical signalling pathway whereby NO activates soluble guanylate cyclase (sGC) to catalyse the conversion of guanosine triphosphate (GTP) to cyclic guanosine monophosphate (cGMP)[2, 3], the role of NO in both physiological and pathological conditions has been extensively studied.

1.1.1 Nitric Oxide Signalling

NO is a heteronuclear diatomic molecule that is a colourless gas in its natural form. In humans, it has an extremely short half-life due to the presence of an unpaired electron[4], being rapidly metabolised in the body primarily to nitrate or nitrite, which are relatively stable and make up the majority of NO metabolites[5].

1.1.2 Nitric Oxide Synthesis

The Nitric Oxide Synthase (NOS) enzyme family catalyses the conversion of L-arginine to NO and L-citrulline *in vivo*. There are three NOS isoforms, endothelial (eNOS, NOS-3), neuronal (nNOS, NOS-1) and inducible (iNOS, NOS-2) (Figure 1). The synthesis of NO from any of the NOS isoforms is dependent on a number of co-factors, these include[6]:

- Nicotinamide-adenine-dinucleotide phosphate (NADPH)
- Flavin adenine dinucleotide (FAD)
- Flavin mononucleotide (FMN)
- Tetrahydrobiopterin (BH4)
- Calmodulin
- Oxygen

eNOS was first identified in the vascular endothelium, but its activity has subsequently been demonstrated in a variety of tissues. It is a constitutive enzyme that produces NO in picomolar concentrations under normal conditions[5]. It is calcium-dependent and acts to stimulate the relaxation of vascular smooth muscle in addition to limiting platelet adhesion and leukocyte activation at the endothelium[5]. Regulation is through interaction with a wide range of stimuli including protein kinase A, 5' AMP-activated protein kinase (AMPK) and Heat Shock Proteins(HSP)[7].

nNOS, as the name suggests was first identified in brain tissue, but it is also found in the kidney[8]. Like eNOS it is a calcium-dependent constitutive enzyme producing low concentrations of NO in its regulatory role.

iNOS was first identified in activated macrophages, however it has been subsequently shown to be present as a constitutive isoform in a number of tissues including renal epithelia, chondrocytes and hepatocytes[6]. By contrast to the other isoforms, iNOS is able to dramatically upregulate NO production and can synthesise NO at concentrations a thousand fold higher than either eNOS or iNOS[9]. A broad range of stimuli can provoke the transcription and activation of iNOS including the bacterial endotoxin lipopolysaccharide (LPS), inflammatory cytokines such as interleukin 1β (IL-1β), tumour necrosis factor α (TNF-α) and Interferon γ (IFN-γ) and other transcription factors such as hypoxia inducible factor 1 (HIF-1)[10] .

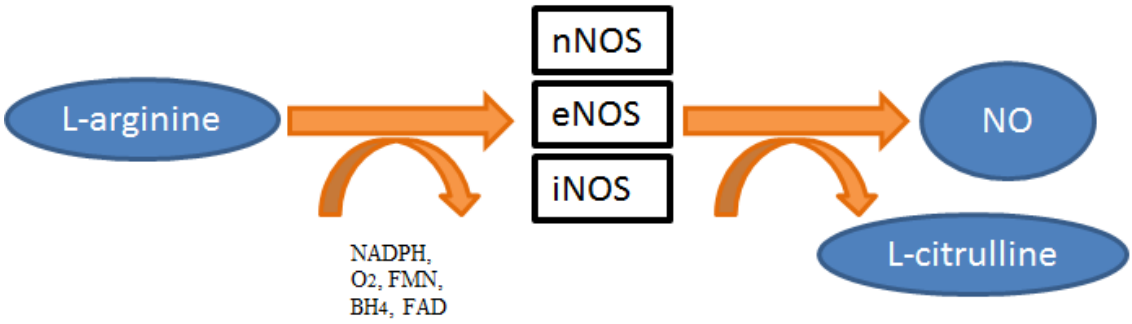

Figure 1: Nitric oxide synthesis.

Nitric oxide synthase isoforms (n-, i-, e-NOS, neuronal-, inducible, endothelial-nitric oxide synthase) catalyse the synthesis of Nitric Oxide (NO) and L-citrulline from L-arginine. The reaction requires the binding of calmodulin protein five co-factors: (NADPH), nicotinamide-adenine-dinucleotide phosphate, oxygen (O_2), flavin adenine dinucleotide (FAD), flavin mononucleotide (FMN) and tetrahydrobiopterin (BH4).

1.1.3 Endogenous Regulation of Nitric Oxide Synthesis

NO synthesis *in vivo* is a complex process which is tightly regulated at every stage from enzyme co-localisation to substrate and co-factor availability[11]. The discovery of a family of arginine derivatives, known as the methylarginines (MA), which act as competitive inhibitors and regulate the binding of L-arginine to the active site of the NOS enzyme is one of few examples where an enzyme system is regulated by endogenous competitive inhibition[12](Figure 2).

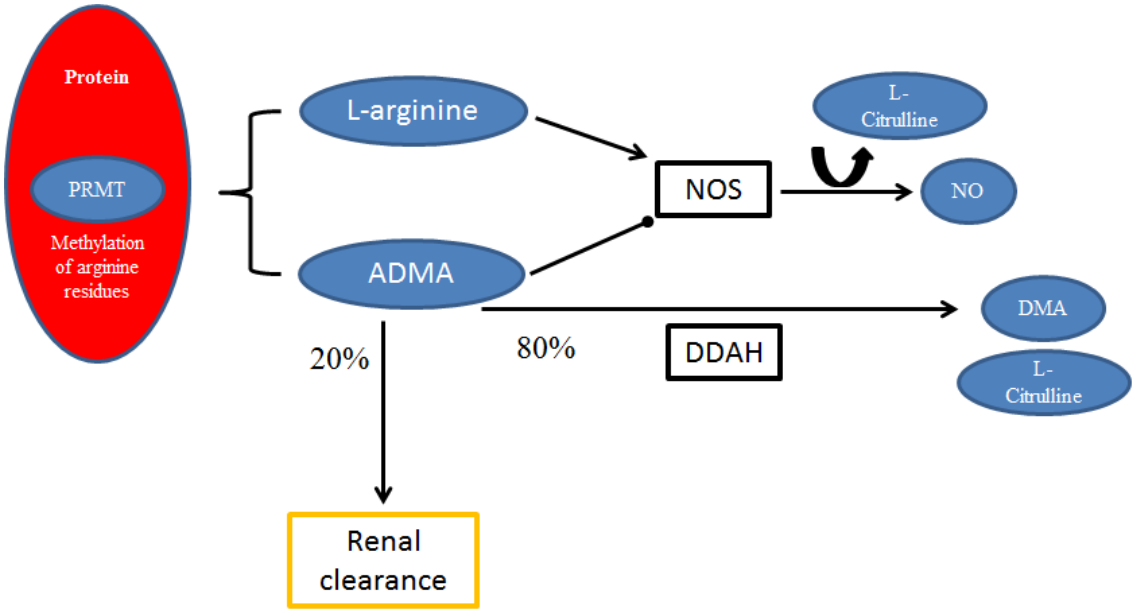

Figure 2:Endogenous regulation of nitric oxide synthesis.

Protein arginine methyl-transferase enzymes (PRMTs) methylate arginine residues within proteins. Arginine and methylarginines are released during proteolysis and are transferred intracellularly by the y+ cationic amino acid transporter family (not shown) and act either as a substrate or inhibitor of nitric oxide synthase enzymes respectively (represented by NOS in the figure). 80% of synthesises asymmetric dimethylarginine (ADMA) and monomethyl arginine (L-NMMA) (not shown) are hydrolysed by dimethlyarginine dimethlyaminohydroxylases 1 and 2 (represented by DDAH in the figure) to L-citrulline and dimethylamine (DMA), thus regulating NOS blockade. The remaining 20% is excreted unchanged in the urine.

1.2 Methylarginines

1.2.1.1 Methylarginine synthesis

Methylarginines are synthesised by the methylation of residues of arginine that lie within certain consensus sites within some proteins a process that is regulated by a family of enzymes known as the protein arginine methyltransferases (PRMTs). Three MA subtypes have been identified[13]. Free methylarginines are released upon proteolysis. (Figure 3):

- NG, NG-dimethyl-L-arginine (asymmetric dimethylarginine; ADMA)
- NG, NG'-dimethyl-L-arginine (symmetric dimethylarginine; SDMA)
- NG-monomethyl-L-arginine (monomethylarginine; L-NMMA)

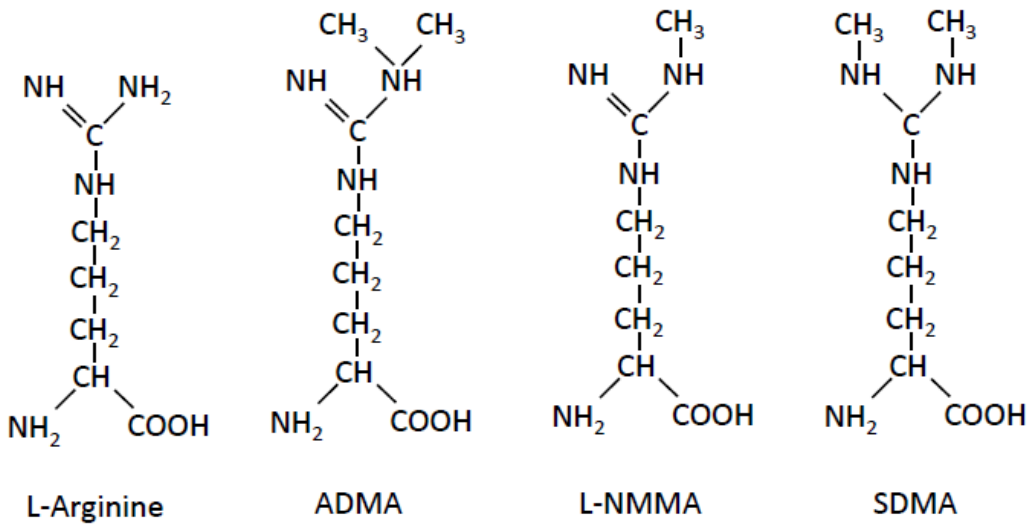

Figure 3: L-arginine and the methylarginines

Representative image of the structure of L-arginine and the methylarginines, L-NMMA: NG-monomethyl-L-arginine (monomethylarginine), SDMA: NG, NG'-dimethyl-L-arginine (symmetric dimethylarginine) and ADMA: NG, NG-dimethyl-L-arginine (asymmetric dimethylarginine).

1.2.1.2 Methylarginine transport and action

MAs are transported between the plasma and tissue compartments via the y+ cationic amino acid transporter (CAT) family which are also responsible for L-arginine transfer[14]. Since both substrate and endogenous inhibitor move into the cell via the same transporter, it has been postulated that this is a further indirect mechanism by which MAs can reduce NO synthesis[15]. The relationship between plasma and intracellular concentrations of MA is not directly proportional, therefore cellular and plasma MA levels may vary significantly[16, 17]. This in turn means that the correlation between intracellular L-arginine and MA levels, useful in determining NOS activity, may not be accurately depicted using plasma measurements. Caution must therefore be employed when interpreting the results of studies associating plasma MA concentrations with DDAH activity and/or NO regulation.

Within the cell, both ADMA and L-NMMA are able to act as competitive inhibitors of NO synthesis by regulating the binding of L-arginine to the active site of the NOS enzyme. L-NMMA is present at only around ten percent of the concentration of ADMA and so plays a lesser role in the regulation of NOS activity in spite of being equipotent[18]. By contrast, SDMA does not compete with L-arginine, has no apparent impact on NOS activity and has historically been considered inert. However, there is emerging evidence to suggest that SDMA may have inflammatory regulatory activity outside of NOS regulation and NO synthesis[19].

1.2.1.3 Methylarginine handling

MAs are either enzymatically degraded or excreted from the body via the renal tract. There are three enzymes that are able to metabolise MAs *in* vivo. They are the two dimethylarginine dimethylaminohydroxylases (DDAH1 and DDAH2), and alanine-glycoxylate (AGXT2), which hydrolyse or deaminate their targets, respectively. Approximately 80% of ADMA and L-NMMA are metabolised to dimethylarginine (DMA) and L-citrulline, whilst the remaining 20% is excreted via the kidney[20]. SDMA is not metabolised by DDAH and until recently was presumed to be cleared entirely by the kidney. However, recent work has led to the discovery of AGXT2 which is able to metabolise all three MAs[21], although only a modest amount of ADMA and L-NMMA are metabolised in this way. AGXT2 is found in both the liver and kidney[22].

1.2.2 Dimethylarginine Dimethylaminohydroxylases

Often found in close apposition to the NOS isoforms, DDAH1 and DDAH2 have differing tissue distributions that may reflect diverging functional roles.

1.2.2.1 Dimethylarginine dimethylaminohydrolase 1

Located on chromosome 1 at the p22 position, DDAH1 has a widespread tissue distribution. In addition to the vasculature[23], it is readily identified in tissue homogenates from the liver, kidney, brain, skeletal muscle and pancreas[24]. Small amounts of DDAH1 have also been found in the pulmonary vasculature[25] and in placental[26] tissues.

Recombinant human DDAH1 has been shown to have high affinity for MAs with results showing Km values of 53.6 and 68.7 μM and Vmax values of 154 to 356 nmol/mg/min for ADMA and L-NMMA, respectively[27, 28]. Short interfering RNA (siRNA)-mediated knockdown and overexpression of DDAH1 in endothelial cells have also both been shown to directly affect MA turnover[29].

1.2.2.2 Dimethylarginine dimethylaminohydrolase 2

The tissue distribution of DDAH2 differs markedly from that of DDAH1. Whilst both isoforms are found in the vasculature, liver and kidney, DDAH2 predominates in the placenta and is not found in the central nervous system. It is also the only isoform found in cardiomyocytes and in immune tissues[23, 24, 30]. The gene for DDAH2 is found at the p21.3 position of chromosome 6. This position lies within the major histocompatibility complex (MHC) III region of the chromosome and is closely associated with a range of genes encoding for inflammatory mediators such as TNF-α and heat shock proteins (HSP)[23]. This, coupled with the tissue distribution of DDAH2, has led to the suggestion that it may play an important role in the response to inflammatory or immune mediated conditions.

In contrast with DDAH1, the measurement of DDAH2 activity has proven to be challenging. This is in part due to difficulties in separating the actions of DDAH1 and DDAH2 when MA turnover is measured in tissues in which both isoforms are present. Purification of the functional DDAH2 protein has also proven difficult[31]. These issues currently render the direct comparison of the activities of the two DDAH enzymes impossible. However, siRNA-mediated knockout of DDAH2 in endothelial cells has been shown to have a similar impact on ADMA and NO synthesis as that observed in experiments on DDAH1[29]. Interestingly, when isolated aortic tissue from DDAH2 knockout animals was incubated overnight, the amount of ADMA that accumulated in the culture medium was significantly elevated compared to control tissues[30].

1.3 Methylarginine dysregulation and disease

This section will consider the existing literature concerning MA dysregulation and its role in disease with a particular focus on animal models of DDAH and on human association and genetic studies. Sepsis will be considered separately later in the chapter.

1.3.1 Association Studies

There are currently over one hundred publications that describe clinical studies on a variety of conditions where an association between plasma concentrations of MAs, particularly ADMA, and disease presence, progression or outcome has been observed. Many of the aforementioned conditions have significant cardiovascular or inflammatory involvement and thus the identification of diseases in which ADMA plays a mechanistic role, instead of acting as a biomarker of inflammatory stress, has proven to be challenging. Some of the risk factors and disease associations are summarised below (Table 1).

Association with cardiovascular risk factors	Disease Association with plasma concentrations	Association with Cardiovascular or mortality outcome
	Higher ADMA levels	
Age	Renal failure	Patients with coronary artery disease
Sex	Peripheral vascular disease	Patients with diabetes mellitus
Lipids	Pulmonary hypertension	Patients with diabetic nephropathy
Tobacco	Atherosclerotic coronary disease	Patients with peripheral vascular disease
Blood pressure	Diabetes mellitus	Patients with chronic kidney disease
Inflammation	Preeclampsia	Patients with pulmonary hypertension
Homocysteine	Alzheimer's disease	
Obesity	Connective tissue disease	
Diabetes mellitus	Liver disease	
Kidney function	Hyperthyroidism	
	Hypothyroidism	
	Stroke	
	Sickle cell disease	
	Alzheimer disease	
	Lower ADMA levels	
	Diabetes mellitus	

Table 1: Association studies of plasma ADMA with cardiovascular risk factors, disease progression and outcome.

Summary table of associations studies of plasma methylarginines. The first column represents studies associating plasma ADMA with specific risk factors for cardiovascular disease, the second, progression of specific diseases and the third, outcomes in cardiovascular disease.

1.3.2 Genetic Studies

A number of clinical studies have looked for a relationship between single nucleotide polymorphisms (SNP) within the genes that encode for the regulatory enzymes DDAH1, DDAH2 and AGXT2, altered MA levels and/or disease. There is some conflicting evidence in this area, with some authors observing no significant correlation between circulatory MA levels and previously published SNPs[32]. However, there are a number of published studies that have shown not only that SNPs of the DDAH or AGXT2 genes can be associated with altered plasma MA concentrations in a variety of disease states, but that they also independently correlate with outcome in a number of conditions (summarised below in Table 2).

Gene	Associations
DDAH1	
rs1146381	Plasma ADMA level[33]
rs233112	Plasma ADMA level[33]
rs233128	Plasma ADMA level[33]
rs11161614	Plasma ADMA level[33]
rs997251	Plasma ADMA level
rs1241321	Progression of Type 2 Diabetes and outcome[34]
rs17384213	Decline in Glomerular filtration rate, ADMA level, DDAH1 mRNA[33]
rs1554597	Independent determinant of ADMA in Diabetes Mellitus[35]
DDAH2	
rs805304	Associated with: renal function T2DM[36] Protective in MI[37]
rs805305	Associated with: 1. Intra-cerebral haemorrhage[38] 2. Paediatric/Adult shock[39, 40] 3.Vasopressor requirement following cardiac surgery[41]
rs138134716	The first functional SNP demonstrated [42]
rs9267551	Associated with Insulin sensitivity[43] CKD[44]
rs805923	Associated with circulating ADMA levels
rs2272592	Associated with T2D
rs3131383	-871 Polymorphism – functionally active.[42]
AGXT2	
rs37369	Plasma SDMA level and Heart rate variability[45]
rs16899974	Plasma SDMA level and Heart rate variability[45]
rs37369	Functional variant Associated with elevation of blood pressure in genome wide association studies[21]
rs28305	Independent determinant of SDMA in Diabetes Mellitus [35]

Table 2: Summary of the existing literature which shows correlation between SNPs found in the genes that encode for methylarginine handling enzymes, and methylarginine MA concentrations and/or human disease.

1.3.3 Animal Models of DDAH in Health and Disease

The development of transgenic animal models has enabled the effects of knockout or overexpression of the MA handling enzymes on basal function and disease response to be further explored. In conjunction with transient short interfering RNA (siRNA) techniques, it has been possible to gain considerable mechanistic insight into the role of these enzymes in health and disease. In addition, evidence has also begun to emerge suggesting potentially important actions for ADMA through mechanisms other than the regulation of NOS activity. However, it is important to exercise caution when analysing these data as assuming a direct association between murine outcome and human disease may be ill considered in light of recent work highlighting the differences between rodents and humans in response to similar pathological stimuli[46].

1.3.3.1 Dimethylarginine dimethylaminohydrolase 1

The effects of the overexpression or knockdown of DDAH1 have been examined in a number of studies using heterozygote[47] or homozygote[48] murine models and siRNA-mediated techniques. In summary, global knockout of DDAH1 has been shown to produce a hypertensive phenotype in rodent models at baseline, with overexpression resulting in a reduction in blood pressure. Table 3 below summarises these findings.

Pharmacological inhibition and genetic knockout of DDAH1 has been shown to be protective in a bleomycin model of pulmonary fibrosis. The same study also found that overexpression of DDAH1 led to increased fibrotic change within the lung parenchyma of the animal model[49]. Proximal tubular knockout of DDAH1 has been shown to be protective against renal fibrosis in both unilateral ureteric obstruction and folate models of chronic kidney injury[8]. Endothelial specific knockout of DDAH1 had no impact on vascular function or systemic ADMA concentrations, but profoundly impaired angiogenesis[50] in another study which refuted earlier work suggesting endothelial knockout completely removed DDAH1 from all tissues[51]. An adipocyte specific model of DDAH1 knockout revealed an increase in cellular ADMA levels which directly up-regulated the mammalian target of rapamycin (MTOR) and caused adipocyte hypertrophy independently of NO regulation[52].

DDAH1 Reduction			
Approach	Species	Plasma ADMA action	Effect
Constitutive exon 1 haploinsufficiency [47]	Mouse	Increased	Increased blood pressure and reduced end diastolic volume
Cre/LoxP exon 4 null [53]	Mouse	Increased	Increased blood pressure
Endothelium targeted exon 4 null [51]	Mouse	Increased	Increased blood pressure and reduced end diastolic volume
siRNA[54]	Rat	Increased	No change in blood pressure or end diastolic volume
DDAH1 Overexpression			
Approach	Species	Plasma ADMA action	Effect
Transgenic overexpression [55]	Mouse	Decreased	Reduced blood pressure
Adenoviral transfection [56]	Rat	Decreased	Reduced blood pressure

Table 3: Summary of existing approaches to modulating DDAH1 protein expression and the observed impact on methylarginine levels and haemodynamics in the rodent resting state (Adapted from [31, 32]).

Mice exposed to hypoxia displayed significant downregulation of DDAH1 within their pulmonary vasculature. This was shown to be mediated by the micro-RNA mir-21 and provided a mechanism for hypoxia-induced pulmonary hypertension.[25] .

Interestingly, the pharmacological inhibition of DDAH1 with the highly selective competitive antagonist L-291 resulted in significantly reduced evidence of pain in animals exposed to a chronic pain model[57].

1.3.3.2 Dimethylarginine dimethylaminohydrolase 2

Global knockout of DDAH2 utilising a high throughput gene trapping strategy has been utilised to explore the impact of DDAH2 deletion in murine models. Under basal conditions, mice deficient in DDAH2 are developmentally and phenotypically normal[58]. When considered over the course of a twenty four hour period under continuous telemetry, no significant differences in haemodynamic indices can be observed when compared to litter mate controls. However, during periods of elevated activity, DDAH2 knockout mice display a modestly elevated blood pressure[30]. Overexpression of DDAH2 in a murine model led to a reduction in systemic ADMA concentrations, but no significant impact on phenotype or haemodynamics, although this study did not include continuous awake haemodynamic monitoring[59].

Less work has been performed on the manipulation of DDAH2 in animal models of disease. However, when human DDAH2 is virally transfected into a rabbit model of atherosclerosis, animals display significantly reduced disease progression when compared to controls[60]. This finding has been confirmed in a murine model of vascular injury using angiotensin II, where mice overexpressing DDAH2 displayed significantly less hypertension and progression of vascular injury[59].

1.4 Sepsis

Sepsis arises when, in response to an infective stimulus, the immune response, designed to eradicate the pathogen becomes dysregulated. This leads to systemic symptoms and organ dysfunction. It is this process of overwhelming systemic compromise in response to infection that defines septic shock.

1.4.1 Systemic Inflammatory Response Syndrome

The systemic inflammatory response syndrome (SIRS) scale is comprised of four indices (three physiological and one haematological) that describe a patient's physiological response to an undefined pathological insult. Meeting any two or more of the criteria defines the patient as having SIRS[61]. The scale is neither highly sensitive nor specific for identifying patients with infection as SIRS may arise as a consequence of a range of disease states including one or more of the following: trauma, surgery, haemorrhage, infection, inflammation or ischaemia[62]. It was developed by the Society of Critical Care Medicine in the United States as a tool to aid the early identification of patients with life threatening infections[61].

The SIRS criteria are:

- Pyrexia of more than 38°C or a core temperature of less than 36°C
- Heart rate higher 90 beats per minute
- Respiratory rate of more than 20 breaths per minute or arterial carbon dioxide tension of less than 4.2kPa
- Deranged white blood cell count (>12,000/μL or < 4,000/μL or >10% immature forms)

1.4.2 Sepsis

Sepsis is the clinical syndrome that arises when the body mounts a systemic inflammatory response to the invasion of a pathogenic microbe. This organism may be bacterial, viral or fungal, although the majority of cases of sepsis are bacterial in origin. The term sepsis, enables the differentiation of inflammatory conditions caused by an infection from those which arise as a consequence of non-infective disease states that provoke a significant inflammatory response[63]. As such, sepsis is defined as the presence of two or more of the SIRS criteria plus the presence of confirmed or suspected infection[61].

1.4.3 Severe sepsis and septic shock

Severe sepsis is defined as sepsis plus organ dysfunction. The term, organ dysfunction, includes a wide range of clinical features and biochemical indices, each designed to demonstrate impaired function of one or more of the organ systems. The following are recognised features of severe sepsis[64]:

- Sepsis-induced hypotension
- Lactate above upper limits of laboratory normal
- Urine output < 0.5mL/kg/hr for more than 2 hrs despite adequate fluid resuscitation
- Acute lung injury with PaO2/FiO2 < 250 in the absence of pneumonia as infection source
- Acute lung injury with PaO2/FiO2 < 200 in the presence of pneumonia as infection source
- Creatinine > 176.8 μmol/L
- Bilirubin > 34.2 μmol/L
- Platelet count < 100,000 μL
- Coagulopathy (international normalized ratio (INR) > 1.5)

Septic shock arises when organ dysfunction persists in spite of adequate intravenous fluid resuscitation and antimicrobial therapy[64].

1.4.4 The Management of Sepsis

The management of sepsis has evolved considerably over the last 20 years with trends in supportive care changing significantly over this time. Improvements in outcomes have been shown with changes in the delivery of supportive therapies but to date, only two agents have been licensed specifically for the treatment of sepsis and both of these have been withdrawn amid fears regarding their efficacy and potential for harm[65-67].

1.4.4.1 Existing therapies in sepsis

Whilst antibiotic therapy is usually effective at eradicating bacteria, the host response to infection drives the process of organ dysfunction that ultimately leads to death. In particular, the profound dilation of blood vessels which leads to a failure of organ perfusion is a significant mechanism underlying mortality in septic patients. The mainstays of supportive therapy in severe sepsis are oxygen, intravenous fluids and vasopressors. The best available guidance for the management of patients with sepsis calls for the early administration of fluids and oxygen therapy, followed by the addition of vasoactive agents in those patients who do not respond[68]. However, there is considerable evidence that both of these therapeutic approaches confer their own morbidity.

Excess fluid administration is strongly associated with harmful side effects including worsened lung function[69]. The nature of the intravenous fluids that are used has also been shown to have harmful impacts on renal function[70, 71] and may increase mortality[71, 72].

Hyperoxia as a consequence of traditional oxygen therapy in critical illness has been associated with harm in a range of disease states including cardiac arrest [73], and has been shown to worsen the degree of acute lung injury in ventilated patients[74].

The administration of agents that restore blood pressure and organ perfusion in sepsis is essential to survival[75]. To date, the bulk of the therapies currently available rely on catecholamine based vasoactive agents[76, 77]. However, these agents confer their own morbidity and have been associated with increased mortality in sepsis[58, 77-79]. Indeed, a recent phase II study has suggested that a 'decatecholaminisation' technique using adrenergic antagonists acting in the opposite way to conventional treatment may offer a protective effect in sepsis[80]. Alternatives to these conventional therapies might offer a significant benefit to patients suffering from septic shock[77, 81].

1.4.5 The Impact of Sepsis as a Disease

Sepsis is a condition with profound implications for the individual, families and society as a whole. The condition is associated with early mortality; however, there is an increasing body of evidence to demonstrate that the sequelae of a relatively short-lived disease may persist long after discharge from hospital.

1.4.5.1 Sepsis mortality

In all countries where data on hospitalisations for sepsis are available, the number of cases has increased steadily[82] and constitutes one of the top ten causes of death worldwide[83]. The United States Centre for Disease Control reports that the number of admissions to hospital due to sepsis increased from 621,000 in the year 2000 to 1,141,000 in 2008[84]. In the USA, up to 750,000 people are admitted to intensive care units with severe sepsis each year. Of these patients, 20 to 45% will not survive their admission to hospital. This equates to up to 330,000 deaths per year in the United States[85] and up to 40,000 people in the UK[86]. The number of hospital admissions with sepsis has tripled over the last 10 years. In comparison, hospital admissions for stroke and myocardial infarction has remained stable over the same period[85]. In fact, the number of hospitalisations with sepsis now exceeds the number of admissions for myocardial infarction in the USA[87]. Even these numbers may underestimate the true scale of the burden based on how the data is collected[88-90].

1.4.5.2 The early economic burden

Treatment for sepsis often involves a prolonged stay in the intensive care unit. The Agency for Healthcare Research and Quality considers sepsis to be the most expensive condition treated in the USA, which, at a cost of $20 billion in 2011, is increasing annually by an average of 11.9%[91].

1.4.5.3 Impact of the sepsis syndrome on long-term survivors

In addition to acute mortality, sepsis also has a major impact on quality of life after discharge from hospital[92]. Patients who survive to hospital discharge after sepsis remain at increased risk of death in the following years[90]. Also, the quality of life of survivors may be severely impaired by psychological and physical effects[93].

Acute kidney injury (AKI) is a common complication arising in up to 35% of patients with sepsis[94]. AKI is not only strongly associated with early mortality[95], but also has a significant impact on long-term outcome in the surviving population where the incidence of severe chronic renal failure is increased by up to 28 fold[96]. It has also been shown that in patients with mild chronic renal impairment, an episode of acute kidney injury leads to a significant increase in the number of patients that are dependent on dialysis[97]. Of patients admitted to intensive care who survive to hospital discharge, one in three patients who were employed prior to admission has not returned to work two years later. This has been associated with reduced quality of life and greater long-term dependency[98]. Severe sepsis is associated with persistent cognitive impairment and functional disability compared to other causes of hospital admission[93]. Other studies have shown that one year after surviving critical illness, cognitive impairment consistent with moderate traumatic brain injury and mild Alzheimer's disease is seen in 34% and 24% of patients, respectively [99].

The long-term impact of sepsis syndrome therefore confers a significant medical, social and health economic burden on survivors and their families.

1.5 The Immune System

The collective systems of the body that mount a defence to an invading pathogen are known as the immune system. The immune system is conventionally divided into the innate immune system, which is the constitutive component, and the acquired or adaptive system, which depends upon stimulus for its activation. The section focuses on the innate immune response to infection.

1.5.1 The Innate Immune System

The innate immune system is comprised of a number of components that constitute the first line of defence against pathogens. These include the skin and mucous membranes as well as a range of immune cells including granulocytes, macrophages, neutrophils, dendritic and mast cells[100]. The innate immune system is activated in response to a broad and non-specific range of stimuli including exogenous and endogenously generated antigens[101]. It provides a rapid pathogen response system, both eradicating the invading organism and facilitating the upregulation of the acquired immune response. The activation of the innate immune response is summarised in Figure 4.

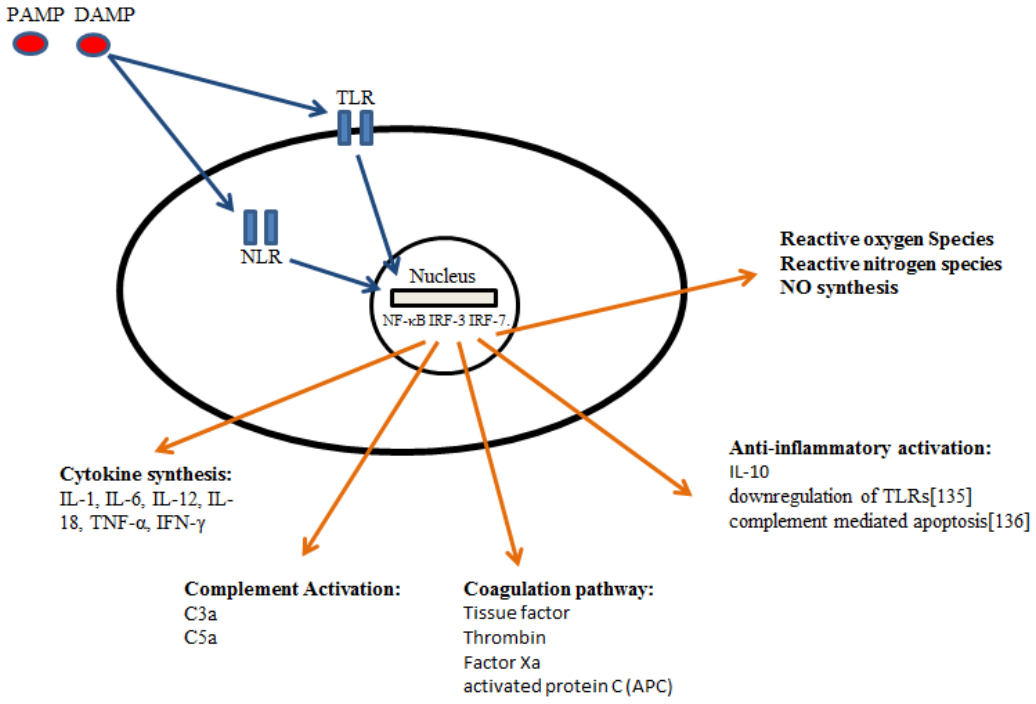

Figure 4: Summary of the activation of innate immune response.

Pathogen associated molecular pattern(PAMP) and danger associated molecular pattern (DAMP) molecules stimulate pattern recognition receptors such as Toll like receptors (TLR) on the cell surface or Nod like receptors (NLR) intracellularly. Myeloid differentiation primary-response protein 88 (MyD88) and the TIR domain-containing adaptor protein-inducing IFN-β (TRIF)-dependent pathways are activated by stimulus of these receptors. This results in the expression of one of three activators (NF-κB, IRF-3 and IRF-7). These in turn stimulate a range of innate responses including cytokine synthesis, complement, coagulation and anti-inflammatory pathways. In addition, Reactive oxygen species and nitric oxide (NO) are synthesised to stimulate local microbiocidal activity and act as signalling molecules.

1.5.1.1 The regulation of the innate immune response

The innate immune response is induced by two main groups of antigens with similar functions, but derived from different sources. The first of these are the pathogen associated molecular patterns (PAMP) which are located on the surface of common pathogens and are conserved across different organisms[102]. They include lipopolysaccharide (LPS), peptidoglycan and bacterial DNA released during cell death[103]. The second category of stimuli is the danger associated molecular patterns (DAMPs). DAMPS are released following cell injury of any kind, such as burns, trauma or necrosis, and include HSPs, S100 proteins, hyaluronic acid and high-mobility group box-1 protein (HMGB-1)[104]. Both DAMPs and PAMPs are recognised by pattern recognition receptors (PRR), which are found both on the surface and within the cytosol of innate immune cells.

PRRs can be divided into several groups. The first of these, the toll like receptors (TLRs), was discovered in the 1990s[105] and is comprised of a group of largely cell surface receptors of which there are ten in humans. In addition to the TLRs, other groups include the Nod-like receptors (NLRs), C-type lectins (CLRs) and RIG-I-Like receptors (RLRs). The bulk of work in the area of infection has been targeted towards the TLRs and NLRs.

TLRs are well conserved across mammalian species with nine of the ten human receptors also found in mice. Mostly responsive to lipoproteins, lipids and nucleic acids, stimulation of a TLR results in the activation of one of two main categories of signalling pathway. These are the myeloid differentiation primary-response protein 88 (MyD88) and the TIR domain-containing adaptor protein-inducing IFN-β (TRIF)-dependent pathways[103]. Initiation of these pathways leads to the activation of one or more of the three effectors NF-κB, IRF-3 and IRF-7. These in turn lead to the induction of many downstream aspects of the immune response including cytokine synthesis and release. TLRs play an important role in the response to infection due to the ligands with which they bind. The Table 4 below summarises some of the key TLRs and their interactions.

Toll Like Receptor	Ligands
TLR2	Lipoproteins Peptidoglycan (Bacterial Cell wall) Lipoteichoic acid (Gram positive bacteria) Zymosan (Fungal wall product)
TLR3	Viral double stranded RNA (dsRNA)
TLR4	Lipopolysaccharide (Gram negative bacterial wall)
TLR 5	Flagellin (bacterial flagella)
TLR 7 and TLR8	Viral single stranded RNA
TLR9	Microbial DNA (bacteria, viruses, parasites)

Table 4: Summary of the key Toll like receptors (TLR) involved in the response to infection and their ligands.

(adapted from [113]

If an organism invades the cytosol, it is recognised by intracellular PRRs located within the cell and the signalling cascade is initiated. The best understood group of intracellular PRRs are the NLRs which, in addition to being able to recognise specific fragments of bacteria, are also able to form complex structures called inflammasomes which respond to a diverse range of DAMPs and PAMPs[102].

1.5.2 Downstream Activation of the Innate Immune Response

Activation of the innate immune response leads to the downstream induction of a diverse range of both pro- and anti-inflammatory pathways. These processes regulate both the innate response and facilitate the initiation of the acquired immune system. Imbalance of these pathways has been associated with both the exaggerated immune response of septic shock[106] and also the impaired ability to mount a response to secondary infection in critically ill patients[107].

Key pathways induced by PRR-mediated signalling include pro- and anti-inflammatory cytokine synthesis, complement and coagulation cascade activation and, in parallel, a series of immunosuppressive pathways.

Cytokines are soluble proteins that have a broad range of roles in regulating both physiological and pathological responses. Their actions are widespread and depend both on the cell type with which they interact and the timing of their release[108]. The term cytokine covers more than one hundred different substances including chemokines, interferons, interleukins and tumour necrosis factors[109].

Traditionally divided into pro and anti-inflammatory groups based upon their apparent function, there is burgeoning evidence to suggest that some cytokines are also able to perform mixed actions[110]. Examples of pro-inflammatory cytokines include IL-1, IL-6, IL-12, IL-18, tumour necrosis factor-α (TNF-α) and Interferon-γ (IFN-γ). Cytokines that have been shown to have anti-inflammatory properties include IL-1, IL-6, IL-10 and transforming growth factor-β (TGF-β)[111-113] .

The downstream immune functions of cytokines are varied, but include macrophage activation (via IFN-γ), migration, proliferation, synthesis of NO and reactive oxygen species (ROS) (IFN-γ, TNF-α) and activation of B and T cells (IL4, IL5, IL6). Other roles include the stimulation of haematopoiesis[114], angiogenesis[115] and the induction of apoptosis[116].

The activation of the complement system offers an additional mechanism of response to infection. Mediated by innate immune signalling, infection results in increased synthesis of complement factors C3a and C5a[117, 118]. This activation has been associated with the biphasic activity of the neutrophil immune response and synthesis of pro-inflammatory mediators by macrophages[119].

Clotting factors and cells that take part in coagulation act via a number of routes to contribute towards the early immune response[120].

Tissue factor (TF), Thrombin, Factor Xa and activated protein C (APC) either directly or indirectly stimulate immune cell protease activated receptors (PARs) which initiate the release of a range of cytokines [121]. TF is also able to directly activate the membrane associated protein kinase (MAPK) enzymes to stimulate cytokine synthesis[122].

The coagulation factor fibrinogen generates a physical barrier within a clot to trap invading microbes as well as stimulating the release of a number of chemotactic stimuli to promote neutrophil recruitment and adhesion[123]. Platelets are able to generate antimicrobial peptides (AMPs) which are part of a group of micro particles synthesised in response to disruption of the vascular endothelial barrier[124]. In addition to stimulating the early phase of platelet aggregation, AMPs have anti-microbial and immune-modulatory properties with some evidence suggesting that they can reduce systemic inflammation in animal models of infection[125].

Immunosuppression has been a recognised feature of the innate response to infection for some time. Originally considered a component of the late compensatory anti-inflammatory response syndrome (CARS)[126], it is now recognised that the induction of both pro- and anti- inflammatory cascades is near simultaneous. During the course of the normal response, anti-inflammatory signalling limits the systemic impact of local infection[127]. In addition to the synthesis of anti-inflammatory cytokines, the immune response is also controlled by the downregulation of TLRs[128], complement mediated apoptosis[129] and the modulation of immune cell function which is induced by other cell types[130].

1.5.3 The Role of the Macrophage in the Innate Immune Response

Found in many tissue types and also in circulation, macrophages are responsible for the removal of cellular debris under normal conditions. During infection, they remove invading pathogens, stimulate the innate and acquired responses and also promote the resolution of inflammation.

1.5.3.1 Macrophage cell types

Macrophages have been classically divided into two groups, M1 and M2. M1 macrophages were the first to be characterised and are the early responder group that mount the immediate defence against an invading pathogen[131]. Originally identified as being stimulated by IFN-γ[132], subsequent work has shown that M1 cells are activated via a variety of TLRs[133]. In response to stimulus, these cells upregulate a range of genes in the three MHC regions and significantly induce NO synthesis by increasing iNOS activity. In addition, a number of cytokines are synthesised including IL-1 and IL-6 which facilitate phagocytosis and bactericidal activity[134].

Like M1 macrophages, M2 cells also upregulate genes in the MHC II region. However, arginine regulation is achieved by Arginase-mediated turnover rather than via iNOS [135]. This IL-4-mediated process appears to promote fibrosis rather than produce a bactericidal phenotype in these cells. It appears that the M2 subdivision is not entirely consistent and that this subtype is in fact able to perform a spectrum of pro and anti-inflammatory roles. As a consequence, three subtypes of M2 cells have now been described with differing actions[136].

1.5.3.2 Phagocytosis

Phagocytosis is one of the key functions of the macrophage given its large surface area that facilitates the formation of vacuoles that can be readily internalised. Phagocytosis typically requires the binding of ligands to a number of cell surface receptors[137], particularly the fragment crystallisable receptors (FcR) and scavenger receptor (SR) families, which stimulate internalisation.

1.5.3.3 Bactericidal activity

Microbial killing by macrophages is undertaken through the generation of two potent groups of toxins, reactive oxygen species (ROS) and nitric oxide (NO). ROS are generated by the action of NADPH oxidase (NOX) enzymes and include superoxide (O_2^-), hydrogen peroxide (H_2O_2) and oxygen free radicals ($O_2^{\cdot}$)[138] . The mechanisms of ROS microbiocidal activity are varied and include the disruption of microbial cysteine residues and damage to the DNA both within the phagosome[139] and external to the cell.

The role of NO in the eradication of pathogens by macrophages is also critical. Mediated by iNOS and the complex regulatory processes described above, NO reacts with ROS to form the reactive nitrogen species (RNS), peroxynitrite and the nitrosothiols that have a number of actions including protein inactivation and damage to bacterial DNA[131].

Macrophages are also able to undertake, within the phagosome, a number of additional processes that contribute towards the eradication of pathogens. These include the removal of essential cations from the phagosome such as magnesium and zinc, the generation of β-defensins that can permeabilise bacterial cell walls[140], the synthesis of proteases which break down carbohydrates[141] and the modification of phagosome pH[142].

1.5.4 Nitric Oxide and the Immune Response

Until relatively recently, there was some contention regarding the role of NO in the human immune response. Whilst murine macrophages are potent producers of NO, it appeared that human cells produce considerably less thus calling into question the importance of iNOS in this system[143, 144]. However, over recent years, it has been clearly demonstrated that NO is an important and tightly regulated mediator of the human innate immune response[145, 146]. Here the role of NO in the response to infection is reviewed.

1.5.4.1 Nitric oxide and redox chemistry

The role of NO in the immune response is intimately related to the other key mediator of oxidative stress, ROS. NO in itself is relatively non-toxic and is dependent upon the presence of ROS to synthesise RNS. The resulting function of the RNS is dependent upon a number of factors that determine the relative bioavailability of ROS and NO. These include the site of the interaction, the redox state of the cell and the proximity of the superoxide source[147, 148]. As a consequence, the close proximity and high concentrations of ROS facilitate the production of bactericidal RNS within the phagosome. In the cytoplasm, NO acts as an antioxidant by binding to ROS and reducing damage to the cell[149].

1.5.4.2 Pathogen-specific actions of nitric oxide

In contrast to ROS, which are largely synthesised within the phagosome, NO and RNS are lipid soluble and readily transition in to and out of the phagosome from their site of synthesis. Conditions inside the phagosome determine which reaction takes place and there is also an organism-specific component.

In the case of bacteria, neither NO nor ROS alone are always potent bactericidal agents. However, when combined in the phagosome, a thousand-fold increase in their ability to eradicate *E-Coli* is observed[150]. In some cases, NO and ROS are unable to eradicate a certain type of bacteria e.g. *Listeria monocytogenes.* In this instance, they combine to limit activity of the organism within the infected cell and reduce its infectivity thus allowing time for alternative pathways to be activated[151].

The protective role of NO signalling in the immune reaction to parasites is apparent when observing the response to *Plasmodium falciparum* infection. Exposure leads to an increase in iNOS activity and thus NO production which is directly toxic to the parasite[152]. NO has also been shown to preserve microvascular flow and reduce parasite adhesion to the vascular endothelium[153].

In the context of viruses, immune cell NO directly interferes with the formation of proteins critical to viral infection, movement and maturation. This is achieved through the nitrosation of cysteine residues on key viral proteins[154]. Within immune cells, NO synthesis in response to viral infection is a protective process. However, excessive NO production has been implicated in the development of haemorrhagic fever[155].

1.5.4.3 The role of nitric oxide signalling in innate immunity

As described above, the induction of iNOS within M1 macrophages is a critical feature of the innate immune response. In addition, NOS also plays an important role in the inflammatory cascade, regulating both pro-inflammatory and immunosuppressive components of the innate immune response.

NO and RNS are both responsible for the upregulation of inflammatory genes including those for the cytokines TNF-α, IL-8 and IL-6[156, 157], particularly during the early phase of inflammation when NO production is at its highest. NF-κB signalling displays a biphasic pattern when exposed to ROS and RNS with low levels augmenting and high levels inhibiting activation[158].

The anti-inflammatory role of NO is also important as it offers an indirect negative feedback process that regulates the response to infection and promotes tissue repair. This process is particularly important when iNOS activity and NO concentrations start to fall after the initial phase of the innate response. During this latter phase, NO promotes increased cAMP and cGMP concentrations via its actions on cyclooxygenase and sGC, respectively. This in turn inhibits further synthesis of TNF-α and IL-1β[159]. Another consequence of the NO-mediated increase in cAMP is that it directly induces the expression of anti-inflammatory cytokines including IL-10. This demonstrates another mechanism by which NO may enable the biphasic regulation of the immune response.

1.5.5 The Pathophysiology of Sepsis

Sepsis is a complex immune-mediated multisystem disorder which arises following pathogen entry into the body. The course and outcome of sepsis is widely variable with type and site of infection, genetic and acquired factors all playing a role in the response to the infective organism.

Under normal circumstances, infection provokes innate and acquired immune activation. A balance of pro- and anti-inflammatory signalling networks regulate a reaction that facilitates eradication of the pathogen and limits the extent of the response. When this process is dysregulated, the local response becomes systemic and sometimes leads to organ dysfunction and death. The exact mechanisms of this process have not yet been fully elucidated. However, a number of pathways have so far been implicated in the pathophysiology of sepsis are discussed below.

1.5.5.1 The infective source

The common feature of all cases of sepsis is by definition confirmed or suspected infection. The source of infection may be acquired from the community or from healthcare environments (e.g. respiratory tract, renal or central nervous system)[160] . It may be iatrogenic following surgery or arise as a consequence of disruption of normal physiological barriers by indwelling lines, tubes and catheters[161]. In addition, typically non-pathogenic organisms can also become infective sources in immunosuppressed individuals[162]. Following pathogen invasion, PRRs are activated by components of the infective microbe (PAMPs) and by endogenous stimuli released in response to infection (DAMPs) as previously discussed.

1.5.5.2 Cytokine production

Historically, it was believed that excessive inflammation mediated by the overproduction of cytokines was responsible for the negative outcomes associated with severe sepsis and septic shock. This belief was derived from the observation that in patients with sepsis, cytokines such as IL-1 and TNF-α were profoundly upregulated with the magnitude of this increase being associated with outcome[163]. Other cytokines that have been implicated include IFN-γ, GM-CSF, IL-8 and IL12 which are all broadly categorised as pro-inflammatory, IL-10 which is considered to be anti-inflammatory and IL-6 which can fulfil both roles[163]. A series of drugs designed to inhibit the activation of pro-inflammatory cytokines in sepsis were therefore developed and over the course of the last decade, numerous phase II and III studies have been undertaken. To date, no agent in this class has been shown to offer a mortality benefit in patients despite promising pre-clinical results. Table 5 below highlights a selection of anti-cytokine treatments that have been unsuccessfully trialled in human sepsis. This suggests that whilst excessive inflammation is an important part of the sepsis syndrome, it is not the only critical pathway involved.

Study	Year	Phase	Intervention	Outcome
Rice et al[164]	2010	III	TLR 4 signalling inhibition	Stopped early - No benefit
Dellinger [165]	2009	III	Endotoxin binding emulsion	Stopped early - excess adverse events
Tidswell[166]	2010	II (III)	Eritoran - TLR blocking agent	Stopped early - No benefit
Albertson[167]	2003	III	MAB - Enterobacterial Ag blocker	Stopped early - No benefit
Abraham[168]	2001	III	TNF-R Fusion protein	No Benefit
RAMSES[169]	2001	III	TNF Monoclonal Ab	Stopped Early - No Benefit

Table 5: Summary of the major clinical studies investigating the impact of cytokine signalling pathway blockade on outcome in patients with severe sepsis and septic shock.

More recently, HMGB-1[170] and macrophage migration inhibitory factor (MIF)[171] have both been shown to be elevated in patients with sepsis. Interest in HMGB-1 is considerable as it appears to be a late mediator of sepsis and thus potentially a more amenable therapeutic target.

In parallel to an exaggerated inflammatory state, anti-inflammatory cytokines are also upregulated during sepsis. It has been shown in some patients, that the synthesis of IL-10 may be preserved whilst the ability to mount a secondary pro-inflammatory response involving TNF-α and IFN-γ may be impaired[172]. This may predispose patients to an increased risk of secondary infection such as ventilator-associated pneumonia which has been shown to independently impact on mortality in patients with sepsis.

1.5.5.3 Complement

Excessive complement activity has been identified as a potential cause of immune dysfunction in sepsis. Increased levels of C5a have been associated with outcome in critically ill patients[173] and are also known to impair phagocytosis and bactericidal activity[174]. As such, C5a has been considered as a potential therapeutic target [175, 176]. Anti-C5a therapy has been shown to reverse the cellular effects of C5a in isolated human monocytes[174] and improve survival in animal models of sepsis[177]. The regulation of C5a is therefore a further therapeutic area currently being explored in sepsis.

1.5.5.4 Coagulopathy

Sepsis results in a pro-coagulant state which is coupled with impaired anti-coagulant pathways and fibrinolysis. Disseminated intravascular coagulopathy (DIC) arises as a consequence and is a common feature of septic shock[103].

The activation of immune cells in sepsis leads to the cell surface expression of TF[178] . TF binds to factor VIIa which results in the activation of factor Xa to promote thrombin formation. In septic shock, this process appears to occur excessively thus leading to the consumption of clotting factors and coagulopathy.

The failure of anti-coagulant processes to balance the pro-coagulant state is another important feature of sepsis-induced DIC. In sepsis, there are three pathways that are particularly important in this process. The first two pathways that are compromised in DIC are anti-thrombin and TPI-mediated anticoagulation which are reduced following a cytokine-induced decrease in endothelial glycosaminoglycans[179]. Protein C synthesis and activation is also deregulated. Protein C is typically activated to form APC following the binding of thrombin to thrombomodulin. APC possess both anti-coagulant and also anti-inflammatory actions.

The deregulation of the clotting pathway as seen in DIC has also been studied as a potential therapeutic target in sepsis. This has led to a number of phase II and III studies which are summarised in the table below (Table 6). Most notably, drugs targeting APC were licensed and were in clinical use for several years before safety concerns prompted further phase III studies and their subsequent withdrawal.

Paper	Year	Phase	Intervention	Outcome
Warren[180]	2001	III	Anti-thrombin III	No Benefit
HERTRASE[181]	2009	II	Un-fractionated Heparin	No Benefit
PROWESS[182]	2001	III	Activated Protein C	Survival Benefit at 28 days
ADDRESS[183]	2005	III	Activated Protein C	No benefit patients with low risk of death
PROWESS SHOCK[66]	2012	III	Activated Protein C	No Benefit

Table 6: Summary of the major clinical studies investigating the impact of modulators of the coagulation cascade on outcome in patients with severe sepsis and septic shock.

1.5.5.5 Cellular dysfunction

Cellular dysfunction is a common feature of sepsis, with a diffuse range of cell types suffering from impaired responsiveness to their stimuli. The causes of this are diverse, but include mitochondrial dysfunction[184, 185], increased expression of inhibitory programmed cell death protein 1 (PD-1) receptors [186] and Tregulatory (Treg) cells and the downregulation of CD88 and HLA-DR mediated pathways[187].

In addition, lymphocyte apoptosis may also be induced, leading to a reduced ability to synthesise cytokines. This finding has been observed in both animal models[188] and also in septic patients where samples were taken immediately post mortem[189].

Previous work has also demonstrated that immune cells are unable to mount an appropriate response due to cellular dysfunction. Clinical trials are therefore underway to explore the potential of immune augmentation in the treatment of sepsis using exogenous agents such as IFN-γ and GM-CSF[190].

1.5.5.6 Nitric oxide and cardiovascular compromise in septic shock

The increase in vascular NO production in response to infection is mediated by iNOS which is upregulated in vascular smooth muscle and endothelial cells[191]. Mediators of the induction of vascular iNOS include IL-1β, IL-6, TNF-α, IFN-γ[192, 193] and adenosine[194]. Under normal conditions, local NO-induced vasodilatation and vascular permeability confer an advantage as they facilitate the delivery of immune cells and oxygen to the site of infection. However, dysregulation of this process plays an important role in sepsis-induced hypotension and hyporeactivity to catecholamine-based vasopressors[195, 196]. Inhibitors of NOS have been shown to increase both arterial pressure and vascular resistance in septic and late-phase haemorrhagic shock[197-199] and to reverse shock in human studies[200].

Mechanisms by which elevated NO levels lead to vasodilatory shock include:

- Activation of myosin light-chain phosphatase.
- Activation of potassium channels in vascular smooth-muscle cells[201-204]. These channels include the cytosolic calcium sensitive (K_{Ca}) channels, which blunt the effect of vasoconstrictors[205]. NO activates K_{Ca} channels via the direct nitrosylation of the channel[201] and activation of cGMP-dependent protein kinases[202].
- Hyperpolarisation of the plasma membrane of vascular smooth-muscle cells in addition to impaired mitochondrial function by cytopathic dysoxia[184, 206].

1.6 Endogenous Regulators of Nitric Oxide Synthesis and Sepsis

This section considers the existing literature regarding the role of MAs and their regulators in sepsis and discusses the available evidence that suggests the involvement of the endogenous NO regulatory pathway in determining disease outcome.

1.6.1 Asymmetric Dimethylarginine

Plasma methylarginines have been examined in a series of small studies. This has led to challenges in interpreting the data as in most cases it has not been possible to correct for potential confounding variables. Nevertheless, studies in this area have generated interesting preliminary data that demand validation in a larger data set.

In 2006, O'Dwyer et al. measured the plasma ADMA levels of 47 patients with severe sepsis following hospital admission and on day one and seven of their critical care stay[40]. They found that when compared to a group of 10 healthy volunteers, ADMA concentrations in septic patients were significantly elevated on admission, and were still raised and somewhat increased by day seven of their intensive care unit (ICU) stay. Increased ADMA was positively correlated with the severity of metabolic acidosis and with levels of blood lactate on both days. In addition, there was an association with the severity of organ failure assessment (SOFA) score.

A further study assessed the changes in ADMA concentration in 30 patients following elective surgery and in a group of 60 patients who were admitted to hospital with a primary diagnosis of sepsis[207]. In this study, ADMA was consistently elevated over the course of the septic insult when compared to healthy volunteers, an effect which persisted to day 28 in survivors. ADMA levels were also found to be consistently higher in patients with acute sepsis-induced liver dysfunction (n=15 on admission) compared to patients with similar disease severity, but normal hepatic function.

In their 2011 study, Davis et al. studied 67 patients with sepsis (20 with septic shock) and explored the potential relationship between plasma ADMA concentrations, shock severity and outcome[208]. Samples were taken on admission and on day two of the patient's ICU stay. The study suggested that patients with ADMA concentrations that fell within the top quartile had a 20-fold increased risk of death by 28 days. However, due to the size of the group in which only 6 patients in total and 5 with septic shock died, the effect is difficult to interpret. ADMA levels also correlated with shock severity, as measured by SOFA score, and the degree of microvascular dysfunction. Of note, univariate analysis indicated that SDMA concentration was also associated with increased mortality. However, this relationship did not persist following correction for the degree of renal failure.

By contrast, the opposite effect is observed in paediatric patients. One particular study compared three groups of participants aged under eighteen with healthy volunteers, non-septic pyrexial patients and children with severe sepsis and septic shock [209]. Each group contained thirty patients with septic participants giving blood samples on each of the first seven days following hospital admission. In this study, sepsis was associated with significantly lower plasma ADMA concentrations in both the febrile and septic groups when compared to controls. However, plasma ADMA concentrations did rise over the course of the study in the septic group. In addition, indices of organ dysfunction and inflammatory state were inversely correlated with ADMA concentration at hospital admission. This is also in contrast to the effects observed in adults. These findings were confirmed by a separate study in Gambian children with severe malaria where both mild and severe disease was associated with a sustained reduction in plasma ADMA concentration[210].

1.6.2 Symmetric Dimethylarginine

Koch et al. examined the plasma SDMA levels of 247 patients that were admitted to intensive care (of whom 160 had sepsis), with samples taken upon admission and on day seven of their hospital stay[211]. They found that SDMA concentrations were higher in critically ill patients when compared to controls and that the highest levels were observed in patients where sepsis was the primary diagnosis. As had previously been shown, SDMA levels correlated with the degree of renal failure and also with the severity of hepatic dysfunction. Interestingly, this study also showed that plasma SDMA concentration at admission was independently associated with mortality at three years.

1.6.3 Dimethylarginine Dimethylaminohydrolase 1

To date, no human studies have as yet been undertaken to explore the association between DDAH1 polymorphisms and outcome in sepsis. However, the availability of a highly selective DDAH1 inhibitor and global knockout mouse model has enabled the phenotypic effects of both transient and lifelong DDAH1 deficiency and its role in sepsis to be further investigated.

Aortic rings taken from heterozygote DDAH1-deficient mice demonstrated preserved vascular responsiveness following stimulation with LPS. $DDAH1^{+/-}$ mice also displayed significantly less reduction in their systemic blood pressure following LPS injection[47, 212].

In both LPS and polymicrobial models of sepsis, the selective DDAH1 inhibitor L-257 has been shown to offer improved survival in rats[213]. In addition, L-257 alone was found to reduce the severity of hypotension and the requirement for noradrenaline therapy in order to maintain blood pressure. These effects were observed even when treatment was delayed until after the onset of shock symptoms. L-257 therapy was shown to improve indices of renal and hepatic function and preserve microvascular flow, but had no effect on immune cell function[213].

1.6.4 Dimethylarginine Dimethylaminohydrolase 2

The question of whether DDAH2 SNPs might be associated with outcome in human sepsis has been raised given its association with disease and position of the gene within the MHC III region of chromosome six. To date, two studies have explored this association, but not on a scale large enough to ensure that observed differences did not occur by chance.

One group conducted a study to determine whether two previously published SNPs located within the promoter region of DDAH2 were associated with plasma ADMA concentration and/or disease outcome in children with sepsis[39] (Figure 5). They found that in 27 patients with septic shock, rs805305, which represents a substitution at the -449 position of the DDAH2 promoter sequence, was associated with lower levels of plasma ADMA. Furthermore, they found that this SNP was associated with a greater incidence of ‘cold shock’. This is thought to arise when the systemic response to infection manifests as a low cardiac output state. However, studies by O’Dwyer et al. in adults showed no association with illness severity, but a positive correlation with plasma ADMA concentration[40].

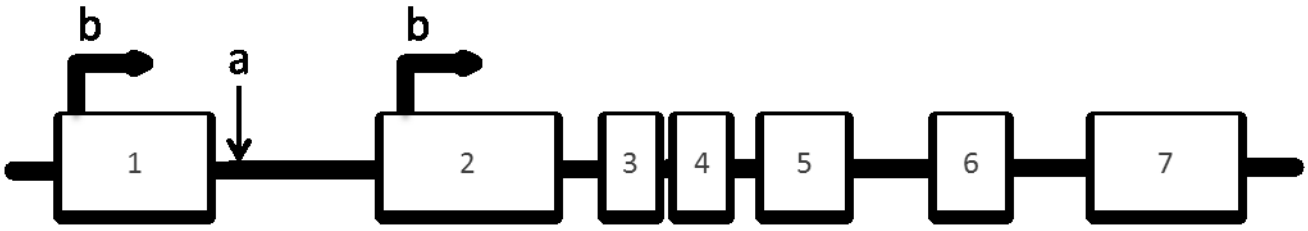

Figure 5: Representative image of the DDAH2 gene

(adapted from www.ncbi.nlm.nih.gov/gene/23564). Exon 1 is considered to be non-coding. However, both exon and intron 1 appear to contain promoter regions. a: represents the site of the rs805305 SNP and b: the proposed translation start sites.

Animal studies have thus far focussed on determining the functional effects of DDAH2 deletion from immune cells. Knockout of DDAH2 using two different transgenic animal models led to a significant reduction in NO synthesis by isolated primary resident macrophages, a phenomenon mediated by increased cellular ADMA concentrations. This apparent impairment of NO synthesis also led to compromise of the normal functions of the animal's macrophages in response to stimulus. This included significantly reduced motility, chemotaxis and bactericidal ability compared to appropriate litter mate controls[30].

1.7 Summary

NO plays a critical role in the immune system and dysregulation of the innate response is an important factor in the development of severe sepsis and septic shock, a condition that has high associated morbidity and mortality. The influence of DDAH on the regulation of NO signalling is well elucidated, however the impact of this process and its role in modulating the immune response is currently not well established. This work will determine the role of monocyte DDAH2 in regulating the immune response to sepsis using cellular, animal and human studies.

2 Hypothesis

2.1 Hypothesis

Immune cell DDAH2 plays a role in the regulation of the systemic immune response and determines outcome in sepsis.

2.2 Objectives

2.2.1 Inflammatory cytokines and the regulation of DDAH2

Using an immortalised cell line and primary murine macrophages, this study aims to determine the role of different pro-inflammatory regulators in DDAH2 expression and evaluate the impact of this on the regulation of NO synthesis.

2.2.2 The role of hypoxia in the DDAH2-mediated immune response

Using primary murine macrophages from wild type and DDAH2 knockout models and human peripheral blood mononuclear cells from healthy volunteers following exposure to normobaric hypoxia, this study will explore NO regulation in response to acute hypoxia and evaluate the role of DDAH2 in this process.

2.2.3 The impact of polymicrobial sepsis in global and macrophage-specific DDAH2 knockout mice

Using *in vivo* radiotelemetry monitoring in a polymicrobial sepsis murine model, this study aims to determine the systemic impact of global and macrophage-specific knockout of DDAH2 in response to life threatening infection.

2.2.4 ADMA, NO and DDAH polymorphisms and outcome in human sepsis

Using a hypothesis based interrogation of a genome wide association study in patients with sepsis, coupled with a prospective analysis of plasma and buffy coat samples from a randomised controlled trial of vasopressor therapy in septic shock, this study will also aim to determine how NO, its endogenous regulators and polymorphisms of DDAH genes relate to a series of outcomes in a robust human population.

3 Methods and materials

3.1 In vitro methods

3.1.1 Isolation and culture of RAW 264.7 murine macrophage cell line

RAW 264.7 are a macrophage cell line that was developed from a murine model of Abelson murine leukaemia virus induced tumour. RAW 264.7 was developed in 1975 and has been well validated[214]. Its ease of use and manipulation have resulted in it becoming one of the most widespread murine macrophage cell lines employed in studies with over 1500 articles relating to its function[215]. The cell line has been used to examine monocyte function and activity, including the regulation of iNOS signalling in response to stimulation[216],receptor signalling and response to Lipopolysaccharide(LPS)[217, 218]. The RAW 264.7 cells were obtained from an existing cell line and incubated in a humidified atmosphere containing 5% carbon dioxide using Dulbecco's Modified Eagle Medium (DMEM) and 10% foetal bovine serum (FBS), 2mM Glutamine and 2mM penicillin/Streptomycin.

3.1.2 Hypoxic Chamber incubation

In order to determine the impact of subacute hypoxia on isolated primary macrophages and RAW 264.7 cells. Cultured cells were incubated for varied amounts of time in a sealed hypoxic incubator at 92% Nitrogen, 3% Oxygen and 5% CO2. Culture medium was placed in the chamber at least 12hours prior to experiment in order to equilibrate medium partial pressure of oxygen with that of the hypoxic atmosphere. Table 7 below describes the changes observed in the medium after 12 hours in the hypoxic chamber.

Measurement	Normal tissue culture incubator	Hypoxic incubator
pH	7.492	7.651
PCO_2 (kPa)	6.55	4.87
PO_2 (kPa)	19.6	7.7
HCO_3^- (mmol/L)	39	40

Table 7: Medium conditions before and after a 12 hour period of equilibration in the a hypoxic chamber with an environment of 3% O2 and 5% CO2

3.2 Molecular Biology Methods

3.2.1 Tissue homogenate preparation

Immediately following sacrifice, tissues were frozen in liquid nitrogen and stored at -80C. Frozen tissue was pulverized using a mortar and pestle and re-suspended in phosphate-buffered saline (PBS) (Invitrogen, UK) supplemented with Complete EDTA-free, Protease Inhibitor Cocktail (Roche, UK). Tissue homogenates were homogenised 3mins at 25Hz then spun at 14,000rpm for 15 minutes, at 4°C. The supernatant was retained for further analysis.

3.2.2 Cell culture protein extraction

Following incubation, culture medium was removed, the cells washed briefly in PBS and replaced with a solution of PBS and protease inhibitor before mechanical clearance from the plate surface.

Following collection, the cells underwent mechanical lysis in an automated homogeniser for 3mins at 25Hz (TissueLyser II, Qiagen, UK). The lysed cells were then centrifuged at 14000rpm for 10mins at 4 degrees Celsius, after this, the supernatant was aspirated and the protein level measured using the Bradford assay in order to standardise the results against protein concentration. Storage was at -80°C prior to use.

3.2.3 Preparation of cell culture samples for mRNA analysis

Cells were scraped from the surface of the culture plate and suspended in 500µL of RLT buffer with 10µL/ml of β-mercaptoethanol before mechanical lysis using a 1ml syringe and 23gauge needle. RNA extraction was performed using column purification as per manufacturer's instructions (Qiagen Ltd, UK)

3.2.4 Protein and RNA quantification

Protein was quantified using either a Bradford assay or the NanoDrop™ device.

3.2.4.1 Bradford Assay

The Bradford assay utilises a calorimetric technique to facilitate measurement of protein concentrations. It utilises a property of Coomassie blue dye which displays a colour change in response to change in pH. The change in pH is mediated by amino acid binding and correlates with protein concentration. This shift in colour may be measured using spectrophotometry[219] and compared to a standard curve of known protein concentrations.

3.2.4.2 NanoDrop™ Device

The NanoDrop device (Thermo Scientific) utilises spectrometry at specific wavelengths to quantify protein, DNA or RNA. 3µL of test solution are loaded, samples analysed in triplicate and an average result obtained.

3.2.5 Polymerase chain reaction

The Polymerase chain reaction (PCR) is a well established method used for a number of applications. In brief, a sample of nucleic acid is added to a solution containing a heat stable DNA polymerase, deoxynucleoside triphosphates (dNTPs) and either complementary DNA fragments or primers. Incremental temperature change results in DNA denaturing, the annealing of complimentary sequences and the binding of dNTPs to form new double stranded DNA, a process which is catalysed by the DNA polymerase. Over multiple repeat cycles, the new DNA acts as a template leading to logarithmic amplification. This process allows specific and quantifiable analysis of DNA.

3.2.5.1 Reverse transcription quantitative polymerase chain reaction

Tissue and cell mRNA turnover was measured using a two stage process. Initially, RNA was purified using RNEasy (Qiagen, UK) as recommended by the manufacturer's protocol. Spectrophotometric quantification of RNA was undertaken by measuring absorbance at 260 and 280nm.

Complementary DNA (cDNA) production by Reverse Transcriptase PCR (RT-PCR) was undertaken from 1000ng of extracted RNA using the iScript cDNA synthesis kit (BioRad, USA) as recommended by the manufacturer.

Component	Volume
iScript reaction mixture	4µL
iScript reverse transcriptase	1 µL
RNA 1000ng + water	Total 15 µL
PCR Protocol (1 cycle only)	Duration
Reverse transcription @ 42°C	30mins
RTase inactivation@ 85°C	5mins

Table 8: cDNA synthesis was undertaken with iScript (BioRad, USA) technology. Materials and protocol are described for the synthesis of 1000ng of cDNA

A commercial Sybr Green-based PCR mix (iTaq Fast SYBR Green Supermix with ROX, BioRad) was added to 100ng of cDNA and using the 7900HT Fast System (Applied Biosystems), fluorescence threshold (CT) was assessed using the established method. Sybr green emits light in the green spectrum once incorporated into a nucleic acid. Samples were analysed in duplicate and the fluorescence threshold (C_T) was set at the base of each exponential curve. The resulting quantitative measure of the mRNA of interest was corrected for housekeeper cDNA.

Several housekeeper genes were considered including β-actin and α-tubulin, however ultimately 18s ribosomal RNA was chosen which is ubiquitous and unaffected by the reactions undertaken. Quantification was based on standard curve plotted on a logarithmic axis and the slope of linear regression used to quantify relative sequence expression.

RT-qPCR protocol step	Duration
Initial step @ 95°C	2min
Thermal cycling x 40	
Denaturation @ 95°C	3 secs
Annealing @ 60°C	30secs
Disassociation step	

Table 9:Protocol for the conduct of RT-qPCR quantitative phase

3.2.5.2 RT-qPCR primer sequences

Primer sequences for qPCR analysis were derived from existing publications or designed using the NCBI Primer blast facility (http://www.ncbi.nlm.nih.gov/tools/primer-blast/index.cgi?LINK_LOC=BlastHome). All sequences were confirmed using blast analysis to confirm 100% concordance with the appropriate sequence.

Primer	forward	reverse
Murine sequences		
DDAH1	TCTCATAGACCTTTGCGCTTTC	CACAGAAGGCCCTCAAGATCA
DDAH2	CCTGGTGCCACACCTTTCCC	AGGGTGACATCAGAGAGCTTCTG
Inducible Nitric Oxide Synthase	CAGCTGGGCTGTACAAACCTT	ATGTGATGTTTGCTTCGGACA
endothelial Nitric Oxide Synthase	AAGACAAGGCAGCGGTGG	GCAGGGGACAGGAAATAGTT
Tubulin	GCCTTCTAACCCGTTGCTATCA	CGGTGCGAACTTCATCGAT
Human Sequences		
DDAH2	CCCTTCTCCACCAACTCTGT	TTGTTTCTTCACCTGTCTCCA
Inducible Nitric Oxide Synthase [220]	TGGCCAGATGTTCCTCTATT	CCAAAGGGATTTTAACTTG
Endothelial Nitric Oxide Synthase[221]	GGGCAGCCTCACTCCTGTT	ACGGCGTTGGCCACTT
Tubulin	GCCTTCTAACCCGTTGCTATCA	CGGTGCGAACTTCATCGAT

Table 10:Summary table of PCR primer sequences used in the conduct of mouse and human studies.

3.2.6 Western blotting

Following preparation of the samples as described above, a known concentration of protein was diluted with a 4x Laemlli buffer solution (see Table 11 below) and heated at 95°C for four minutes. Each sample was then added to a lane of sodium dodecyl sulfate-polyacrylamide gel electrophoresis (SDS-PAGE) gel. The recipes utilised in DDAH2 western blotting can be seen in Table 12 below. 2µL of a protein ladder was added to one lane of each gel. Following electrophoresis, gel was transferred onto PVDF membrane (GE Healthcare, UK) and then blocked in PBS with 0.1% tween-20 (Sigma-Aldrich, USA) and 5% non-fat milk (Sigma-Aldrich, USA).

Substance
277.8mM Tris-HCl, pH 6.8
4.4% LDS (lithium dodecyl sulfate)
44.4% (w/v) glycerol
0.02% bromophenol blue
10% v/v β-mercaptoethanol

Table 11:Contents of Laemlli buffer solution

Primary antibodies for DDAH1 and DDAH2 were raised in goats against peptide sequences, which are conserved across rats, humans, and mice as previously described[30, 222]. Purification of these antibodies is described below. Secondary antibody for alpha Tubulin was purchased from Abcam (Cambridge, UK). Secondary horse-radish peroxidase conjugated antibodies, ECL+ reagents, and ECL film was used to visualize blots (all GE Healthcare). Protein levels were quantified by densitometry and ImageJ (NIH).

Resolving	Stacking
4.35mL dH2O	6.32mL dH2O
3mL 40% acrylamide/Bis 37.5:1;	1mL acrylamide/Bis 37.5:1
2.5mL 1.5M Tris-HCl pH8.8;	2.52mL 0.5M Tris-HCl pH6.8
100uL 10% SDS;	100uL 10% SDS
5uL TEMED;	10uL TEMED
50uL 10% APS	50uL 10% APS

Table 12:Ingredients for the preparation of two 12% SDS-PAGE gels for the conduct of western blotting for DDAH2

The protocol for the conduct of a DDAH2 western blot was as follows:

Stage	Protocol
Run SDS PAGE	10-20uL protein/well plus 2uL protein marker (All Blue; BioRad). 150V
Rinse gel and membrane	Wash gel in transfer buffer for 30mins Soak Membrane in methanol for 10mins, wash x 2in dH_2O, soak in transfer buffer for at least 15mins
Transfer to membrane	Hybond-P (Immobilon), 260mA, 70mins Cooled with ice
Wash in PBS Tween 0.1%	3x10mins in large volumes
Dry in air	60mins
Primary antibody incubation (In 5% milk with PBS-T)	in 5% milk PBS-T with continuous agitation @ 4°C overnight
PBS-T washes	3x10mins in large volumes
Secondary antibody incubation (In 5% milk with PBS-T)	Room temperature 1 hour with agitation
PBS-T washes	3x10mins in large volumes
Visualisation either:	
Chemiluminescence	Amersham ECL kit

Table 13: Protocol for the conduct of Western blots in cell culture, animal tissue and human studies.

3.2.6.1 DDAH antibody synthesis

Commercially available antibodies to DDAH1 and DDAH2 produce variable outcomes. Our group has developed polyclonal goat antibodies to both genes based on sections of the sequence conserved across both rodents and humans.

Working antibody solutions were extracted from goat serum through a process of affinity purification using beads with covalently bound DDAH peptides, which were passed through purification columns, a low pressure chromatography system. Extracted fractions were passed through a UV filter and the selected fractions run separately through a SDS-PAGE gel to confirm the presence of the eluted protein. Definitive confirmation was obtained by the conduct of western blotting of tissue lysates of appropriate samples to confirm successful detection of DDAH1 and DDAH2.

3.2.7 Liquid chromatography-mass spectrometry / mass spectrometry

Analysis of methylarginine and L-arginine concentrations was undertaken using a liquid chromatograph, triple quadrupole mass spectrometry technique as previously demonstrated[30, 47, 223]. This is a high specificity and sensitivity method for the detection of methylarginines in concentrations as low as the picomolar range.

Biological samples underwent methanol protein precipitation in a 1:5 dilution of methanol for cell lysate and culture medium and a 1:10 dilution for plasma. An internal standard of 7-deuterated (D7) ADMA (Cambridge isotope laboratories, USA) was added at the precipitation stage to facilitate correction for extraction efficiency. Following extraction, solutions were evaporated to dryness on a heat block and resuspended in mobile phase (0.1% formic acid).

3.2.7.1 High performance liquid chromatography

During the HPLC phase samples were pumped at high pressure through a column which contains a number of adsorbent materials, to which solutes bind. The column is then washed with an elution buffer across a pH or salt gradient, and solutes are separated based on their affinity for the column. In this study, a hypercarb chromatography column was used (Thermo, UK), and through it, a mobile phase of 0.1% formic acid was passed in conjunction with 1% acetonitrile, which increased to 50% for minutes five to ten of each sample run. The total run time was fifteen minutes per sample. A standard curve of ADMA samples of 10 known concentrations was prepared for 96 well plate (0 to 10μM). Samples were prepared and run immediately

3.2.7.2 Mass Spectrometry

Mass spectrometry involves the ionisation of a substance and then detection of that substance or fragments of it through comparison of their mass/charge (m/z) ratio. This study employed the Agilent 6400 LCMS/MS system.

The first step was electro- spray ionisation. The substance to be analysed was presented to the analyser in solution, having travelled through the liquid chromatograph. The solution is is nebulised to form a fine spray [224]. These nebulised droplets are heated and dry nitrogen is applied in order produce charged analytes which are in turn transferred into the high vacuum chamber via a small opening[225]

Once into the vacuum chamber the analyte passes through a quadrupole. This is made of four metal rods which are used to generate varying voltages which facilitate the passage of particles with different m/z ratios. A series of fixed voltages in the quadrupole causes the analyser to detect specific analytes in a sample based on their mass/charge ratio[225]. This initial phase forms part of the triple quadrupole system. The second component is made of a quadrupole that has an inert gas such as argon at low pressure within it and accelerates the fragments towards the third quadrupole. Collisions of the analyte with this gas result in the phenomenon of collision induced dissociation. Passage of these fragments through a third quadrupole analyser allows identification of the m/z ratio of these breakdown products. This in turn permits differentiation of structures that may not be separated by single chamber mass spectroscopy alone. The ability to set and then vary voltages for the first and third quadrupoles makes it possible to examine multiple analytes and their products during the course of a sample run. This is known as multiple reaction monitoring (MRM).

Standardisation of the measurements is achieved using labelled analytes inserted at the beginning of the purification process. This accounts for losses during sample preparation as well as variation in the analytical process[225].

3.2.7.3 Detected fragments

The precursor ion/product ions measured were:

- D7 ADMA: 210/46.0
- Arginine: 175/60
- ADMA: 203.1/46
- SDMA: 203.2/172 and 203.2/72
- L-NMMA: 189.1/57

3.2.8 Promoter reporter construct preparation and utilisation

3.2.8.1 Promoter reporter development

Promoter reporter constructs had been developed by the group using a method described previously[42, 226]. In brief, a restriction fragment spanning the nucleotides contained with the -1755 to -216 territory of the human DDAH2 gene was isolated from a human genomic clone and added to a pGL3 basic luciferase vector (Promega, US) (to generate pGL3sal), a promoter reporter construct containing a firefly luciferase reporter. Specific regions of the promoter sequence were selected which represented specific areas likely to represent important transcription factor binding sites (Genomatix) and from that a series of 5' deletion sequences were also generated and cloned to the same pGL3 basic reporter construct. The 5' oligonucleotide sequences were designed and tagged with MluI restriction sites and PCR was performed using these primers and a 3' vector oligonucleotide. Following digestion with MluI and SalI, constructs were verified by sequencing prior to cloning of the new construct. A 270 base pair fragment spanning nucleotides −927 to −658 was generated by PCR and cloned into the pGL3 basic vector (PPIRF). From this, a site specific construct was also made by deleting four base pairs from the relevant consensus region (IRFKO) using established methods.

A representative image of the promoters utilised in these studies can be seen in Figure 6 below.

Frozen stocks of these promoter reporter constructs had been stored at -80°C prior to use in these studies. Following thawing, aliquots of these stocks underwent plating and then maxiprep (Qiagen, UK) to extract the construct and amplify its concentration prior to experiment. Before use, all of the constructs underwent repeat sequencing in order to confirm their identities.

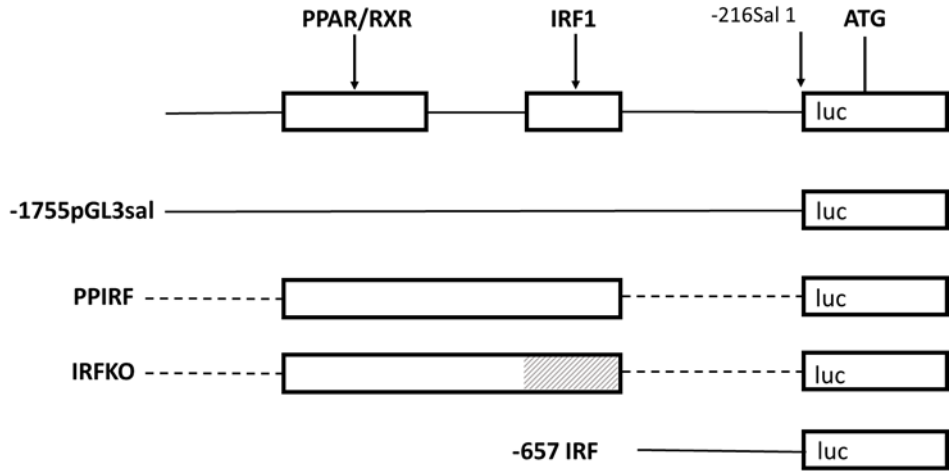

Figure 6: DDAH2 Promoter constructs used in exploring response to pro-inflammatory stimulus

Top image: key promoter regions, -1755pGL3sal - whole promoter region synthesised, PPIRF - Active region of DDAH2 promoter construct, IRFKO – PPIRF promoter with deletion of a portion of the sequence in the IRF1 region, -657 IRF - downstream region.

3.2.8.2 Agar plating

Agar was sterilised in an autoclave for 60mins before cooling to room temperature. The liquid Agar was then divided into aliquots of 30mls in sterile 100mm plates under a Bunsen flame. Ampicillin was added to each plate under the same conditions because pGL3 constructs also contain a resistance gene to this antibiotic, which allows for selection of plasmid containing bacteria. Plates were allowed to set at 4°C prior to use.

Aliquot of Cells from glycerol stock or water suspension were applied to individual plates and incubated at 37°C in 5% CO_2 and 21% Oxygen overnight. Following incubation, a starter culture was selected from each plate and added to 5mls of LB medium and incubated at 37°C in 5% CO_2 and 21% overnight with vigorous shaking at 300rpm.

The following day, aliquots of this fluid were collected for DNA measurement using the NanoDrop device and preparation for DNA sequencing to confirm the position of each construct within the promoter region of the DDAH2 gene.

3.2.8.3 Maxi Prep

The conduct of the plasmid DNA extraction was undertaken using the Maxiprep kit (Qiagen) and based upon their recommended protocol. Following confirmation of the correct identities of the constructs by sequencing, the collected sample was diluted 1:500 in fresh LB medium and incubated for 16 hours at 37°C in 5% CO_2 and 21% Oxygen with agitation. The resultant suspension was centrifuged at 4°C for 15minutes.

In the next phase, the pellet was resuspended, the bacteria exposed to a lysis buffer and then incubated on ice for 15mins. Following a thirty minute centrifugation step at 4°C, the plasmid containing supernatant was removed and this step repeated with a further 15 minute centrifuge cycle.

The supernatant from this is then passed through a proprietary resin column to which the plasmid DNA adheres. The column is washed to remove non-adherent contaminants and then the plasmid DNA is collected by the passage of an elution buffer through the column into a collection vessel. This DNA is precipitated using isopropanol and collected after a further 30minute centrifuge step. Washed with 70% ethanol and allowed to dry in air, the plasmid pellet was then resuspended and concentration of the collected plasmid DNA measured by UV spectrometry at 260nM.

3.2.8.4 Electroporation

Nucleofection is an electroporation technique that facilitates insertion of plasmid DNA or siRNA into the nucleus of a target cell. It is a well-established technique in RAW 264.7 cells and delivers a high degree of efficiency. RAW 264 cells were cultured and two million cells were harvested per sample. Following centrifugation, cells were resuspended in 100µL proprietary of Nucleofector solution (Lonza, GER) and injected into a purpose made cuvette and exposed to electroporation in a nucleofector device. After electroporation, cells were reincubated for 12 hours in culture medium.

Two plasmids were inserted into the RAW 264 cells. The first, one of the previously described human DDAH2 promoter/reporter constructs containing a portion of the promoter region and also a reporter construct expressing firefly luciferase following stimulus. The second construct was a pGL4 control promoter (Promega, US) to act as a positive control expressing *renilla* (sea pansy) luciferase.

The efficiency of this process was determined using a green fluorescent protein (GFP) reporter simultaneously electroporated into the RAW cells with the pGL3 construct. The degree of fluorescence was then measured at eight hours after electroporation using fluorescence microscopy which demonstrated a >90% efficiency in surviving cells. A representative image can be seen below in Figure 7.

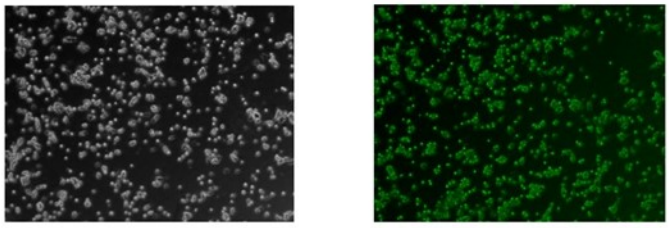

Figure 7: Light microscopy and Fluorescent microscopy images of electroporated RAW 264.7 cells

Left image: Representative brightfield image of RAW 264.7 cells 14 hours following electroporation and transfection with GFP reporter. Right image: Representative GFP fluorescent image of RAW 264.7 cells 14 hours following electroporation and transfection with GFP reporter.

3.2.8.5 Dual Luciferase Assay

Following insertion of the human DDAH2 promoter into the RAW 264.7 cells, medium was changed and cells exposed to a pro inflammatory cocktail or control stimulus, followed by incubation at 37°C in 5% CO_2 and 21% Oxygen for 8 hours prior to analysis. Following incubation, cells were washed and lysed (Passive Lysis Buffer).

Luminescence was determined using the dual Luciferase reporter assay (Promega, USA). An aliquot of cell lysate was applied to a firefly luciferase reporter to generate a stable luciferase signal from the pGL3 construct. Following measurement of luminescence, the primary reaction was quenched and Renilla (Renilla reniformis or sea pansy) luciferase intensity from the pGL4 control promoter stimulated. Luminescence was then reassessed and used to correct each individual measurement for variability of cell number and electroporation efficiency.

3.3 Biochemical Methods

3.3.1 Measurement of nitric oxide concentrations

3.3.1.1 The Griess reaction

The Griess reaction offers a reliable method for determining the amount of nitrite produced by a chemical reaction[227]. Nitrite is the stable end product of NO generation and is the result of the interaction between nitroxides and sulfanilic acid that then goes on to react with N-(1-napthyl) ethylenediamine. This then produces a purple azo-dye compound that can be measured using spectrophotometric techniques since it absorbs maximally at 546nm [228-230].

Griess reagent is prepared from the mixing of two solutions immediately prior to experimentation. Solution A is 1% (w/v) sulphanilamide in 5% phosphoric acid. Solution B is 0.1% (v/v) napthylethylenediamine prepared in distilled water. Both solutions are stored at 4°C until shortly before use, when equal volumes of each are mixed together. 100µL of the supernatant from the different conditions was removed at each time point under investigation and applied in triplicate to a well of a 96 well plate with an equal amount of the newly mixed Griess reagent also added to each well at room temperature. After an incubation period of 10 minutes, a micro plate reader measured absorption of light at 540nm in each of the wells. In order to determine the nitrite production, a standard curve of absorbance (0 to 100 µM) was prepared for each sample. Untreated medium containing monocytes usually only contains less than 1µM concentration of nitrite[231, 232].

3.3.1.2 Chemiluminescent measurement of nitrate and nitrite

The Sievers NOA 280i (GE Analytical Instruments) was used to measure Nitrate + Nitrite (NOx) content of biological samples. Tissue and plasma samples underwent methanol precipitation using 1:10 dilution fraction. Samples were run in duplicate and the mean value taken as the final result.

The measurement of NO using a chemiluminescent technique requires the re-derivation of NO from nitrites and nitrates (stable end-products of NO activity) by reduction in heated vanadium chloride. NO is released as a gas by this reaction which is detected and quantified by reaction within the detector with ozone which produces light in the red/infra-red spectrum. NO produced by this reaction is quantified by comparison against a standard curve of sodium nitrate in the range 0 to 100µM.

3.4 *In vivo* Methods

3.4.1 Animal Husbandry

Animals were house in accordance with home office guidelines and procedures were performed under Project Licence (70/7049) and Personal License (76/26000). Throughout the care and experimental phases animals were kept in standard conditions with free access to food and water.

3.4.2 Transgenic models

3.4.2.1 Generation and Identification of DDAH2 knockout mice

Heterozygous DDAH2 genetic knockout mice (ddah2$^{+/-}$), were obtained from the Texas Institute for Genomic Medicine (http://www.tigm.org/). The genetic knockout of DDAH2 was generated in a high throughput gene-trapping strategy using retroviral vectors and insertion of multiple terminal repeat sequences in the DDAH2 gene[233]. Global Knockout mice were produced by breeding DDAH2 $^{+/-}$ and subsequent breeding of DDAH2$^{-/-}$ offspring to produce a breeding line of globally deficient in DDAH2 (Figure 8).

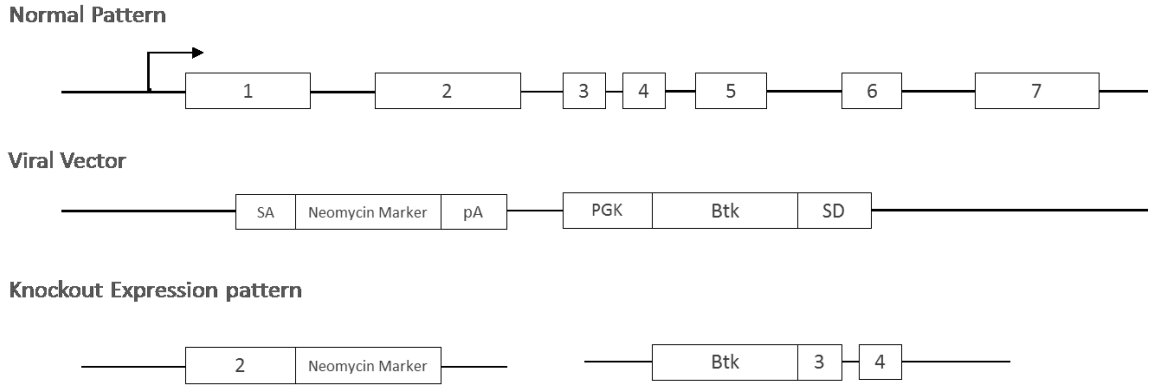

Figure 8: Schematic representation of the development of a global Ddah2 knockout mouse using high throughput gene trapping strategy.

Tandem PCR was used to identify the virally inserted long terminal repeat (LTR) or the wild-type allele (ddah2^{+}). This process used a forward primer common to both sequences and can be seen in Table 15.

Thermal cycling conditions were as follows:

95°C for 5 minutes

40 cycles of 95°C for 30 seconds

57°C for 40 seconds

72°C for 1 minute

72°C for 5 minutes

PCR products were analysed using standard agarose gel electrophoresis methods and visualized with ethidium bromide (Sigma-Aldrich, USA).

3.4.2.2 Generation of Macrophage specific (LysMCre) knockout mice

DDAH2$^{flox/flox}$LysMCre animals employ the LoxP Cre recombinase technique with tissue specificity delivered via Cre expression at the murine M lysozyme locus using a previously established method[234] (Figure 9). This results in 88-98% of deletion of ddah2 in mature macrophages and 100% in granulocytes. This specificity can be achieved in murine models because unlike in humans there are two lysozyme genes coding for myeloid cells (M) and Paneth Cells (P). The impact of this process is that DDAH2 knockout can be achieved in the two immune cell types described with only microglial cells (the only other cell type expressing the M lysozyme) also deficient in DDAH2 [235].

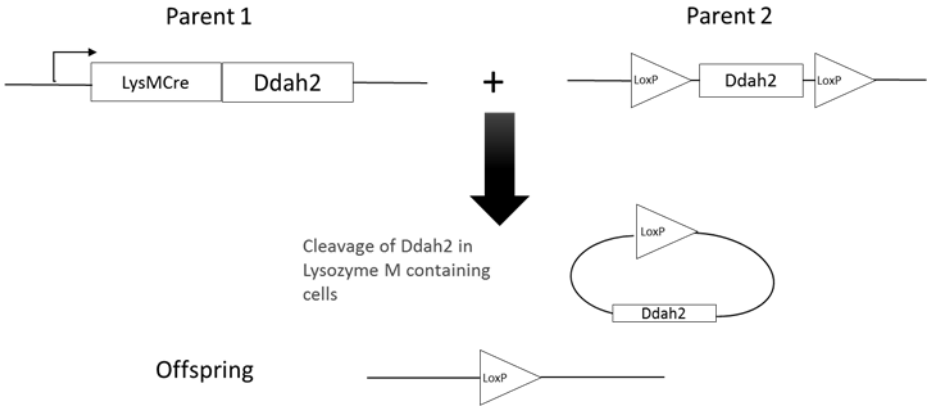

Figure 9: Schematic representation of the LoxP Cre recombinase model employed to delete Ddah2 from murine macrophages

Schematic representation of the LoxP Cre recombinase model employed to delete Ddah2 from Murine cells containing the M Lysozyme (Macrophages, Granulocytes and Glial cells). Mice Cre positive in the Lysozyme M locus were bred with LoxP positive mice at the Ddah2 gene. Resulting offspring had Ddah2 cleaved from the M Lysozyme resulting in tissue specific Ddah2 knockout.

Dual PCR was undertaken to demonstrate the presence of the Cre Recombinase and DDAH2 LoxP in knockout animals. PCR protocol and primer sequences can be found in Table 14 and Table 15.

Sequence detection protocol	
Cre Recombinase	LoxP
94°C for 2minutes	94°C for 2minutes
40cycles of 94°C for 20seconds	35 Cycles of 94°C for 30 seconds
60°C for 40seconds	65°C for 30seconds
72°C for 1minute	68°C for 1minute
72°C for 5minutes	68°C for 7minutes

Table 14:PCR protocol for the identification of Cre recombinase and LoxP sequences

Primer Name	Target	Sequence (5'-3')
F	Common forward primer	CACCCTTTCTGTTTCTTCTCT
Wt	reverse primer, Ddah2+ allele	AAATGGCGTTACTTAAGCTAGCTTGC
KO	reverse primer, Ddah2- allele	AGTACTCCATGCTCCCTTTGA
Cre	Forward Primer	GCCTGCATTACCGGTCGATGCA
Cre	Reverse Primer	GTGGCACATGGCGCGGAAC
ddah2 flox	Forward primer	GGGCAGGGCTATGGTGAAGG
ddah2 flox	Reverse Primer	ACCTCCTGGCTGTTGGGCAG

Table 15:Primer sequences for genotyping PCR, RT-PCR

3.4.3 *In vivo* radiotelemetry of blood pressure and activity

All studies were undertaken using animals aged between eight and ten weeks of age. Anaesthesia was induced in spontaneously breathing animals using isoflurane at a concentration of 2-5% in an induction chamber. When fully anaesthetised, animals were shaved and delivered subcutaneous analgesia with buprenorphine at 0.2mg/kg.

Animals were transferred onto a microsurgery operating table and anaesthesia maintained with 1-2% isoflurane. The left internal carotid artery was exposed and two ligatures loosely applied to the vessel. The proximal tie was tightened to obstruct blood flow and the vessel cannulated with the HD-X11 radiotelemetry probe (DSI ltd, St Paul, MN, USA) as per the manufacturer's instructions. Following probe insertion, the distal ligature was tied to obstruct flow and the proximal tie secured around the probe. The unit containing the battery and radiotelemetry transmitter were inserted subcutaneously on a left side of the abdominal wall.

Following surgery, animals were recovered in for at least one hour in a warming chamber and then once fully active returned to individual cages where they were housed for 14 days. Following recovery, telemetry recording was commenced. Data regarding heart rate, blood pressure and activity was continuously recorded of a 24 hour baseline data period. BP readings averaged every minute over the measurement period were used and downloaded to Excel (Microsoft, US) for analysis.

3.4.4 Intermittent radiotelemetry monitoring of temperature

Recording of subcutaneous using a radiotelemetry probe inserted into the subcutaneous tissue of the anterior abdominal wall temperature (Bio Medic Data Systems, Seaford, DE, USA) was used as an index of sepsis severity and objective experimental endpoint as previously demonstrated[236].

3.4.5 Determination of Aortic Vascular reactivity

Following schedule one termination, the thoracic cavity was opened, anterior and middle mediastinal structures removed and the aorta dissected. The isolated aorta was washed in warm PBS, slices were mounted on the myograph (Danish Myotechnology, DK) and bathed in physiological salt solution (PSS) at pH 7.4 containing the following solutes:

- NaCl 115mM
- KCl 4.7mM
- MgSO4 1.4mM
- NaHCO3 5mM
- K2HPO4 1.2mM
- Na2HPO4 1.1mM
- CaCl2 1.0mM
- HEPES 20mM
- Glucose 5mM

Functional integrity of the endothelium was demonstrated by the presence of relaxation induced by acetylcholine 10-6 mol/L during contraction obtained with phenylephrine 10^{-3}mmol/L. Concentration-response curves to phenylephrine(Sigma-Aldrich, USA) (10-5 to 10^{-1}mmol/L), acetylcholine(Sigma-Aldrich, USA) (10^{-6} to 10^{-3}mmol/L) and sodium nitroprusside (Sigma-Aldrich, USA) (10^{-8} to 10^{-3}mmol/L) were made for each aortic ring sampled.

Phenylephrine contraction was expressed as absolute tension in mNewtons (mN). Relaxation was expressed as a percentage of the phenylephrine-induced contraction. The concentrations of agonist producing half-maximum effect (EC_{50} values) was determined from the individual concentration-response curves by nonlinear regression analysis and expressed as moles/L. Two-way ANOVA was used for comparison of concentration dependent effects in knockout mice and their appropriate controls.

3.4.6 Invasive Cardiovascular Hemodynamic Measurements in anaesthetised animals

Mice were anaesthetised as described above, shaved and placed on a micro surgery table. The right common carotid artery was identified and a 1.4French gauge Millar MikroTip pressure catheter inserted and advanced distally until stable blood pressure traces were obtained. Following a fifteen minute period of haemodynamic stability, values were recorded using the PowerLab and Chart 5 software (ADInstruments Ltd, UK).

3.4.7 Echocardiography

Trans-thoracic echocardiography was performed under general anaesthesia using a Vivid 7 echocardiography machine (GE Healthcare, UK) and a 14MHz transducer in spontaneously breathing mice anesthetised with isoflurane. Pulsewave Doppler was used to measure aortic outflow tract velocity which results in the acquisition of time integral envelopes to give the velocity time integral (VTI). Following completion of the study, stroke volume index (SVi) was calculated as follows:

SVi = (VTI x 0.0143)/weight

Where VTI = Stroke distance, 0.0143 = standardised aortic diameter and weight = the animal body weight.

Cardiac output was calculated as the product of stroke volume and heart rate.

3.4.8 Isolation of primary macrophages

Following schedule one termination, the animal was positioned and anterior abdominal wall fur removed. The peritoneal cavity was exposed and immediately filled with 3mL cold PBS (Invitrogen, UK) and gently agitated for thirty seconds. The peritoneal washout was carefully collected by aspiration and spun for ten minutes at 1000 RPM, at 4ºC to sediment the cells. Cells were suspended in Dulbecco's modified Eagles medium (DMEM) cell culture media with L-glutamine (all Invitrogen, Paisley, UK), and then incubated for one hour at 37°C and 5% CO_2 to allow macrophages to adhere to the wells. Once the cells had adhered, media was removed and cells were gently washed with PBS to remove any non-adherent macrophages. Fresh media was then added. Total cell number was counted using a haemocytometer prior to experimental application (approximately $2x10^6$ cells viable were retrieved from each animal).

3.4.9 Collection of murine plasma

Plasma was obtained via transcutaneous cardiac puncture of anaesthetised mice. Following collection of blood, samples were placed in Lithium-heparin coated tubes (Sarstedt, GER) and centrifuged at 2000g for 5mins at 20°C. After collection, animals were culled using schedule one techniques. Plasma was separated from the samples and stored at -80°C prior to analysis.

3.4.10 Induction of sepsis in animals

The Caecal Ligation and Puncture model was used to induce sepsis in male mice from 8-10 weeks old. Following induction and maintenance of anaesthesia with isoflurane animals were weighed and a modified laporotomy performed utilising a lateral incision in the lower left quadrant of the abdominal wall. The large intestine in the mouse was exposed and a 50% portion of the caecum was ligated using 2/0 silk suture. The portion of caecum distal to the obstruction was surgically perforated in two places using a 21G needle. Before being returned to the peritoneal cavity, manual pressure was applied to extrude faeces and ensure patency of the iatrogenic perforation. The proportion of caecum ligated and gauge of puncture needle determine severity of this model[237]. The peritoneum and abdominal walls were closed with 5/0 and 4/0 ethilon sutures respectively. The operative steps are summarised in Figure 10. Analgesia with buprenorphine 0.2mg/kg was administered to all animals at induction of surgery and every 12 hours until termination. Fluid resuscitation with 30ml/kg 0.9% sodium chloride solution was administered via subcutaneous injection at completion of surgery and at each 24 hour time point until cessation of the experiment. In order to minimise animal suffering and to facilitate determination of differences in plasma NO production and ADMA level the end point used was independent blinded assessment of illness severity based on an established severity score by an experienced named animal care and welfare officer.

A sample size of 8 animals per group was chosen based on previous mortality model estimates of inter group difference, an alpha error of 5% and a beta error of 80%[238].

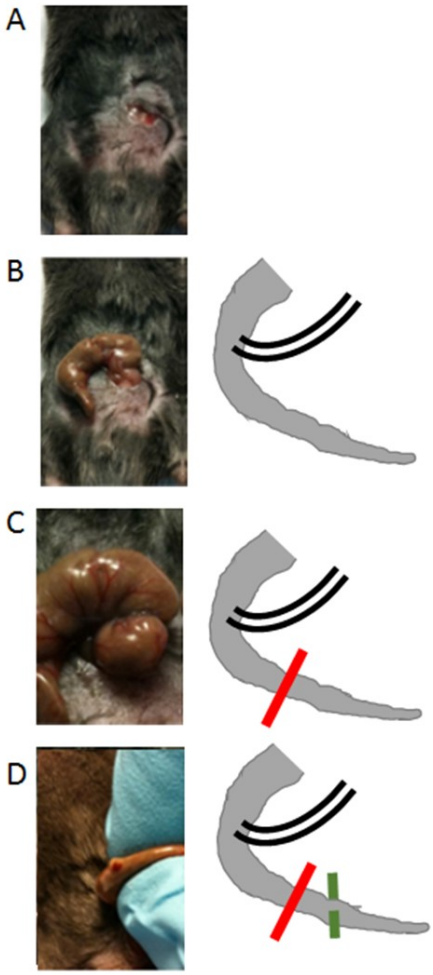

Figure 10: Schematic Representation and representative images of the conduct of caecal ligation and puncture (CLP) in a murine model of polymicrobial sepsis.

A: Following the induction of anaesthesia and administration of subcutaneous buprenorphine. The left lateral abdominal wall is shaved and prepared with topical antiseptic. Following draping, the skin and peritoneal connective tissue is incised using a lateral incision in the left lower quadrant of the abdomen. B: The terminal ileum and ileo-caecal junction is exposed and the blind ending portion of caecum identified. C: A variable portion of the terminal ileum (typically the distal third) is ligated using a 2/0 silk suture. D: Following ligation, a 21G hypodermic needle is used to puncture the ligated portion of bowel at two points. A small amount of faeces is extruded to ensure that the puncture sites are patent and the ileo-caecal region is returned to the peritoneal cavity which is closed with 5/0 silk, the skin is closed with 5/0 dissolvable ethilon

3.4.11 Estimation of whole blood and peritoneal bacterial load

Samples of whole blood and peritoneal washout fluid were collected as described above. Following serial dilutions, aliquots were plated onto freshly prepared 50mm tryptic soy agar plates without antibiotic and incubated overnight at 37°C, 21% O_2 and 5% CO_2. The following day the most appropriate dilution was identified and counted for Colony Forming Units (CFU). Correction was made for dilution and bacterial loads compared.

3.4.12 Polyinosinic polycytidylic acid stimulus

Polyinosinic polycytidylic acid (Poly I:C)(Sigma Aldrich) was used as a non-infective model of the early response to TLR3 mediated stimulus. Intraperitoneal injection was undertaken and observation over the experimental period was undertaken using established end points described above. Poly I:C was injected at 2mg/kg in all reported experiments based on a dose determined in previously published models[239].

3.5 Human studies

3.5.1 Human Hypoxia Study

Ethical Approval was received from the University College London Ethical review panel on 4th March 2014 ref: 2416.001. The title of the study was ' A prospective observational study into the effects of acute normobaric hypoxia on endogenous regulators of Nitric Oxide synthesis on healthy volunteers'.

3.5.1.1 The Hypoxic Chamber

The study was conducted in a normobaric hypoxic chamber which is a purpose built device supplied and installed by Hypoxico ltd (NY, USA) and installed at the University College London Institute for Sports and Exercise Health. The chamber generates a temperature, humidity controlled hypoxic environment with ambient fraction of inspired oxygen of 11-21%. The temperature was regulated at between 22°C and 24°C to optimise participant comfort and eliminate change in temperature as a source of variation throughout the experiment. CO_2 was removed using a purpose built carbon dioxide scrubber that limits the CO_2 level within the chamber to 0.2%. The chamber is $8m^2$ in size and made of transparent plastic to facilitate continual external safety assessment. Participants were encouraged to remain in the chamber throughout the 8 hour assessment period and a low nitrate lunch was provided for all volunteers as well as ad libitem access to water. If at any stage a participant requested extraction from the chamber this was done immediately.

3.5.1.2 Cardiovascular assessment

Cardiovascular assessment was undertaken using a variety of methods including traditional non-invasive techniques such as non-invasive blood pressure (Omron Ltd, NL) and digital pulse oximetry (Nonin Ltd, USA), which gives accurate values of both heart rate and peripheral arterial oxygen saturations.

In addition, cardiac output, stroke volume and systemic vascular resistance were assessed non-invasively using the Clearsight™ device (Edwards Life Sciences, USA) which utilises a modified Penaz technique and is now a well established and validated mode of continuous assessment of blood pressure[240]. In addition to measuring heart rate and blood pressure using this method, the Clearsight™ device was able to interrogate the morphology of the arterial pressure waveform to calculate stroke volume and systemic vascular resistance. The Clearsight device has been extensively against other methods of cardiac output assessment including oesophageal Doppler and transpulmonary thermodilution[241, 242].

3.5.1.3 Assessment of adverse events

The impacts of acute or subacute hypoxia may or may not be detected by an individual exposed to the hypoxic environment, and can, in a small proportion of people be serious. In order to ensure that adverse events were detected early and an optimal safety profile maintained, a modified Lake Louise Acute Mountain Sickness (AMS) assessment tool was developed. The Lake Louise Scoring system combines two domains, subjective and objective. The subjective component includes a series of questions regarding symptoms of acute mountain sickness whereas the objective, a series of assessments undertaken by a third party of potential altitude related neurological sequelae[243, 244]. This tool has been validated for the assessment of potential mountain sickness both at sea level in hypobaric chambers[244] and at the effective altitude generated by the hypoxic chamber in this study[245]. Based on these studies an incidence of one or more symptoms of AMS of around 30% would be expected. Due to the daytime only nature of the study, the objective measure of sleep quality which is included in the complete Lake Louise assessment was excluded. Each remaining domain was scored between 0 and 4 with a total score of 3 plus a headache being considered positive for AMS, an indication for immediate cessation of the study and removal of the volunteer from the chamber.

Domains assessed in the modified questionnaire are displayed in Table 16. Assessments were undertaken at twenty minutes after entry into the chamber and on an hourly basis throughout the study thereafter, unless the volunteer reported any positive symptoms in which case, the study supervisor conducted subjective and objective analyses every twenty minutes throughout the study.

Subjective assessment criteria -Symptom	Objective assessment criteria - Sign
Headache: No headache 0 Mild headache 1 Moderate headache 2 Severe, incapacitating 3	Change in mental status: No change 0 Lethargy/lassitude 1 Disoriented/confused 2 Stupor/semi consciousness 3
Gastrointestinal: No GI symptoms 0 Poor appetite or nausea 1 Moderate nausea or vomiting 2 Severe N&V, incapacitating 3	Ataxia(heel to toe walking): No ataxia 0 Manoeuvres to maintain balance 1 Steps off line 2 Falls down 3 Can't stand 4
Fatigue/Weakness (F/W) Not tired or weak 0 Mild fatigue/weakness 1 Moderate fatigue/weakness 2 Severe F/W, incapacitating 3	Peripheral Oedema: No oedema 0 One location 1 Two or more locations 2
Dizziness: Not dizzy 0 Mild dizziness 1 Moderate dizziness 2 Severe, incapacitating 3	

Table 16: Modified Lake Louise acute mountain sickness questionnaire.

The Lake Louise questionnaire was utilised to determine the presence and severity of features of acute mountain sickness and has been widely validated[245]. The sleep quality index was removed due to the study duration.

3.5.1.4 Isolation of Peripheral blood mononuclear cells

Blood collected from the patient was diluted with twice the volume of balanced salt solution and layered carefully over an equal volume of Ficoll-Paque Premium (GE Life Sciences, UK) separation medium to avoid mixing of the two liquids.

The sample was centrifuged at 400g at 18-20°C for 40mins in a bucket centrifuge without break to facilitate separation of the sample into plasma/platelets, monocyte and erythrocyte/granulocyte layers. Following separation, the plasma portion of the separated blood is removed using manual pipetting and stored for later analysis. The mononuclear cell layer is removed without disruption of the Ficoll Medium and resuspended in RLT buffer for subsequent mRNA analysis or PBS with protease inhibitor for protein determination and Western blotting. The separation process is summarised in Figure 11.

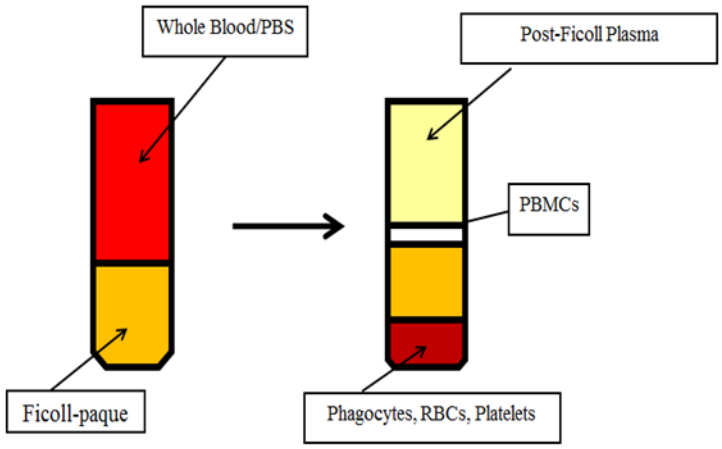

Figure 11: Isolation of peripheral blood mononuclear cells (PBMCs) using Ficoll separation

Schematic representation of the isolation of human Peripheral Blood Mononuclear Cells (PBMCs). Fresh whole blood anticoagulated with EDTA is diluted with 2x the volume of a balanced salt solution and carefully layered upon a separation medium (Ficoll-Paque). Samples are then centrifuged at 400g for 40minutes at 400g without break at termination. Post separation plasma is collected for experiment and the remainder carefully removed from the PBMC layer. The PBMCs are collected, washed twice with PBS and stored at -80°C.

3.5.1.5 Plasma sample preparation for analysis

Whole blood is collected in EDTA at 1.5mg/ml and stored on ice for subsequent preparation. Within 60mins of collection, the Cells are removed from plasma by centrifugation for 15 minutes at 1,000-2,000g at 4°C which removes platelets from the plasma sample. The separated plasma was stored separately at -80 °C pending subsequent analysis.

3.5.2 Genome wide association study

Genome wide association studies (GWAS) have become an important form of translational study in a range of disease areas. By conducting widespread screens of SNPs in human samples taken from patients with a pre-defined illness, it is possible to identify genes which are associated with that disease state. This can offer diagnostic and risk stratification in the clinic but it can also offer the opportunity for 'back-translation' where a finding in a GWAS can drive mechanistic investigation in the laboratory. There are some challenges associated with GWAS however, not least is the observation that due to the extensive correction that must be undertaken for multiple comparisons, common SNPs are more likely to reach the level of significance typically required in this kind of work[246, 247]. This exposes the risk that important regulators of response and outcome could be missed for this reason.

An alternative approach is the hypothesis based interrogation of these data sets once collected. In the presence of a mechanistic finding and a valid hypothesis, specific SNPs or genes within a GWAS data set may be interrogated for insights into outcome that are significant on this level but do not reach the significance level typically required (usually set at a p value of 10^{-8}).when more than 1million polymorphisms are being examined across the whole genome

In the field of Nitric Oxide regulation, this method has been successfully employed to explore the relationship between MA regulating genes and outcome in chronic kidney disease. In 2012, Caplin et al [21], demonstrated that based on a hypothesis driven approach, it was possible to confirm an observation made in animal models that SNPs of the AGXT2 gene are associated with systolic and diastolic blood pressure in a large healthy volunteer cohort.

3.5.2.1 The Genetics Of sepsis and Septic shock in Europe (GenOSept) and Genome wide Association in Sepsis (GAinS) Studies

The GenOSept and GAinS studies were conducted in seventeen countries across Europe between 2005 and 2011. The GenOSept study recruited 1525 patients with severe sepsis and septic shock in 143 hospitals in sixteen countries. Patients included in this study were suffering from sepsis as a consequence of either community acquired pneumonia (CAP) (n=794) or faecal peritonitis (FP) (n=731). This study was completed in 2009 at which time the GAinS study started to recruit patients with CAP (n=241) in the UK. In the original study[248], two additional data sets were interrogated that had been collected from the Vasopressin in Septic Shock Trial (VASST)[76] and the Human Activated Protein C Worldwide Evaluation in Severe Sepsis (PROWESS)[249] trials. The study found that in patients with CAP only, a single SNP of the *FER* gene (rs4957796) was associated with survival at the genome wide level.

In our study, we drew on our previous work showing that in animal models, knockout of DDAH1 and DDAH2 both have significant – and in fact opposite – impacts on outcome in septic shock[30, 213]. We interrogated the GAinS and GenOSept cohorts with the specific hypothesis that SNPs of DDAH1 and DDAH2 are associated with outcome in human sepsis.

Our hypothesis based testing was conducted on both the directly measured SNPs within the territory of our two genes of interest and also on indirectly measured genes, using imputation to identify SNPs in linkage disequilibrium with those that are directly measured.

This combination of direct and indirect measures is a well established approach and resulted in the analysis of 601 SNPs of the DDAH1 gene and 36 for DDAH2. Explored SNPs are published in Appendix 1.

3.5.3 VAsopressin versus Noradrenaline as Initial therapy in Septic sHock (VANISH) study

The VANISH study was undertaken between 2013 and 2015 and was a randomised controlled trial in a 2x2 format of vasopressin vs. noradrenaline with or without the addition of exogenous corticosteroids in patients with septic shock. The VASST study[76] had suggested that vasopressin might offer a favourable profile over conventional catecholamines in patients with septic shock and that this benefit might particularly prominent in patients who also received steroids as an adjunct to their management of sepsis. This study recruited 412 participants with vasopressor dependent septic shock from eighteen intensive care units in the UK. The full protocol for this study can has been published[250].

The primary endpoint of the study was the number of renal failure free days, with secondary end points including 28 day mortality and length of hospital and ICU stay. The study included the collection of an extensive amount of data including routinely collected clinical data and detailed information regarding illness severity (SOFA score[251]), degree of shock and level of organ support required during the ICU stay. In a subpopulation of patients recruited to three of the study centres, regular blood sampling was undertaken during the first seven days of admission to the critical care unit.

Score	1	2	3	4
PaO2/FiO2 ratio (mmHg)	<400	<300	<200 and mechanically ventilated	<100 and mechanically ventilated
Glasgow Coma Scale	13-14	10-12	6-9	<6
Mean Arterial Pressure or Vasopressor use (mcg/kg/min)	<70mmHg	Dopamine <5 or Dobutamine any dose	Dopamine >5 or epinephrine <0.1 or norephinephrine <0.1	Dopamine >15 or epinephrine >0.1 or norephinephrine >0.1
Liver (µmol/L)	20-32	33-101	102-204	>204
Coagulation (platelet count x1000/µL)	<150	<100	<50	<20
Renal Creatinine (µmol/L) or urine output (mL/day)	110-170	171-299	300-440 or <500mls/day	>440 or <200mls/day

Table 17: The table summarises the Sequential Organ Failure Assessment (SOFA) score criteria.

The maximum score is 24 and both admission and peak SOFA score are predictors of outcome in critical illness[252].

Samples were collected at admission to the ICU prior to the commencement of the intervention and on study day one (24-36 hours), two (48-72 hours) and four (96-120 hours) after enrolment. In 215 patients, plasma and buffy coat samples were collected by centrifugation of whole blood at the collection centre immediately following collection. In a further 75 patients, whole blood samples were collected in EDTA tubes and prepared as described in below. All samples were marked with appropriate anonymised study ID and reference and frozen at -80°C for storage. Figure 12 summarises with samples collected and their analysis.

- Collection of plasma and buffy coat samples
- The EDTA bottle was placed in a centrifuge and spun for ten minutes at 1,000 RCF.
- Following spin, the plasma was immediately transferred into cryo-tubes in 1mls aliquots.
- The buffy coat layer was transferred into one cryo-tube.

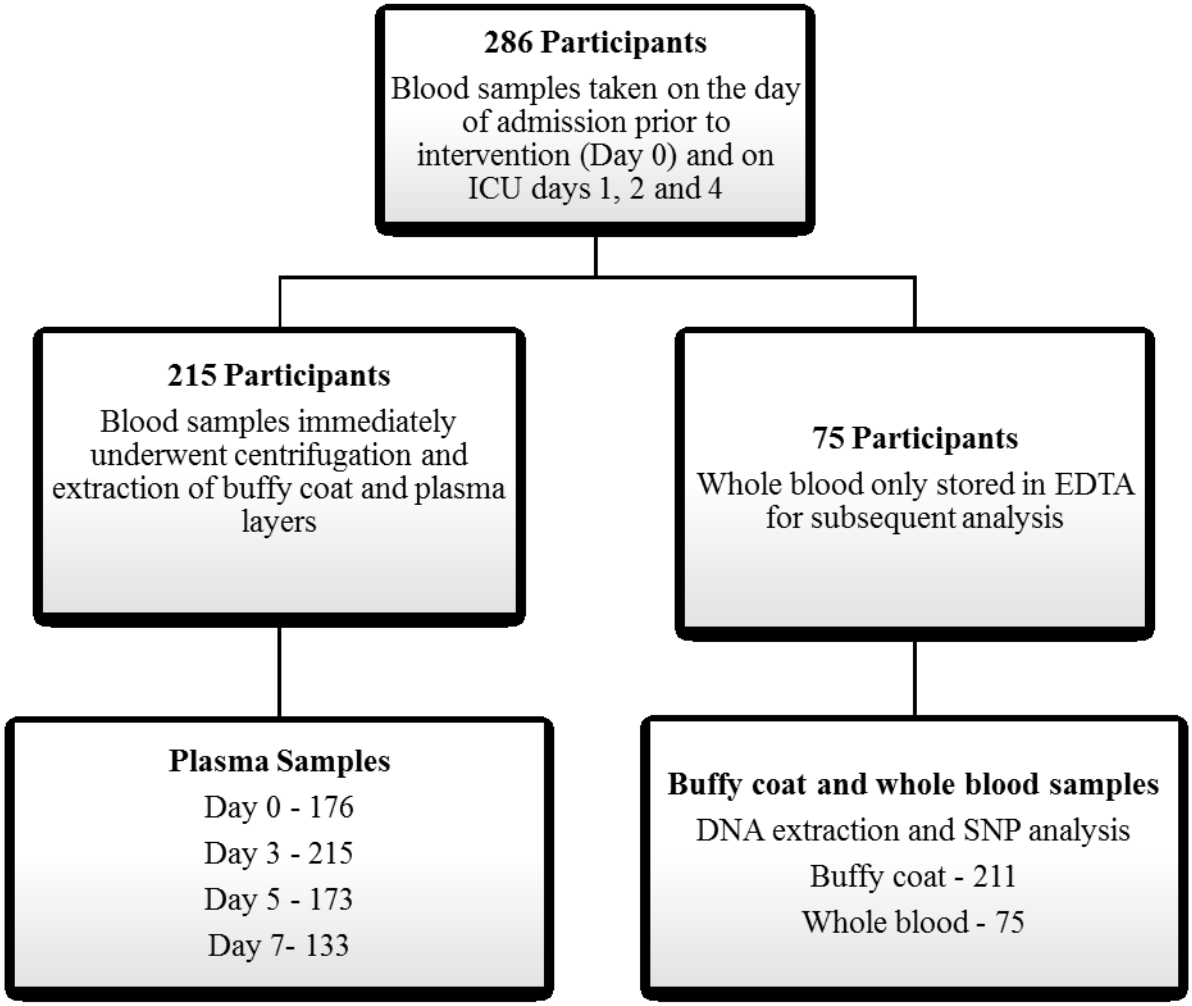

Figure 12: Schematic representation of sample handling of blood and plasma collected from patients in the VANISH trial

Access to these samples for analysis of methylarginines and hypothesis based SNP analysis was secured. Buffy coat samples and whole blood were sent for analysis of a series of SNPs based on the results of other human studies in this project. Methylarginines, Arginine and plasma NOx were analysed as described above. In order to ensure result consistency across a large number of mass spectrometry analysis and account for potential drift of the results over time, on each plate a standard curve using the same set methylarginine standards was prepared and run. An example of the standard curves for ADMA seen in each of the study plates can be seen in

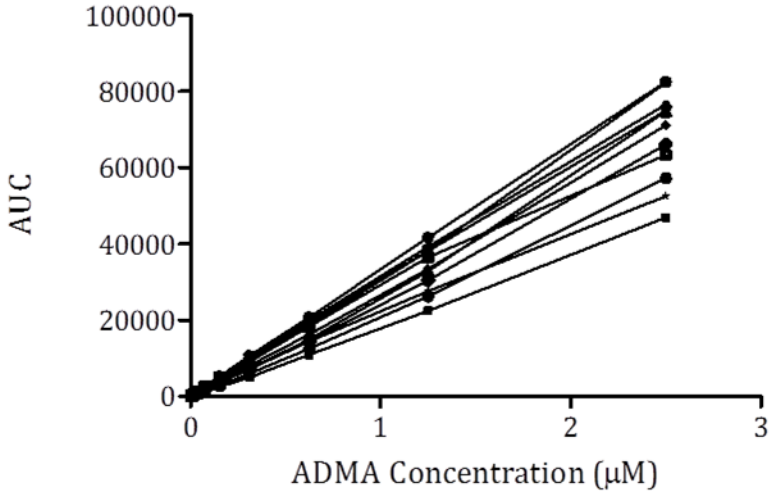

Figure 13 below. Between each set of patient samples, a blank sample of mobile phase was run to ensure that there was no run over between samples. All biochemical analysis was undertaken in a blinded fashion and only once complete were the outcomes and treatment groups made available for analysis.

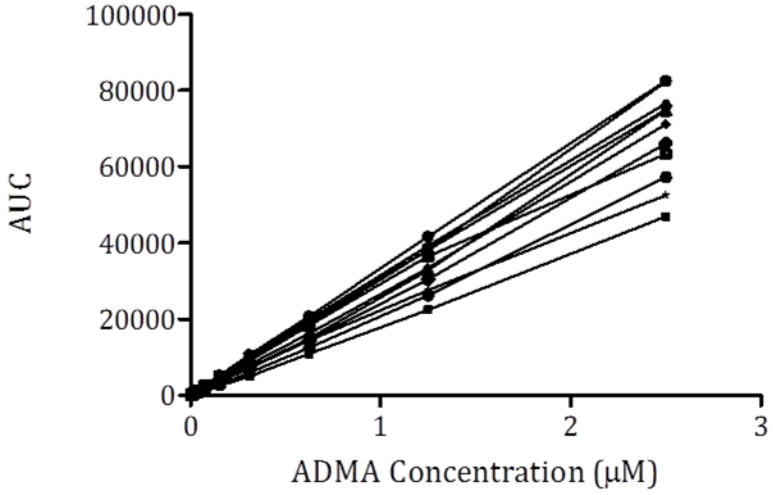

Figure 13: Relationship between area under the curve (AUC) of the chromatogram for ADMA specific fragments against the concentration of known standard concentrations of ADMA.

r^2 for all curves > 0.995.

The following analyses were undertaken of the association between the following biochemical and clinical indices and the SNPs that were identified:

Clinical Outcome	Biochemical measures
shock duration	Plasma Nitrate + Nitrite
Sequential organ failure assessment (SOFA) score	Plasma ADMA
Incidence and duration of renal failure	Plasma SDMA
28 day mortality	Plasma L-Arginine

Table 18: Clinical outcomes and biochemical indices measured in the patients recruited into the VANISH study and for whom plasma was available.

3.6 Statistics

Statistical analysis was performed using the Prism software package (GraphPad Inc, CA, USA). Normally distributed data was analysed using a t test or Analysis of Variance (ANOVA) with Bonferroni post-test comparison of groups as appropriate. In cases where samples were taken before and after intervention from a single participant, paired analyses were used. Non parametric data was analysed using a Mann Whitney U test. Correlations were analysed with Spearman's and Pearson's coefficients, Kaplan Meier analyses using the Log Rank test. Values are expressed as either mean +/- standard deviation or Median +/- interquartile range.

4 The regulation of monocyte DDAH2 by hypoxia

4.1 Introduction

4.1.1 Hypoxia and the innate immune response

Hypoxia is a common feature of critical illness and may arise as a consequence of a range of mechanisms. Failure to adequately oxygenate the blood as it traverses the lungs, impaired delivery due to vascular obstruction and the cell's inability to utilise it effectively are all ways in which cells may be exposed to a hypoxic environment. In addition to this, in inflamed or infected tissue, hypoxia may be severe and arise as a result of reduced perfusion, microvascular injury and increased interstitial pressure all of which may be coupled with increased oxygen utilisation by immune cells[253-256].

Under normal conditions the oxygen tension to which cells are exposed lies in the range of 2-9kPa. This equates to around 2.5-9% oxygen. However, in the context of infection, markedly lower levels of oxygen may be available with nadir values of less than 1% reported[253]. There is burgeoning evidence to suggest that hypoxia is not simply an epiphenomenon associated with infection, but that it does in fact regulate a range of immune processes and contributes towards the activation of the innate response.

These studies explore the hypothesis that as a regulator of the immune response to inflammation, DDAH2 may itself play an important role in modulating NO production in hypoxia.

4.1.1.1 Hypoxia inducible factor regulates the hypoxic response

Hypoxia inducible factors (HIF) were originally discovered in the early 1990s as one of the mechanisms by which erythropoietin was synthesised in hypoxic conditions[257, 258]. Regulated by both oxygen and iron levels, HIF is found in all mammalian cells and has been shown to regulate more than 100 genes in response to hypoxic stress. HIF regulated genes modulate metabolism, vascular tone, new vessel development and apoptosis, with implications in both healthy and disease states[259-262].

The HIF complex is comprised of the constitutive HIF1β which binds to one of two inducible components, HIF1α and HIF 2α. Under normal conditions, the inducible subunits are unstable and as a consequence are readily turned over via the ubiquitin-proteasome pathway[263] and by asparaginyl hydroxylase[264]. In hypoxia, these hydroxylase pathways are inhibited and the HIF proteins are stabilised. As a consequence, HIF1α and HIF 2α accumulate, translocate to the cell nucleus and form a heterodimer with HIF1β. This heterodimer then binds directly to regions of the promoter sequence of its target genes (Hypoxia response elements, HREs) to initiate transcription.

4.1.1.2 Hypoxia inducible factor and innate immune cells

Global knockout of HIF 1α is not compatible with life in murine models, however using a similar technique to that employed in this study, a mouse has been developed that is HIF1α-deficient only in macrophages, granulocytes and microglial cells. Whilst this mouse is phenotypically normal under control conditions, when exposed to an inflammatory stress, it displays significantly impaired macrophage activation and induction of the local inflammatory response[265].

The impact of the reduced macrophage function observed in the HIF1α knockout mouse is an impaired capacity to kill both Gram-positive and Gram-negative bacteria[265, 266]. By contrast, a hypoxic environment appears to improve bactericidal activity of normal macrophages and neutrophils[266, 267]. This process may be mediated by a number of mechanisms including, in part, by the HIF1α-induced upregulation of iNOS [266] and increased cytokine production[267]. It is interesting to note that in contrast to these hypoxia-mediated processes, HIF does not appear to modulate reactive oxygen species (ROS) synthesis by macrophages which appears to be independent of the presence of HIF1α[268]

This hypoxia-mediated augmentation of the innate response appears to be synergistically regulated by nuclear factor κB (NF-κB)[269] whereby hypoxia stimulates the activation of NF-κB by inhibiting metabolising hydroxylases. NF-κB can in turn provoke the upregulation of HIF1α, thus HIF synthesis is a major regulator of innate immune response[270].

In animal models of sepsis, HIF1α deletion in macrophages and granulocytes is protective against a normally fatal dose of LPS and significantly reduces the systemic inflammatory state [268].

4.1.1.3 The impact of hypoxia on the inflammatory response

Hypoxia has been shown to induce the synthesis of a number of pro and anti-inflammatory mediators of inflammation by innate immune cells. The list is extensive and includes IL-1, TNF-α, PGE2, IFN-γ and IL-10. This has been demonstrated in both human and murine macrophages with a significant number shown to be HIF-mediated[271, 272].

Studies also report a number of mechanisms by which hypoxia can regulate NO production by immune cells. It is well established that oxygen is essential for the oxidation of NADPH by NOS in the synthesis of NO. Two moles of oxygen are required for the production of 1 mole of NO[273]. For this reason, it is well established that in low oxygen conditions, isolated macrophages, particularly in murine cell lines and primary culture, produce only minimal NO when exposed to a pro-inflammatory stimulus in a hypoxic environment[274].

However, in murine and human cells it has been demonstrated that hypoxia, via the HIF1α-mediated stimulation of iNOS HRE elements, is able to upregulate iNOS synthesis and thus protein expression[272, 275]. As a consequence, murine cells display increased iNOS expression, but no apparent elevation of NO synthesis when cultured in hypoxic conditions. If however, they are subsequently returned to a normoxic environment, this upregulation of iNOS rapidly leads to the increased synthesis of NO[276]. This pattern is less apparent in human cells which produce less NO in response to pro-inflammatory stress and therefore are not as oxygen-dependent as murine macrophages.

4.1.2 Hypoxia studies in humans and animals

The growing interest in the hypoxia-mediated response has led to the development of a number of techniques designed to further examine the impact of hypoxia on biological systems. They can be divided into those which involve the culture of primary cells or immortalised cell lines in a hypoxic environment (*ex vivo* studies), the exposure of whole animals to hypoxic conditions whilst in a controlled environment (*in vivo* animal studies) and studies in humans, which can be divided into normobaric and hypobaric hypoxia trials.

4.1.2.1 *Ex vivo* studies of hypoxia

Tools for exploring the role of hypoxia in tissue culture can be categorised into two groups. The first, the hypoxic chambers, are generally smaller devices that rely on sealing the tissue culture plate or plates within an airtight container before delivering a known concentration of oxygen. Typically, this is achieved using nitrogen/oxygen mix cylinders to generate anoxia/hypoxia within the container. This method is straightforward, but is limited by the ability to adjust and regulate the environment, particularly the ambient CO_2 and humidity. The alternative and gold standard approach for studies in this area is a modified glove box. Nitrogen and CO_2 are delivered by regulators at concentrations that can be set and continuously measured electronically. The result is that a titratable oxygen concentration of between 1 and 100% can be achieved. Other advantages of systems such as this include the capacity to regulate humidity, adjust the environment during a tissue culture experiment and also the availability of an air lock system, meaning that equipment and cells can be introduced to the chamber without disrupting the conditions within. The size of the chamber and glove box also means that it is possible to collect and, in some cases, analyse samples without exposing them to atmospheric conditions. For this reason, the hypoxic glove box was used in all cell culture studies of murine cells reported in this study.

4.1.2.2 *In vivo* animal models of hypoxia

It is also possible to expose whole animals to hypoxic conditions using modified hypoxic chambers. These may take the form of modified individual cages or larger chambers into which the animal is placed. Some chambers may permit normal atmospheric pressure (normobaric), low pressure (hypobaric) or high pressure (hyperbaric) environments; this facilitates the study of both hypoxia and also altitude (or diving) as pathological stressors. No studies including whole animal models of hypoxia are reported here.

4.1.2.3 Human hypoxia studies

Human studies of hypoxia are a well recognised way to explore the impact of low oxygen tensions on a range of pathophysiological responses and have been considered to be a model of critical illness worthy of considerable investigation[277, 278]. Hypoxia is also an established training tool for endurance athletes in whom chronic hypoxic exposure leads to increased erythropoietin synthesis, haemoglobin concentrations and therefore tissue oxygen delivery during sport[279]. Broadly, human studies exploring hypoxia are divided into two groups, normobaric and hypobaric hypoxia. Each group is associated with different advantages and compromises.

It has long been recognised that altitude exposure results in a series of adaptations leading to improved exercise tolerance over time and that some individuals or ethnic groups are better adapted to tolerate such exposures. The discovery that changes in atmospheric pressure at altitude reduce available oxygen (although not the actual percentage) and that this provokes a range of physiological adaptations is now well established. Hypobaric hypoxia has been shown to affect a range of systems including coagulation, cardiovascular function and metabolism[280-282]. The advantages of hypobaric hypoxia studies include the ready availability of volunteers, the ability to titrate the severity of the hypoxic exposure based on height climbed and the fact that studies can be undertaken with clinically relevant durations of up to several weeks.

The limitations associated with this technique relate to the nature of the hypoxic exposure and environmental conditions. At altitude, the fraction of inspired oxygen remains at 21% (as it is at sea level), however, due to the reduction in atmospheric pressure, the available number of oxygen molecules is reduced leading to a relative hypoxic exposure. This differs from the mechanisms discussed previously that are responsible for hypoxia in clinical populations. Furthermore, at altitude there are significant changes in the environment that make this technique less representative of clinical exposure. These include barometric pressure, temperature and dietary variation as well as increased ultraviolet light exposure. The impact of these differences has been debated and results from studies undertaken in these environments must therefore be interpreted with these confounders in mind[283]. Of note is that it is also possible to conduct hypobaric hypoxia studies at sea level using chambers out of which a portion of the gas is pumped in order to simulate the lower barometric pressure seen at altitude.

The alternative strategy for modelling hypoxia in humans is to deliver hypoxic gas mixtures to healthy volunteers at sea level. Normobaric hypoxia may be delivered using a facemask or alternatively using larger chambers in which the environment is regulated. It is both feasible and practical to deliver hypoxic mixtures by facemask, however the tolerability of this approach and the duration of therapy are limited. Also, because the peak inspiratory flow rate typically exceeds the rate of gas flow that can be delivered by a cylinder, even one with a dual stage pressure reducing demand valve, the actual percentage of inspired oxygen cannot be defined exactly. Indirect measures such as arterial oxygen concentrations must therefore be used which may not reflect subtle changes in hypoxic exposure.

The second approach, and the one used in the studies reported here, is the hypoxic chamber. These systems include a sealed container of variable size into which a controlled hypoxic mixture is pumped and set at a known inspired percentage or target altitude. Within the chamber, humidity and temperature can be readily controlled and CO_2 is removed through the use of an extraction system that also records the concentrations in the atmosphere. This system confers the advantages that it is a safe, easily monitored and readily reversible environment. It allows continual observation without the requirement for the supervisor to be exposed to hypoxia, it is titratable and exposes the volunteer to none of the other environmental variation seen at altitude. The main limitation is time, as spending long periods of time in the chamber can prove claustrophobic and uncomfortable. As a result, the duration of studies is typically limited to hours rather than days of continuous exposure. Nonetheless, this mode has been well validated for use in studies of the pathophysiology of hypoxia[284-290].

4.1.3 Hypoxia and the endogenous regulation of nitric oxide synthesis

Whilst it has been well established that hypoxia has a direct effect on NOS expression and NO synthesis in both humans and animals [291, 292], relatively little work exists that explores the relationship between MAs, DDAH and NO synthesis in hypoxia. These limited studies do however pose interesting questions regarding the regulation of NO synthesis by DDAH in hypoxic conditions and its relevance to disease.

4.1.3.1 Methylarginines in hypoxia

There is some evidence from association studies to suggest that ADMA is elevated in disease states in which hypoxia is a feature such as chronic obstructive pulmonary disease[293] and asthma[294]. Little is known about the regulation of MA levels in the context of hypoxia alone, however some evidence is emerging regarding the mechanistic role that they play in regulating the hypoxic response.

One study of human pulmonary endothelial and smooth muscle cells in culture showed that the administration of exogenous ADMA stabilised HIF1α, activated STAT3 and resulted in a phenotype consistent with *in vitro* models of pulmonary vascular dysfunction[295]. In this study, ADMA also appeared to act synergistically with hypoxia to regulate cytokine synthesis by these cells. In healthy human volunteers, a study exploring the relationship between MAs and normobaric hypoxia suggested that an acute increase in ADMA was associated with increased pulmonary artery pressure. However, they also observed that a fall in ADMA made participants more likely to experience symptoms of altitude sickness[296]. The size of this study makes the interpretation of this data challenging since only modest correlations were observed and the change in ADMA was small.

Animal studies in yaks have shown that ADMA levels are reduced in animals that have adapted to living at high altitude and that their cardiac and pulmonary pressures are normalised[297]. However, one study compared male cows at 760m altitude to male yaks at 3000m. Interpretation of these results is therefore challenging. In mice, increased ADMA was found to be a feature of a three-week whole animal hypoxic exposure. This study also observed that this may in part be mediated by an increase in protein arginine methyltransferase 2(PRMT2) in alveolar type II cells[297].

4.1.3.2 Dimethylarginine Dimethylaminohydrolase in hypoxia

A number of studies have looked at the expression and activity of DDAH in hypoxia models at sea level and have primarily explored the mechanisms of hypoxia-induced pulmonary hypertension. In 2003, by utilising hypobaric hypoxia in a pig model of lung development and pulmonary hypertension, Arrigoni et al. showed that the development of pulmonary hypertension was associated with significant reductions in DDAH2 expression and overall DDAH activity[298]. Following 10% oxygen exposure for one week, a rat model demonstrated reduced DDAH1 expression and activity leading to an increase in ADMA concentrations [299]. Following these experiments, a second rat model of hypoxia showed reduced expression of both DDAH1 and DDAH2 which mediated the development of pulmonary hypertension. This study also showed that the mechanism by which DDAH1 was regulated in response to hypoxia was via increased microRNA-21[25].

The yak study described above also proposed increased DDAH2 expression and activity as a potential mechanism for the observed reduction in ADMA, although the same previously mentioned experimental caveats still apply [297].

Taken together these experiments have shown that over the course of chronic exposure to low oxygen, reduced DDAH expression within the pulmonary vasculature mediates increased ADMA concentrations, reduced NO production and provokes pulmonary hypertension. These models reflect the impact of medium to long term hypoxia on the development of pulmonary hypertension. However, to date, no studies have explored the acute modulation of DDAH expression by hypoxia, what happens in innate immune cells or the impact that any changes may have on the innate immune response.

4.2 Study design

The goal of the studies presented here was to explore, for the first time, the impact of normobaric hypoxia on the endogenous inhibitors of NO synthesis and their immune cell regulatory enzyme, DDAH2. These studies were undertaken in primary cell culture models and findings were validated in a human study.

4.2.1 Murine macrophage studies

These studies utilise a glove box hypoxic chamber to explore the regulation and functional role of DDAH2 in immune cells exposed to hypoxia. In the first series of studies, using primary peritoneal macrophages extracted from wild type mice, the regulation of DDAH2 expression, ADMA level and NO synthesis is explored following exposure to 3% oxygen.

In the subsequent experiments, the relationship between DDAH2 and NO synthesis is explored using primary peritoneal macrophages from macrophage specific DDAH2 knockout mice and their floxed littermate controls.

4.2.2 Human normobaric hypoxia studies

Building upon the *ex vivo* animal studies described above, a human observational healthy volunteer study is presented in which 12 male participants were exposed to a systemic hypoxic insult with an inspired oxygen fraction of 12% (equivalent to around 4500m in altitude) at normal atmospheric pressure. Peripheral blood mononuclear cells were isolated before and after an eight-hour exposure and DDAH2 expression, ADMA concentration and cellular NO synthesis was determined.

4.2.2.1 Power calculation

The study was powered to detect a 20% drop in plasma ADMA concentration associated with an eight-hour hypoxic exposure. Sample size was based on a power of 90%, an alpha error of 0.05 and a standard deviation of plasma ADMA concentration of 0.1μM. This gave an estimated sample size of 11. 13 participants were therefore recruited following a two person pilot study to ensure adequate sample collection.

4.3 Results

4.3.1 Murine macrophages and hypoxia

4.3.1.1 The impact of hypoxia on NO synthesis and its inhibitors

The synthesis of nitric oxide by isolated wild type primary murine monocytes exposed to hypoxic and normoxic conditions was determined using the chemiluminescent technique as described in Chapter 2. Cells were isolated from twelve mice, counted and allocated to either hypoxic exposure at 3% oxygen (with 5% CO_2, 37°C and 40% humidity) or 21% oxygen, but otherwise identical conditions. After 12 hours exposure, culture medium was changed and both sets of cells were returned to normal incubation conditions. Medium samples were collected at baseline, seven and 24 hours. Whilst control cells displayed no significant difference in NOx concentrations over the course of 24 hours, hypoxia treated cells displayed a significant induction of NOx synthesis after 7 and 24 hours of reoxygenation (mean(SD), 6.3(0.78)μM at 7 hours and 13.7(3.1)μM at 24 hours ($p<0.01$ by two-way ANOVA)) (Figure 14).

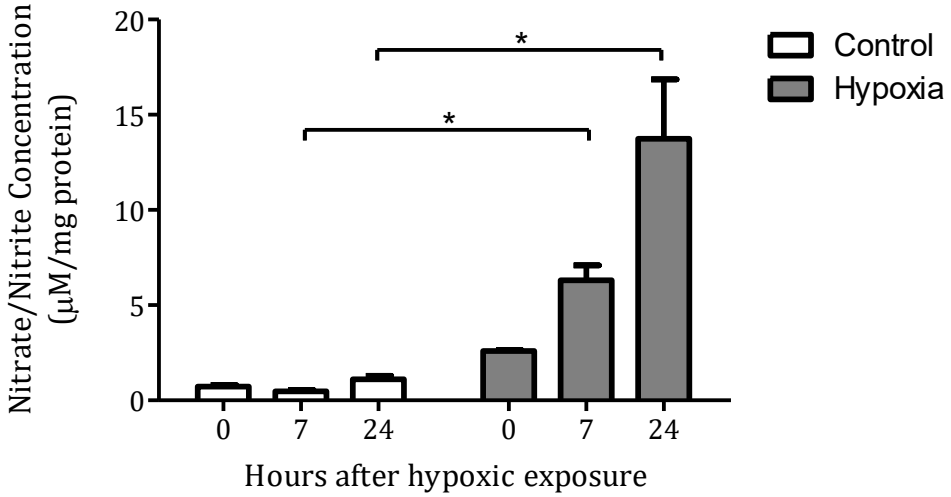

Figure 14: The impact of hypoxia on nitric oxide synthesis in medium taken from primary peritoneal murine macrophages.

Serial measurements of the accumulation of Nitrate/Nitrite in culture medium during reoxygenation after 12 hours hypoxic exposure or control incubation. Nitrate/Nitrite concentrations were corrected for cell lysate protein concentration at the time of experimental cessation due to differential rates of cell death in the hypoxia and control groups. n=6 per group, *= p<0.01 over control cells at the same time point.

At 24 hours after the reoxygenation phase, in addition to medium collection, cell lysate was taken, protein concentration was determined and samples were analysed for levels of NOx. When corrected for protein concentration, lysate NOx was 13.21(2.4)μM/mg protein in hypoxia treated cells and 8.0(1.7)μM/mg protein in control macrophages (p=0.04) (Figure 15).

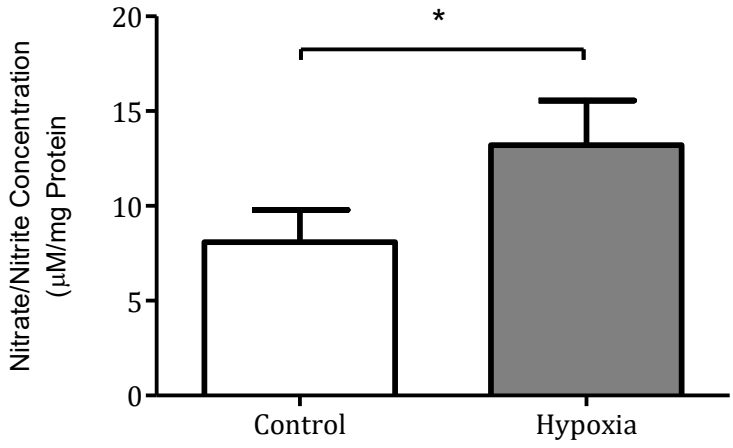

Figure 15: The impact of hypoxia on nitric oxide synthesis in cell lysate of primary peritoneal murine macrophages.

Nitrate/Nitrite concentrations were measured using a chemiluminescent technique and corrected for cell lysate protein concentration at the time of experimental cessation. n=6 per group, *p=0.038 over control cells at the same time point.

The induction of iNOS was also evaluated in cell lysate mRNA using quantitative PCR. iNOS displayed a 6- fold increase following hypoxic exposure and reoxygenation compared to control cells exposed to normal culture conditions (p=0.01)(Figure 16).

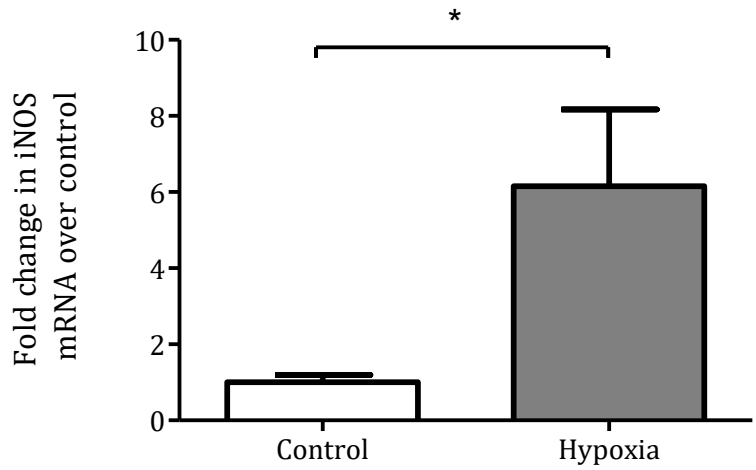

Figure 16: Cell lysate analysis of iNOS mRNA in cells exposed to hypoxia compared to controls.

qPCR measurement of inducible Nitric Oxide Synthase mRNA expression in cell lysate from resident peritoneal macrophages following culture under normal and hypoxic conditions (n=6 per group, * p=0.01).

Cell lysate L-arginine concentrations were similar in both cell types, 53.9(10.2)µM/mg protein in controls vs. 50.29(2.5)µM/mg protein (p=0.60) (Figure 17). In contrast, ADMA concentration, when corrected for cell lysate protein was reduced in hypoxia-exposed cells (0.24(0.03)µM/mg protein) compared to 0.32(0.04)µM/mg protein in control cells (p=0.02) (Figure 18). L-NMMA was unchanged across the two groups (0.78(0.013)µM/mg protein and 0.77(0.01)µM/mg protein, p=0.74) (Figure 19). SDMA could not be measured for technical reasons.

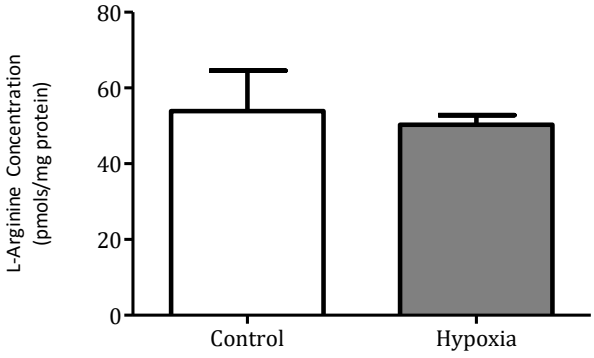

Figure 17: L-arginine concentrations in control and hypoxia treated primary murine macrophages.

Cell lysate L-arginine was measured in control and hypoxia treated murine macrophages following correction for cell lysate protein concentration (n=6, p=0.60).

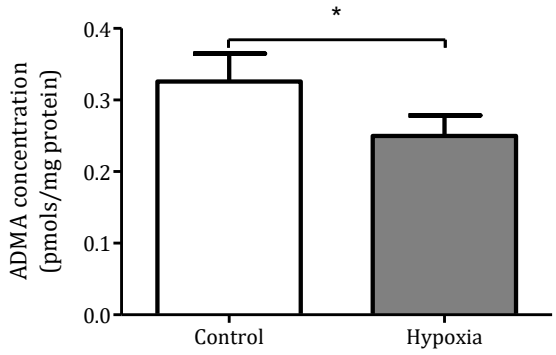

Figure 18: ADMA concentrations in control and hypoxia treated primary murine macrophages.

Cell lysate ADMA was measured in control and hypoxia treated murine macrophages following correction for cell lysate protein concentration (n=6, p=0.02).

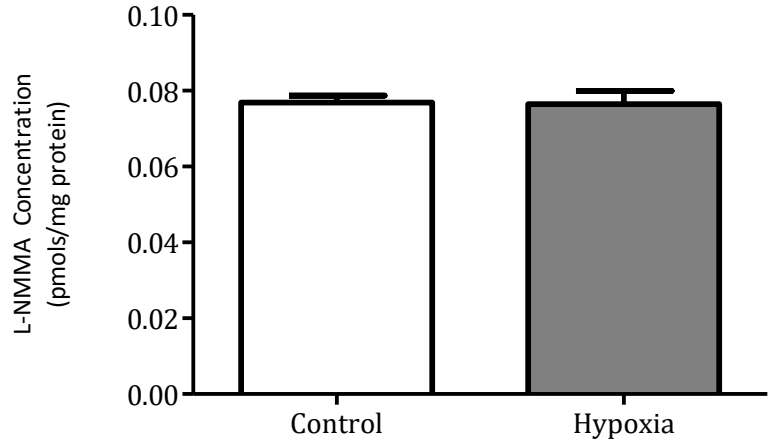

Figure 19: L-NMMA concentrations in control and hypoxia treated primary murine macrophages.

Cell lysate L-NMMA was measured in control and hypoxia treated murine macrophages following correction for cell lysate protein concentration (p=0.7)

4.3.1.2 The impact of hypoxia on DDAH2 expression in wild type murine macrophages

Cell lysate was collected and mRNA and protein was extracted as described above. Quantitative PCR revealed a 3.6(0.1)-fold (mean(SD)) increase in DDAH2 mRNA compared to control cells ($p<0.01$). DDAH2 protein levels showed a similar pattern when evaluated by Western blot. When the relative density of bands was compared, DDAH2 expression was shown to be significantly increased (4.5(2.3) fold, $p=0.026$).

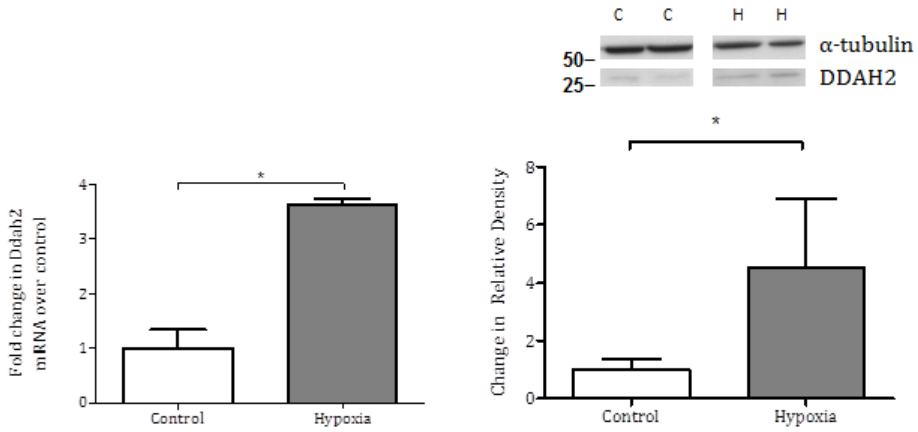

Figure 20: DDAH2 mRNA and protein expression changes in primary macrophages following hypoxic exposure.

Left imge) QPCR measurement of DDAH2 mRNA expression in resident peritoneal macrophage lysates from wild type (C57Bl6) mice following culture in normal conditions or after 12 hours of hypoxic exposure (n=6 per group, * p<0.05). right image) Change in DDAH2 protein expression following culture in control (C) and hypoxic (H) conditions as evaluated by Western blot densitometry analysis (n=6 per group, (* p<0.05).

4.3.1.3 Hypoxia and pro-inflammatory activation

In order to explore a potential synergistic relationship between hypoxia and pro-inflammatory stimuli, a series of experiments were conducted involving four groups. Primary peritoneal macrophages were exposed to IFN-γ, hypoxia at 3%, IFN-γ and hypoxia together or control conditions for 12 hours. Medium was then changed and cells were exposed to normal culture conditions (21% oxygen, 5% carbon dioxide, 37% humidity) for 24 hours. Medium was collected at baseline, 7 and 24 hours and cell lysate was collected after 24 hours of reoxygenation.

Significant increases in medium Nitrite/Nitrate levels were observed following separate treatment with either IFN-γ or hypoxia as has been shown previously (Table 19, Figure 21). When exposed to both stimuli in conjunction, an exaggerated NOx synthesis was observed compared to either stimulus alone, ($p<0.01$ for both stimuli).

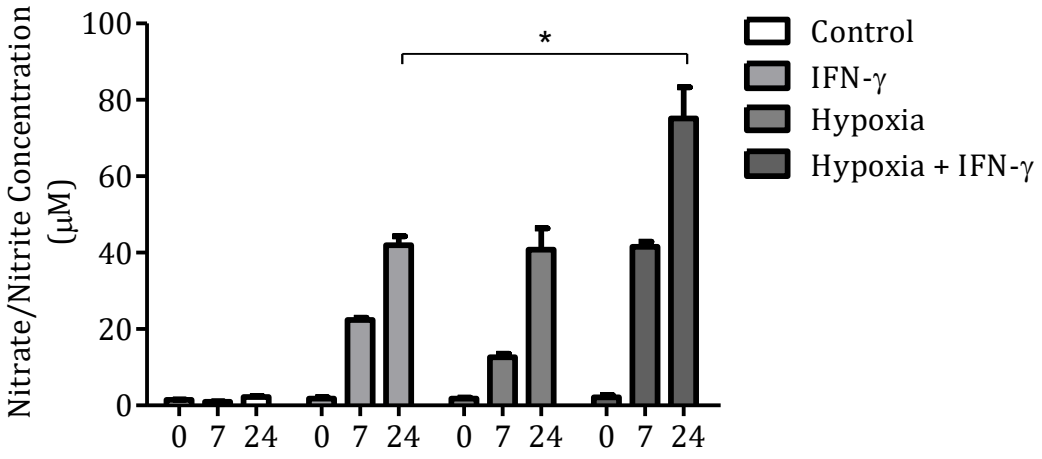

Figure 21: Medium Nitrate/Nitrite synthesis in response to Hypoxia, Interferon-gamma or hypoxia plus interferon treatment.

Isolated murine macrophages were incubated in either control or hypoxic (3%) conditions for 12 hours. In each condition, one group of cells was exposed to normal medium and the other to stimulus with IFN-γ. Medium was then replaced and cells were returned to normal incubation conditions. Medium was collected at baseline, seven and 24 hours after the medium change. All treatments resulted in significant increases in NOx at seven and 24 hours. Treatment with IFN-γ and hypoxia in combination resulted in a significantly greater induction of NO synthesis in comparison to either hypoxia or IFN-γ treatment alone ($p<0.01$ for both).

	Control		IFN-γ		Hypoxia		Hypoxia + IFN-γ	
Time	Mean (μM)	SD	Mean(μM)	SD	Mean (μM)	SD	Mean (μM)	SD
Baseline (0)	1.43	0.18	1.7	0.43	1.9	0.59	2.1	1.0
Seven	0.96	0.11	22.4	0.96	12.6	1.57	41.52	2.37
Twenty four	2.21	0.36	41.9	4.03	40.8	9.68	75.11	14.17

Table 19: The impact of hypoxia, Interferon-gamma or both stimuli on medium Nitrate plus Nitrite concentrations.

The mechanism of these differences was explored by evaluating iNOS and DDAH2 levels using RT-qPCR. Similar elevations in iNOS induction were observed in both IFN-γ and Hypoxia + IFN-γ treated groups (Figure 22, Table 20), however in cells exposed to both stimuli, DDAH2 mRNA was significantly higher compared to either hypoxia or IFN-γ treated cells alone ($p<0.01$ compared to both stimulus alone) (Figure 23, Table 20).

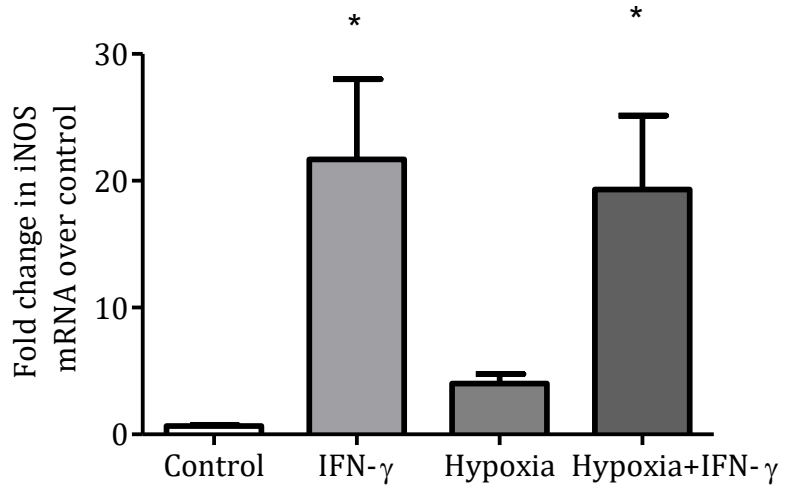

Figure 22: RT-qPCR analysis of the impact of treatment with hypoxia and Interferon-γ either alone or in combination on iNOS mRNA expression.

Cell lysate was collected following culture for 12 hours in control (21%) or hypoxic (3%) conditions with or without IFN-γ before a further 24 hours at 21% oxygen. iNOS mRNA expression was significantly elevated in all treatment conditions over control ($p<0.01$). Similar levels of iNOS induction were observed in IFN-γ and hypoxia + IFN-γ conditions ($p>0.05$ by Bonferroni comparison following one-way ANOVA).

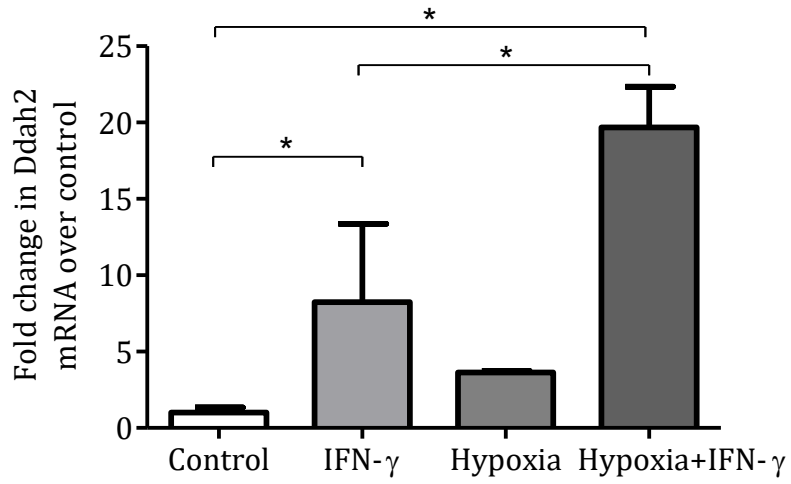

Figure 23: RT-qPCR analysis of the impact of stimulation with hypoxia and Interferon-gamma either alone or in combination on DDAH2 mRNA expression.

DDAH2 mRNA expression was significantly elevated in all treatment conditions over control ($p<0.01$). Significantly greater induction was observed in IFN-γ plus hypoxia treated cells compared to IFN-γ or hypoxia alone ($p<0.01$ by Bonferroni comparison following one-way ANOVA).

iNOS mRNA				
Mean	1	21.69	4.011	19.32
SD	0.1258	10.93	1.316	10.08
DDAH2 mRNA				
Mean	1	8.25	3.632	19.67
SD	0.3466	5.125	0.1169	2.677

Table 20: Change in iNOS and DDAH2 mRNA expression following hypoxia, IFN-gamma and combination therapy measured using RT-qPCR.

4.3.2 The impact of hypoxia on DDAH2 deficient murine macrophages

Macrophage-specific knockout mice ($Ddah2^{M\Phi-}$) and litter mate floxed controls ($Ddah2^{flox/flox}$) were used as the source of primary peritoneal macrophages. Animals were sacrificed at 8-10 weeks using cervical dislocation and peritoneal washout undertaken as described in Chapter 2, followed by hypoxic or control incubation as above.

4.3.2.1 Comparison of Nitric Oxide synthesis and inhibitors in DDAH2 knockout cells and controls

Nitric oxide concentration was measured before and after hypoxic exposure in the cell lysate of primary peritoneal macrophages from $Ddah2^{M\Phi-}$ mice and their $Ddah2^{flox/flox}$ littermate controls. Cells deficient in DDAH2 displayed reduced intracellular NOx concentrations at baseline compared to controls (mean (SD), 5.15(0.61)µM/mg protein vs. 7.7(0.87)µM/mg protein ($p=0.014$)) (Figure 24). After hypoxic exposure for 12 hours and reoxygenation for a further 24 hours, $Ddah2^{flox/flox}$ cells displayed a significant induction of NOx synthesis (11.6(0.94)µM/mg protein ($p<0.01$). By contrast, peritoneal macrophages from $Ddah2^{M\Phi-}$ mice displayed no significant increase in intracellular NOx following hypoxic exposure ($p=0.10$) (Figure 24).

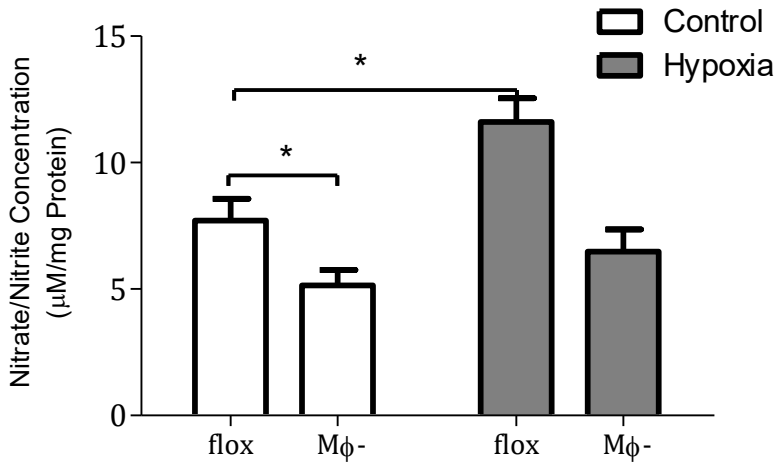

Figure 24: Nitric oxide synthesis in DDAH2 deficient primary peritoneal macrophages following hypoxic exposure.

Change in macrophage intracellular NOx concentration (corrected for cell lysate protein concentration) following 12 hours of hypoxic exposure and 24 hours of reoxygenation in DDAH2 macrophage-specific knockout (MΦ-) and littermate flox/flox control mice (flox). Floxed control cells displayed a significant induction of NO synthesis in response to hypoxia and reoxygenation ($p<0.01$). Macrophage-specific knockout cells had significantly lower baseline NO concentrations and did not display an increase in NO synthesis in response to hypoxic stimulation ($p=0.10$) ($n=6$ per group, $*p<0.05$).

Intracellular ADMA in $Ddah2^{flox/flox}$ mouse macrophages displayed a similar change to that seen in peritoneal macrophages from wild type animals (mean(SD), 0.30(0.015)pmol/mg protein falling to 0.12(0.01)pmol/mg protein, p=0.01) (Figure 25). Ddah2MΦ- macrophages showed no fall in ADMA levels following hypoxic treatment. In contrast to the floxed cells, they instead displayed a two-fold increase with concentrations of 0.13(0.04) μM/mg protein in controls and 0.28(0.03) μM/mg protein in treated cells (p=0.06) (Figure 25).

SDMA concentrations were measured and shown to be unchanged after hypoxic exposure in floxed cells (mean(SD), 0.78(0.13)pmol/mg protein vs. 0.80(0.35)pmol/mg protein, p=0.92) (Figure 26). $Ddah2^{MΦ-}$ mouse macrophages also displayed no change in SDMA levels between control and hypoxic treated groups with concentrations of 2.27(1.5) mol/mg protein and 2.06(1.6)mol/mg protein, respectively (p=0.88) (Figure 26).

L-arginine concentrations were also unchanged across the two floxed groups with mean(SD) L-arginine concentrations of 4.6(0.68)pmol/mg protein in control conditions and 4.39(0.62)pmol/mg protein after hypoxic stress (p=0.62). This pattern was similar in the DDAH2 deficient macrophages where L-arginine concentrations were 5.92(0.62) pmol/mg protein in control and 5.6(0.58) pmol/mg protein in hypoxic conditions (p=0.63) (Figure 27).

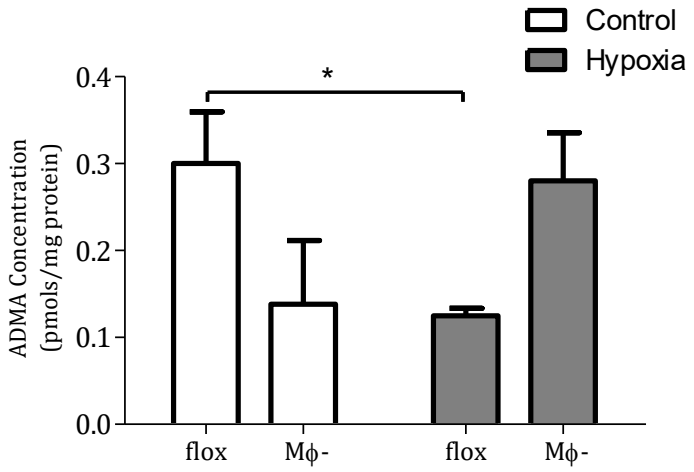

Figure 25: Intracellular ADMA concentration in control and DDAH2 macrophages following exposure to hypoxia.

Floxed control cells demonstrated a significant reduction in ADMA concentration following hypoxic exposure. A trend towards increased ADMA was observed in DDAH2 deficient macrophages following hypoxic incubation (p=0.06) (n=6 per group, *p=0.01).

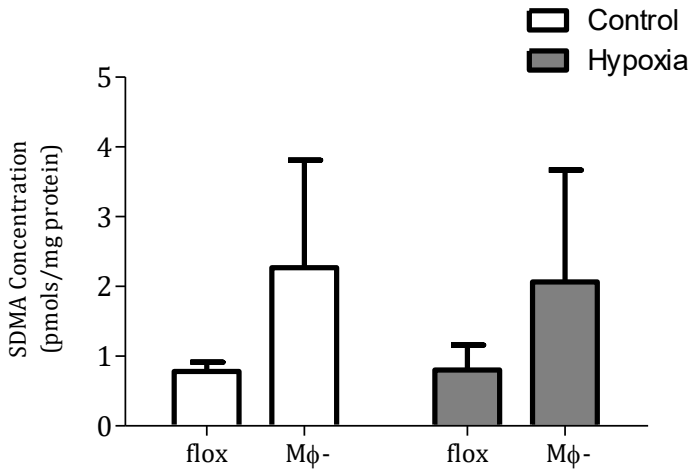

Figure 26: Intracellular SDMA concentrations in control and DDAH2 deficient macrophages following exposure to hypoxia.

Floxed control cells demonstrated no changes in SDMA concentration following hypoxic exposure (p=0.92). A similar pattern was seen in DDAH2 deficient cells where SDMA concentrations were similar in both hypoxia treated and control groups (p=0.88) (n=6 per group).

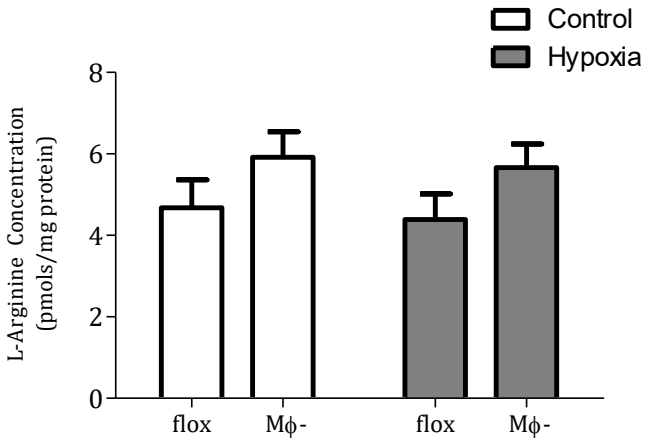

Figure 27: Intracellular L-arginine concentrations in control and DDAH2 deficient macrophages following exposure to hypoxia.

Floxed control cells demonstrated no changes in L-arginine concentration following hypoxic exposure (p=0.62). A similar pattern was seen in DDAH2 deficient cells where L-arginine concentrations were similar in both hypoxia treated and control groups (p=0.63) (n=6 per group).

4.3.3 The impact of hypoxia on human peripheral blood mononuclear cells

A healthy volunteer study was undertaken as described in Chapter 2 using a normobaric hypoxic chamber following ethics committee review by the UCL research ethics committee. Following a 2 volunteer pilot study to determine technical aspects and tolerability, thirteen participants completed a study involving an eight-hour exposure to a 12% inspired oxygen concentration which is equivalent to approximately 4500m of altitude. A blood sample, baseline observations and haemodynamic assessment was undertaken prior to entering the hypoxic chamber. Haemodynamic monitoring was performed twenty minutes after entry and at least once per hour thereafter. Upon completion of the study period, volunteers underwent repeat blood sampling whilst still in the chamber.

4.3.3.1 Baseline physiology in healthy volunteers prior to hypoxic exposure

Participants were eligible for inclusion in the study if they were male, had no significant co-morbid illnesses, and had not been exposed to prolonged periods at altitudes above 3000m. The demographics of the volunteers are described in Table 21 below.

	Mean	SD
Age	31.17	12.64
Weight(kg)	78.08	8.754
Height(cm)	178.3	5.294
BMI(kg/m^2)	24.54	2.089
$SaO_{2(\%)}$	97.25	1.055

Table 21: Baseline physiological characteristics of healthy male volunteers in the normobaric hypoxia study.

4.3.3.2 Safety and tolerability of hypoxic chamber exposure in healthy volunteers

Of the fifteen participants that were included in the pilot and subsequent study, four volunteers exhibited subjective symptoms of acute mountain sickness with a modified Lake Louise score (described in the methods section) of between 1 and 3. No significant objective signs could be elicited upon examination. One volunteer suffered from an episode of nausea during the main study and he was withdrawn from the hypoxic chamber immediately. Observation for 1 hour revealed no subjective or objective sequelae. Follow up at 24 hours revealed no residual symptoms in the participant; however he was excluded from the study and further analysis. Of the participants that completed the study, nine volunteers underwent physiological, plasma and paired-monocyte sample collection and a further three underwent plasma and physiological measurement analysis only.

4.3.3.3 The cardiorespiratory impact of hypoxic exposure in healthy volunteers

Careful monitoring of cardiovascular and respiratory function was undertaken throughout the study period. This offered a robust validation of the degree of hypoxic stress and also important safety information.

Digital arterial oxygen saturations (SaO_2) were measured and the saturations recorded in each volunteer. SaO_2 fell rapidly upon entry into the chamber and remained similar throughout the hypoxic exposure. Mean(SD) saturations were 86(2.9)% at the one hour time check and 87(2.0)% at the final check (Figure 28).

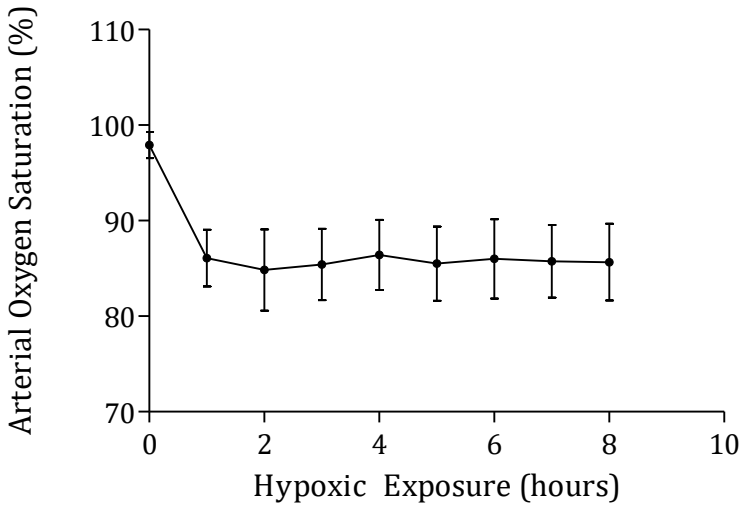

Figure 28: The impact of exposure to a 12% hypoxic environment on healthy volunteer arterial oxygen saturations.

The impact of exposure to 12% inspired oxygen fraction on healthy volunteer peripheral arterial oxygen saturations measured at rest prior to entrance (0). Subsequent regular measurements are summarised hourly (n=12).

There was no significant impact on heart rate during the course of the hypoxia study period. Mean(SD) heart rate was 68(11)beats/min prior to entry into the chamber and 72(9) on completion of the study (Figure 29).

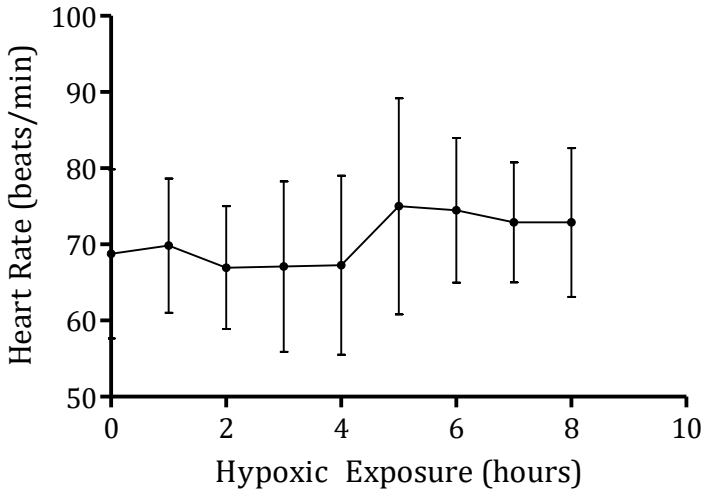

Figure 29: The impact of exposure to a 12% hypoxic environment on healthy volunteer heart rate.

The impact of exposure to 12% FiO2 on healthy volunteer heart rate measured at rest prior to entrance (0). Subsequent regular measurements are summarised hourly (n=12).

Blood pressure was assessed at each time point using a non-invasive device. Systolic and diastolic blood pressure appeared to fall slightly over the first hour of hypoxic exposure (mean(SD) systolic 128(21)mmHg to 118(11)mmHg and diastolic 74(6.3)mmHg to 70(13)mmHg, however neither of these trends were significant (p=0.16 and 0.34 respectively). Blood pressure was otherwise unchanged over the course of the study period.

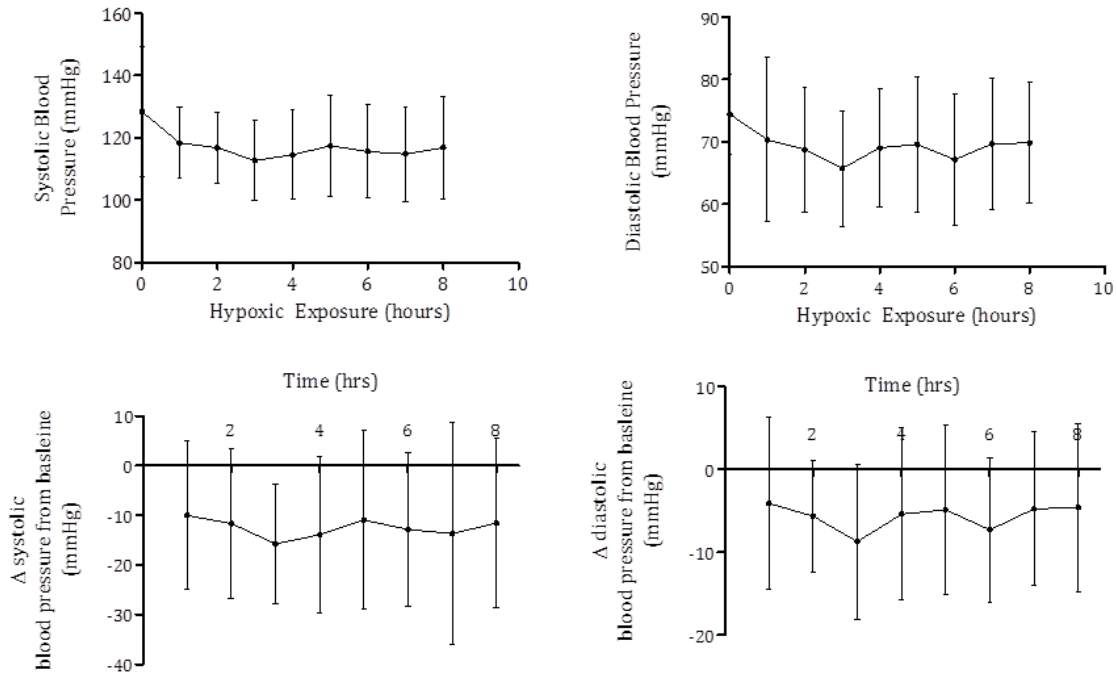

Figure 30: The impact of exposure to a 12% hypoxic environment on healthy volunteer systolic and diastolic blood pressure.

The impact of exposure to 12% FiO2 on healthy volunteer systolic (top left) and diastolic (top right) blood pressure measured using the DINAMAP device at rest prior to entrance (0). Subsequent regular measurements are summarised hourly. Lower panels represent change in systolic (lower left) and diastolic (lower right) blood pressure from baseline. Data is presented as mean(SD) blood pressure (mmHg) (n=12).

Non-invasive assessment of cardiac output in normobaric hypoxia

Cardiac output was measured using the Clearsight™ device, disposables for which were provided as an unrestricted research tool from Edwards Lifesciences (UK). This provided a non-invasive assessment of haemodynamic changes over the course of the experiment. The device uses a modified Penaz technique as described in Chapter 2 to record pressure variation in the digital arteries following partial occlusion of the vessel. This information is then converted into an arterial pressure waveform and from this the stroke volume is derived based on the shape of the curve and a nomogram of standard values. Although the device is licensed for continuous use for four hours without interruption, this study was the first to use it in a hypoxic environment and so in order to minimise any risk of impaired oxygenation of the digit, volunteers underwent 15 minute periods of assessment at each time point. After calibration, the mean value over the final five minutes of each assessment period was taken as the measurement at that time point. The device provided information regarding cardiac output and systemic vascular resistance. Both of these values were automatically corrected for body surface area to allow comparison between volunteers.

Cardiac index and systemic vascular resistance were stable over the course of the experimental period, however between hours four and six, paired analysis revealed increased cardiac index and reduced systemic vascular resistance ($p<0.01$ and ($p<0.01$, respectively) (Figure 31). This was consistent with changes associated with the consumption of a low nitrate meal that was provided at this time in the study period.

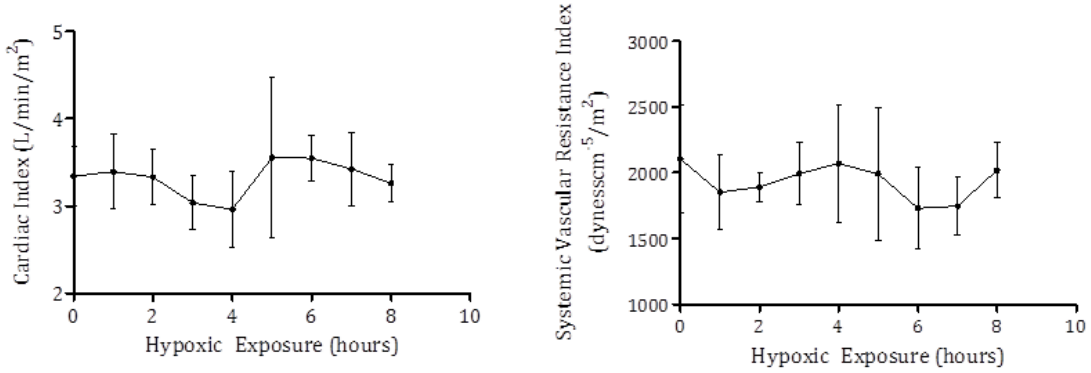

Figure 31: The impact of normobaric hypoxia on cardiac and systemic vascular resistance indexes in healthy human volunteers.

The Clearsight™ device was used to analyse the impact of a 12% hypoxic exposure on healthy volunteers. No significant differences were observed over the whole course of the study, however paired analysis revealed an increase in cardiac index and reduced systemic vascular resistance around the time of eating ($p<0.01$ for this interaction in both assessments).

4.3.3.4 Nitric oxide and inhibitors of nitric oxide synthase in the plasma of hypoxia-exposed volunteers

In the twelve healthy volunteers that completed the main study, eight-hour hypoxic exposure led to a significant increase in plasma Nitric Oxide concentration from mean(SD) 3.6 (1.8)µM to 6.4 (3.2)µM ($p=0.01$) (Figure 32).

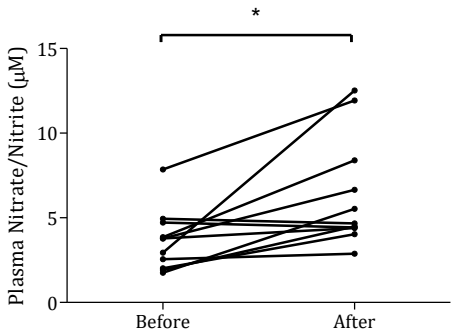

Figure 32: Plasma Nitric Oxide concentration of healthy volunteers before and after exposure to an eight-hour hypoxic challenge.

Plasma Nitric Oxide concentration was measured using a chemiluminescent technique. Plasma from twelve healthy volunteers underwent protein extraction using methanol followed by analysis. Nitric Oxide concentration increased significantly over the course of the study period (paired t-test, $p=0.01$)

Plasma L-arginine was unchanged over the course of the experiment (mean(SD), 102(31)µM to 111(19)µM, p=0.31). Plasma ADMA concentration fell significantly from 0.42(0.12)µM at baseline, to 0.29(0.05)µM after exposure (p<0.01). No changes were observed in plasma SDMA (0.42(0.1)µM to 0.46(0.14)µM, p=0.119) or L-NMMA levels (0.043(0.01)µM to 0.046(0.007)µM, p=0.24) (Figure 33).

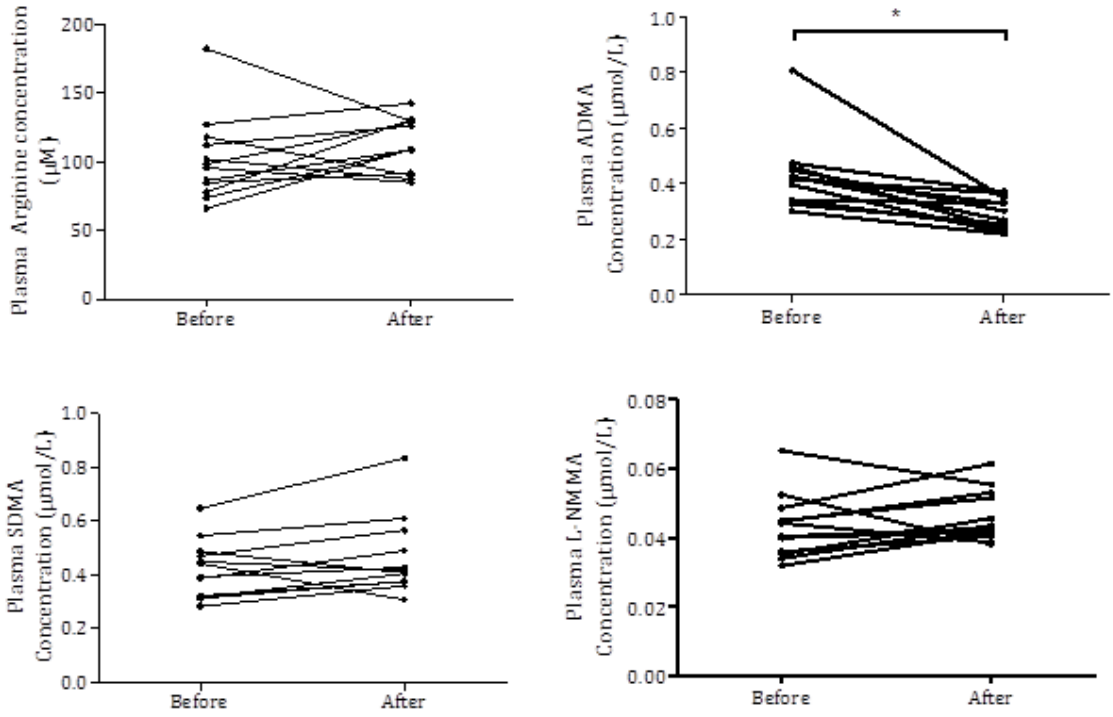

Figure 33: Plasma L-arginine and methylarginine concentrations of volunteers before and after an eight-hour hypoxic exposure.

No significant differences were observed between plasma L-arginine (p=0.31), SDMA (p=0.119) or L-NMMA (p=0.24). Plasma ADMA concentration fell significantly as evaluated by paired analysis (p<0.01).

The plasma ADMA:Arginine ratio was also significantly reduced by hypoxia, falling from a mean(SD) ratio of 0.042(0.01) to 0.027(0.004) (p<0.01) (Figure 34).

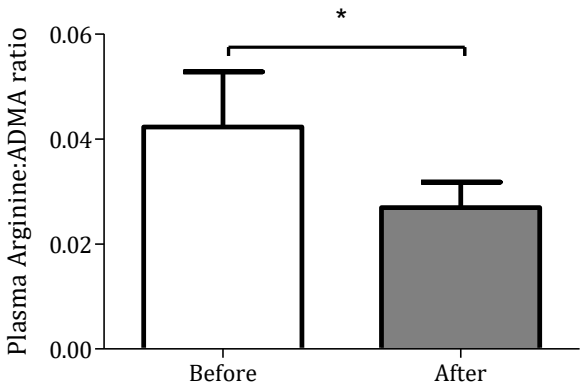

Figure 34: The impact of hypoxia on the plasma ADMA:L-arginine ratio in healthy volunteers exposed to an eight-hour period of hypoxia.

Plasma ADMA:L-arginine ratio fell significantly following the hypoxic challenge (p<0.01).

4.3.3.5 Endogenous inhibitors of Nitric Oxide synthesis in peripheral blood mononuclear cells of hypoxia exposed volunteers

Peripheral blood mononuclear cells (PBMC) were isolated using a Ficoll separation technique and analysed for the concentrations of L-arginine and methylarginines as described in Chapter 2. Results were corrected for cell lysate protein concentration and compared using paired analysis of individual results before and after the hypoxic exposure. PBMC L-arginine was unchanged at mean(SD) of 24.4(5.1)pmol/mg protein to 24.9(5.0)pmol/mg protein (p=0.86). PBMC ADMA fell from 0.43(0.13)pmol/mg protein to 0.29(0.06)pmol/mg protein (p<0.01). L-NMMA was unchanged (0.43(0.07)pmol/mg protein to 0.42(0.06)pmol/mg protein, p=0.62) as was SDMA (4.3(0.70)pmol/mg protein to 4.7(0.75)pmol/mg protein, p=0.15) over the course of the study period (Figure 35)

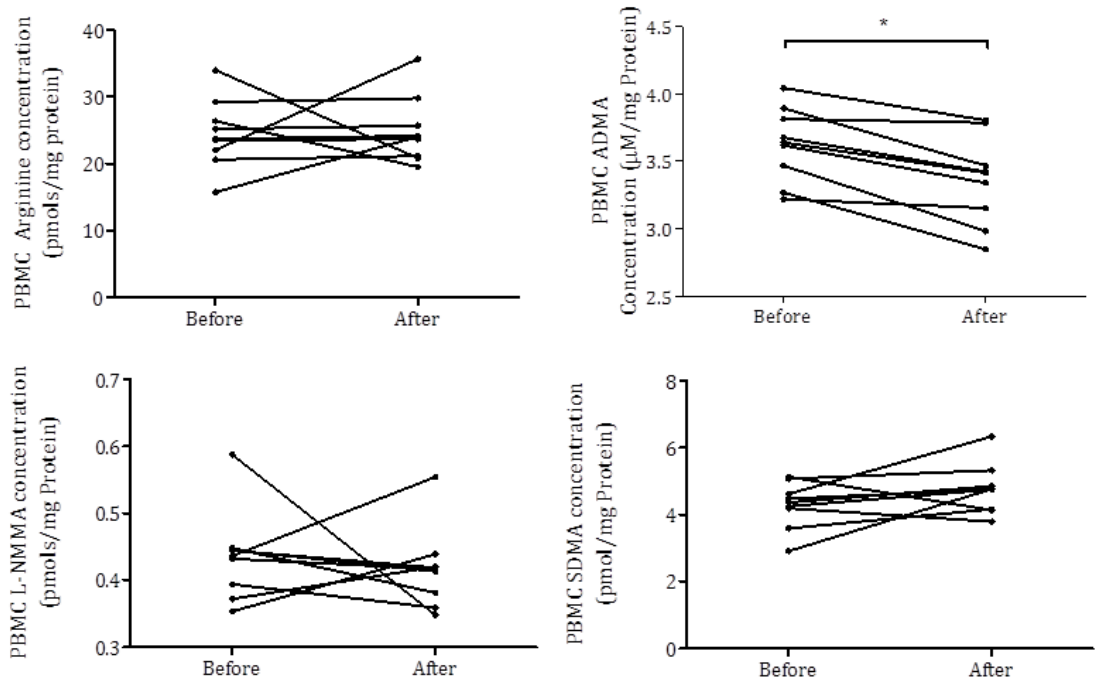

Figure 35: Peripheral blood mononuclear cell L-arginine and methylarginine concentrations of volunteers before and after an eight-hour hypoxic exposure.

Peripheral blood mononuclear cell L-arginine and methylarginine concentrations in twelve healthy volunteers exposed to an eight-hour period of hypoxia. No significant differences were observed between plasma L-arginine (p=0.86), SDMA (p=0.15) or L-NMMA (p=0.62). Plasma ADMA concentration fell significantly as evaluated by paired analysis (p<0.01) (n=9).

The PBMC ADMA:arginine ratio was also reduced after hypoxic exposure (mean(SD) ratio of 0.18(0.03) to 0.14(0.02), p=0.05) (Figure 36).

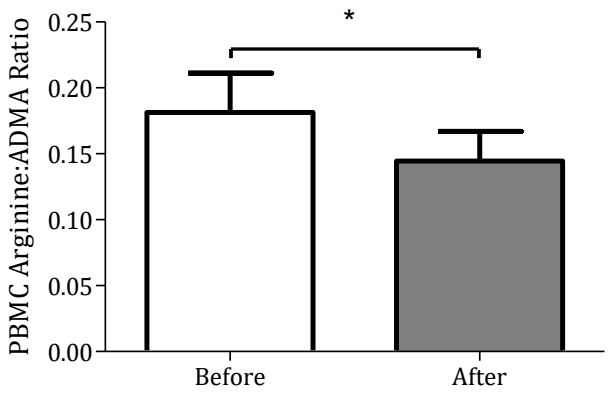

Figure 36: The impact of hypoxia on the peripheral blood mononuclear cell ADMA:arginine ratio in healthy volunteers exposed to an eight-hour period of hypoxia.

The plasma ADMA:arginine ratio fell significantly following the hypoxic challenge (p=0.05).

4.3.3.6 The relationship between plasma and mononuclear cell methylarginine concentrations

There was no significant correlation between plasma and PBMC ADMA concentrations before the hypoxic study (r^2 0.047, p=0.57). However, at the end of the hypoxic study period, a positive correlation between the cell and plasma concentrations was observed (r^2 0.531, p=0.026) (Figure 37).

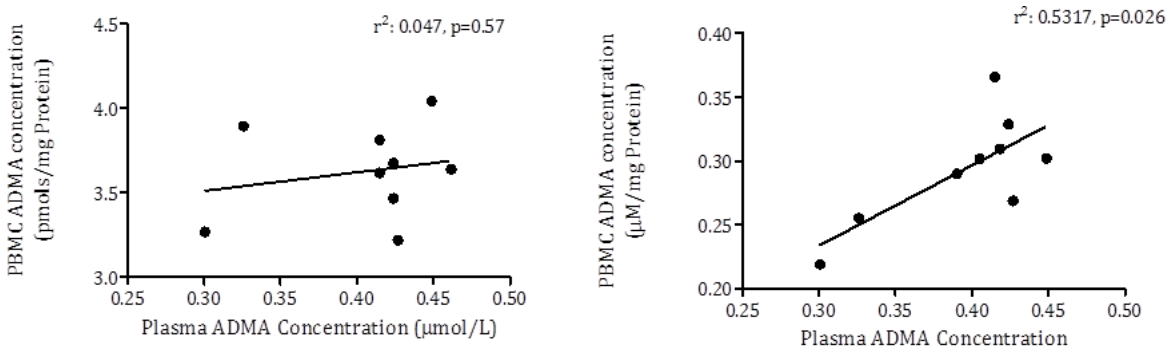

Figure 37: Correlation between plasma and peripheral blood mononuclear cell ADMA concentrations before and after eight-hour hypoxic exposure.

The relationship between plasma and intracellular concentrations of ADMA was determined before and after the hypoxic challenge in volunteers where both kinds of sample were available (n=9). No apparent correlation was observed before the challenge (p=0.57), however, a positive correlation was detected at the end of the study period (p=0.026).

4.3.3.7 Change in DDAH2 expression in the mononuclear cells of humans exposed to a hypoxic challenge

Cell lysate from the healthy volunteer study was examined for DDAH2 mRNA and protein expression using methods described previously. DDAH2 mRNA expression (mean(SD) increased 1.9(0.6)-fold over baseline (p=0.03). DDAH2 protein expression showed a similar magnitude of increase with a 2.5(0.94)-fold change (p=0.034)(**Error! Reference source not ound.**).

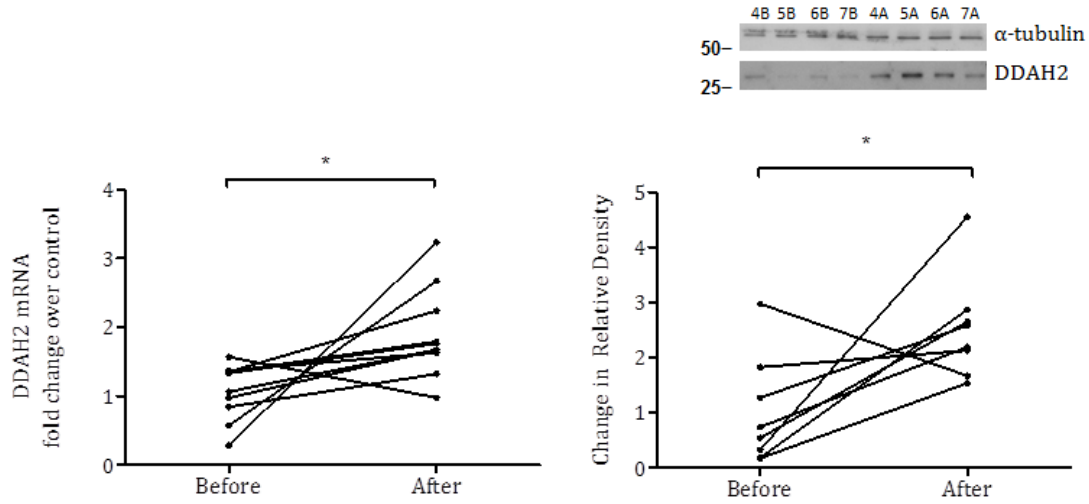

Figure 38: DDAH2 mRNA and protein expression changes in peripheral blood mononuclear cells following hypoxic exposure.

Left image) QPCR measurement of DDAH2 mRNA expression in peripheral blood mononuclear cells from healthy volunteers before and after an eight-hour hypoxic challenge (*p=0.03). Right image) Change in volunteer DDAH2 protein expression following eight-hour hypoxic exposure as evaluated by Western blot densitometry analysis compared to Tubulin controls (* p<0.01). Representative Western blot of four volunteers before (B) and after (A) hypoxic challenge.

4.3.3.8 Nitric Oxide synthase expression in human mononuclear cells exposed to hypoxia

Human peripheral blood mononuclear cells were examined for the presence of Nitric Oxide synthase isoforms. iNOS was not detectable at the mRNA or protein level, however eNOS mRNA expression was shown to display a trend towards being downregulated following hypoxic challenge (relative reduction in eNOS mRNA (mean(SD)% 33(30), p=0.08) (Figure 39).

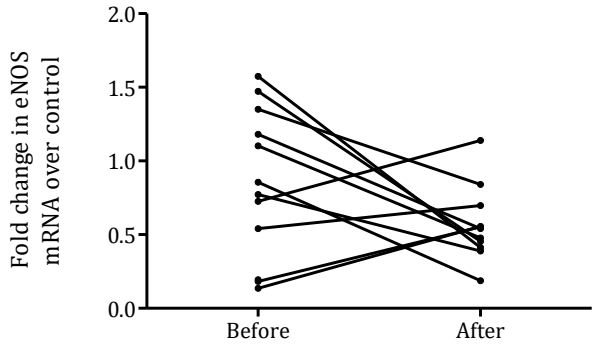

Figure 39: Change in eNOS mRNA expression in human peripheral blood mononuclear cells following eight-hour hypoxic exposure.

eNOS mRNA was determined in nine healthy volunteers following exposure to an eight-hour 12% inspired oxygen challenge. A trend was observed towards a reduction in eNOS mRNA expression (p=0.08).

4.4 Discussion

In the introduction to this chapter, the mechanisms by which hypoxia regulates the innate inflammatory response were reviewed. It is clear that low oxygen tensions are more than a consequence of infection or inflammation and are a key regulator of physiological response. This study considers for the first time how endogenous inhibitors of Nitric Oxide Synthase and their immune cell regulatory enzyme, DDAH2 contribute towards the hypoxic response. By advancing our understanding of the interactions between hypoxia, ADMA and DDAH, this study offers an insight into the way in which hypoxia regulates the synthesis of NO in immune cells.

4.4.1 Murine macrophages

4.4.1.1 Nitric Oxide Synthase induction and inhibition in murine macrophages

This study confirms the previous observation that in murine macrophages, NO synthesis is upregulated in response to hypoxia and that this is mediated by the induction of iNOS[272, 275]. In addition, the observation that in murine macrophages, hypoxic environments limit the ability of increased iNOS protein to synthesise NO is recapitulated [273, 274]. The induction of iNOS and degree of NO synthesis is consistent with the literature and reflective of the ability of murine macrophages to synthesise more NO in response to stimulus than human cells[276].

This study did not identify any significant changes in the concentrations of L-arginine or L-NMMA in cell lysates after the hypoxia and reoxygenation period. However, a significant reduction in intracellular ADMA concentration was observed. This is consistent with reduced intracellular NOS inhibition and suggests an additional mechanism by which hypoxia might induce increased NO synthesis, particularly in circumstances where NOS protein expression is increased but the availability of the key co-factor for NO production, oxygen is limited.

Also, in wild type cells we were able to show that DDAH2 protein expression was significantly increased in response to hypoxia. This led to the hypothesis that increased DDAH2 expression in response to hypoxia might mediate reduced ADMA concentrations and therefore increase NO synthesis by macrophages.

4.4.1.2 The impact of hypoxia and pro-inflammatory co-stimuli on Nitric Oxide Synthesis

Given the co-existence of hypoxia and pro-inflammatory states during the infective process, the impact of simultaneous stimulation with hypoxia and IFN-γ, both of which have been shown to induce DDAH2 expression, was explored. This study demonstrated a similar degree of iNOS induction in cells exposed to IFN-γ alone and hypoxia + IFN-γ together over the study period. Interestingly, the combination of stimuli results in significantly greater NO synthesis than IFN-γ alone. A number of mechanisms for this observation are possible and include changes in protein expression not reflected in mRNA levels and also changes in eNOS expression not represented here. However, a possible explanation is found with the observed increased expression of DDAH2 mRNA in the co-stimulus group over either stimulus alone. This suggests that increased DDAH2 expression mediates reduced ADMA and NOS inhibition which results in increased NO production in response to a pathophysiological stress.

4.4.2 The impact of hypoxia on DDAH2 deficient macrophages

In order to explore the hypothesis that the upregulation of DDAH2 in wild type macrophages when exposed to hypoxia was also responsible for the observed increase in NO synthesis, primary peritoneal macrophages were extracted from $DDAH2^{flox/flox}$ and $DDAH2^{M\Phi-}$ mice. When exposed to the hypoxia-reoxygenation model, differences were observed between floxed control cells and DDAH2 deficient macrophages. In control incubations, NO concentrations in the cell lysate of floxed macrophages were significantly higher than those of $Ddah2^{M\Phi-}$ mice. However, following hypoxic incubation, floxed cells showed a significant additional increase in NO synthesis in contrast to knockout cells in which no significant difference was observed. In control cells, as might be expected in tissues with DDAH2, ADMA concentrations fell to a similar degree as demonstrated previously in wild type cells. By contrast, ADMA concentration in $Ddah2^{M\Phi-}$ mice rose significantly. This suggests that DDAH2 does not simply play a role in reducing the ADMA concentration within cells in response to hypoxia, but also that it prevents a stress-induced increase in ADMA levels in these circumstances. This may offer a mechanism in which animals deficient in DDAH2 demonstrate impaired immune function and may in part explain the association between polymorphisms of the human *DDAH2* gene and outcome in patients with septic shock[300]

4.4.3 Human normobaric hypoxia

Having made the observation that DDAH2 expression increased in murine macrophages and that this mediated changes in NO synthesis, the human normobaric hypoxia study was designed to determine whether this mechanism was conserved across mice and humans.

4.4.3.1 The conduct of a normobaric hypoxia study in humans

This was the first study of its kind to be conducted at the Institute of Sports and Exercise Health at UCL and as such presented a number of challenges in terms of study conduct and sample collection. However, it was possible to recruit an adequate number of healthy volunteers without previous high altitude exposure and conduct a study at the limit of acute hypoxia that most humans can tolerate without acclimatisation.

As expected following this kind of exposure, a proportion of patients did display minor symptoms of altitude sickness and whilst carefully monitored, one had to be withdrawn from the study. The duration, the lack of mandated physical activity and the absence of overnight stay in the hypoxic chamber lead to a reduced incidence of acute mountain sickness in this study. One participant was withdrawn from the study following an episode of nausea. His data collection was not completed and so is not included in the presented results.

The hypoxic chamber at UCL allowed us to generate a reliable and consistent degree of hypoxia in our healthy volunteers, as demonstrated by the rapid and stable reduction in arterial oxygen saturations observed in the study group.

This study was the first to use non-invasive cardiac output analysis using the Clearsight™ device and this offered useful insights into the cardiovascular impact of hypoxia beyond what is possible using conventional non-invasive technology. In particular, we were able to observe a significant increase in cardiac output and reduction in systemic vascular resistance following the meal with which the participants were provided. This is consistent with splanchnic vasodilatation which may be exaggerated in conditions of reduced oxygen availability.

The key goal of this study was to validate the observation that hypoxia in isolation increases DDAH2 expression, reduces ADMA levels and enhances NO synthesis. The normobaric hypoxia chamber allows us to eliminate the other effects of a study conducted at altitude whilst still delivering clinically relevant degrees of hypoxia. The duration of the study was designed to be the maximum tolerable in order to allow a model consistent with the duration of hypoxia that might be seen in acute illness. By using a 'whole animal' model of human hypoxia such as this, the physiological response can be more accurately modelled and the impact determined.

This study showed that as in mice, hypoxia leads to an increase in plasma concentrations of NO. In addition, an acute reduction in ADMA concentrations is observed, consistent with that seen in mice. This occurs in conjunction with an increase in DDAH2 expression in human PBMCs recapitulating the findings from our murine models and suggesting that this mechanism is conserved across species. This study builds upon a previous observation that plasma and PBMC methylarginine concentrations do not correlate in healthy volunteers[17] and also demonstrates that after a hypoxic stress, a correlation develops between plasma and intracellular ADMA concentrations. This suggests that under conditions of pro-inflammatory stress, monocyte ADMA synthesis may play a role in determining systemic ADMA concentrations.

This study validates previous observations that NOS induction in humans differs from that seen in mice. An increase in iNOS was observed in hypoxia treated murine macrophages consistent with previous studies [301]. By contrast, in humans, a trend towards reduced eNOS expression was observed. This is consistent with studies showing that in the absence of a pro-inflammatory cytokine, iNOS induction is not observed in human hypoxia[302]. There is conflicting evidence in the literature regarding the impact of hypoxia on eNOS in different tissues, however a number of stimuli have been shown to regulate eNOS in isolated human monocytes[303] and hypoxia may be one of these.

In summary, the human hypoxia study translates the findings made in the animal models and confirms that DDAH2 plays a role in the regulation of NO synthesis in response to hypoxia. This may play an important role in the human immune response and in part explain the association between polymorphisms of DDAH2, plasma ADMA concentrations and shock in human sepsis studies[300].

4.4.4 The tissue-specific actions of DDAH2 in hypoxia

This study provides an interesting insight into the regulation of DDAH2 in macrophages. However, it contrasts with the limited published literature that has previously explored the impact of hypoxia on DDAH2 expression. In a study examining pulmonary artery smooth muscle and endothelial cell lines, Iannone et al. evaluated the impact of hypoxic exposure and showed that in cells exposed to 2% oxygen for up to 48 hours there was a time-dependent reduction in DDAH2 mRNA and protein. This is in contrast to the observations made here and leads to the question of how similar stimuli could lead to differential tissue effects. In the vascular tissue models studied, both DDAH1 and DDAH2 were co-expressed whereas in immune cells only one is present. It is possible that tissues with differing DDAH distributions may react variably in response to stress or that the DDAH2 promoter may contain specific response elements that drive differential changes in DDAH2 translation. Interrogation of potential transcription factor binding sites of the DDAH2 promoter using the Matinspector™ software reveal multiple potential sites that could facilitate transcription and be relevant to a differential tissue response, including NF-κB and HIF-1 ancillary sequence. This latter binding site forms an essential part of the hypoxia response element (HRE) described earlier[304], although its role in the absence of the HIF-1 binding site, the other key component of the HRE is uncertain.

4.4.5 Strengths and limitations

4.4.5.1 Murine models

The strengths of this study lie in the demonstration of the induction of NO synthesis as mediated by iNOS in a well-validated model and using primary murine cells. The observation that this is associated with increased DDAH2 expression was translated to a causative one through the use of cells from knockout animals to confirm that in the absence of DDAH2 this phenomenon was abated.

It must be noted that the LoxP Cre recombinase model of transgenic mouse development is a well-utilised and validated one, however there are well-established 'off target' effects of this technique which may play a role in the immune response. These issues are addressed in more detail in subsequent chapters.

As described above, the mechanism by which hypoxia drives DDAH2 expression is not yet clear. In the vascular endothelium, mir-21 has been implicated in the regulation of DDAH1, however it was not shown to regulate DDAH2 expression. The mechanism for this action remains unclear and merits future exploration.

4.4.5.2 Human Hypoxia study

This human study provided direct evidence that the mechanism observed in mice could be conserved across species. By using healthy volunteers in normobaric conditions, it allowed the most controlled assessment possible of the impact of hypoxia on PBMC DDAH2. Clinical and altitude populations come with multiple confounding observations that limit the ability to derive information specifically on hypoxia. The highly controlled nature of this study with environment, diet and exposure tightly regulated makes this a robust observation.

As with many studies of this kind, it is small in nature, and whilst the sample size target was reached, an error caused by this is less likely, but still possible. Furthermore, for technical reasons, it was not possible to sort the PBMCs by flow cytometry since that facility was not available. Therefore, it is possible that the changes observed in DDAH2 expression are mediated by changes in circulating monocyte type. Whilst the observation remains valid that this has a systemic effect, understanding the circulating immune cell types involved and how they change in hypoxia would also have been informative.

For pragmatic reasons, the study duration was limited to eight hours in the chamber. This limitation precluded longer exposure to hypoxia which may have provided further information relevant to clinical cohorts.

4.4.6 Future work

Future work in this area can be divided into two areas, first in *ex vivo* models and secondly the translation of these observations into clinical populations. In primary cells, understanding the mechanism by which DDAH2 is regulated is an important step, as is determining if the same patterns can be seen in the other major tissue type that only expresses DDAH2 – the heart. In humans, identifying clinical cohorts in which hypoxia and inflammation are important components of disease and understanding how DDAH2 is modified in response to these stressors may provide useful insights for therapies in these areas.

4.4.7 Summary statement

- Hypoxia induces nitric oxide synthesis in primary murine macrophages isolated from the peritoneal cavity of wild type mice.
- In addition to increased iNOS, increased DDAH2 expression and reduced ADMA levels provoke elevated NO synthesis in primary murine cells exposed to hypoxia for twelve hours followed by reoxygenation for a 24 further hours.
- DDAH2 deficient macrophages do not display this pattern of response, and ADMA levels increase after hypoxia in contrast to wild type cells.
- In humans, an eight-hour hypoxic exposure recapitulates the increased systemic NO synthesis, reduced ADMA and increase DDAH2 expression seen in animals.

5 Regulation of DDAH2 by Interferon-gamma

5.1 Introduction

5.1.1 Inflammation and Nitric Oxide signalling

Extensive work has demonstrated that macrophages upregulate nitric oxide (NO) synthesis in response to a range of stimuli through the induction of iNOS as discussed previously. However, to date, limited work has been undertaken in which the impact of pro-inflammatory agents on the endogenous inhibitor of NOS, ADMA and its regulator in immune cells, DDAH2 has been explored. Existing evidence suggests that DDAH2 may play an important role in the human inflammatory response[39, 300]. Understanding its regulation in macrophages may therefore provide insights into how SNPs of DDAH2 have come to be associated with severity of shock in humans.

One study has explored the impact of exogenous ADMA on the LPS-induced synthesis of NO. In 2013, Pekarova et al. co-incubated RAW 264.7 cells and alveolar macrophages with LPS and increasing doses of ADMA[9]. Using high doses of ADMA (10-50μM), which is beyond the normal physiological range, they observed that ADMA induced a dose-dependent reduction in NO synthesis. Of note is that in addition to the established mechanism of competitive inhibition, the group also observed a dose-dependent reduction in iNOS expression following ADMA treatment. This latter finding has not been replicated in any other tissues.

5.1.2 Tissue culture macrophage models

There are more than 25 monocyte or macrophage cell lines available for tissue culture use at present, each offering a differing pattern of response to stimulus, function and ease of use. The choice of cell line is therefore a complex one and can be broadly divided into two groups, human and rodent.

The more common human monocyte cell lines such as U-937 and THP-1 have been derived, in most cases, from patients with leukaemia or lymphoma. Like U-937 and THP-1, they are often undifferentiated monocytes and must undergo several days of treatment with stimuli such as phorbol-12-myristate-13-acetate (THP-1 cells), phorbol esters, vitamin D3, interferon-γ, tumour necrosis factor-α and retinoic acid (U-937 cells) to induce their differentiation into macrophages. The advantage of these cell lines is that their inflammatory response is similar to that seen in humans. However, the experimental process of differentiating cells of this kind into terminal macrophages induces a degree of pro-inflammatory stress. This means that cells are already activated prior to the initiation of the experiment which may distort results[305].

Rodent cell lines have more widespread origins. Some are immortalised through retroviral recombination such as ANA-1[306], others from bone marrow isolates (C7[307]) and the third group, like most human cell lines, from leukemic models[214].

RAW 264.7 cells were employed in the studies presented here. They are a macrophage cell line that was developed from a murine model of Abelson murine leukaemia virus-induced tumour. RAW 264.7 was developed in 1976 and has since been well-validated[214]. Its ease of use and ability to manipulate have resulted in it becoming one of the most widespread experimental murine macrophage cell lines, with over 1500 articles relating to its function[215]. The cell line has been used to examine monocyte function and activity, including the regulation of iNOS in response to stimulation[216], receptor signalling and LPS[217, 218].

5.1.3 Polyinosinic polycytidylic acid

Polyinosinic polycytidylic acid (Poly I:C) is a non-infective model of the response to TLR3-mediated stimulation. Poly I:C is a double stranded RNA (dsRNA) and naturally occurring TLR3 agonist that mimics viral infection. It activates the transcription of Type 1 interferons, NF-κB and STAT1 which are key mediators of the early anti-viral response[308, 309].

The binding of Poly I:C to TLR3 results in the activation of a number of downstream signalling pathways which drive gene expression[310]. As described previously, TIR-domain-containing adapter-inducing interferon-β **(**TRIF) is a critical signalling protein which contributes to the activation of all four TLR3-mediated signalling pathways, these being interferon regulatory factor-3 (IRF-3), NF-κB, c-Jun N-terminal kinases **(**JNK) and P38. Activation of these pathways stimulates the transcription of target genes via their interferon sensitive response elements (ISRE) (IRF-3), κB binding sites (NF- κB) or AP1 (JNK and P38) regions. Activation of these transcription sites leads to the synthesis of Type I interferons, TNF-α, NADPH oxidase and STAT1, all of which have diverse pro-inflammatory actions[308].

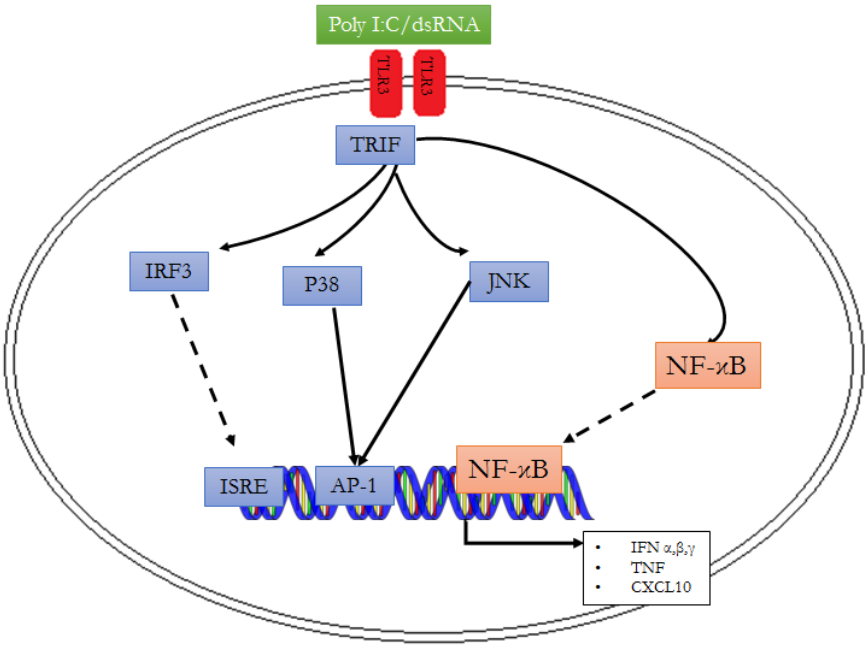

Figure 40: Representative image of the inflammatory response to Poly I:C stimulation.

The binding of Poly I:C to the TLR3 receptor activates TIR-domain-containing adapter-inducing interferon-β (TRIF), an adaptor protein that facilitates downstream TLR signalling. This complex activates interferon regulatory factor-3 (IRF-3), P38, c-Jun N-terminal kinases (JNK) and NF-κB. Once activated, they bind to either interferon sensitive response elements (ISRE), κB binding sites (NF- κB) or AP1 regions (JNK and P38) to stimulate the transcription of a range of pro-inflammatory genes.

The administration of Poly I:C in animal models has been a widely employed method of mimicking viral infection. In addition, it has been used in human therapeutic studies as an adjuvant therapy in H1N1 and H5N1 influenza vaccination [311] and in randomised controlled trials of chronic fatigue syndrome[312]. In the studies presented here, the administration of Poly I:C into the peritoneal cavity of mice at a dose of 12mg/kg was undertaken based on dosage information derived from the literature[239] and pilot work.

5.2 Study Design

5.2.1 Tissue culture models of the inflammatory response

This series of studies employs the RAW 264.7 murine macrophage cell line to explore the hypothesis that DDAH2 is a regulator of the acute inflammatory response. In these studies, the stimulation of cells with a number of pro-inflammatory agents representing key inflammatory pathways was performed in order to determine their effects on endogenous inhibitors of NO synthesis.

Observed differences between the pro-inflammatory stimuli and their effects on the synthesis of and/or responses to the endogenous inhibitor ADMA provoked further mechanistic exploration.

All studies presented here represent 6-8 independent experiments unless otherwise specified. Samples for Nitrite/Nitrate analysis, quantitative PCR and mass spectrometry were analysed in duplicate.

5.2.2 Modelling the viral infection using a TLR3 stimulus

This study involves macrophage and granulocyte-specific DDAH2 knockout mice developed using the LoxP Cre recombinase technique and their floxed littermate controls. Poly I:C was used as a non-infective model of viral infection. A single 12mg/kg bolus of Poly I:C or sham injection was administered into the peritoneal cavity of knockout and control animals and the systemic response to Poly I:C administration observed.

The physiological response was monitored using subcutaneous temperature probes inserted into the scruff of the neck 24 hours prior to the experimental injection. Blood was taken from the animals at the end of the six-hour experiment using cardiac puncture under general anaesthesia and followed by schedule one termination. Plasma was isolated and measurement of methylarginines and cytokines undertaken as previously described.

5.3 Results

5.3.1 Pro-inflammatory stimuli and endogenous inhibitors of Nitric Oxide Synthase activity

Consistent with the existing literature, RAW 264.7 cells stimulated with Lipopolysaccharide (LPS) (Salmonella Typhosa) (Sigma, UK) displayed a significant induction of NO synthesis [9] (Figure 41). This was largely mediated by the inducible isoform of Nitric Oxide Synthase as demonstrated by co-incubation with 1400W (Sigma, UK), a potent and selective iNOS inhibitor, which completely inhibited LPS-induced NO synthesis. Mean(SD) NOx synthesis in control cells was 2.0(0.15)µM, it was 27.5(1.3)µM following LPS stimulus and 2.19(0.05)µM in LPS+1400W treated cells ($p<0.01$).

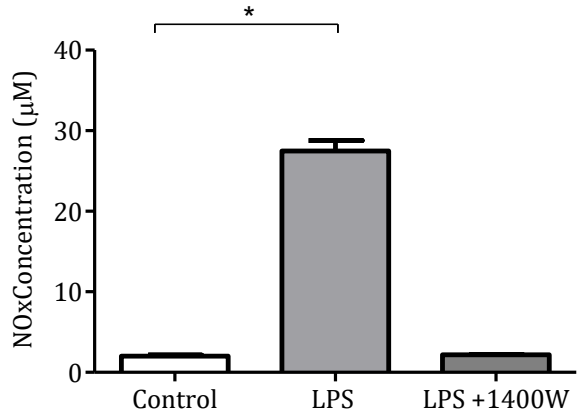

Figure 41: Impact of LPS and LPS+1400W on NOx synthesis in RAW 264.7 cells.

The impact of 5µg/mlL of the pro-inflammatory stimulus, lipopolysaccharide (LPS) alone or in combination with the selective iNOS inhibitor, 1400W on Nitrite synthesis in RAW 264.7 cells cultured for 12 hours (data presented as mean(SD), * = p<0.01).

There was no significant change in cell lysate ADMA levels when corrected for sample protein concentration, (mean(SD) 0.63(0.1)pmol/mg protein in controls vs. 0.66(0.06)pmol/mg protein in LPS treated cells) (Figure 42), however, there was an increase in ADMA concentration in the culture medium following incubation (ADMA of 0.89(0.18)µM in control cells vs. 1.16(0.05)µM, p=0.03) (Figure 42).

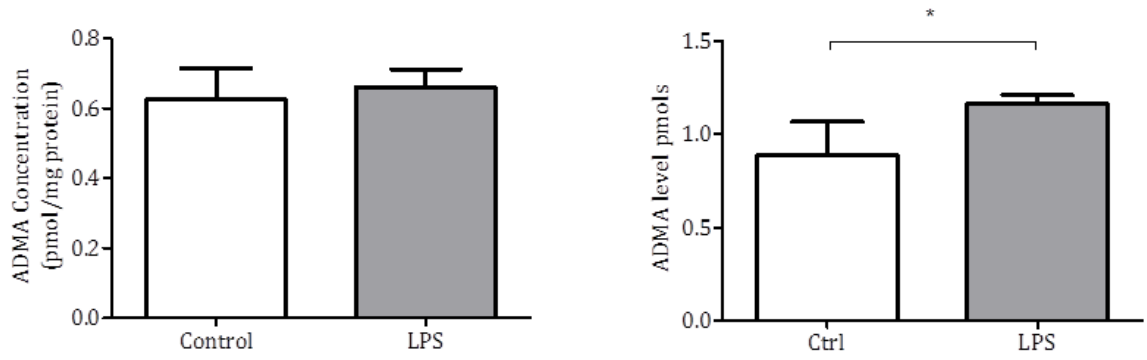

Figure 42: ADMA concentrations in cell lysate and culture medium following eight-hour incubation with LPS.

Cell lysate (left panel) and culture medium (right panel) were analysed using mass spectrometry. No significant differences were observed between the cell lysates following treatment with LPS, however, accumulation of ADMA within the medium was significantly increased at the end of the study period (*p=0.03).

The uptake of ADMA by RAW cells was measured using two doses of ADMA. Cell lysate ADMA increased from 0.01(0.005)pmol/mg protein in control cells to 0.26(0.16) pmol/mg protein in cells exposed to 100µM ADMA and 0.44(0.26)pmol/mg protein in 200µM-treated cells ($p<0.01$ for both) (Figure 43).

NOx synthesis was measured following treatment with two doses of LPS. 100ng/mL LPS resulted in medium NOx concentrations of 22.6(1.6)µM, and 5µg/mL resulted in a level of 22.3(0.9)µM suggesting maximal stimulus of the TLR4-mediated response by the lower dosing. Exogenous ADMA administration at a concentration of 100µM resulted in significant and similar reductions in NOx synthesis in both dosage groups (15.6(0.65)µM and 16.6(0.65)µM, respectively, $p<0.01$) consistent with the existing literature[9] (Figure 43).

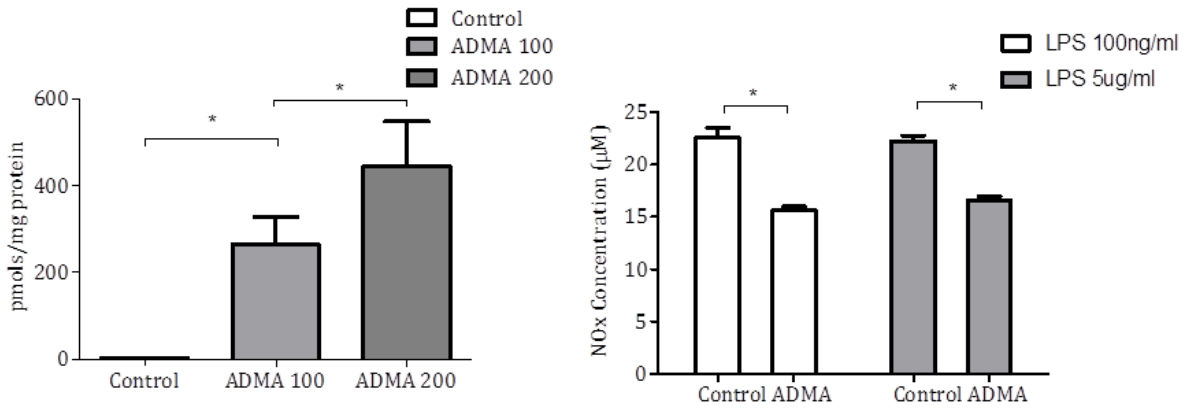

Figure 43: The impact of ADMA treatment on LPS-induced NOx synthesis.

Left panel: ADMA accumulates within RAW 264.7 cells in a dose-dependent fashion following 12-hour incubation with 100μM (ADMA 100) or 200μM (ADMA 200) ADMA as measured by mass spectrometric analysis of the cell lysate (* = p<0.01). Right panel: Exogenous ADMA administration (100μM in culture medium) results in a significant reduction in NOx synthesis by 100ng/mL and 5μg/mL LPS treated cells (* = p<0.01 for both).

NOx synthesis in LPS treated cells was compared to levels induced by a cocktail of LPS, TNF-α and IFN-γ. LPS treatment alone increased NOx synthesis as previously shown ($p<0.01$). Following overnight incubation, the cocktail treatment resulted in a further increase in NOx synthesis with levels of 50(4.5)μM in cocktail treated medium compared to 41.1(1.8)μM in LPS treated cells ($p<0.01$). Treatment with the iNOS inhibitor 1400W inhibited the action of the pro-inflammatory cocktail, confirming iNOS as the primary mechanism for NOx synthesis in this treatment (Figure 44).

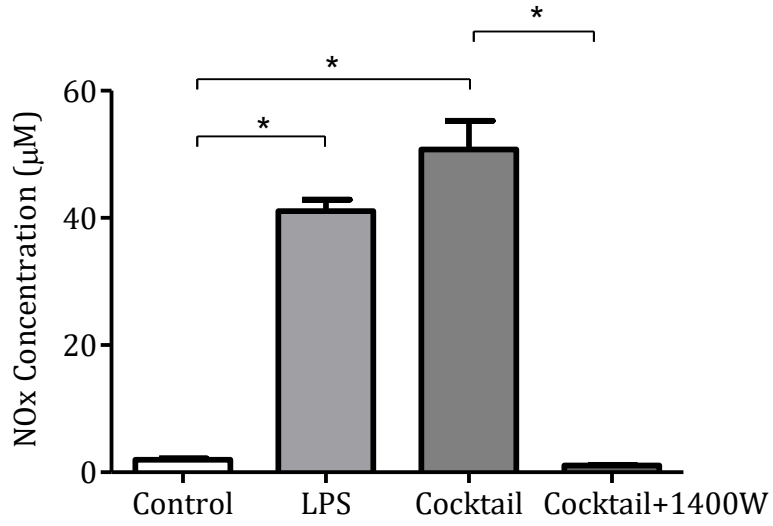

Figure 44: Comparison of NOx synthesis following LPS and inflammatory cocktail stimulation.

The impact of LPS and cocktail (LPS + IFN-γ+TNF-α) stimuli on NOx synthesis by RAW 264.7 cells after an eight-hour incubation period. Significant increases were observed in both treatment groups. Cocktail treatment resulted in a greater increase in NOx synthesis than LPS alone. Treatment with 1400W inhibited cocktail-induced NOx synthesis (* = p<0.01).

The increased accumulation of NOx within the culture medium over the course of the incubation following cocktail treatment was shown to be modest when compared to LPS alone. However, there was a significantly greater induction of iNOS mRNA in cocktail treated cells (mean(SD), 101(27)-fold compared to 51(13)-fold in LPS treated cells, p<0.01)(Figure 45).

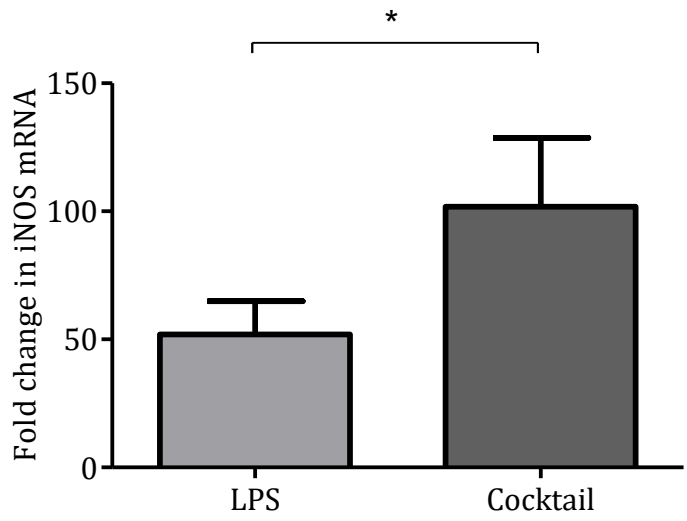

Figure 45: Change in iNOS induction following LPS and inflammatory cocktail treatment.

Quantitative PCR analysis of iNOS induction in RAW 264.7 cells treated with LPS and a pro-inflammatory cocktail for eight-hours. Data represents the fold change in iNOS mRNA compared to untreated control cells and normalised to 1 (* = p<0.01).

Following the same incubation, significantly lower ADMA accumulation was observed in culture medium of cocktail treated cells compared to those exposed to LPS, (0.86(0.04)µM vs. 1.16(0.05)µM respectively), p<0.01(Figure 46).

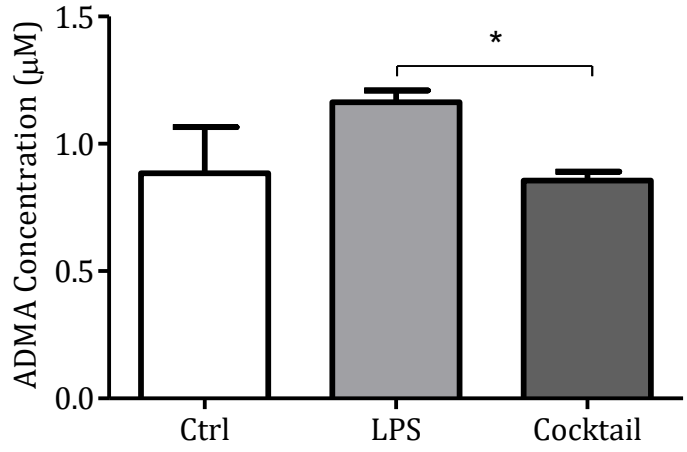

Figure 46: Accumulation of medium ADMA in cells incubated with LPS and a pro-inflammatory cocktail.

Medium ADMA was collected and measured using mass spectrometry at the end of eight hour incubation with LPS or a pro-inflammatory cocktail. ADMA concentration was significantly lower in inflammatory cocktail treated cells compared to cells exposed to LPS, p<0.01.

Accumulation of SDMA in the medium of RAW cells cultured in control, cocktail and LPS only conditions revealed no significant differences between the groups, p=0.54 by one way ANOVA (Figure 47). L-NMMA could not be analysed for technical reasons.

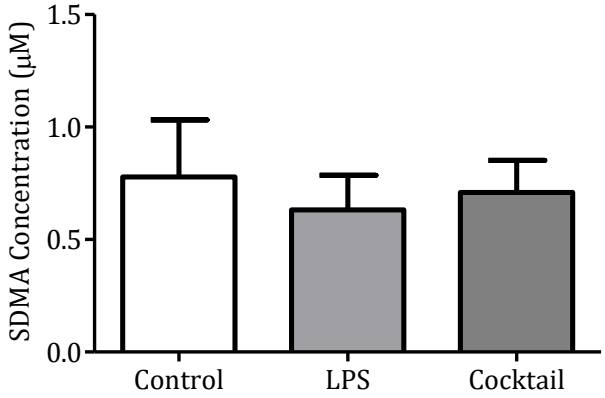

Figure 47: Accumulation of SDMA in culture medium of RAW 264.7 cells incubated with LPS, a pro-inflammatory cocktail or control.

Medium SDMA was collected and measured using mass spectrometry at the end of eight hour incubation with LPS or a pro-inflammatory cocktail. ADMA concentration was unchanged in inflammatory cocktail and LPS treated cells compared to controls, p=0.54.

In contrast with the previous observation that exogenous ADMA treatment reduced NOx synthesis in response to LPS, ADMA treatment at 100µM had no significant impact on NOx production in cells exposed to the pro-inflammatory cocktail, mean(SD) 28.4(4.6)µM vs 25.7(3.3)µM respectively, p=0.23 (Figure 48). A dose escalation study confirmed the observation that there was no impact of increasing doses of ADMA on NOx synthesis following cocktail incubation, p=0.85 (one way ANOVA) (Figure 48).

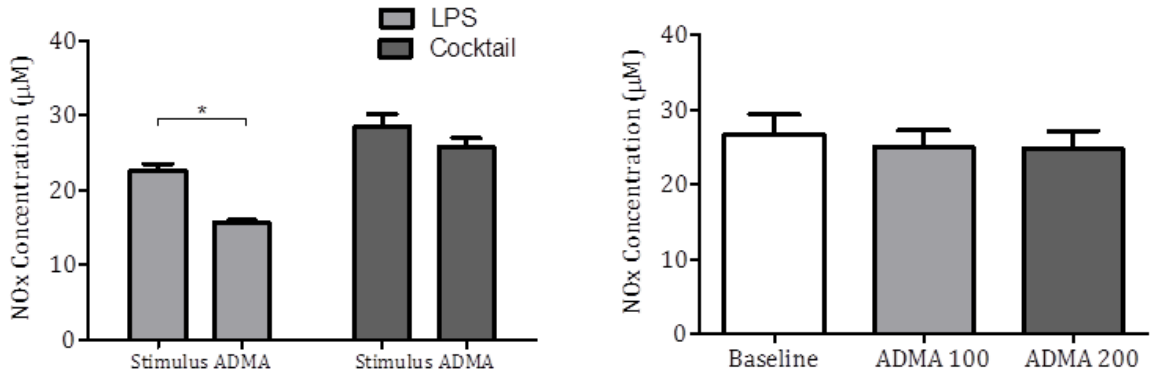

Figure 48: The impact of exogenous ADMA administration on NOx synthesis in cells treated with LPS or a pro-inflammatory cocktail.

Left panel: Comparison of the effect of exogenous ADMA (100µM) on NOx synthesis following stimulus of RAW 264.7 cells with either LPS or a pro-inflammatory cocktail. ADMA significantly reduced NOx synthesis in LPS treated cells ($p<0.01$) but had no effect on cocktail treated cells (p=0.23). Right panel: Increased doses of ADMA has no effect on NOx synthesis in cells treated with a pro-inflammatory cocktail, p=0.85. ADMA 100µM (ADMA 100) and ADMA 200µM (ADMA 200).

In order to ensure that supraphysiological L-arginine concentration in culture medium was not responsible for the apparent lack of activity of ADMA on cocktail treated cells, a study of 3 concentrations of L-arginine was undertaken. Doses ranged from a near physiological 100µM to normal medium concentration of 300µM. Simultaneously, a comparison of two doses of ADMA was conducted. ADMA at 50µM and 100µM did not have any effect on iNOS activity in cocktail treated cells regardless of medium L-arginine concentration , although an increase in NOx synthesis was observed in a dose dependent fashion as L-arginine concentration increased (Figure 49).

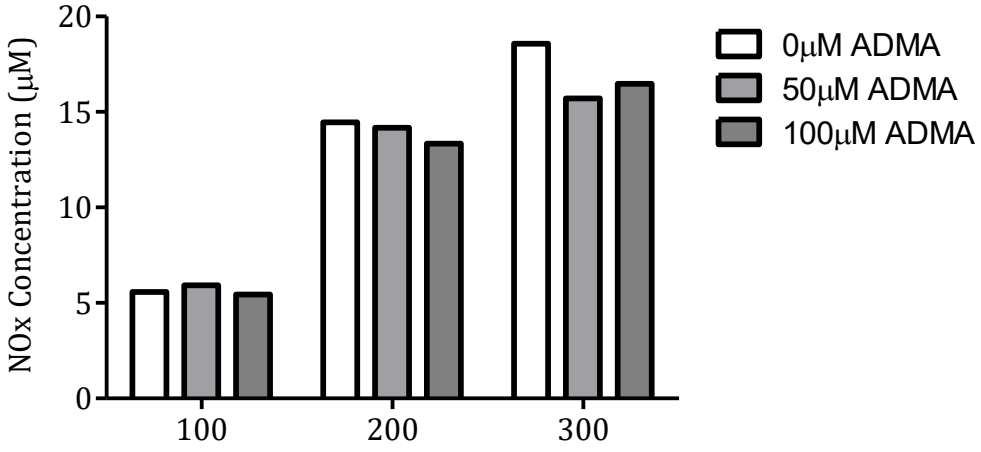

Figure 49: The impact of varied two doses of exogenous ADMA on inflammatory cocktail treated cells cultured in medium with differing L-arginine concentrations.

RAW 264.7 cells were incubated in culture medium containing L-arginine at three concentrations 100μM (100), 200μM (200) and 300μM (300). Co-administration of a pro-inflammatory cocktail and either 0, 50 or 100μM ADMA. Increasing the L-arginine concentration resulted in a dose dependent increase in NOx synthesis, ADMA had no apparent effect on the synthesis of NOx.

5.3.2 The regulation of DDAH2 by Interferon-γ

A comparison of different components of the pro-inflammatory cocktail was undertaken in order to explore the different responses observed between LPS alone and the cocktail conditions. A significant reduction in mean(SD) cell lysate ADMA concentration was observed following IFN-γ (0.55(0.07)pmol/mg protein and cocktail (0.59(0.06)pmol/mg protein) conditions compared to LPS treatment alone (0.66(0.05)pmol/mg protein, $p<0.01$ and 0.03 respectively (Figure 50). Cell lysate SDMA concentration was unchanged across the treatment groups ($p=0.71$ by one way ANOVA)(Figure 51).

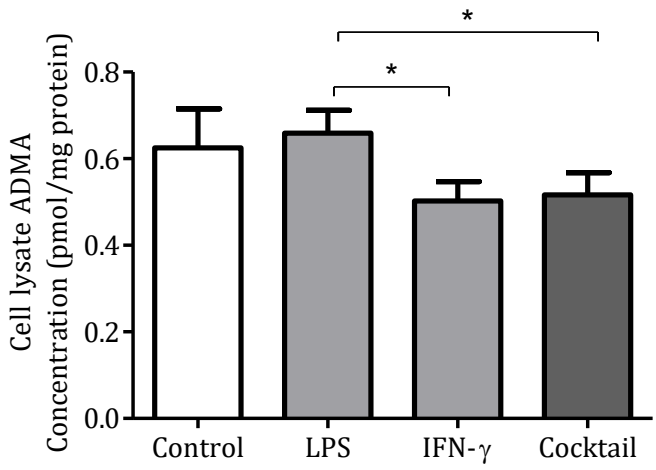

Figure 50: The impact of incubation with a combination of stimuli on cell lysate ADMA concentrations.

The cell lysate ADMA concentration of cells treated with LPS, IFN-γ or the pro-inflammatory cocktail was assessed using mass spectrometry. Significant reductions in lysate ADMA were observed following incubation with IFN-γ alone or cocktail conditions ($p<0.01$ and $p=0.03$ respectively).

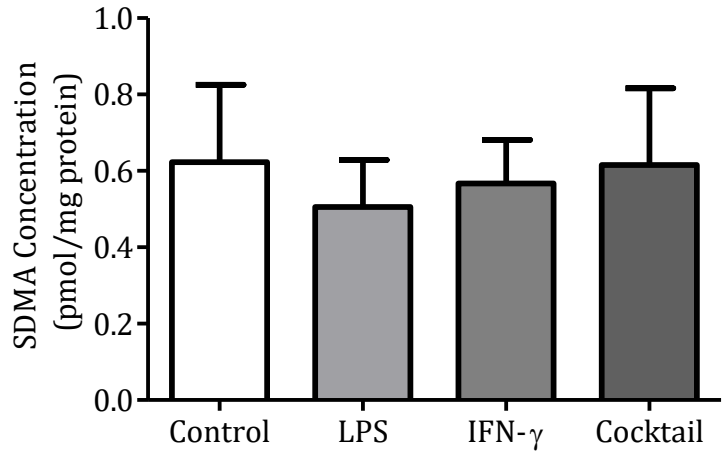

Figure 51: Cell lysate SDMA concentration following stimulus with LPS, IFN-γ or a pro-inflammatory cocktail.

The cell lysate SDMA concentration of cells treated with LPS, IFN-γ or the pro-inflammatory cocktail was assessed using mass spectrometry. No significant differences were observed between the groups ($p=0.71$) by one way ANOVA.

iNOS mRNA was differentially induced by the treatments, however as observed previously cocktail conditions induced greater iNOS induction that LPS alone. IFN-γ however also demonstrated a trend towards increased expression following incubation with RAW cells, mean(SD) 78.9(23.3) fold increase (p=0.13 compared to LPS) (Figure 52).

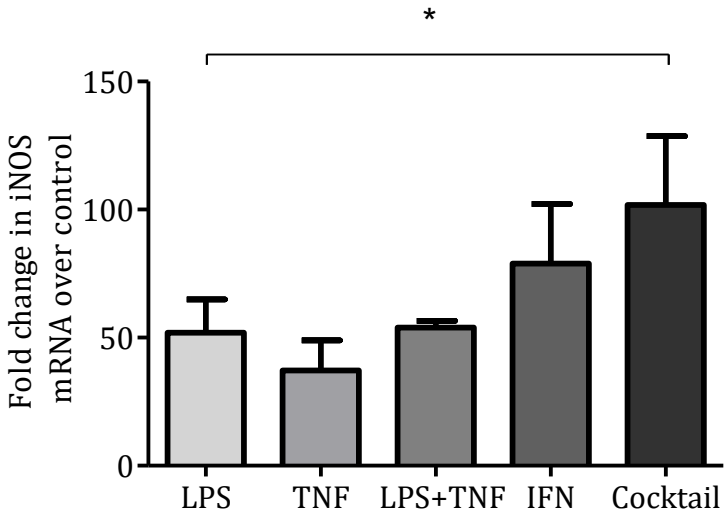

Figure 52: The impact of a range of pro-inflammatory stimuli on iNOS mRNA expression.

Fold change in iNOS mRNA was measured following eight hour incubations with a series of pro-inflammatory stimuli (LPS, IFN-γ, TNF-α) as well as LPS+ TNF-α and all three together (cocktail). Significantly greater iNOS induction was observed in cocktail treated cells($p<0.01$).

DDAH2 mRNA was induced to a similar degree in IFN-γ and cocktail conditions (mean (SD) 1.29(0.14) fold and 1.39(0.09) fold over control cells respectively, $p<0.01$ for either treatments compared to control or LPS alone after an eight hour incubation(Figure 53).

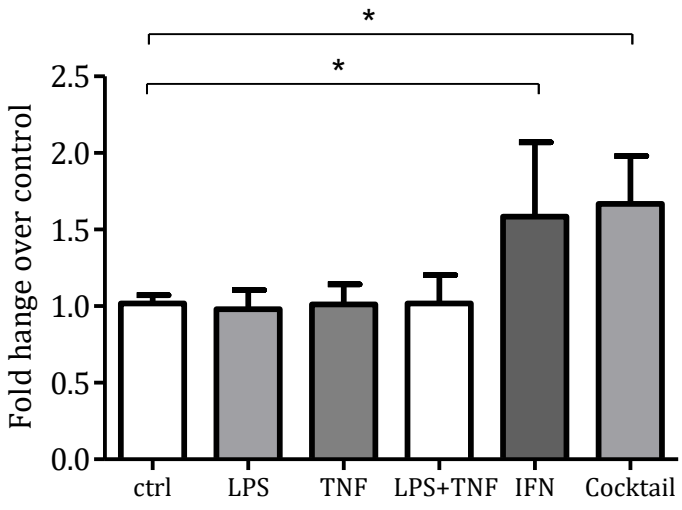

Figure 53: Change in DDAH2 mRNA expression following incubation with a range of pro-inflammatory stimuli.

Fold change in DDAH2 mRNA was measured following eight hour incubations with a series of pro-inflammatory stimuli (LPS, IFN-γ, TNF-α) as well as LPS+ TNF-α and all three together (cocktail). Significantly greater DDAH2 induction was observed in IFN-γ and cocktail treated cells($p<0.01$).

Time course analysis revealed dynamic iNOS mRNA expression and that DDAH2 mRNA appeared to follow a similar pattern over the twenty four hour study period (Figure 54).

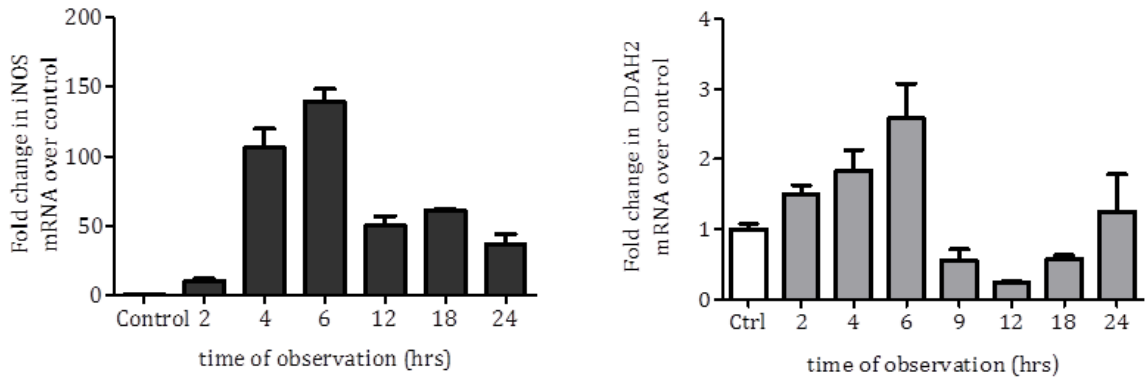

Figure 54: Time course analysis of the relationship between iNOS and DDAH2 mRNA expression over 24 hours of IFN-γ treatment.

Cell lysate was collected from cells incubated with IFN-γ at a series of time points over a 24 hours period. iNOS (left panel) and DDAH2 (right panel) mRNA were determined at each time point. Fold change compared to untreated control cells at 24 hours and normalised to 1.

5.3.3 The Janus Kinase(JAK)/ Signal Transducer and Activator of Transcription(STAT) pathway of DDAH2 transcription

In order to understand the mechanisms of the apparent IFN-γ mediated upregulation of Ddah2, a number of mechanistic studies were undertaken. The canonical IFN-γ signalling pathway was explored through inhibition of the key cellular signalling component Janus tyrosine Kinase (JAK)(Figure 55). The three isoforms of this enzyme can be specifically inhibited with CAS 457081-03-7[313] (Merck Millipore, Herts, UK). This agent has a high sensitivity for the JAK enzymes and a dose response experiment revealed that a dose of 4μM obtunded IFN-γ mediated NO synthesis completely and so this dose was used for further experiments. Co-incubation of this agent with IFN-γ or pro-inflammatory cocktail resulted in the abolition of the effects of interferon treatment on Ddah2 expression, $p=0.38$ by two way ANOVA (Figure 56).

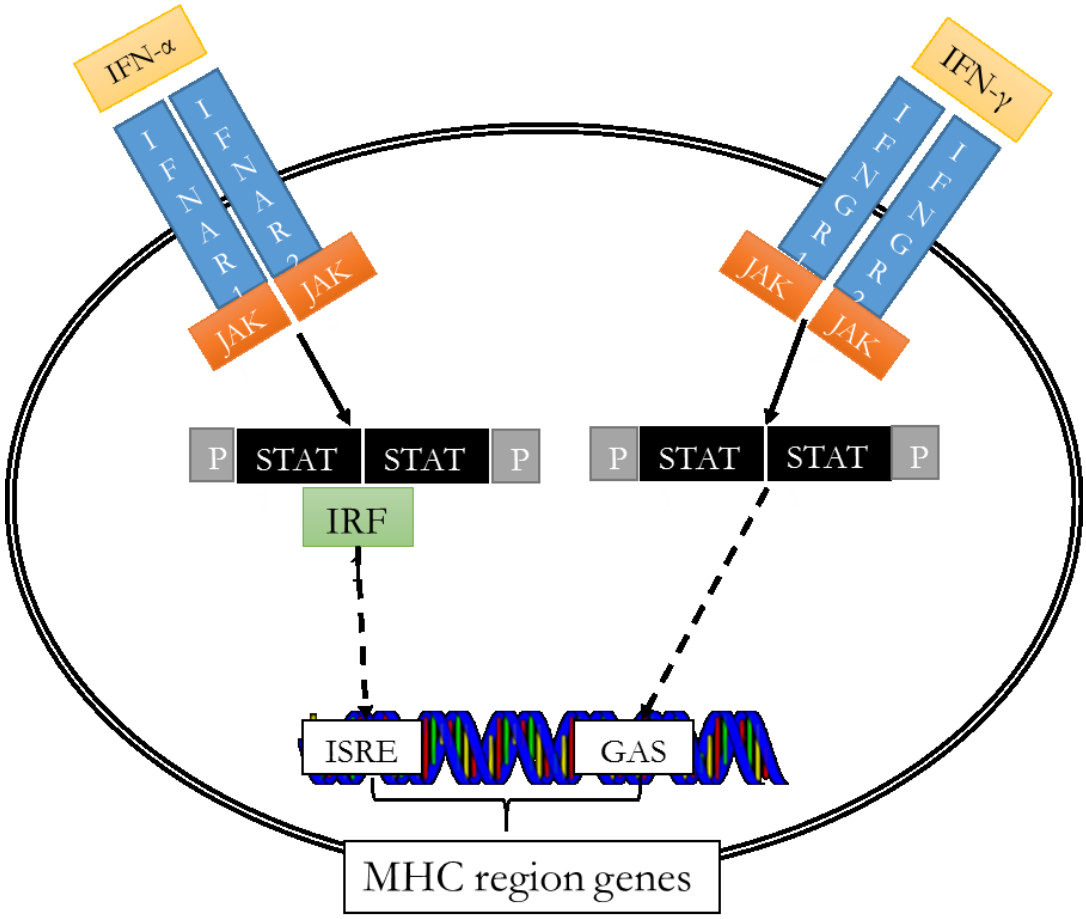

Figure 55: Schematic representation of the canonical Type I and II interferon signalling pathway.

Interferon-γ(IFN-γ) binds to the heterodimeric receptor interferon gamma response element (IFNGR 1 and 2). This activates constitutive Janus Kinase (JAK) which phosphorylates Signal Transducer and Activator of Transcription(STAT) and directly activates Gamma Activated Sites (GAS) in the promoter regions of a number of regions including the major histocompatibility complex (MHC). Interferon α (IFN- α)and β(not shown) bind to the heterodimeric receptor interferon alpha response element (IFNAR 1 and 2). This activates constitutive Janus Kinase (JAK) which phosphorylates Signal Transducer and Activator of Transcription(STAT) and stimulates Interferon Regulatory Factor to bind to the Interferon sensitive response element of target promoter regions.

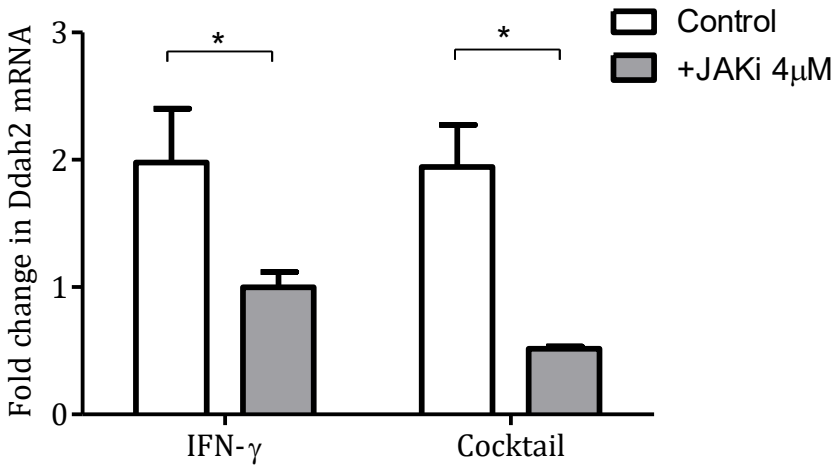

Figure 56: the impact of Janus Kinase inhibition on the increase in DDAH2 mRNA expression mediated by IFN-γ or pro-inflammatory cocktail treatment.

RAW 264.7 cells were incubated with either by IFN-γ or pro-inflammatory cocktail. Treatment groups were co-incubated with a Janus Kinase inhibitor at 4μM. Cells lysate was analysed for fold change in DDAH2mRNA expression and compared to untreated control cells which were normalised to 1.

The co-incubation of IFN-γ with Cycloheximide ($C_{15}H_{23}NO_4$) (Sigma, UK) had no impact on IFN-γ mediated increase in Ddah2 mRNA level. This suggests that the signalling pathway that increases Ddah2 expression does not require protein translation[314] for efficacy (Figure 57), p=0.70.

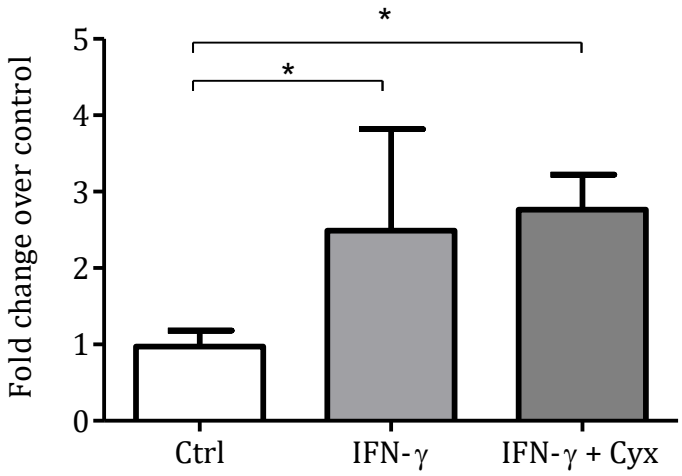

Figure 57: The impact of cycloheximide co-incubation on IFN-γ mediated induction of DDAH2 mRNA.

Raw 264.7 cells were incubated in either IFN-γ alone or in combination with the inhibitor of translation cycloheximide. The co-administration of cycloheximide had no impact on the induction of DDAH2 mRNA synthesis. Comparison made to untreated controls and normalised to 1.

5.3.4 Activation of the Human DDAH2 promoter

A number of potential sites of direct activation of the Ddah2 promoter were identified by interrogation of consensus promoter sequences[315]. These included Interferon Regulatory Factor 1 (IRF1) and Signal transducer and activator of transcription sites. Electroporation was used to successfully transfect RAW264.7 cells with a group of promoter reporter constructs in order to explore this hypothesis. A high degree of successful transfection was achieved using the Nucleofector™ system. This was demonstrated by using a proprietary GFP promoter construct to explore the efficiency of electroporation as described above. Success was defined by GFP positivity at 12 hours (Brightfield image and GFP image, Figure 58).

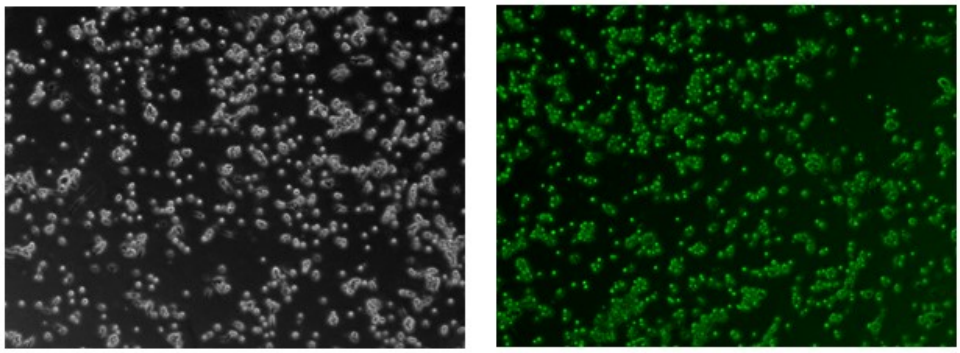

Figure 58: Representative bright field and Fluorescence images of RAW264.7 cells electroporated with DDAH2 promoter and GFP control vectors.

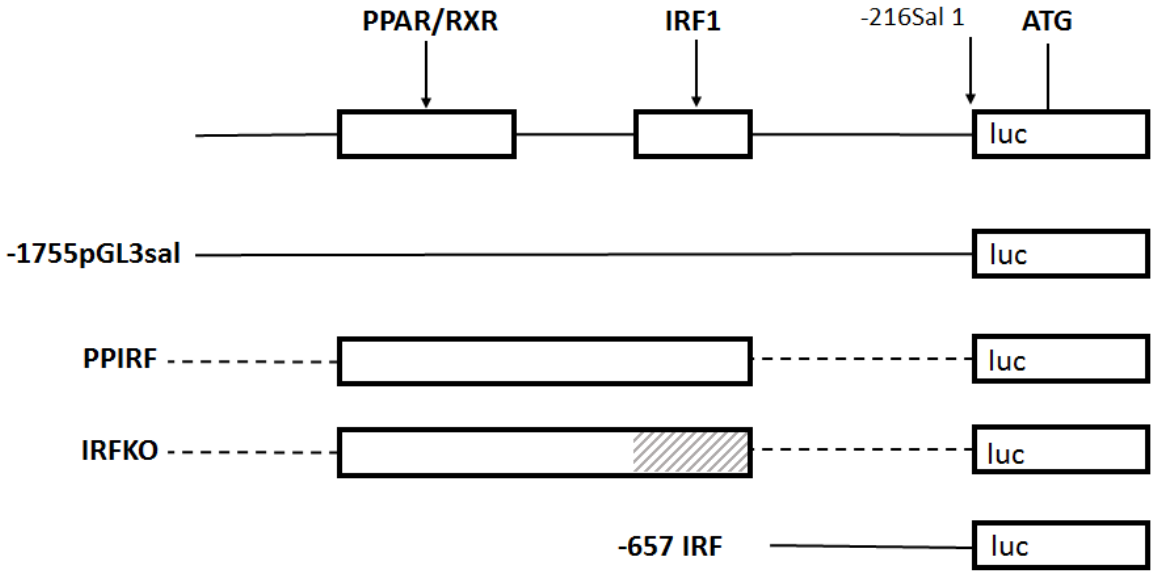

Figure 59: Representative image of DDAH2 promoter constructs used in the exploration of IFN-γ signalling.

Top image represents a stylised representation of the DDAH2 promoter sequence with postulated PPAR and IRF1 transcription factor binding sites highlighted. The second image represents the control promoter sequence containing the whole sequence. The third image represents the PPRIF promoter, with a section of the promoter sequence containing the PPAR and IRF1 transcription sites only present. The fourth image describes the IRFKO promoter in which the IRF1 section of the PPIRF promoter was replaced with nonsense sequence. The bottom image represents the truncated promoter containing only the sequence proximal to the IRF1 site.

Analysis of the impact of IFN-γ treatment on DDAH2 promoter activity was determined by comparison of the whole promoter region (PGl3sal) to a section of the promoter (PPIRF), containing the PPAR and IRF1 transcription sites only, the IRFKO – made up of the PPIRF section with scrambled sequence in the IRF region or a truncated promoter sequence (IRF) (Figure 59). Reductions were observed in the PPIRF and IRFKO compared to the whole sequence (mean(SD) reductions 38(16)% and 25(5%) respectively and in the truncated sequence 87(1)%, $p=0.01$, $p=0.08$, $p<0.01$ respectively(Figure 60).

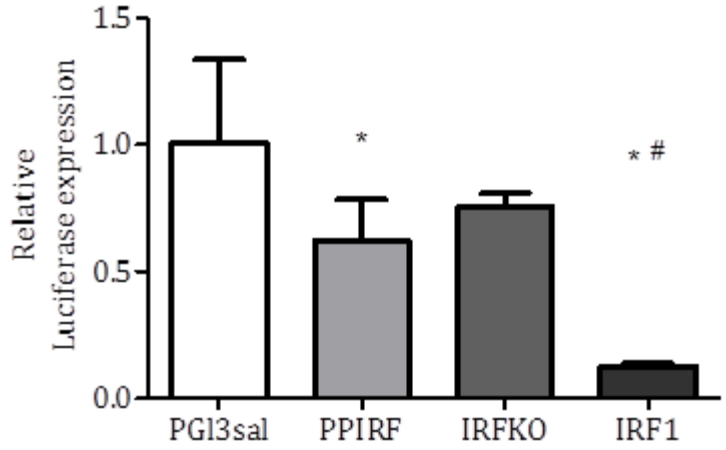

Figure 60: Response of the DDAH2 promoter reporter constructs to IFN-γ stimulus.

Impact of IFN-γ stimulus upon firefly luciferase fluorescent intensity in RAW 264.7 cells transfected with human DDAH2 promoter reporter constructs representing differing regions of the promoter. pGL3sal - whole promoter region synthesised, PPIRF - Active region of DDAH2 promoter construct, IRFKO – PPIRF promoter with nonsense code in the IRF1 region, IRF - downstream region (n=6, *=p<0.05 compared with whole promoter region construct (PGL3sal) #=p<0.05 compared with IRFKO and PPIRF promoter constructs). Results are corrected for transfection efficiency using a dual luciferase reporter assay technique employing *renilla* luciferase.

5.3.5 Polyinosinic Polycytidylic acid

5.3.5.1 *Ex vivo* pilot study

Overnight incubation of isolated wild type primary murine macrophages revealed significant induction of NOx in response to Poly I:C treatment from 1.3(0.2)µM in the medium of control cells and 14.3(1.0)µM in treated medium, $p<0.01$ (Figure 61). Evaluation of cell lysate revealed that in wild type cells, Poly I:C treatment resulted in a fall in medium ADMA accumulation from 0.25(0.05)µM in untreated cells to 0.20(0.02)µM in treated conditions, $p<0.01$ (Figure 61).

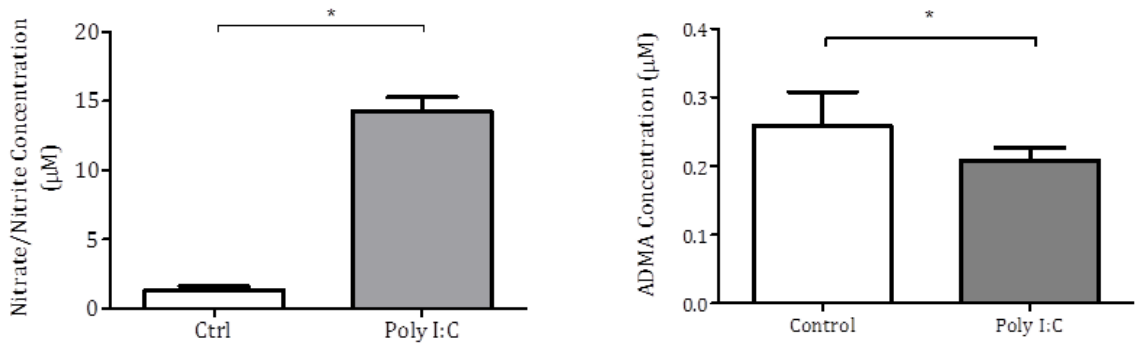

Figure 61: Impact of Poly I:C treatment on NOx synthesis and ADMA accumulation by primary peritoneal macrophages.

Left panel: impact of Poly I:C treatment of isolated primary peritoneal macrophages on Nitrate/Nitrite accumulation in culture medium, p<0.01. Right panel, Change in accumulation of ADMA in medium of primary macrophages treated with PolyI:C and measured using mass spectrometry, p<0.01.

5.3.5.2 The systemic response to Poly I:C administration

Subcutaneous radiofrequency temperature probes were inserted into the scruff of the neck and animals allowed 24 hours recovery period. Six animals of each genotype were allocated to sham injection or intraperitoneal administration of Poly I:C.

Control animals showed no significant variation in temperature over the study period (Mean(SD), 35.3(0.44)°C in floxed controls and 35.3(0.26)°C in Ddah2$^{M\Phi-}$ mice, p=0.97 by two way ANOVA(Figure 62). In animals treated with Poly I:C, both groups showed significant and similar increases in temperature (36.1(0.61)°C in floxed animals and 36.1(0.55)°C in macrophage specific DDAH2 knockout mice, p=0.96 (Figure 62). No significant difference in maximum temperature change was observed across the genotypes, p=0.39 (Figure 63).

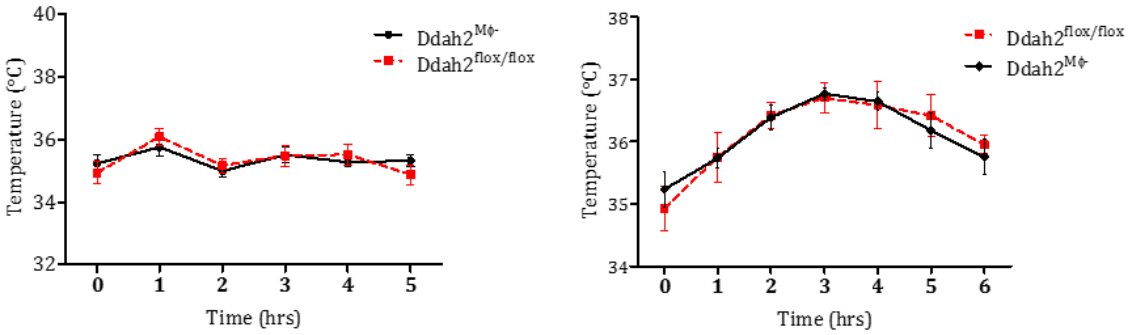

Figure 62: Change in subcutaneous temperature over a six hour time course in macrophage specific knockout and floxed control animals exposed to 12mg/kg Poly I:C injection.

DDAH2 macrophage specific knockout mice or floxed controls were allocated to either sham or Poly I:C groups. Radiofrequency monitoring of temperature was undertaken before injection of both groups and on once per hour thereafter. No change was noted in the temperature of animals in the control group, however both knockout and control mice displayed significant increases in temperature over the course of the study, $p<0.05$ for both groups.

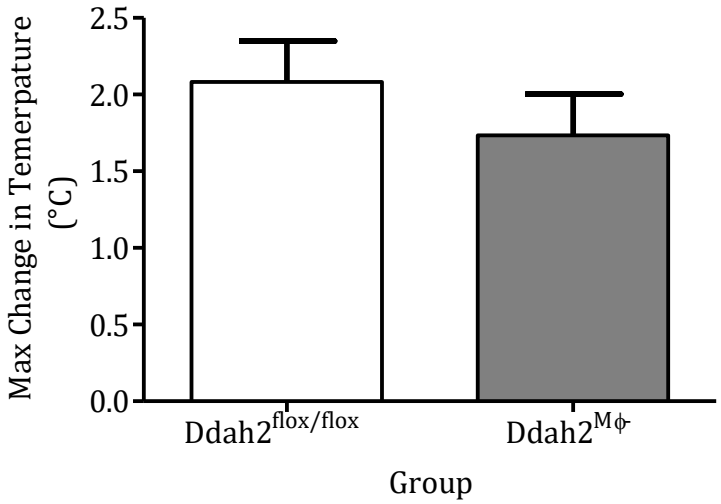

Figure 63: Peak temperature change in macrophage specific DDAH2 knockout and floxed control animals following Poly I:C injection.

Peak change in temperature over baseline in macrophage specific DDAH2 knockout mice and floxed control mice over the course of a six hour observation following Poly I:C injection, no significant difference was observed in the two groups of mice ($p=0.39$).

Plasma methylarginines were measured in macrophage specific DDAH2 knockout mice and their floxed litter mate controls using established methods. Plasma ADMA concentration was slightly elevated at baseline in Ddah2$^{MΦ-}$ compared to floxed controls (mean(SD) 1.69(0.10)µM vs 1.42(0.12)µM respectively, (p=0.049) but remained unchanged when sham and Poly I:C groups in both knockout (p=0.41) and controls (p=0.54) (Figure 64). Plasma SDMA concentrations were unchanged across genotypes and also in the response to Poly I:C injection, p=0.13 by one way ANOVA(Figure 65). Plasma L-NMMA concentration fell significantly in floxed control animals following Poly I:C treatment, p<0.05 (Bonferroni comparison following one way ANOVA, no fall in L-NMMA was observed in Ddah2$^{MΦ-}$ mice treated with Poly I:C, p=0.94.

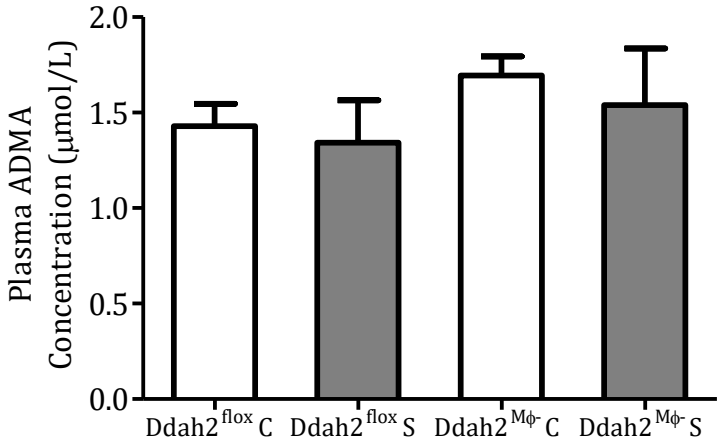

Figure 64: Plasma ADMA concentration in macrophage specific DDAH2 knockout mice and controls in untreated animal and at 6 hours after Poly I:C injection.

Plasma methylarginines were measured using mass spectrometry. Plasma ADMA was increased in sham injected macrophage specific DDAH2 knockout mice (Ddah2$^{MΦ-}$ C) compared to floxed controls (Ddah2^{flox} C), p=0.04. No significant change in ADMA was observed following Poly I:C injection (Ddah2$^{MΦ-}$ S, Ddah2^{flox} S)

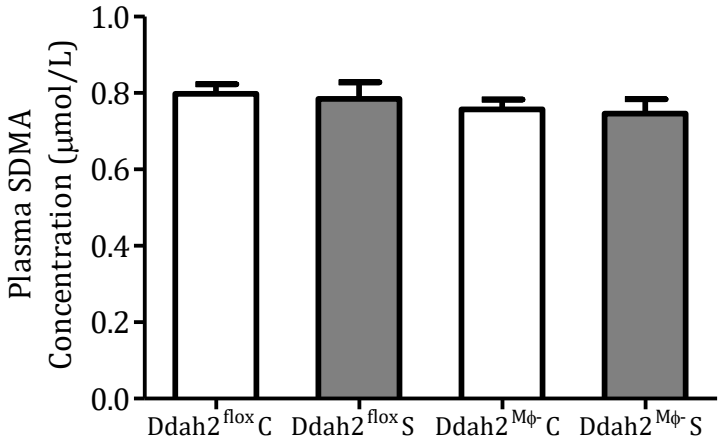

Figure 65: Plasma SDMA concentration in macrophage specific DDAH2 knockout mice and controls in untreated animal and at 6 hours after Poly I:C injection.

Plasma methylarginines were measured using mass spectrometry. Plasma SDMA was unchanged in sham injected macrophage specific DDAH2 knockout mice (Ddah2$^{MΦ-}$ C) compared to floxed controls (Ddah2^{flox} C). No significant change in SDMA was observed following Poly I:C injection (Ddah2$^{MΦ-}$ S, Ddah2^{flox} S)

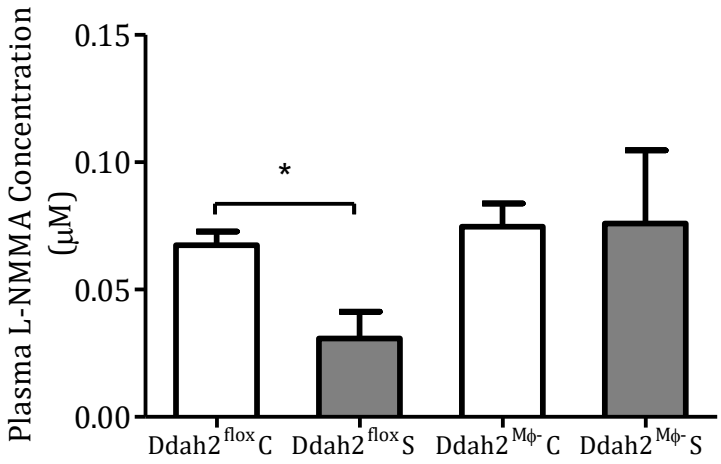

Figure 66: Plasma L-NMMA concentration in macrophage specific DDAH2 knockout mice and controls in untreated animal and at 6 hours after Poly I:C injection.

Plasma methylarginines were measured using mass spectrometry. Plasma L-NMMA was unchanged in sham injected macrophage specific DDAH2 knockout mice (Ddah2$^{MΦ-}$ C) compared to floxed controls (Ddah2^{flox} C). No significant change in SDMA was observed following Poly I:C injection in macrophage specific knockout mice (Ddah2$^{MΦ-}$ S) but a significant fall was observed in floxed control animals injected with Poly I:C, $p<0.05$ (Ddah2^{flox} S).

Plasma cytokines were examined using enzyme linked immunosorbent assay (ELISA) techniques. IL-6 was 253(114)pg/ml in floxed animals compared to 194(49)pg/ml in knockout mice, p=0.47. IL-10 levels were similar in $Ddah2^{flox}$ animals (mean(SD)) 163(66)pg/ml compared to $Ddah2^{M\Phi-}$ 140(43)pg/ml, p=0.67. IFN-γ was significantly elevated in knockout mice (11.13(6.4)pg/ml) compared to (0.67(0.57)pg/ml in floxed controls, p<0.01(Figure 67).

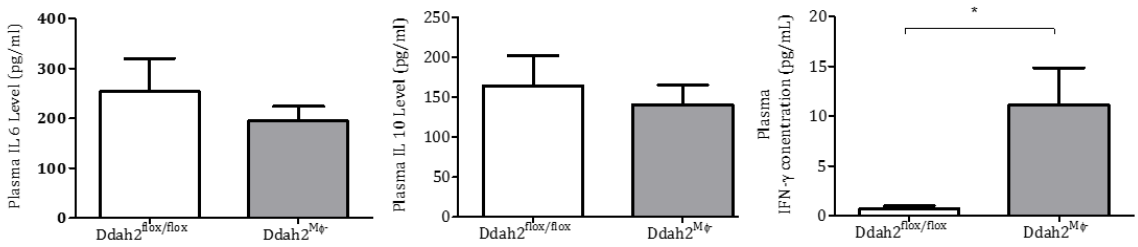

Figure 67: Impact of Poly I:C injection on plasma cytokine expression.

Plasma from mice treated with Poly I:C was compared to plasma of control mice using ELISA analysis of cytokine expression. No significant differences were observed between the control and treated mice in IL-6 or IL-10 expression. Significant increase was observed in IFN-γ expression in macrophage specific DDAH2 knockout mice ($Ddah2^{M\Phi-}$) compared to floxed controls ($Ddah2^{flox}$), p<0.01.

5.4 Discussion

5.4.1 Induction of Ddah2mRNA transcription in murine cells by IFN-γ

This study shows for the first time that a cytokine which is a well-established regulator of the NOS signalling cascade is also a regulator of DDAH2 expression in a murine macrophage cell line, and offers further evidence that in the context of an acute inflammatory response, upregulation of DDAH2 by IFN-γ is a potential mechanism by which this stimulus is able to induce NO synthesis by immune cells. By reducing the amount of ADMA in the cell, DDAH2 limits the ability of ADMA to compete with L-arginine at the NOS binding site and therefore results in greater NO synthesis in response to the stimulus.

It is of note that the change in Ddah2 mRNA expression observed in the course of a 24 hour incubation followed a similar pattern to that seen in iNOS mRNA. This suggests that the regulation of these two enzymes, both of which have a role controlling NO synthesis in response to inflammatory stress, may have similar regulatory pathways. This may in part also explain why NO synthesis does not appear to consistently match the degree of NOS expression in activated immune cells[316].

Further to the observation that IFN-γ is able to induce Ddah2 mRNA transcription is the finding that it is not the case that either LPS or TNF-α have any effect on DDAH2 expression. Whilst only performing a limited screen, this may in part explain differences observed in experimental models of the inflammatory response and the inconsistent relationship between these and studies of more complex polymicrobial insults[317].

5.4.2 Activation of the DDAH2 promoter

It has been shown previously that the human DDAH2 promoter may be stimulated with retinoic acid[226], however no studies to date have demonstrated the regulation of DDAH2 transcription using a physiological stimulus. Here we show that IFN-γ stimulates transcription of DDAH2 mRNA via its canonical signalling pathway and activation of at least two sites on the human promoter. One of these postulated sites lies within the PPIRF due to the partial reduction in luciferase activation seen when this region only is stimulated. The binding site is unlikely to be the in the IRF1 region however as replacing the IRF1 sequence within the PPIRF promoter with nonsense has no significant impact on the degree of luciferase expression observed. The second binding site for IFN-γ mediated transcription appears to lie proximal to the PPIRF region since the whole promoter demonstrates higher levels of activity compared to the PPIRF region alone and the promoter that represented the region distal to the IRF1 site had negligible response to IFN-γ stimulus. Interrogation of the Matinspector™ database (www.genomatix.de/online_help/help_matinspector.html) revealed predicted STAT1 binding sites within the PPIRF region and also proximal to this as predicted by the promoter reporter constructs (Figure 68)[315].

This experiment relies upon inserting the human promoter sequence into the murine macrophage cell line RAW 264.7 and utilising the cells own signalling machinery to initiate transcription factor binding to the promoter. Whilst the promoter sequences of the two species are somewhat different, the IFN-γ/JAK/STAT pathway is well conserved across species.

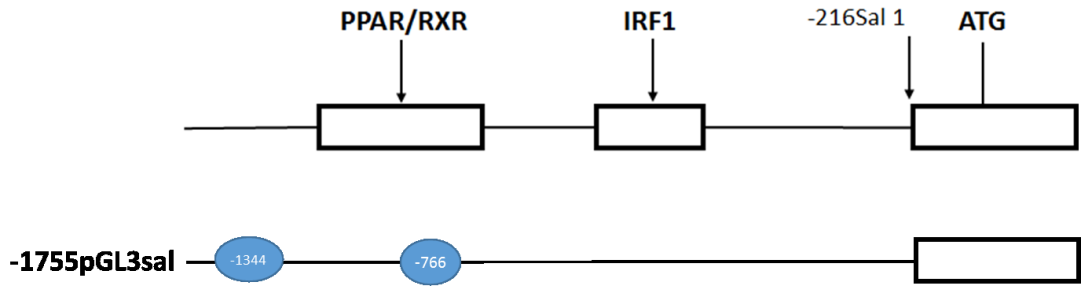

Figure 68: Postulated STAT1 binding sites in the human DDAH2 promoter sequence.

Interrogation of the matinspector™ website https://www.genomatix.de/online_help/help_matinspector/matinspector_help.html) revealed possible transcription factor binding sites for STAT1 on the forward and reverse sequences within the PPIRF region and also distal that that section in the DDAH2 promoter (blue boxes).

The choice of RAW 264.7 cells for this project is a pragmatic one. Whilst initially challenged, there is extensive evidence that human macrophages produce considerable amounts of NO in response to stimulus via an iNOS mediated mechanism[318]. However in cell culture models, human monocyte cell lines must first be differentiated into the mature macrophages of interest which results in upregulation of iNOS at baseline and also cellular stress that impairs the response of the cells to the experimental intervention.

5.4.2.1 Interferon-γ signalling

IFN-γ modulates a number of immune responses including viral clearance and the early response to viral infection. Impaired function of the signalling pathway is associated with increased susceptibility to viral infection[319]. In addition to the anti-viral role, IFN-γ has been implicated in a range of autoimmune diseases such as systemic lupus erythematosus[320], multiple sclerosis[321] and diabetes[322].

Named because they were discovered through their action inhibiting viral replication[323], the interferons are divided into two classes, the Type I which include up to twenty subtypes of IFN-α and IFN-β and the type II which contains only IFN-γ[324]. IFN-γ is secreted by a broad range of immune cells and synthesis is controlled by pro-inflammatory cytokines such as IL-12 and IL-18 and negatively regulated by IL-4 and IL-10[325]. This process facilitates the link between IFN-γ and the innate response[326].

The interferon gamma receptor (IFNGR) is formed of two components (IFNGR1 and IFNGR2) which are both constitutively expressed but lack the intrinsic signalling machinery to facilitate signal transduction. The IFNGR1 intracellular domain contains binding elements for both Janus Tyrosine Kinase (JAK)1 and signal transducer and activator of transcription (STAT)1. Both of these are required for induction of the induction of downstream activity.

Binding of IFN-γ to the IFNGR complex results in phosphorylation and activation of JAK1 and JAK2 which in turn allows the IFNGR1 to form two docking sites for STAT1. The recruitment and phosphorylation of a pair of latent STAT1 proteins results in the translocation of the STAT1 homodimer into the nucleus of the target cell[327]. Binding of this group to Gamma Activation Site (GAS) sequences on target genes results in either activation or suppression of transcription[325, 328].

IFN-γ has been previously shown to be an potent regulator of a range of class I and II MHC region molecules including iNOS[329]. In addition, it plays a role in regulating cell growth by protecting against pathogen induced apoptosis and proliferation[330]. The microbiocidal activity of IFN-γ includes the induction of NADPH oxidase, upregulation of lysosomal enzymes and importantly priming of macrophages for NO synthesis[331].

5.4.3 Polyinosinic polycytidylic acid

It is well established that IFN-γ plays an important role in modulating the response to viral infection. Therefore given the impact that had been observed of IFN-γ on immune cell DDAH2, an experiment was conducted to understand whether the viral ‘mimic’ Poly I:C led to differing systemic responses in mice deficient in DDAH2 within macrophages when compared to their floxed litter mate controls. Using this ‘upstream’ stimulus allowed the exploration of a more physiological model compared to the administration of single cytokines alone.

In isolated cells, Poly I:C led to significant induction of NO synthesis and, like IFN-γ alone led to a significant reduction in ADMA accumulation within the cell culture medium.

The intraperitoneal injection of Poly I:C led to pyrexia consistent with previous experiments[239] and was similar in both genotypes. The impact of the stimulus on plasma indices of methylarginine metabolism was measured and no significant differences were seen following treatment with Poly I:C in either genotype. A small elevation over controls was seen in macrophage specific knockout mice compared to floxed controls at baseline although this was small and statistical significance was borderline.

SDMA was unchanged in the plasma of these groups of mice at baseline and following treatment consistent with the lack of activity of DDAH2 on SDMA. Interestingly, L-NMMA fell significantly in floxed control mice treated with Poly I:C but not in macrophage specific knockout animals. L-NMMA is metabolised by DDAH2 but due to its relatively low physiological concentrations, is thought to play a less important part in the regulation of NOS activity.

Whilst the animals appeared systemically similar in their responses to Poly I:C injection and levels of the cytokines IL-6 and IL-10 were not significantly different, an interesting observation was that IFN-γ synthesis was elevated almost tenfold in macrophage DDAH2 deficient mice. This, combined with the observation that DDAH2 is regulated by IFN-γ suggests that DDAH2 plays a role in regulating IFN-γ synthesis and also in turn is regulated by it, suggesting a mechanism of synthesis of this pro-inflammatory cytokine that is previously unidentified.

5.4.4 Strengths and limitations

This study was a pragmatic one, exploring in an *in vitro* model the regulation of endogenous inhibitors of nitric oxide synthase in macrophages. This study used a widely validated model of differentiated murine macrophages. This meant that it was unnecessary to differentiate the cells prior to experiment which reduced the degree of baseline inflammatory activation present. This in turn made it possible to identify small differences in NOx synthesis between groups and reliably identify them as due to the intervention being studied. Also, as potent producers of iNOS mediated NO, murine macrophages provide a good model to study subtle signalling changes that affect NO synthesis.

The use of a human promoter reporter construct to validate the observation that murine DDAH2 was induced by IFN-γ provided a degree of translation and offers some confidence that this finding may also be conserved in humans.

This study is limited by the observation that all the findings reported relate to changes in mRNA expression and protein changes are not directly demonstrated. However, work done in hypoxia and presented in a separate chapter does demonstrate that there is a strong relationship between DDAH2 mRNA and protein induction. Also, the downstream physiological effects of increased DDAH2 protein are observed through changes in ADMA concentration, making it unlikely that only mRNA changes have taken place.

Furthermore, this study identifies one potential mechanism for the regulation of ADMA and NO synthesis by IFN-γ. It is possible that other processes including synthesis of ADMA, expression of iNOS and protein translation all contribute to the observed changes in NO synthesis.

This study was conducted in a murine macrophage immortalised cell model, and as discussed previously, there are differences between murine and human macrophages in terms of function and in particular NO synthesis. Therefore extrapolating the downstream effects of changes in DDAH2 expression on these cells to the human immune response may not be representative of the *in vivo* phenotype.

The conduct of a short term Poly I:C study meant that the long term impact of this viral mimic could not be studied. Also, measuring only plasma indices of methylarginine turnover does not preclude tissue specific impacts not reflected in the plasma. In measuring just three cytokines it is possible that other differential impacts on the systemic immune response exist that have not been observed which may contribute to differences in the immune response.

5.4.5 Future work

This results of this study pose a number of questions regarding the regulation of DDAH2 *in vivo* and the impact that this may have in disease states. Future work would involve primary human cells treated with IFN-γ to determine if this effect is conserved across species. In addition it could address the role of other pro- and anti-inflammatory stimuli on DDAH2 expression and explore the impact of these stimuli in combination following inflammatory stress in whole animal models.

In parallel, interrogation of human studies currently underway using IFN-γ as an immunomodulatory agent may answer the question of whether DDAH2 regulation is one mechanism by which it is able to stimulate the immunoparetic patient[332].

Building on the Poly I:C study, further work will explore the role of TLR3 stimulus and viral infection and the endogenous inhibition of NO synthesis, particularly focussing on the apparent co-regulatory mechanism of IFN-γ and DDAH2. Also, longer term studies may reveal a more significant phenotype not seen in the short term study undertaken.

5.4.6 Summary statement

- Unlike LPS or TNF-α, IFN-γ is able to upregulate the expression of DDAH2 which results in reduced ADMA concentrations and facilitates increased NO synthesis in a tissue culture model of macrophage activity.
- IFN-γ mediated transcription of DDAH2 mRNA is mediated by the canonical JAK/STAT pathway in murine macrophages.
- Treatment with IFN-γ of RAW 264.7 cells electroporated with human DDAH2 promoter reporter constructs demonstrates that the human DDAH2 promoter has two regions that contain plausible STAT1 binding sites which may mediate activation of the promoter.
- Systemic administration of Poly I:C results in differential synthesis of IFN-γ by mice deficient in DDAH2 within macrophages compared to floxed litter mate controls.

6 The role of global and macrophage specific knockout in polymicrobial sepsis

6.1 Introduction

6.1.1 Transgenic techniques

Two distinct transgenic techniques were used in this study in order to develop the global DDAH2 knockout ($DDAH2^{-/-}$) and the DDAH2 macrophage specific ($DDAH2^{M\Phi-}$) mice, high throughput gene trapping and the LoxP Cre recombinase methods respectively. These techniques generate with a high degree of reliability, DDAH2 knockout in the whole animal or in macrophages. Importantly, correct choice of control animals is essential, and in studies presented here, $DDAH2^{-/-}$ mice were compared to wild type litter mate controls ($DDAH2^{+/+}$) and $DDAH2^{M\Phi-}$ mice were compared to floxed litter mate controls ($DDAH2^{flox/flox}$).

6.1.1.1 Generation of DDAH2 global knockout mice

The high throughout gene trapping strategy used in the development of the $DDAH2^{-/-}$ mice has been described previously[233] and was used to develop heterozygous DDAH2 null animals which were secured from the Texas institute of genomic medicine (http://tigm.org/technologies.html).

In brief, embryonic stem (ES) cells are infected with a retroviral vector which contains two active regions which preferentially insert at the 5' end of genes. The first is made up of a splice receptor sequence, an antibiotic marker (Neomycin) and a polyadenylation (pA) signal. Following infection, a fusion fragment is created which contains a 5' fragment of the target gene, the antibiotic marker and pA signal within the target gene. This process facilitates identification of ES cells which have undergone successful retroviral integration.

The second active region of the viral vector is made up of an ES cell active promoter, e.g. mouse phosphoglyceratekinase (Pgk), a marker exon such as Bruton's tyrosine kinase (Btk) and a splice donor signal(SD). Splicing of the vector from the SD as far as the exons downstream of the insertion site results in a fusion transcript that can be readily identified using high throughput PCR screening. This is then used to reveal the location of the inserted sequence within the gene. The Btk exon contains termination codons that prevent translation of downstream transcripts. In this case, the DDAH2 gene was disrupted through the insertion of a 5kb viral gene trap into the first exon of the gene.

Once identified, ES cells containing the new recombined sequence without a functional DDAH2 gene were injected into developing embryos which, if successful, results in a chimeric foetus. If a fertilised oocyte taken from one of these chimeric populations reaches term, heterozygotes will be created of the target genotype. Selective breeding of these heterozygote animals will then result in wild type, homozygote knockout and heterozygote animals (Figure 69).

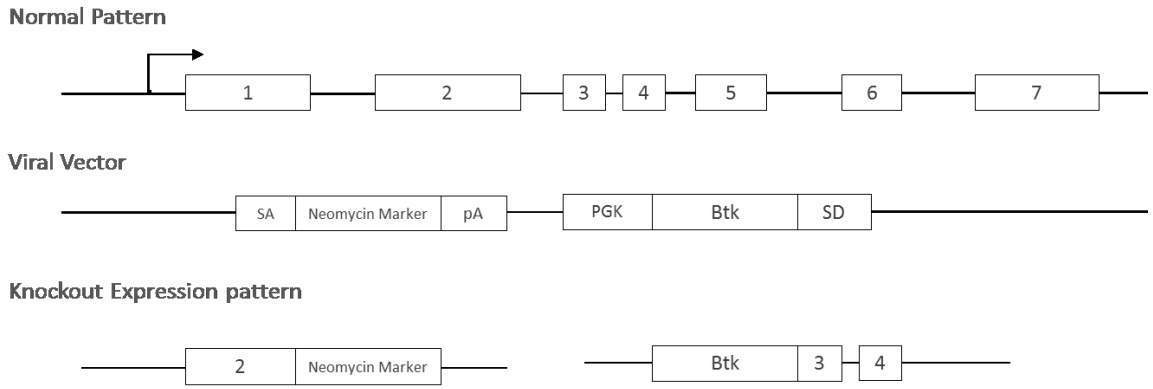

Figure 69:Schematic representation of the high throughput gene trapping strategy used in the development of the DDAH2 global knockout mouse.

The normal intronic pattern of DDAH2 is displayed with the conventional translation start site marked. At the 5' end of the viral vector is a neomycin marker and a polyadenylation signal (pA). The second part of the vector is a stem cell promoter, marker exon and a splice donor signal. Following vector insertion, a 5kb section of nonsense sequence was inserted into the first exon resulting in disruption of the sequence and loss of function. Btk: Bruton's tyrosine kinase, Pgk: phosphoglyceratekinase, SD: splice donor signal

6.1.1.2 Generation of the macrophage specific knockout mouse

The generation of a macrophage specific knockout mouse model is possible because unlike humans, mice express two types of lysozyme genes, M and P. A highly specific LysM Cre strain has been developed that delivers around 90% deletion of LoxP flanked target genes in macrophages, 100% in granulocytes but normal expression in other immune cells. With the development of CRISPR Cas9 technology, alternative methods may become available however at present, the LysMCre method provides the most effective tool for work in this area. In this technique, a site specific DNA recombinase (Cre) expressing animal is bred with mice with LoxP sites flanking the target gene. This results, depending on the orientation of the LoxP sites, in cleavage of the gene in tissues expressing LoxP only. This produces, a Cre LoxP mouse in which the original target gene is disrupted (Figure 70).

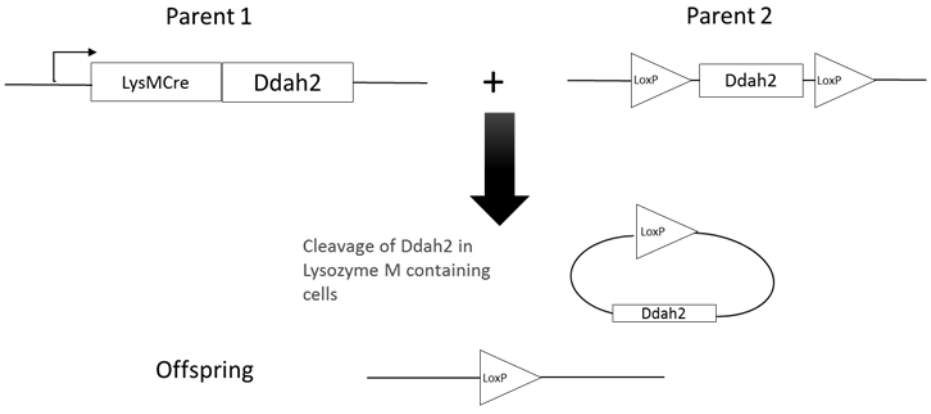

Figure 70: Schematic representation of the development of the LoxP Cre recombinase model of macrophage specific DDAH2 knockout mice.

Cre-mediated recombination between two LoxP sites results in the splicing of DDAH2 and one LoxP site from the offspring DNA sequence.

6.1.2 Mouse models of sepsis

A number of models are available for the study of sepsis in rodents. They offer a range of mechanism, severity and challenges in safe delivery. Selecting appropriate animal models is critical in undertaking valid studies in this area.

6.1.2.1 Rodent models vs human studies in sepsis

The use of rodents in the study of sepsis has been widely employed for many years to explore the pathophysiology or mechanism of disease or to testing potential therapeutic agents and targets. Significant controversy has arisen surrounding sepsis models due to concern about their validity in pre-clinical testing of novel therapeutics[333, 334]. Over the course of the last twenty years, numerous agents have shown great promise in animal studies, only to prove ineffective in human trials[333, 335]. A number of potential reasons have been cited for the disconnection between successful animal studies and human trials. They include the timing of administration of the agent to be tested, the absence of adequate resuscitation and the lack of adjunctive therapies such as antibiotics. All of these may serve to exaggerate the benefits of an agent in animal models.

Coupled with this are significant differences between rodents and humans in terms of their inflammatory response to sepsis. In a recent study of the impact of inflammatory stress (burns, trauma and endotoxaemia) in rodents and humans, poor correlation was observed between genes upregulated in humans and animals[46]. In the context of NO signalling, these differences are particularly relevant. There is a high degree of conservation across species in terms of genes involved, their regulation and mechanisms of activation, however there are differences in the absolute amount of NO synthesised [336].

In spite of this, the murine models of sepsis can offer significant mechanistic insights into the role of particular genes in the pathophysiological response to disease and whilst absolute differences must be interpreted with caution, the impact of genetic knockout on outcome in disease remains an important tool in the understanding of pathology.

The choice of model is an important part of study design. Models can be broadly divided into two groups, those that rely on non-infective stimuli to mimic the systemic response to infection or those that involve the exposure of the animal to one or more live bacterial species.

6.1.2.2 Non-infective models of the response to infection

The most common stimulus used in studies of this type is bacterial endotoxin (lipopolysaccharide, LPS). Derived from the cell wall of Gram negative bacteria, LPS directly stimulates TLR4[337] and induces, following intravenous or intraperitoneal injection, haemodynamic, haematological and metabolic derangement consistent with sepsis. Unfortunately, this response tends to be short lived, severe in terms of cytokine synthesis and result, after a short hyperdynamic phase in a hypodynamic circulatory state. However, LPS does offer the further advantage that as a model of inflammatory stress, it can also be administered to humans with resultant systemic symptoms, although the dose that must be administered to humans is much less than that required in rodents to generate a similar response[338]. Fundamentally however, this is a non-infective model without the sustained and multifactorial initiating steps that we see in bacterial infection. As such, the use of LPS as a model can only provide limited insights when studying the role of specific genes on the pathophysiological response to infection. It is perhaps for this reason that some agents that were tested using this model were ultimately shown to be ineffective in treating human disease[317].

Polyinosinic polycytidylic acid (Poly I:C) is a further non-infective model of the early response to a TLR3 mediated stimulus. Poly I:C is double stranded RNA (dsRNA), a naturally occurring TLR3 stimulus that mimics a viral infection. It particularly activates the transcription of type 1 interferons, NF-κB and STAT1 which are key mediators of the early anti-viral response[308, 309]. Poly I:C has been widely used in animals and has remained popular since it is both a straightforward and safe technique delivering an alternative route of activation to that of bacterial stimuli. It is rarely fatal, producing a hyperdynamic response lasting hours rather than days before resolution. Of note is that not only is Poly I:C safe for use as an experimental model in humans, it has also been used therapeutically or tested as an immunostimulant to induce a more robust immune response to such diseases as stroke[339], viral infection[340] and various subtypes of neoplastic disease[341].

Zymosan is a fungal cell wall glucopolysaccharide that stimulates TLR2 and causes a sterile, non-infective stimulus which induces the release of reactive oxygen species, cytokines and lysosomal enzymes and results in a sepsis like syndrome[342]. When introduced intraperitoneally, it causes features consistent with peritonitis[343]. Zymosan produces a catabolic state, with reduced muscle mass followed by a clinically relevant recovery phenotype[344] and has been used as a model of the sepsis survivor syndrome[345].

6.1.2.3 Infective models of murine sepsis

There are a number of methods available for inducing bacterial sepsis in rodent models. These include bacterial, viral and fungal infections. Only bacterial modalities will be reviewed here. The simplest of these is the intravenous administration of a live bacterial culture, these models are limited by the absence of a septic focus – a normal finding in human disease - and also the catastrophic nature of the model with animals typically dying within four hours of exposure, making it difficult to detect differences in outcome between genotypes[346].

The administration of live bacteria to model respiratory tract infection has also been undertaken. Models include amongst others, Gram negative infection with Pertussis species[347] and inhalation of pseudomonas species to model respiratory tract infection, particularly as a recurrent stimulus to model the effects of infection on cystic fibrosis models[348]. Challenges of delivery, titrating severity and managing associated respiratory failure in severe limit their employment in septic shock models.

The most common and clinically relevant models of bacterial sepsis in rodents are the peritonitis group of techniques. These can be created using either caecal ligation and puncture (CLP) or its variants[349] or intraperitoneal slurry administration. They involve the exposure of the normally sterile peritoneal cavity to a largely gram negative bacterial load and induce an initial hyperdynamic response consistent with human disease[350]. CLP results in a continuous leak of faecal contents into the peritoneal cavity whereas slurry administration is a one-off injection. The techniques may be modified to titrate the severity of the systemic response and deliver a similar inflammatory state to that seen in humans[351] by altering the amount of caecum ligated, the size or number of perforations or in the case of intraperitoneal slurry, the volume administered.

This study employs the caecal ligation and puncture model with regular, clinically relevant fluid resuscitation to create a septic insult that, in a wild type mouse leads to approximately 50% mortality at 4 days. The model is therefore both clinically relevant and adequately severe.

6.1.3 Haemodynamic monitoring in sepsis models

Haemodynamic monitoring is an important tool in understanding physiology and pathophysiology in transgenic models. Techniques can be divided into non-invasive and invasive approaches.

6.1.3.1 Non-invasive techniques

The primary non-invasive method of haemodynamic monitoring is tail cuff measurement. Analogous to a sphygmomanometer used in clinical practice, the tail cuff is able to record intermittent, awake, non-invasive blood pressure directly measuring systolic and mean arterial pressure and calculating diastolic blood pressure. This technique is useful for long term intermittent monitoring of trends in cardiovascular function[352]. However in conditions such as sepsis where the pulse pressure is narrowed by vasoconstriction of the peripheral circulation and continuous monitoring is an advantage, tail cuff measurements are less useful[353].

6.1.3.2 Invasive assessment of haemodynamics

Invasive techniques used to record blood pressure, cardiovascular and other data can be divided into those that are undertaken during general anaesthesia and those that permit continuous awake recording. All anaesthetic agents have some impact upon cardiovascular function[354] and this must be considered when interpreting measurements undertaken in this way, particularly if a subtle effect is expected.

The most commonly used intermittent monitoring tool is the Millar catheter, a solid state transducer inserted into either the femoral or carotid artery of the mouse[355]. This is the most sensitive and high frequency device available, offering a rapid response and analysis of the arterial pressure waveform. It is however associated with a high morbidity and must be undertaken under general anaesthesia.

Two invasive methods are in common use that permit continuous awake monitoring of haemodynamic function. The first, the fluid filled catheter system requires the insertion of an aortic cannula that is in turn attached to a pressure transducer which may be externalised and attached to a tether. This means that the animal may be conscious and allowed relatively free movement around its cage and permits not only direct continuous monitoring but also the potential to deliver drugs to the animals via the indwelling catheter[356]. This technique is a useful one for continuous monitoring during short studies, however, long term observation using this approach is more challenging.

The second approach, and the one used in the studies presented here is continuous haemodynamic monitoring using an indwelling catheter attached to a radiotelemetry signalling device. This permits continuous monitoring over protracted periods whilst still allowing free movement of the animal within the cage. Using a gel filled catheter in a similar way to that utilised in the fluid filled catheter model, the carotid artery is cannulated and a signalling box sited in the subcutaneous tissues which wirelessly relays the recorded data to a receiving device[357]. Monitoring can be initiated and halted as desired using an externally applied magnet. Limitations of the technique include a mortality associated with insertion even in expert hands of 5-10% and the requirement for a recovery period of at least seven days before continuous monitoring can begin. This is however the gold standard for physiological monitoring in models of this kind.

6.1.4 End point assessment in murine sepsis models

There is a considerable amount of interest in non-mortality end points in sepsis models in mice. Whilst it is important to ensure that any end point selected is predictive of death, a non-mortality end point reduces the degree of animal suffering and also facilitates collection of biological samples including blood. Studies included here use a combination of validated severity score and subcutaneous temperature as robust clinical end points.

6.1.4.1 Clinical assessment of illness severity

A number of scoring tools have been developed to provide a reliable non-mortality endpoint in sepsis models. These scores include a range of clinical observations, the presence, absence or extent of which can be graded[358, 359]. The cumulative score for each of these indices provides an objective assessment of illness severity and offer a threshold for experimental termination. This study employs a five point scale of illness severity validated extensively in sepsis[360-362] which proved to be straightforward and reliable (Table 22). In studies undertaken here, illness severity was assessed by a member of the animal technical team, blinded to the genotype. Scoring was undertaken at least once every eight hours through the study period and upon reaching a score of four, repeated once every hour until a score of five was reached, at which point the severity threshold was considered to have been met. At this point, death was considered inevitable and under general anaesthesia, cardiac puncture for collection of blood was undertaken and the animal sacrificed using schedule one methods.

Characteristic	Scoring range
Hunched	0-1
Bloated	0-1
Conjunctival injection/mucky eyes	0-1
Lack of movement	0-2
Lack of alertness	0-2

Table 22: Characteristics of the score used in the assessment of illness severity in mice with sepsis induced by caecal ligation and puncture.

Based on [362], a score of 1-3 implies mild to moderate sepsis and ≥4 severe sepsis. If a score of 4 was reached, monitoring was undertaken every hour until a score of 5 was detected which heralded schedule one sacrifice.

6.1.4.2 Subcutaneous temperature

In circumstances where non-terminal end points are sought, subcutaneous temperature can be used as an index of illness severity and the development of progressive hypothermia is a predictor of death in murine sepsis[236, 363, 364]. The insertion of a subcutaneous temperature probe into the dorsum of the neck or between the peritoneal and the abdominal walls either some days before surgery or at the time of sepsis induction is a minimally invasive technique which allows the animal to move freely following recovery from anaesthesia. Whilst not offering continuous monitoring, it is readily measureable in the conscious animal without causing distress. Measuring temperature as a secondary end point can offer objective confirmation that the severity threshold determined by blinded assessment is consistent.

6.1.5 Study design

The studies reported here describe a series of experiments exploring the impact of knockout of global and macrophage specific knockout of DDAH2 on survival, haemodynamics and regulators of NO synthesis in sepsis. The model chosen for the induction of sepsis was caecal ligation and puncture (CLP). Each study included eight animals per group (unless otherwise stated) and the length of survival studies was censored at 72 hours following the induction of sepsis in illness severity studies. The duration of other short term assessments of the septic response in knockout mice are described on a per experiment basis in the text.

Specific studies of the pathophysiological response to sepsis include *in vivo* haemodynamics, aortic vascular reactivity, estimation of bacterial load and measures of methylarginines and NO synthesis.

6.2 Results

6.2.1 The impact of DDAH2 knockout at baseline

6.2.1.1 Demonstration of the global knockout of DDAH2

There were no apparent phenotypic differences between the DDAH2$^{-/-}$ and their wild type litter mate controls. At the time of experiment at age 8-10 weeks, weights were similar across the two groups of animals, mean (SD) weight (g): DDAH2$^{+/+}$ 24.3 (2.8) vs DDAH2$^{-/-}$ 24.4 (1.1) p=0.971.

Western blots of kidney, heart and liver tissue homogenates showed complete absence of DDAH2 protein in Ddah2 knockout animals (Figure 71). This was confirmed with formal DDAH2 quantification. DDAH2 Protein was demonstrated in aortic tissue in wild type animals and shown to be absent from knockout mice (Figure 72).

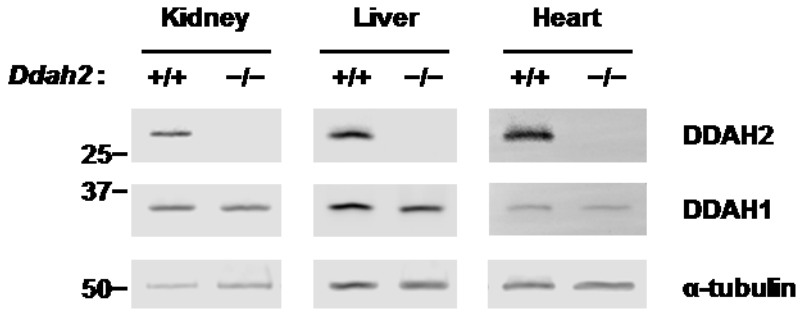

Figure 71: Representative images demonstrating the absence of DDAH2 from kidney, liver and heart tissue homogenates in the global DDAH2 knockout mouse.

Reproduced with permission from Dr Ben Lee.

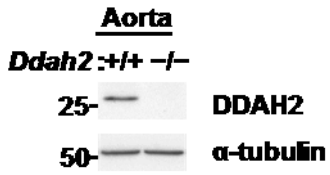

Figure 72: Representative image of the knockout of DDAH2 protein in global DDAH2 knockout mice compared to wild type litter mates.

Reproduced with permission from Dr Ben Lee.

6.2.1.2 Baseline methylarginine concentrations

In the Ddah2$^{-/-}$ animals there were significant changes in tissue methylarginine concentrations compared to Ddah2$^{+/+}$ litter mate control mice. Results are presented as Mean (SD)µmols/mg protein in tissues, µM in plasma measurements and urinary methylarginine concentrations are presented as µM corrected for urinary creatinine, also in µM

In myocardial tissue homogenate, ADMA concentration was elevated 0.89(0.20) vs 0.67(0.13), p=0.02. Mean L-NMMA concentration was unchanged at 0.215 vs 0.213, p=0.97 as was SDMA at 0.10 vs 0.11,p=0.85(Figure 73).

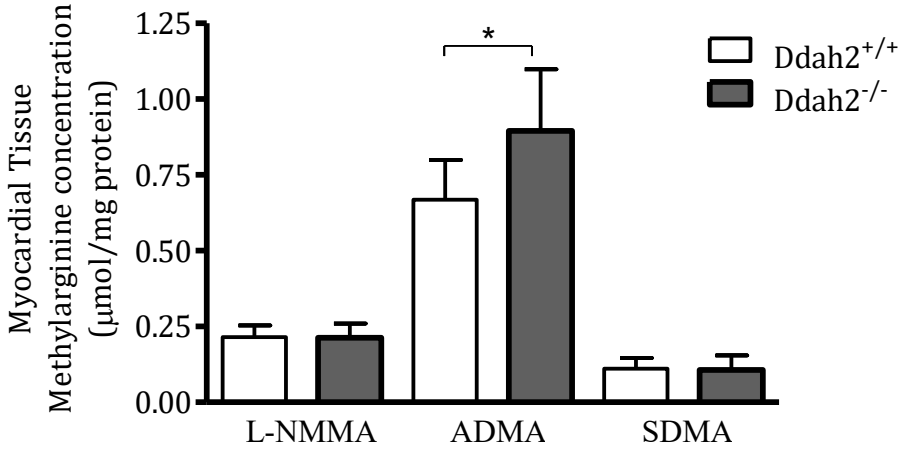

Figure 73: Myocardial tissue methylarginine concentrations in DDAH2 global knockout and wild type litter mate controls.

Tissue homogenates underwent protein extraction followed by methylarginine estimation using liquid chromatograph, triple quadrupole mass spectrometry. Mean(SD) concentrations presented, corrected for tissue lysate protein concentration measured by Bradford assay. ADMA concentration was elevated in DDAH2 knockout mice (Ddah2$^{-/-}$) compared to wild type controls (Ddah2$^{+/+}$), p=0.02. No significant differences were observed in L-NMMA or SDMA concentrations.

In renal tissue, ADMA was significantly higher in Ddah2$^{-/-}$ mice at 0.85(0.23) vs 0.44(0.14), p<0.01 (Figure 74). A modest but statistically significant increase in Mean(SD) L-NMMA level was also observed in the kidney of knockout mice, 0.56(0.14)µmol/mg protein vs 0.39(0.16) µmol/mg protein, p=0.04. Mean renal SDMA concentration was unchanged at 0.32µmol/mg protein vs 0.36µmol/mg protein, p=0.48.

In the plasma, there was an increase in L-NMMA level (0.4(0.11)µmol/mg protein vs 0.28(0.17)µmol/mg protein, p=0.016 (Figure 75). Plasma ADMA (p=0.50) and SDMA (p=0.78) were unchanged when the two groups were compared.

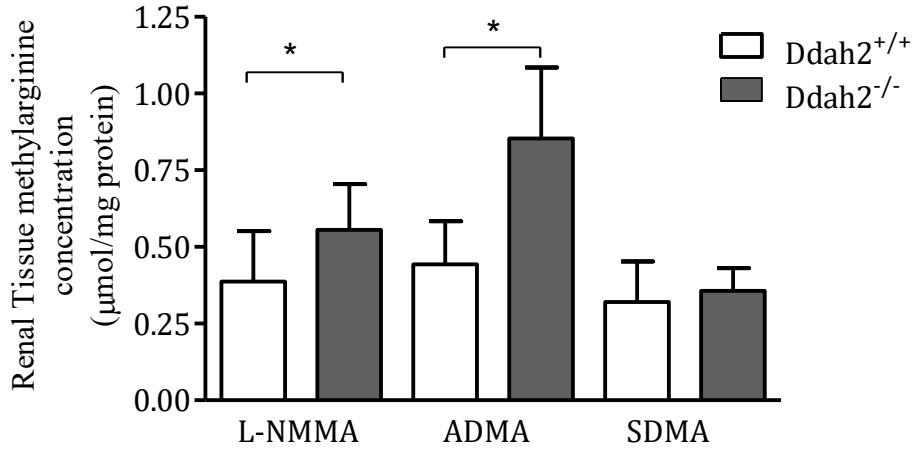

Figure 74: Renal tissue methylarginine concentrations in DDAH2 global knockout and wild type litter mate controls.

Tissue homogenates underwent protein extraction followed by methylarginine estimation using liquid chromatograph, triple quadrupole mass spectrometry. Mean(SD) concentrations presented, corrected for tissue lysate protein concentration measured by Bradford assay. ADMA and L-NMMA concentration was elevated in DDAH2 knockout mice ($Ddah2^{-/-}$) compared to wild type controls ($Ddah2^{+/+}$), p<0.01 and 0.04 respectively. No significant difference was observed in SDMA concentration.

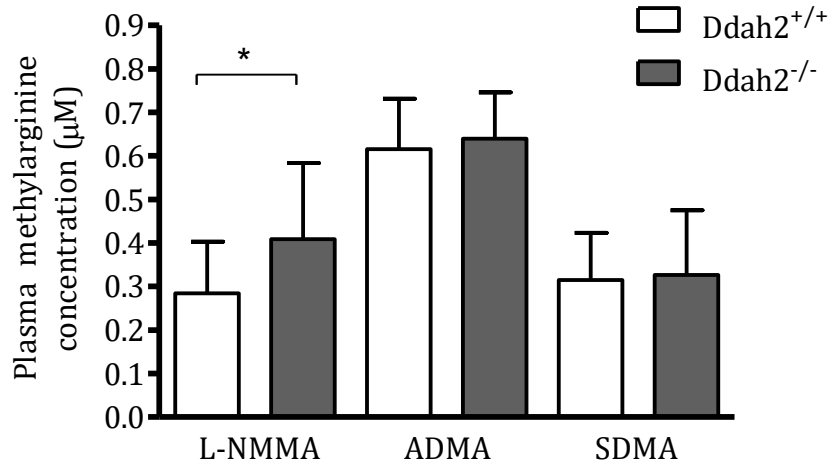

Figure 75: Plasma methylarginine concentrations in DDAH2 global knockout and wild type litter mate controls.

Plasma methylarginine was estimated using liquid chromatograph, triple quadrupole mass spectrometry. Mean(SD) concentrations presented. L-NMMA concentration was elevated in DDAH2 knockout mice ($Ddah2^{-/-}$) compared to wild type controls ($Ddah2^{+/+}$), p=0.016. No significant differences were observed in ADMA or SDMA concentrations.

Renal clearance of methylarginines by the kidneys (as measured by urinary methylarginine concentration and corrected for urinary creatinine) was significantly deranged in Ddah2$^{-/-}$ animals when compared to the wild type litter mates (Figure 76). When corrected for urinary creatinine, ADMA clearance was significantly increased from 0.018(0.004)µM/µM creatinine in the wild type animals to 0.031(0.005)µM/µM creatinine in the knockout mice, p<0.01. SDMA excretion was also elevated 0.012(0.004)µM/µM creatinine vs 0.028(0.005)µM/µM creatinine respectively, p<0.01. L-NMMA clearance was unchanged, p=0.22.

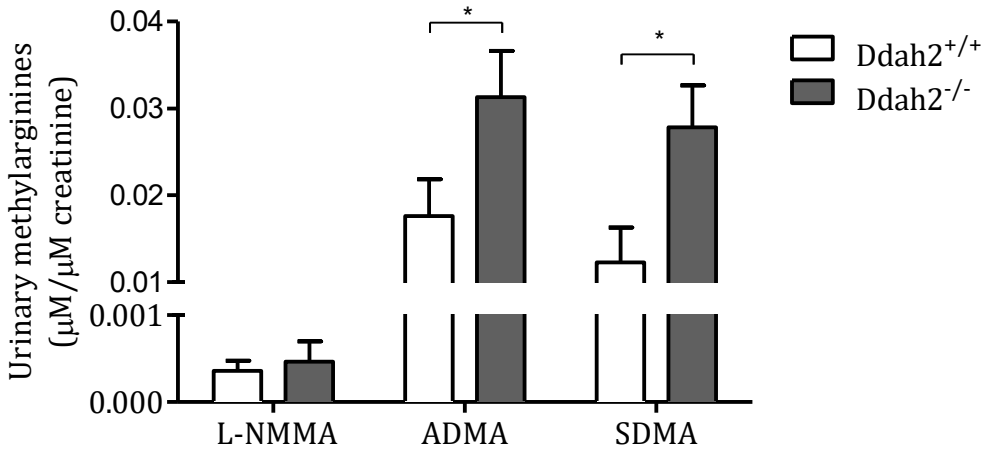

Figure 76: Urinary methylarginine concentrations in DDAH2 global knockout and wild type litter mate controls.

Urine underwent protein extraction followed by methylarginine estimation using liquid chromatograph, triple quadrupole mass spectrometry. Mean(SD) concentrations presented, corrected for urine creatinine concentration measured by mass spectrometry (µM). ADMA and SDMA clearance was elevated in DDAH2 knockout mice (Ddah2$^{-/-}$) compared to wild type controls (Ddah2$^{+/+}$), p<0.01 for both. No significant difference was observed in L-NMMA concentrations (p=0.22). Kindly provided by Dr James Tomlinson.

When fed on a nitrate free diet for 12 days prior to analysis, plasma NOx was significantly reduced in knockout animals compared to wild type controls 41.2(24.0)µM vs 21.5(10.8)µM, (p=0.04) (Figure 77) (Data provided by Dr Laura Dowsett).

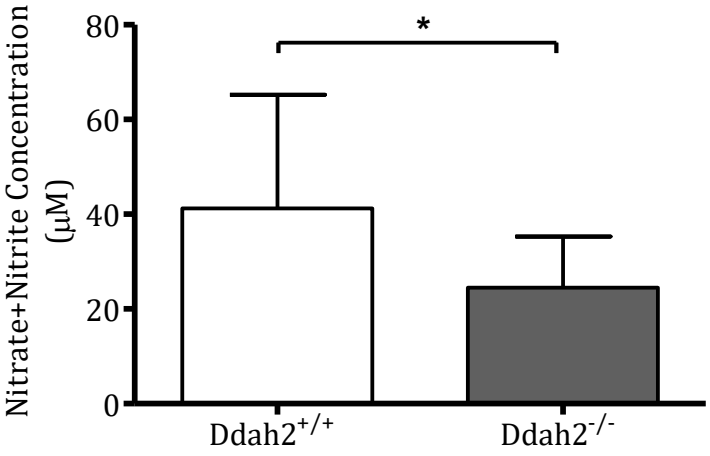

Figure 77: Plasma nitrate+nitrite concentration in DDAH2 global knockout and wild type litter mate controls fed a nitrate free diet.

Plasma Nirate+Nitrite (NOx) concentration was measured in murine plasma using a chemiluminescent technique. Animals were fed a nitrate-free diet for 12 days prior to blood sampling. Whole blood was collected in tubes containing EDTA and underwent separation of the plasma fraction by centrifugation. Plasma then underwent protein extraction using methanol and was analysed as described above. Plasma NOx was significantly reduced in DDAH2 knockout mice (Ddah2$^{-/-}$) compared to controls (Ddah2$^{+/+}$), p=0.04. Data provided by Dr Laura Dowsett.

6.2.1.3 Baseline haemodynamics

Radiofrequency telemetry probe insertion was undertaken in ten Ddah2$^{+/+}$ animals and eleven Ddah2$^{-/-}$ mice. In one animal from each group, features consistent with significant vascular injury caused early sacrifice of the animal and in one animal from the knockout group, the probe was non-functional at the time of baseline assessment so the animal was excluded. Following a 14 day recovery period, animals were placed in individual cages on radiofrequency monitoring platforms. After one hour to allow adaptation for environmental change, a twenty four hour recording period was commenced to facilitate *in vivo* assessment of circadian changes in haemodynamics. All blood pressure results are reported as mean(SD)mmHg

The data were interrogated for differences between the two groups tested. Systolic blood pressure in Ddah2$^{-/-}$ mice was 118.5(8.7)mmHg vs 112.7(7.5)mmHg, p=0.40 (Figure 78). Although no significant difference was observed in the primary analysis of systolic blood pressure, when level of activity was taken into account in a secondary analysis undertaken by Dr Ben Caplin, Ddah2 knockout mice displayed significantly higher blood pressure when their activity level recorded by the radiotelemetry device was greater than 45 counts per minute with blood pressures of 131.0(8.7)mmHg vs 112.1(7.4)mmHg, p=0.025.

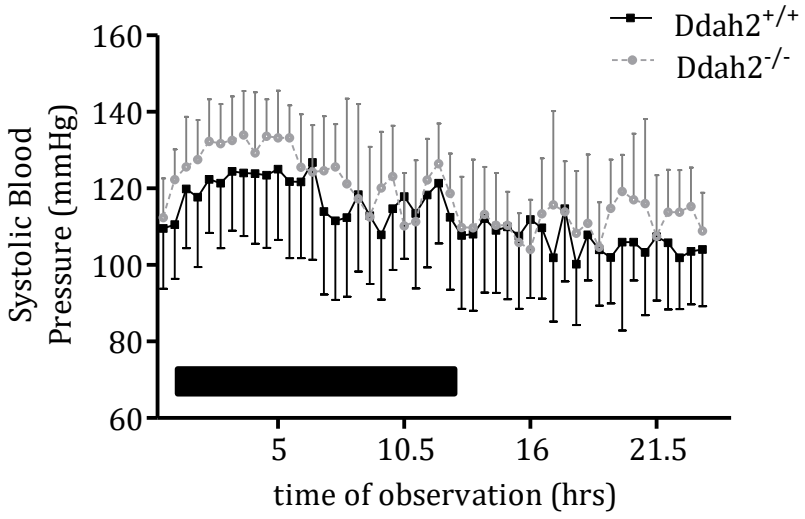

Figure 78: Systolic blood pressure in DDAH2 global knockout mice and wild type controls monitored using *in vivo* radiotelemetry.

***In vivo* radiotelemetry monitoring was undertaken for a continuous 24 hour period 14 days after the insertion of monitoring devices. No significant differences were observed when blood pressure was considered over the whole period of monitoring in DDAH2 global knockout ($Ddah2^{-/-}$) when compared to wild type litter mates ($Ddah2^{+/+}$),p=0.40. Secondary analysis revealed a signifcantly higher blood pressure during periods of high activity in $Ddah2^{-/-}$ mice. Data recorded every 20 seconds and averaged over each minute for calculation. Data presented with each data point at 30minutes for clarity.**

Diastolic blood pressure was not significantly different across the two groups with Ddah2 knockout mice expressing a mean diastolic blood pressure of 93.7(7.1)mmHg and wild type control animals 87.76(5.7)mmHg, p=0.27 (Figure 79).

Heart rate was recorded during the 24 hour observation period, there was no difference between heart rates of the two groups of animals, p=0.42. Mean(SD) heart rate over the observation period was 523(57)bpm in the wild type animals and 539(57)bpm in the global knockout mice(Figure 80).

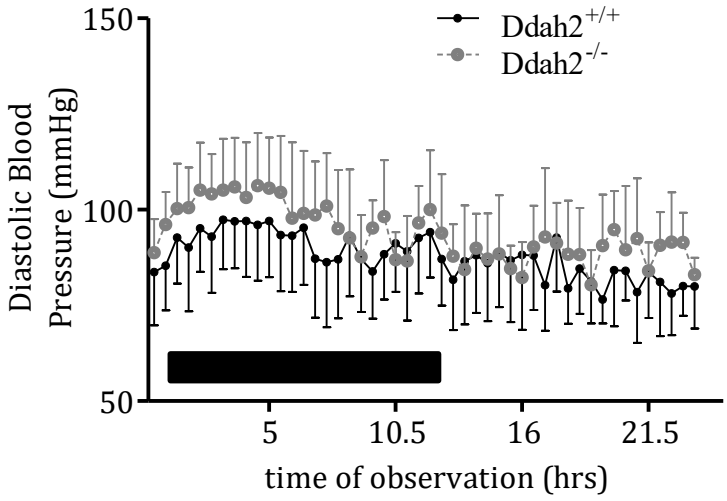

Figure 79: Diastolic blood pressure in DDAH2 global knockout mice and wild type controls monitored using in vivo radiotelemetry.

In vivo **radiotelemetry monitoring was undertaken for a continuous 24 hour period 14 days after the insertion of monitoring devices. No significant differences were observed when blood pressure was considered over the whole period of monitoring in DDAH2 global knockout ($Ddah2^{-/-}$) when compared to wild type litter mates ($Ddah2^{+/+}$),p=0.27. Data recorded every 20 seconds and averaged over each minute for calculation. Data presented with each data point at 30minutes for clarity.**

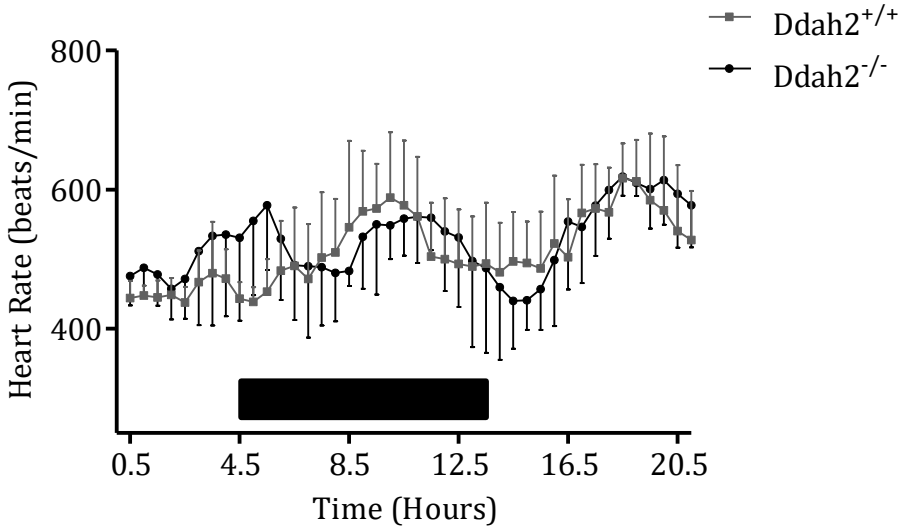

Figure 80: *in vivo* heart rate monitoring in global DDAH2 knockout mice and litter mate controls.

In vivo **radiotelemetry monitoring was undertaken continuously for 24 hours following a 14 day recovery period after probe insertion. Heart rate was similar in DDAH2 global knockout ($Ddah2^{-/-}$) when compared to wild type litter mates ($Ddah2^{+/+}$) (p=0.42). Data recorded every 20 seconds and averaged over each minute for calculation. Data presented with each data point at 30minutes for clarity.**

6.2.1.4 Anaesthetised models of cardiac function

Cardiac function was assessed under anaesthesia as described above in two groups of ten animals. As expected, systemic blood pressure was reduced with a mean (SD) pressure (measured using a simultaneous tail cuff sphygmomanometer) mean arterial blood pressure of 105.2(6.4)mmHg in Ddah2$^{-/-}$ mice and 99.58(12.3)mmHg in Ddah2$^{+/+}$ animals, p=0.40. Assessment of heart rate during anaesthesia revealed no significant differences between the knockout animals (539(54)bpm) compared to the wild type mice in whom the mean heart rate was 505(62)bpm, p=0.25.

Stroke volume (SV) was measured as described above and cardiac output calculated accordingly. In wild type mice, the mean stroke volume was measured as 56(10.9)µL. This compared to 49(9.0)µL in the knockout rodents, p=0.14 (Figure 81). Cardiac output was calculated and corrected for the animal's body weight in grams at the induction of anaesthesia. In Ddah2$^{+/+}$ mice it was 1.1(0.3)ml/min/g compared to 0.97(0.20)ml/min/g in Ddah2$^{-/-}$ mice, p=0.31(Figure 81).

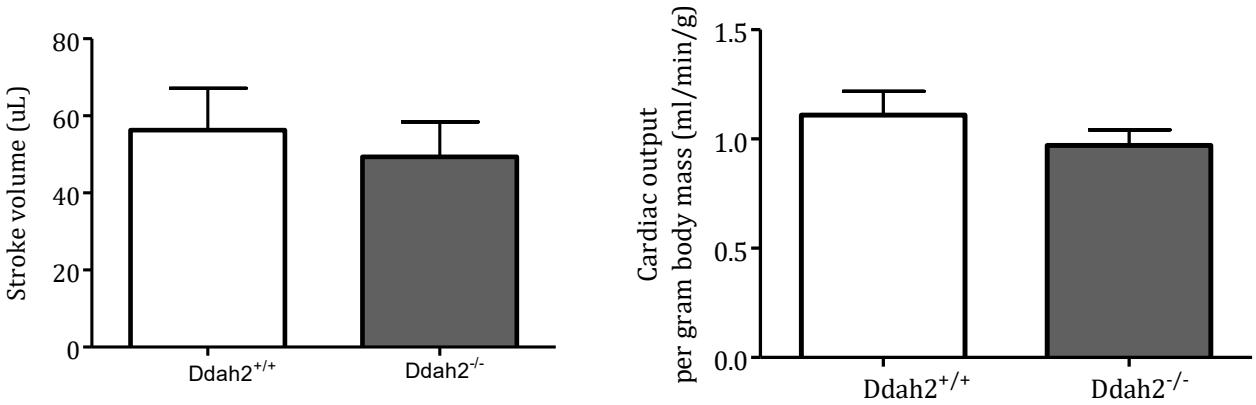

Figure 81: Assessment of left ventricular function in anaesthetised DDAH2 knockout mice and their controls.

Under general anaesthesia, mice underwent transthoracic echocardiographic assessment of stroke volume and cardiac output (Corrected for body weight in grams). No differences were observed between the DDAH2 knockout mice (Ddah2$^{-/-}$) when compared to wild type litter mates (Ddah2$^{+/+}$) in stroke volume or cardiac output, p=0.14 and 0.31 respectively.

6.2.1.5 Aortic vascular reactivity

Aortic vascular reactivity was measured on a subgroup of animals from both genotypes. EC_{50} values can be seen in Table 23 below. Vessels from DDAH2 deficient mice displayed impaired relaxation in response to ACh compared to the wild types ($p < 0.01$, n=3) (Figure 82). (Analysis by Dr A Slaveiro)

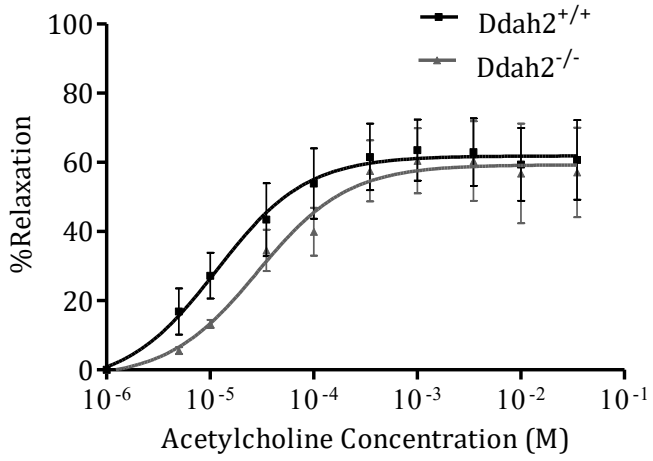

Figure 82: Aortic Vascular relaxation in global DDAH2 knockout mice and their controls following incremental doses of Acetylcholine.

Aortas were isolated from DDAH2 knockout mice (Ddah2$^{-/-}$) and compared to wild type litter mates (Ddah2$^{+/+}$). Following maximal contraction with Phenylephrine, incremental doses of acetylcholine were administered and degree of relaxation assessed. Analysis of genotype specific effects was undertaken using two way Analysis of variance (ANOVA). Acetylcholine was associated with significantly reduced relaxation in knockout mice compared to wild type controls, p<0.01. (Analysis conducted by Dr Anna Slaveiro)

The half-maximal dose of Phe-induced contraction was significantly lower in Ddah2$^{-/-}$ animals than in Ddah2$^{+/+}$ mice ($p<0.01$, $n=3$) (Figure 83).

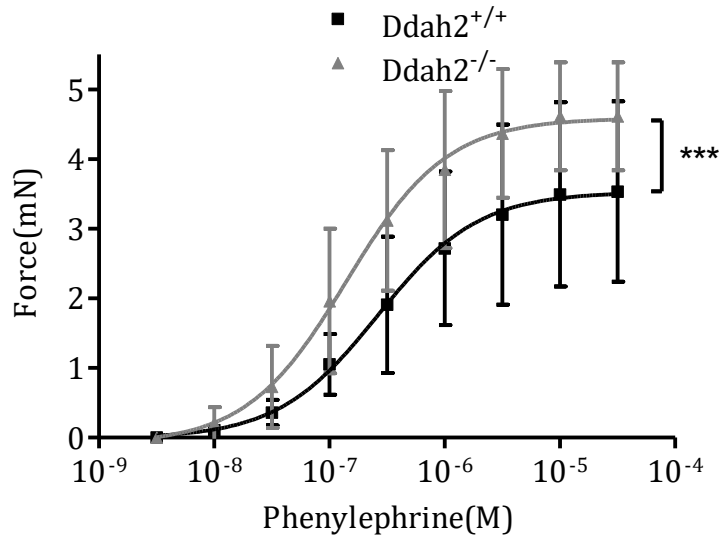

Figure 83: Aortic Vascular force of contraction in global DDAH2 knockout mice and their controls following incremental doses of Phenylephrine.

Aortas were isolated from DDAH2 knockout mice (Ddah2$^{-/-}$) and compared to wild type litter mates (Ddah2$^{+/+}$). Degree of contraction in response to incremental doses of phenylephrine was assessed (mN). Analysis of genotype specific effects was undertaken using two way analysis of variance (ANOVA). Phenylephrine was associated with significantly reduced contraction in knockout mice compared to wild type controls, p<0.01. (Analysis conducted by Dr Anna Slaveiro)

The EC50 of the response to the NO donor SNP was slightly and statistically significantly decreased in knockout mice (Figure 84).

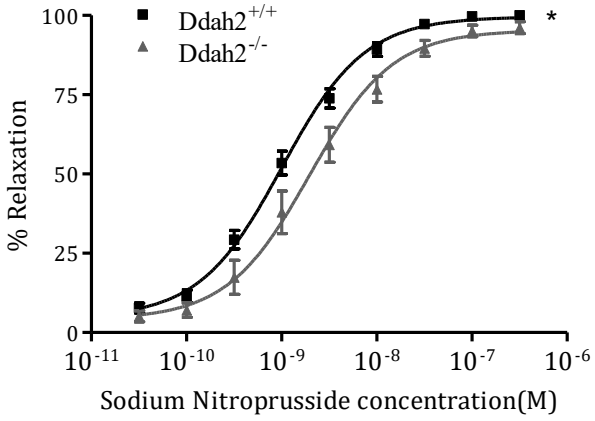

Figure 84: Aortic Vascular relaxation in global DDAH2 knockout mice and their controls following incremental doses of Sodium Nitroprusside.

Aortas were isolated from DDAH2 knockout mice (Ddah2$^{-/-}$) and compared to wild type litter mates (Ddah2$^{+/+}$). Following maximal contraction with Phenylephrine, incremental doses of sodium nitroprusside were administered and degree of relaxation assessed. Analysis of genotype specific effects was undertaken using two way Analysis of variance (ANOVA). Sodium nitroprusside administration was associated with significantly reduced relaxation in knockout mice compared to wild type controls, p<0.01. (Analysis conducted by Dr Anna Slaveiro)

	Ddah2$^{+/+}$		Ddah2$^{-/-}$		
	EC_{50}	95% C.I.	EC_{50}	95% C.I.	p
Phenylephrine	2.638 x 10^{-7}	1.258 – 5.530(x $^{10-7}$)	1.408 x $^{10-7}$	0.8506 – 2.330(x $^{10-7}$)	<0.001
Acetylcholine	4.345 x 10^{-8}	2.104 – 8.969(x $^{10-8}$)	8.091 x $^{10-8}$	3.538 – 18.50(x $^{10-8}$)	0.0057
Sodium Nitroprusside	1.009 x 10^{-9}	0.8357– 1.219(x $^{10-9}$)	1.975 x $^{10-9}$	1.407 – 2.772(x $^{10-9}$)	<0.001

Table 23: Summary of EC50 (95% confidence intervals) data for baseline assessment of aortic vascular reactivity in Ddah2$^{+/+}$ mice and their Ddah2$^{-/-}$ litter mates. (Analysis conducted by Dr Anna Slaveiro)

Comparison made by two way analysis of variance (ANOVA).

6.2.1.6 Right ventricular phenotyping

In a subgroup of five animals of each genotype, the right ventricular systolic pressure (RVSP) was analysed using transthoracic echocardiography assessment of the regurgitant jet across the tricuspid valve. In addition, at termination of the experiment, the heart was dissected out and the right ventricle removed and weighed. When corrected for total body weight, this gave an index of relative right ventricular size.

This gave an average RVSP of 13.1(4.6)mmHg in wild type animals and 14.2(2.5)mmHg in global knockout mice (p=0.79) and corrected mean ventricular masses of 0.81 vs 0.77 (p=0.64) (Figure 85).

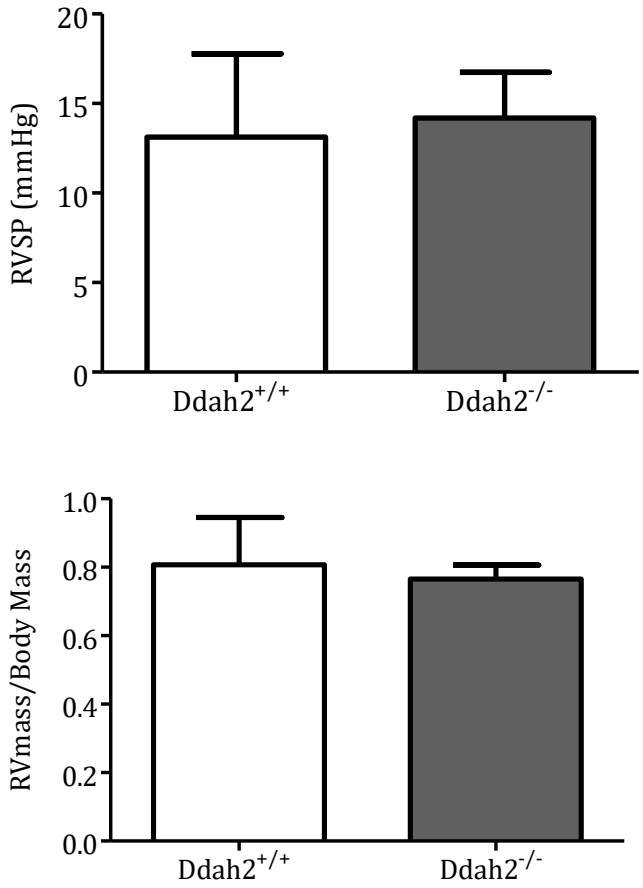

Figure 85: Assessment of right ventricular function in global DDAH2 knockout mice and controls.

Right ventricular systolic pressure was similar in both DDAH2 global knockout mice ($Ddah2^{-/-}$) and wild type litter mates ($Ddah2^{+/+}$), p=0.79 when assessed using transthoracic echocardiography. When corrected for body mass, right ventricular mass following dissection from the rest of the heart was the same in both group, p=0.64.

6.2.2 The role of global DDAH2 knockout in sepsis

6.2.2.1 Survival studies in polymicrobial sepsis

Utilising the severity scoring system described above as an objective endpoint for termination of studies of CLP in sepsis, it having been agreed *a priori* that a severity score of five or more predicted death with a high degree of accuracy. Our mortality study revealed significant differences in mortality between knockout and wild type mice. At 72 hours after the induction of sepsis, 45% of the $Ddah2^{+/+}$ mice had died whereas 87.5% of the $Ddah2^{-/-}$ animals had reached the severity threshold and been culled ($p<0.01$), with a median survival of 63 vs 33 hours respectively (Figure 86).

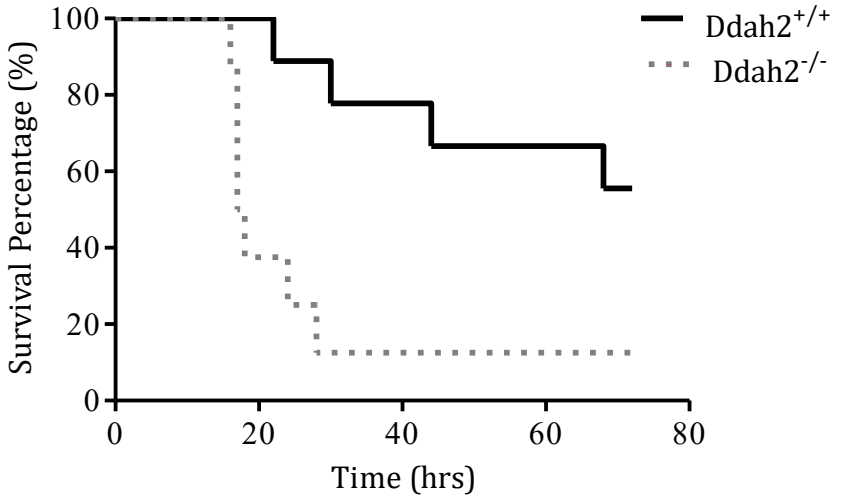

Figure 86: Kaplan Meier curve comparing survival following caecal ligation and puncture in DDAH2 global knockout mice and their wild type litter mate controls.

DDAH2 knockout mice ($Ddah2^{-/-}$) and their litter mate controls ($Ddah2^{+/+}$) had sepsis induced using a caecal ligation and puncture model. A blinded assessment of illness severity was used to predict death, a severity threshold score of five or more was considered highly predictive of death and an indication for experimental cessation. $Ddah2^{-/-}$ mice displayed significantly increased mortality (87.5%) compared to controls (45%), $p<0.01$. Median survival was 63 hours in controls and 33 hours in knockout mice.

In addition to the severity score as an index of outcome, intermittent monitoring of temperature via a subcutaneous radiofrequency probe was undertaken at each monitoring stage. At 18 hours after the onset of sepsis, the recorded temperature had dropped significantly more in the DDAH2 knockout animals consistent with their higher level of illness severity (Figure 87). Knockout mice had displayed a reduction in core temperature of -11(6.1)°C compared to -1.4(3.9)°C in wild type controls with sepsis ($p<0.01$).

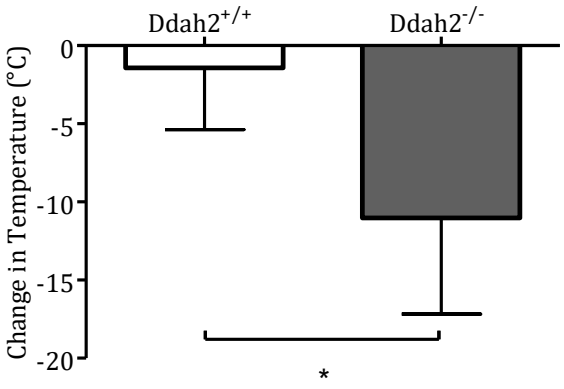

Figure 87: Radiofrequency monitoring of temperature at 18 hours after the onset of sepsis in DDAH2 knockout and wild type control mice.

Radiofrequency temperature probes were inserted into the abdominal wall at the time of sepsis induction and temperature monitored during the course of sepsis. DDAH2 knockout ($Ddah2^{-/-}$) and their litter mate controls ($Ddah2^{+/+}$) were compared at 18 hours after the onset of sepsis. Mean temperature was significantly lower (-11.0°C) in knockout mice than in controls (-1.4°C), p<0.01.

In those animals deemed to have reached the severity score threshold for termination, core temperatures were significantly reduced in both groups, however knockout animals displayed a lower mean reduction in temperature of -13.9(1.6) °C vs -10.6(2.3) °C, p=0.02. (Figure 88).

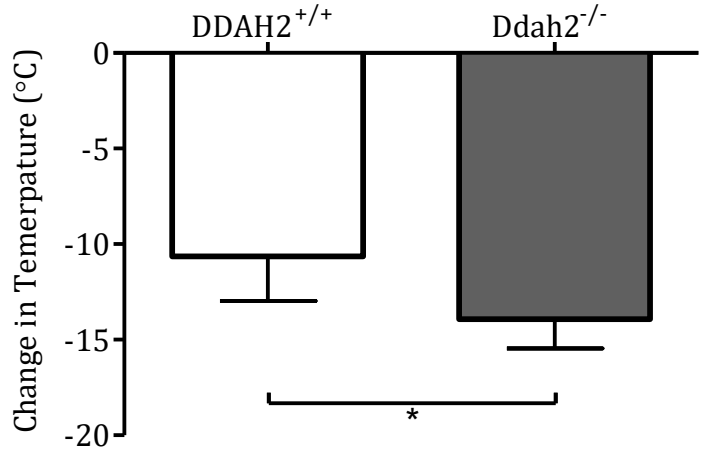

Figure 88: Radiofrequency monitoring of temperature at illness severity threshold in sepsis in DDAH2 knockout and wild type control mice.

Radiofrequency temperature probes were inserted into the abdominal wall at the time of sepsis induction and temperature monitored during the course of sepsis. DDAH2 knockout ($Ddah2^{-/-}$) and their litter mate controls ($Ddah2^{+/+}$) were compared at the time that animals reached the pre-determined severity threshold as defined by blinded assessment. Mean temperature was -13.9°C in knockout mice and -10.6°C in controls, p<0.01.

6.2.2.2 Haemodynamic response to caecal ligation and puncture

Continuous radiofrequency haemodynamic monitoring of the Ddah2$^{-/-}$ animals and their wild type littermates was undertaken over the course of their septic insult. Displaying the whole course of illness for both groups as a single figure is challenging due to the significant differences observed in length of survival (Figure 89). A more robust interrogation of the data is possible if a direct comparison is made of the last 24 hours of life for each of the experimental groups. Mean systolic blood pressure was similar in both groups of animals over the last 24 hours of life (p=0.236), however when blood pressure 12 hours before death was directly compared, significant hypotension was observed in the Ddah2$^{-/-}$ mice (83(32)mmHg) against 129(45)mmHg in Ddah2$^{+/+}$ animals, p=0.039, suggesting that blood pressure was maintained for longer in the wild type control animals (Figure 90).

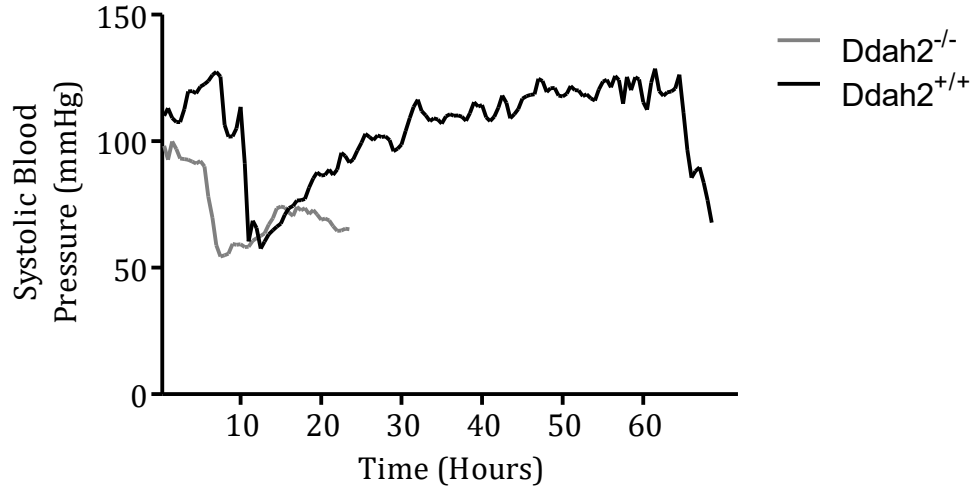

Figure 89: Representative images of systolic blood pressure of two mice undergoing in vivo radiotelemetry monitoring over the course of the experiment in DDAH2 knockout mice and litter mate controls with sepsis.

***In vivo* radiotelemetry monitoring was undertaken continuously following the induction of sepsis using a moderate severity model of caecal ligation and puncture. Representative curves of two individual mice for the period of global DDAH2 knockout and wild type litter mate control are shown. Reported period is from induction of sepsis until the time that the severity threshold was reached.**

Diastolic blood pressure displayed a similar pattern overall to systolic pressure with no significant differences detected by two way ANOVA in the data sets as a whole (p=0.44). A trend to earlier onset of cardiovascular compromise persisted however with wild type animals maintaining a mean diastolic blood pressure of 97.5(32)mmHg vs 68.4(29)mmHg in Ddah2 deficient mice (p=0.096) (Figure 91).

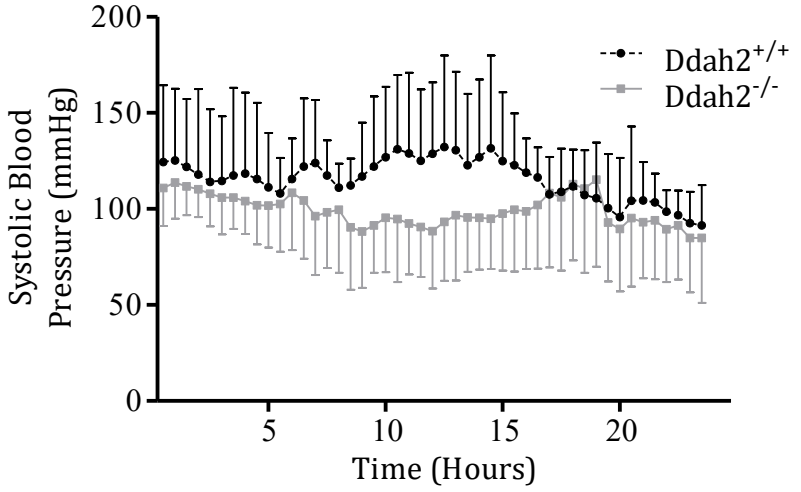

Figure 90: *In vivo* radiotelemetry monitoring of systolic blood pressure over the final 24 hours of life in DDAH2 knockout mice and litter mate controls with sepsis.

***In vivo* radiotelemetry monitoring was undertaken continuously following the induction of sepsis using a moderate severity model of caecal ligation and puncture. No significant differences were observed when blood pressure was considered over the whole period of monitoring in DDAH2 global knockout ($Ddah2^{-/-}$) when compared to wild type litter mates ($Ddah2^{+/+}$), however 12 hours prior to experimental cessation, $DDAH2^{-/-}$ mice were more hypotensive than controls, p=0.039. Data recorded every 20 seconds and averaged over each minute for calculation. Data presented with each data point at 30minutes for clarity.**

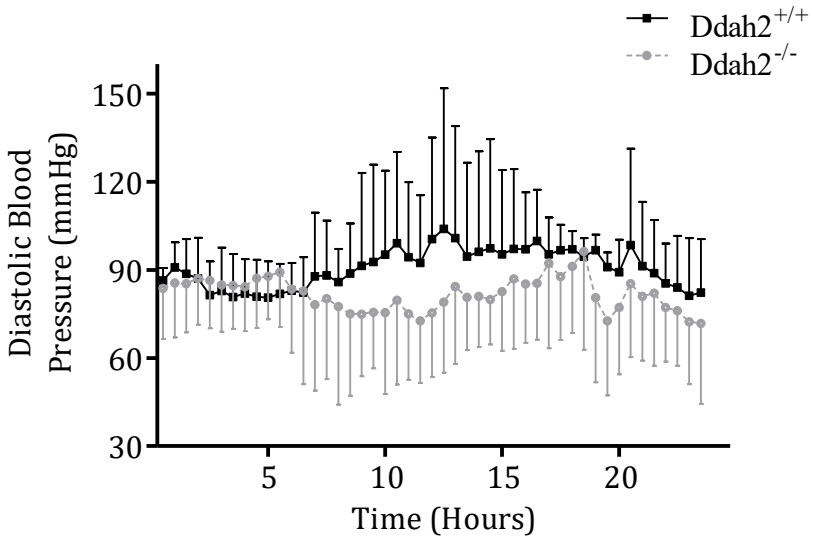

Figure 91: In vivo radiotelemetry monitoring of diastolic blood pressure over the final 24 hours of life in DDAH2 knockout mice and litter mate controls with sepsis.

***In vivo* radiotelemetry monitoring was undertaken continuously following the induction of sepsis using a moderate severity model of caecal ligation and puncture. No significant differences were observed when diastolic blood pressure was considered over the whole period of monitoring in DDAH2 global knockout ($Ddah2^{-/-}$) when compared to wild type litter mates ($Ddah2^{+/+}$), however 12 hours prior to experimental cessation, there was a trend to lower blood pressure in $DDAH2^{-/-}$ mice (p=0.096). Data recorded every 20 seconds and averaged over each minute for calculation. Data presented with each data point at 30minutes for clarity.**

When mean arterial pressure (MAP) is considered, a Ddah2$^{-/-}$ mice were consistently hypotensive 12 hours prior to reaching the severity threshold compared to their litter mate controls, with mean MAPs of 78.2(29) and 118.1(34) respectively, p=0.03. Although once again, no difference was observed in blood pressure overall, p=0.25 (Figure 92).

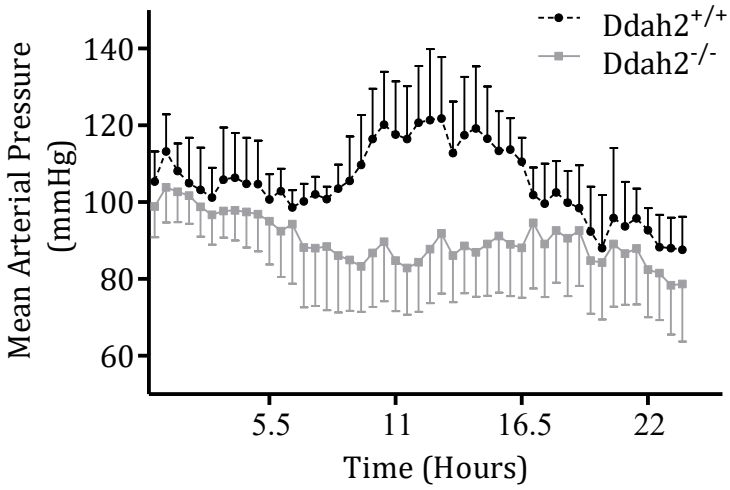

Figure 92: In vivo radiotelemetry monitoring of mean arterial blood pressure over the final 24 hours of life in DDAH2 knockout mice and litter mate controls with sepsis.

***In vivo* radiotelemetry monitoring was undertaken continuously following the induction of sepsis using a moderate severity model of caecal ligation and puncture. No significant differences were observed when mean arterial blood pressure was considered over the whole period of monitoring in DDAH2 global knockout (Ddah2$^{-/-}$) when compared to wild type litter mates (Ddah2$^{+/+}$), however 12 hours prior to experimental cessation, there was a lower blood pressure in DDAH2$^{-/-}$ mice (p=0.03). Data recorded every 20 seconds and averaged over each minute for calculation. Data presented with each data point at 30minutes for clarity.**

Heart rate was continuously monitored throughout the period of the sepsis study. When compared to wild type controls, DDAH2 knockout mice had similar heart rates throughout the last 24 hours of life although a trend was noted on overall analysis towards a lower heart rate in Ddah2$^{-/-}$ mice, mean(SD) heart rate(bpm) 488(53) compared to 571(25) in controls (p=0.22) (Figure 93).

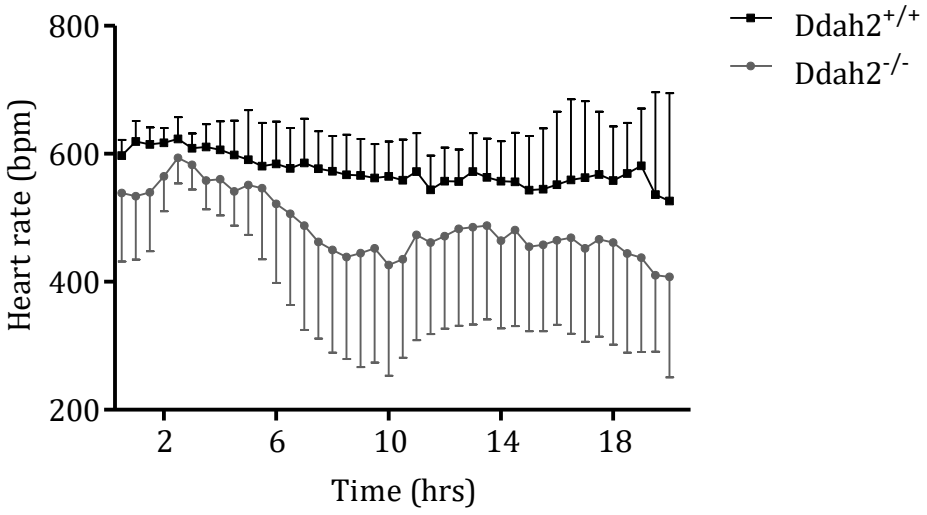

Figure 93: Radiotelemetry monitoring of heart rate in the final 24 hours of life in septic DDAH2 knockout mice and litter mate controls.

***In vivo* radiotelemetry monitoring was undertaken continuously following the induction of sepsis using a moderate severity model of caecal ligation and puncture. A trend (p=0.1049) to lower heart rate in the last 24 hours of life was seen when heart rate was analysed over the whole period of monitoring in DDAH2 global knockout ($Ddah2^{-/-}$) when compared to wild type litter mates ($Ddah2^{+/+}$), however 12 hours prior to experimental cessation, there was a no significant difference in heart rate between the two groups(p=0.22). Data recorded every 20 seconds and averaged over each minute for calculation. Data presented with each data point at 30minutes for clarity.**

6.2.2.3 Aortic vascular reactivity in sepsis

Aortic vascular reactivity was modelled in global knockout mice and their controls using the same technique employed in earlier models. As expected, when the aortas were isolated six hours after the induction of sepsis, overall vascular reactivity was grossly impaired (Figure 94). Of note however is that whilst there were no significant differences in the response to the vasopressor phenylephrine or acetylcholine treatment, an exaggerated response to sodium nitroprusside administration was observed in the DDAH2 knockout mice compared to wild type animals($p<0.01$), EC_{50} may be seen for each of these experiments in Table 24 below. (Analysis by Dr A Slaveiro)

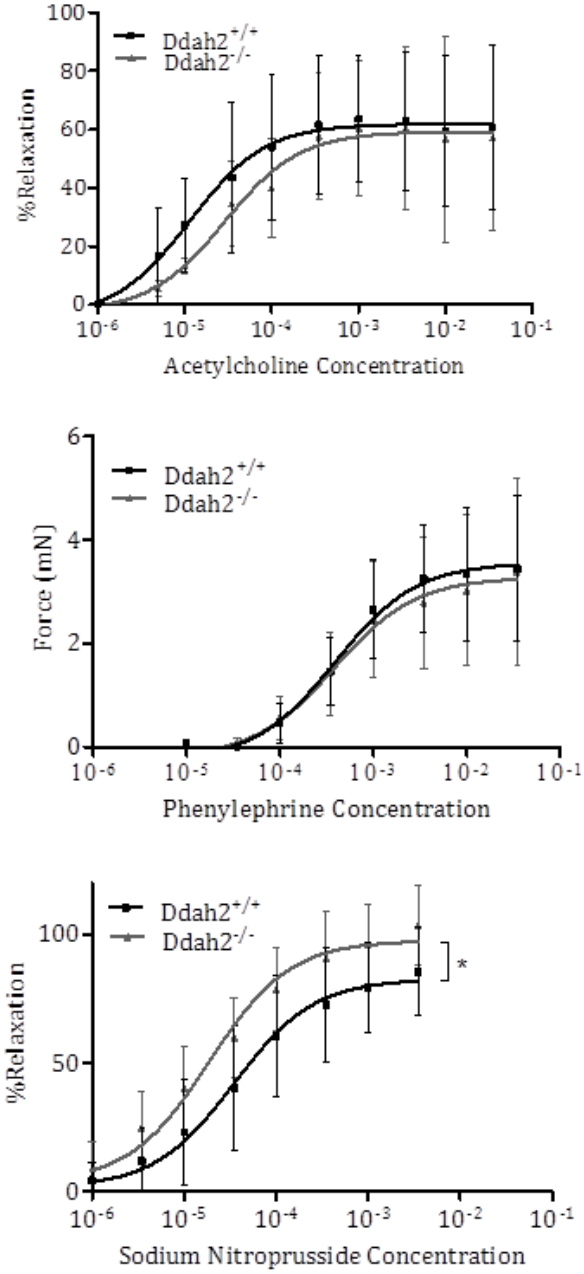

Figure 94: Aortic Vascular relaxation in septic global DDAH2 knockout mice and their controls following incremental doses of acetylcholine, phenylephrine and sodium nitroprusside.

Aortas were isolated from DDAH2 knockout mice (Ddah2$^{-/-}$) and compared to wild type litter mates (Ddah2$^{+/+}$) at six hours after the onset of sepsis. Following maximal contraction with phenylephrine, incremental doses of sodium nitroprusside were administered and degree of relaxation assessed. A repeat incremental scale of phenylephrine was undertaken and force of contraction recorded. Sodium nitroprusside was then applied at increasing doses and relaxation assessed. Analysis of genotype specific effects was undertaken using two way Analysis of variance (ANOVA). No significant differences were observed between groups of septic mice in response to phenylephrine (p=0.59) or acetylcholine (p=0.17), however sodium nitroprusside administration was associated with significantly reduced relaxation in knockout mice compared to wild type controls, p<0.01. (Analysis by Dr A Slaveiro)

	Ddah2$^{+/+}$ sepsis		Ddah2$^{-/-}$ sepsis		p
	EC_{50}	95% C.I.	EC_{50}	95% C.I.	
Phenylephrine	1.37×10^{-4}	2.1×10^{-5}–7.8×10^{-4}	1.27×10^{-4}	2.7×10^{-5} –6.8×10^{-4}	0.59
Acetylcholine	2.7×10^{-5}	8.0×10^{-6}-9.0×10^{-5}	8.0×10^{-6}	1.9×10^{-6} -3.4×10^{-5}	0.17
Sodium Nitroprusside	1.9×10^{-5}	1.2×10^{-5} – 3.0×10^{-5}	3.5×10^{-5}	1.9×10^{-5} - 6.6×10^{-5}	<0.001

Table 24: Summary of EC50 (95% confidence intervals) data for assessment of aortic vascular reactivity in Ddah2$^{+/+}$ mice and their Ddah2$^{-/-}$ litter mates at six hours after the onset of sepsis. Comparison made by two way analysis of variance (ANOVA). (Analysis by Dr A Slaveiro)

6.2.2.4 Systemic nitric oxide levels in sepsis

Plasma NOx was measured using the chemiluminescent technique described above. Nitrate + Nitrite concentration was significantly elevated in all Ddah2$^{-/-}$ mice and also non surviving Ddah2$^{+/+}$ animals when compared to wild type mice who did not reach the pre-defined illness severity threshold (Figure 95). Mean(SD) nitric oxide concentration was 98.9(30)µM in Ddah2$^{-/-}$ mice, 91.9(37)µM in non-surviving wild type mice and 53.0(26)µM in surviving Ddah2$^{+/+}$ rodents, p=0.018 and 0.046 respectively. NOx concentrations were similar in non-surviving animals of both knockout and control groups, p=0.75.

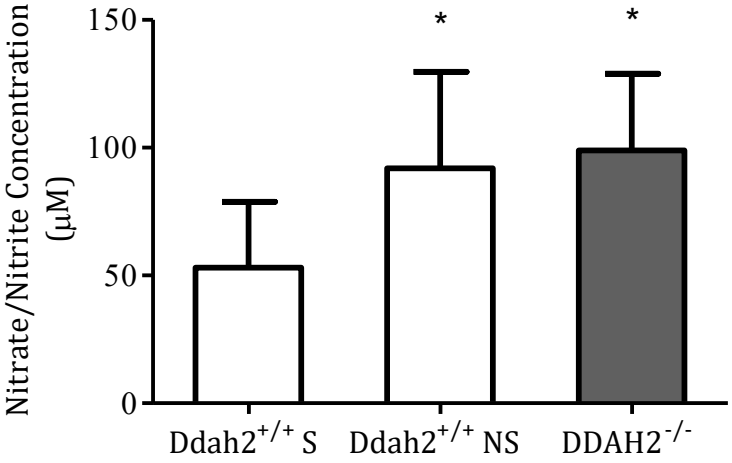

Figure 95: Plasma Nitrate+Nitrite(NOx) concentrations in DDAH2 knockout animals and surviving and non-surviving litter mate controls at the end of a sepsis study.

A chemiluminescent technique was used to determine plasma NOx concentrations at the end of a caecal ligation and puncture mediated sepsis model in DDAH2 knockout mice ($Ddah2^{-/-}$) and compared to wild type litter mates ($Ddah2^{+/+}$) which survived (S) or reached the pre-defined severity threshold (NS). Plasma NOx concentrations were significantly higher on non-surviving animals but no difference was observed between genotypes, p=0.75.

6.2.2.5 Methylarginines in global DDAH2 knockout models of sepsis

Severe sepsis was associated with significant derangement of the plasma methylarginines in both groups of animals, however there increases in ADMA and L-NMMA increased more in global Ddah2 knockout animals. ADMA (Mean (SD)μM) in the $Ddah2^{+/+}$ mice was 4.3(0.73) compared to $Ddah2^{-/-}$ mice in which it was elevated further to 6.3(1.6), p=0.015 (Figure 96). L-NMMA increased to 0.43(0.28) in wild type mice and 0.93(0.32), p=0.01 (Figure 96) with no significant difference in plasma SDMA level detected between the genotypes (p=0.63).

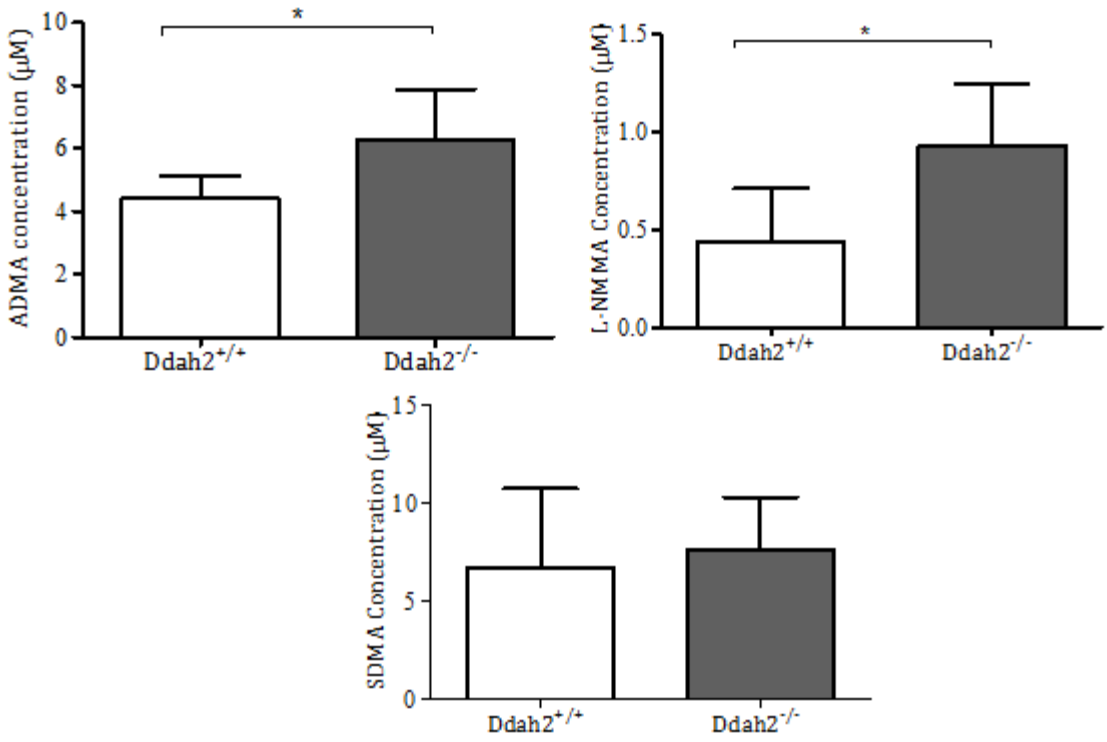

Figure 96: Plasma concentrations of methylarginines in DDAH2 knockout mice and wild type controls with sepsis.

Following experimental cessation, plasma taken at terminal bleed by cardiac puncture was analysed for methylarginine concentrations. Whilst all methylarginines were elevated over control levels, ADMA and L-NMMA were significantly higher in DDAH2 knockout animals (Ddah2$^{-/-}$) compared to controls (Ddah2$^{+/+}$), p=0.015 and 0.01 respectively.

6.2.2.6 Peritoneal and whole blood bacterial load in sepsis

In a short term model of sepsis induced using CLP with experimental termination at 6 hours after the onset of sepsis, bacterial load was significantly increased in peritoneal lavage fluid in global knockout mice. Representative images of plates exposed to peritoneal lavage fluid at a range of dilutions can be seen in Figure 97below. Total bacterial load was 1.00 x10^7 (IQR 1.17 x10^6 -1.20 x10^9) in Ddah2 knockout mice and in wild type animals was lower at 1.01 x10^6 CFU/ml (IQR 13650-9.50 x10^6) (p=0.04). There was also a trend to elevated bacterial load in whole blood in knockout mice compared to controls (1084 (IQR 25-6364) vs 373 (IQR 0-670) (p=0.052)) (Figure 98).

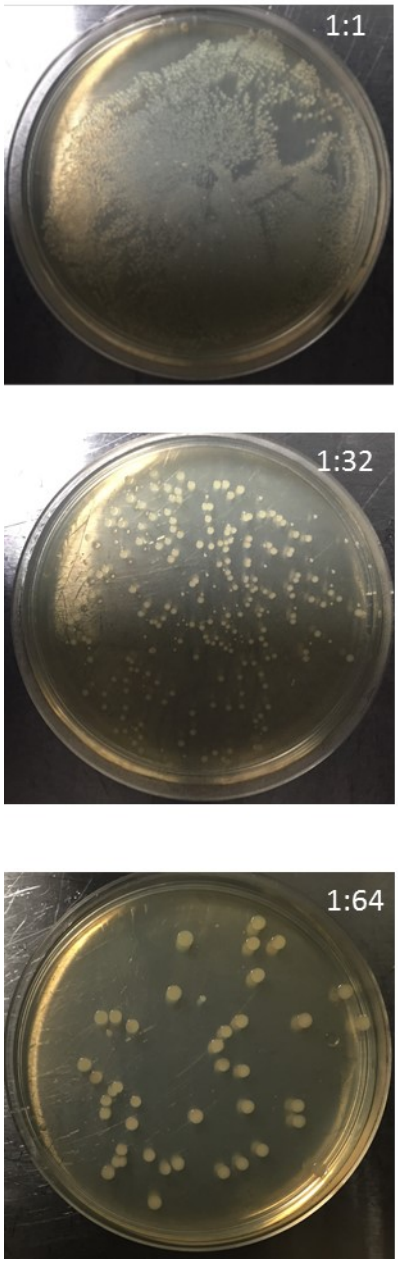

Figure 97: Representative images of peritoneal fluid plating following serial dilution after collection at six hours after caecal ligation and puncture and 24 hour incubation.

Representative images of selected dilutions of peritoneal fluid collected from DDAH2 knockout mice and their litter mate controls collected six hours after the onset of sepsis were plated on Agar and the appropriate dilution counted for assessment of bacterial load at 24 hours.

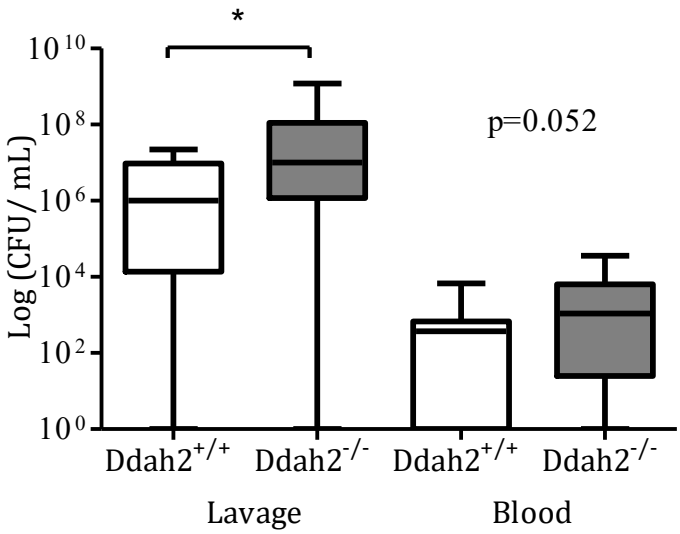

Figure 98: Whole blood and peritoneal washout bacterial loads in DDAH2 knockout mice and controls six hours after the onset of sepsis.

Serial dilutions of blood and peritoneal fluid collected from DDAH2 knockout mice and their litter mate controls collected six hours after the onset of sepsis were plated on Agar and the appropriate dilution counted for assessment of bacterial load at 24 hours. DDAH2 knockout mice (Ddah2$^{-/-}$) had significantly higher peritoneal (p=0.04) and a trend towards higher blood (p=0.052) bacterial loads compared to wild type litter mate controls (Ddah2$^{+/+}$). Data presented as Log_{10} colony forming units (CFU)/ml fluid.

6.2.3 Macrophage specific DDAH2 knockout

In order to explore the role of macrophage DDAH2, a macrophage specific Ddah2 deficient mouse was developed using the loxP Cre Recombinase technique (Ddah2$^{MΦ-}$). All studies involving these mice were compared to Ddah2$^{flox/flox}$ litter mate controls in order to limit the impact of transgenic technique on observed differences in the response to sepsis.

6.2.3.1 Demonstration of the macrophage specific knockout of DDAH2

Western blots of kidney, heart, liver and aortic tissue homogenates showed preservation of DDAH2 protein in Ddah2 monocyte specific knockout animals (Figure 99). DDAH1 protein was also shown to be present in these tissues.

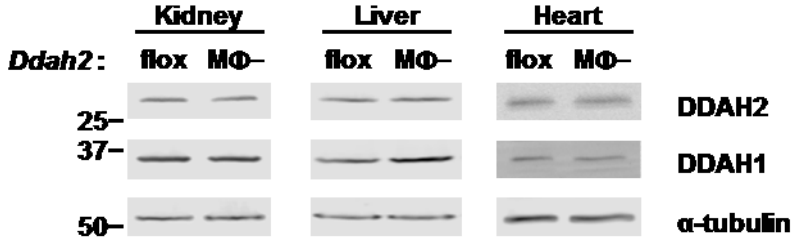

Figure 99: Representative images demonstrating the presence of DDAH2 in kidney, liver and heart tissue homogenates in the global DDAH2 macrophage specific knockout mouse (MΦ-).

Compared to floxed litter mate control mice (flox). Reproduced with permission of Dr Ben Lee.

DDAH2 protein and mRNA was shown to be absent from isolated resident peritoneal macrophages (Figure 100).

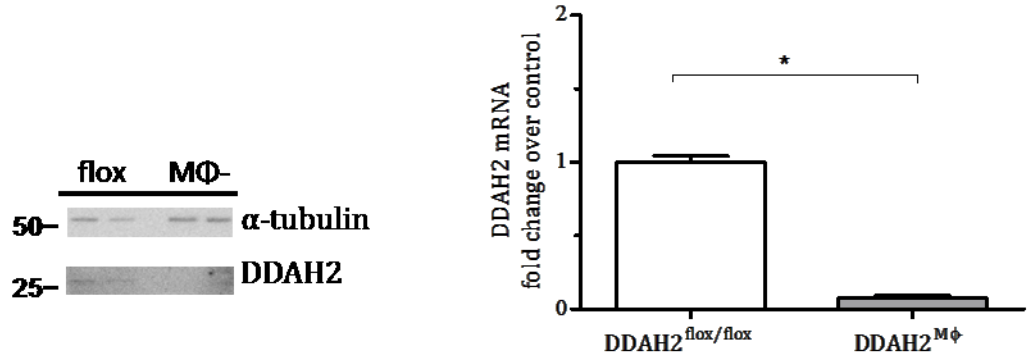

Figure 100: Demonstration of the absence of DDAH2 protein and mRNA from macrophages from DDAH2 knockout mice.

Representative image displaying the absence of DDAH2 from the macrophages of DDAH2 knockout mice MΦ- compared to floxed controls (flox). Second image: quantitative analysis of DDAH2 mRNA expression in (Ddah2$^{MΦ-}$) mice compared to floxed controls (Ddah2$^{flox/flox}$).

Both the Ddah2$^{MΦ-}$ mice and Ddah2$^{flox/flox}$ controls appeared phenotypically normal although at the time of experiment at 8 -10 weeks there was a trend towards lower body weight in Ddah2$^{MΦ-}$ compared to their control litter mates, Mean(SD) Ddah2$^{flox/flox}$ 24.5(2.5)g vs DDAH2$^{MΦ-}$ 23.0(1.8)g p=0.09.

6.2.3.2 Survival studies in polymicrobial sepsis

Survival studies in the macrophage specific knockout animals were conducted in identical fashion to studies undertaken in global knockout mice. Using blinded independent assessment of severity and the surrogate marker of subcutaneous temperature as described above, DDAH2$^{MΦ-}$ mice displayed a similar pattern of early excess mortality to Ddah2$^{-/-}$ animals with 100% of mice reaching the pre-determined severity threshold compared to 50% of the Ddah2$^{flox/flox}$ mice ($p<0.01$), median survival was 24 hours in the macrophage specific knockouts and 72hours in floxed control mice(Figure 101). Greater change was observed in subcutaneous temperature at 18 hours post CLP in the knockout mice, mean(SD) temp change °C and Ddah2$^{flox/flox}$ -0.8(3.7)°C vs Ddah2$^{MΦ-}$ -9.32(6.4)°C, $p<0.01$ (Figure 102). Consistent severity of illness at time of sacrifice of those animals reaching illness severity threshold was demonstrated by similar body temperatures at sacrifice, p=0.26 (Figure 102).

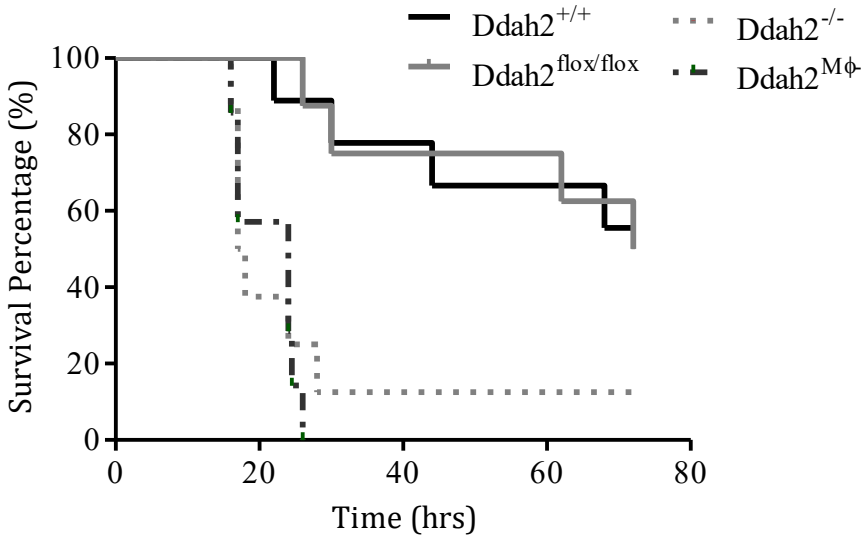

Figure 101: Kaplan Meier curve comparing survival following caecal ligation and puncture in DDAH2 macrophage specific knockout mice and their floxed controls.

DDAH2 macrophage specific knockout mice ($Ddah2^{M\Phi-}$) and their litter mate controls ($Ddah2^{flox/flox}$) had sepsis induced using a caecal ligation and puncture model. A blinded assessment of illness severity was used to predict death, a severity threshold score of five or more was considered highly predictive of death and an indication for experimental cessation. $Ddah2^{-/-}$ mice displayed significantly increased mortality (100%) compared to controls (50%), $p<0.01$. Median survival was 72 hours in controls and 24 hours in knockout mice. Global DDAH2 knockout ($Ddah2^{-/-}$) and Wild type ($Ddah2^{+/+}$) control survival curves are provided for comparison.

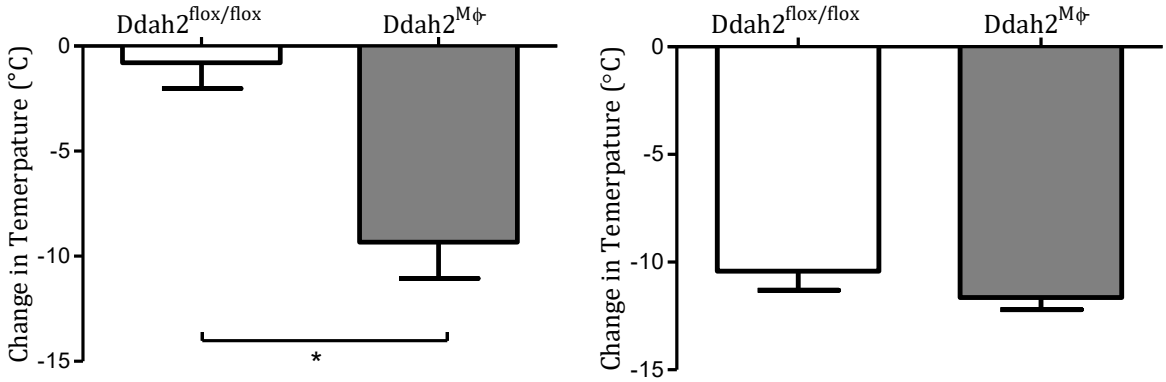

Figure 102: Radiofrequency monitoring of temperature at 18 hours after the onset of sepsis and at termination in DDAH2 macrophage specific knockout and floxed controls.

Temperature monitoring was undertaken in DDAH2 macrophage specific knockout mice ($Ddah2^{M\Phi-}$) and floxed controls ($Ddah2^{flox/flox}$). No differences were observed at experimental cessation however at 18 hours after the onset of sepsis, DDAH2 macrophage specific knockout mice displayed significantly greater mean drop in temperature (-9.32°C) compared to floxed controls (-0.8°C), $p<0.01$.

6.2.3.3 Radiotelemetry probe insertion in macrophage specific knockout mice

In order to model the physiological impact of macrophage specific Ddah2 knockout on haemodynamic response in sepsis, radiotelemetry probe insertion was undertaken in a group of nine $DDAH2^{flox/flox}$ mice and nine $DDAH2^{M\Phi-}$ mice utilising the same technique described previously and successfully employed in the global knockout animals and their controls.

Telemetry probe insertion was uneventful with no apparent haemorrhagic complications and all animals displaying a good recovery after one hour in a heated chamber. Animals were returned to their cages and allowed to recover overnight.

By 12 hours after probe insertion, all animals from both groups displayed significant evidence of distress, with limited movement, piloerection and hypothermia prominent. Fluid resuscitation and analgesia with burprenorphine was administered with minimal apparent effect. Based on the level of apparent distress, it was decided, in conjunction with the animal welfare team to terminate the experiment. Animals were euthanised and post mortem examination undertaken at the time of probe removal.

There was no evidence of haemorrhagic complication or cerebrovascular accident and the thoracic cavity appeared normal. Upon dissection of the peritoneal cavity however, there was gross discolouration of the proximal small bowel, consistent with mesenteric artery ischaemia present to some degree in all animals of both Ddah2 macrophage specific knockout and floxed control mice(Figure 103). Further investigation revealed no displacement of the monitoring catheter and no gross abnormality of the great vessels. Possible mechanisms for this are considered in the discussion below.

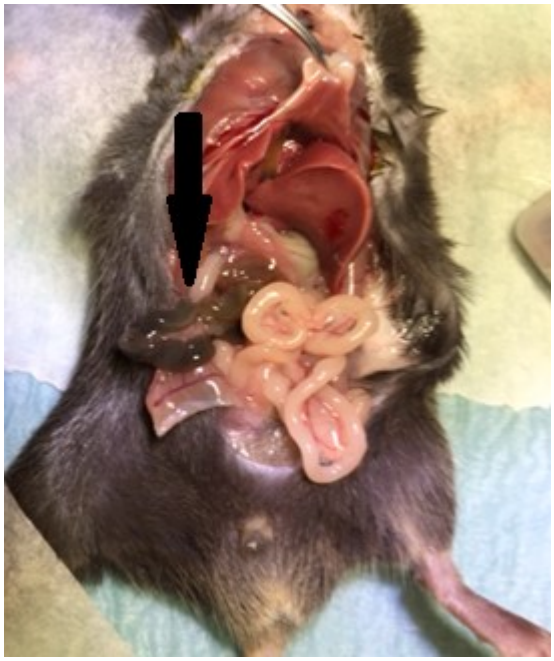

Figure 103: Representative image of proximal bowel ischaemia in LoxP animals. Arrow highlights region of small bowel ischaemia.

6.2.3.4 Haemodynamic response to caecal ligation and puncture

As an alternative approach to assessing haemodynamics in the macrophage specific mice, sepsis was induced using the previously described CLP model including fluid resuscitation and analgesia followed by anaesthesia and in vivo assessment of blood pressure undertaken using a Millar fluid filled catheter technique. Blood pressure at 6 hours after the onset of sepsis did not reveal any significant differences between the two groups of animals although significant haemodynamic compromise was noted in both groups (Figure 104). Anaesthetised systolic blood pressure (mean(SD)) was 77.7(39)mmHg in floxed animals compared to 80.7(9.6)mmHg in macrophage specific knockout mice, p=0.87. Diastolic blood pressure was similarly reduced compared to normal levels with pressures of 57.7(35)mmHg and 62(8.7)mmHg respectively, p=0.79.

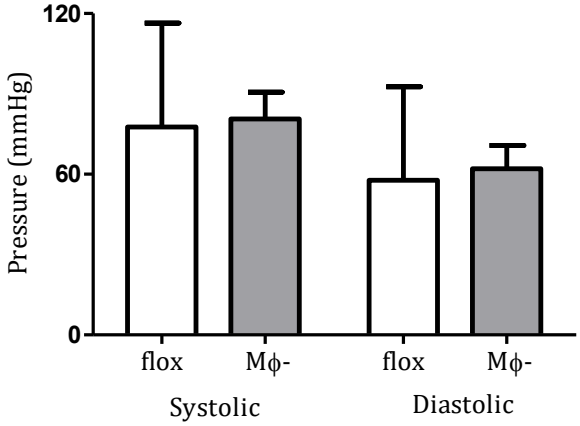

Figure 104: Anaesthetised haemodynamic assessment in DDAH2 macrophage specific knockout mice with sepsis and floxed controls.

Six hours after the induction of sepsis, animals were anaesthetised and the right internal carotid artery exposed. Once a stable level of anaesthesia had been achieved, a Millar catheter was inserted and after a 15 minute period of stability blood pressure was recorded in DDAH2 macrophage specific knockout (Ddah2$^{+/+}$) and floxed litter mate controls (Ddah2$^{flox/flox}$). No differences were observed between the systolic and diastolic blood pressures of the two groups, p=0.87 and 0.79 respectively.

6.2.3.5 Aortic vascular reactivity in sepsis

In the same model of sepsis used to explore aortic vascular reactivity in global knockout animals, no significant differences between responses of Ddah2$^{MΦ-}$ and their Ddah2$^{flox/flox}$ litter mates (Figure 105) although in all cases, sepsis related vascular reactivity was significantly impaired compared to normal values. EC50 for all experiments can be seen in Table 25 below. (Analysis by Dr A Slaveiro)

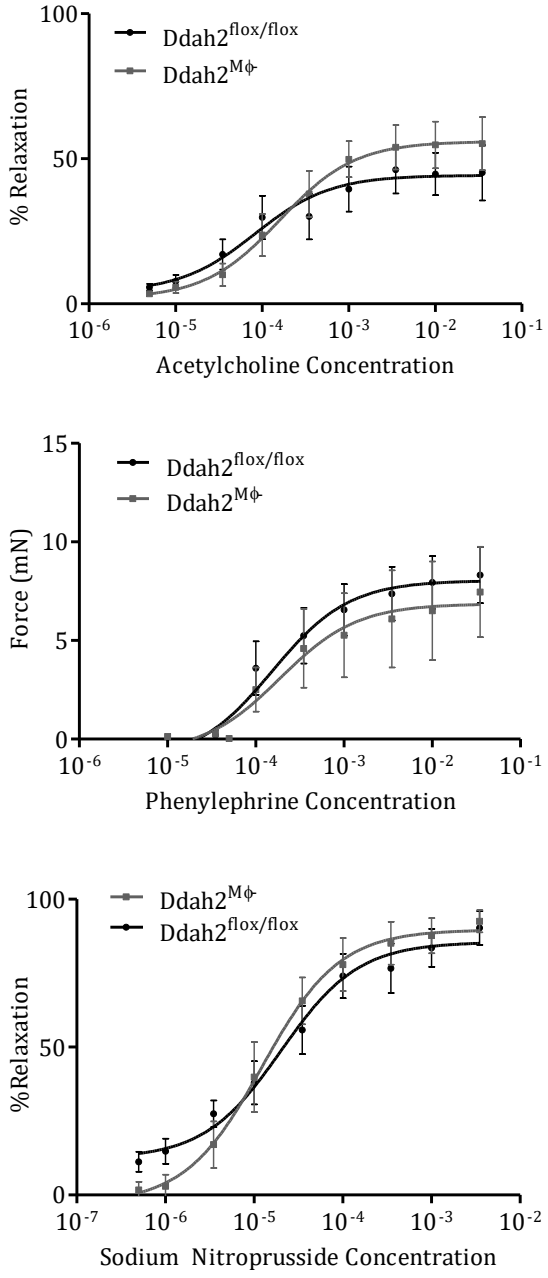

Figure 105: Aortic Vascular responsiveness in septic macrophage specific DDAH2 knockout mice and their controls following incremental doses of acetylcholine, phenylephrine and sodium nitroprusside.

Aortas were isolated from DDAH2 knockout mice ($Ddah2^{M\Phi-}$) and compared to floxed litter mates ($Ddah2^{flox/flox}$) at six hours after the onset of sepsis. Following maximal contraction with phenylephrine, incremental doses of sodium nitroprusside were administered and degree of relaxation assessed. A repeat incremental scale of phenylephrine was undertaken and force of contraction recorded. Sodium nitroprusside was then applied at increasing doses and relaxation assessed. Analysis of genotype specific effects was undertaken using two way Analysis of variance (ANOVA). No significant differences were observed between groups of septic mice in response to phenylephrine (p=0.299), sodium nitroprusside(p=0.97) or acetylcholine (p=0.32), however sodium nitroprusside administration was associated with significantly reduced relaxation in knockout mice compared to wild type controls, p<0.01. (Analysis by Dr A Slaveiro)

	$Ddah2^{flox/flox}$ Sepsis		$Ddah2^{M\Phi-}$ sepsis		
	EC_{50}	95% C.I.	EC_{50}	95% C.I.	
Phenylephrine	1.5×10^{-4}	5.1×10^{-5}–4.6×10^{-4}	1.9×10^{-4}	2.7×10^{-5} – 1.3×10^{-4}	0.299
Acetylcholine	8.3×10^{-5}	2.0×10^{-5}–3.4×10^{-4}	1.6×10^{-4}	6.4×10^{-5} – 4.0×10^{-4}	0.320
Sodium Nitroprusside	2.0×10^{-5}	1.0×10^{-5}–4.0×10^{-5}	1.2×10^{-5}	6.6×10^{-5} – 2.3×10^{-5}	0.966

Table 25: Summary of EC50 (95% confidence intervals) data for baseline assessment of aortic vascular reactivity in $Ddah2^{M\Phi-}$ mice and their $Ddah2^{flox/flox}$ litter mates. (Analysis by Dr A Slaveiro)

Comparison made by two way analysis of variance (ANOVA).

6.2.3.6 Systemic nitric oxide levels in sepsis

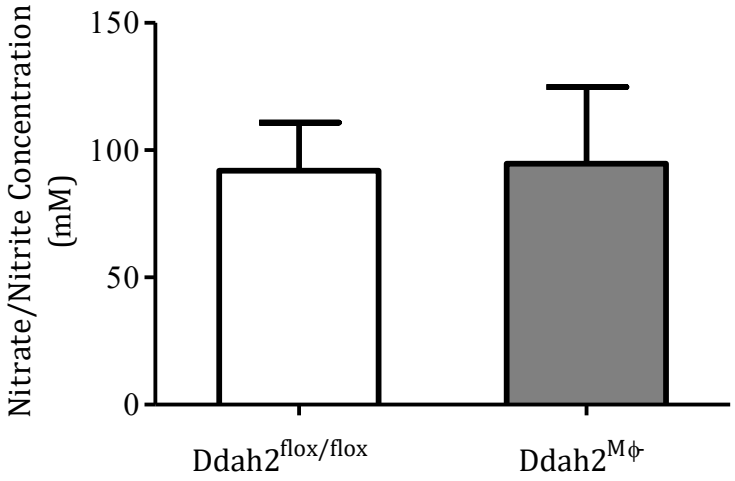

Figure 106: Plasma Nitrate+Nitrite(NOx) concentrations in DDAH2 macrophage specific knockout animals and floxed litter mate controls at the end of sepsis study.

A chemiluminescent technique was used to determine plasma NOx concentrations at the end of a caecal ligation and puncture mediated sepsis model in DDAH2 knockout mice ($Ddah2^{M\Phi-}$) and compared to floxed litter mates ($Ddah2^{flox/flox}$) Plasma NOx concentrations were similar in both groups at experimental cessation, p=0.95.

Systemic levels of nitric oxide were measured in plasma collected from mice at the time of termination, either upon reaching the pre-determined severity threshold or at the censor point of the experiment at 72 hours (Figure 106). No significant differences were observed between $Ddah2^{flox/flox}$ mice (Mean(SD) 91.9(37.7)µM) and $Ddah2^{M\Phi-}$ mice (94.7(30.0) µM), p=0.95.

6.2.3.7 Methylarginines in macrophage specific DDAH2 knockout models of sepsis

Systemic derangement of ADMA and SDMA consistent with severe sepsis was observed in the Ddah2$^{MΦ-}$ animals and their controls (Figure 107) (mean(SD)μM). ADMA concentrations were similarly elevated in both groups at 4.54(0.74) in floxed animals and 5.5(2.0) in the macrophage specific knockout mice (p=0.226).SDMA was elevated in Ddah2$^{flox/flox}$ mice at 6.0(3.9) and similarly increased in Ddah2$^{MΦ-}$ animals at 6.9(2.4), p=0.68. For technical reasons L-NMMA could not be reliably measured in these animals.

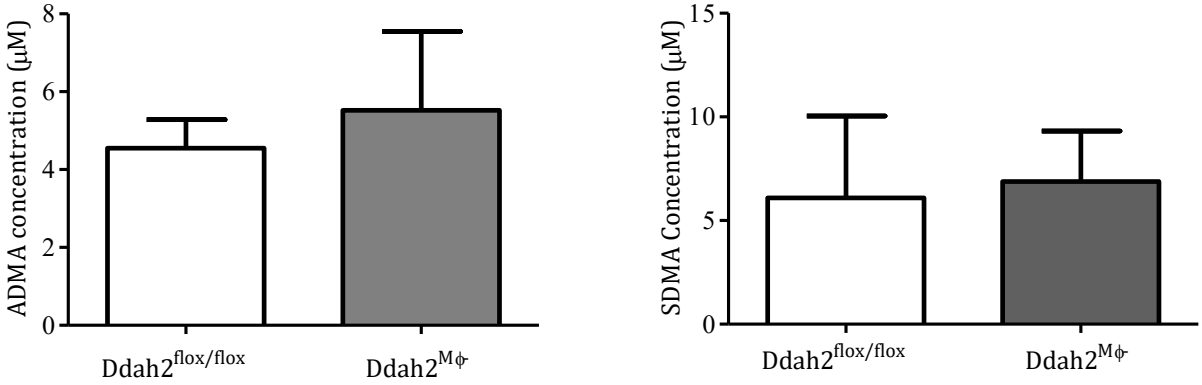

Figure 107: Plasma concentrations of methylarginines in DDAH2 macrophage specific knockout mice and floxed controls with sepsis.

Following experimental cessation, plasma taken at terminal bleed by cardiac puncture was analysed for methylarginine concentrations. All methylarginines were elevated over control levels, ADMA and SDMA were similar in both macrophage specific DDAH2 knockout mice (Ddah2$^{MΦ-}$) and floxed litter mates (Ddah2$^{flox/flox}$) , p=0.226 and 0.68 respectively.

6.2.3.8 Peritoneal and whole blood bacterial load in sepsis

Peritoneal bacterial load was significantly elevated in Macrophage specific knockout mice (Median (IQR)CFU/ml 9.0x10^5 (3.93 x10^5-1.72x10^6) against 1.0x10^5 (3.05 x10^5-3.0 x10^5), p=0.03 in Ddah2$^{flox/flox}$ animals. A similar trend was observed in whole blood of the Ddah2$^{MΦ-}$ mice 1800(1300-3500) vs 200(0-1400) in floxed control mice, p=0.056, Figure 108.

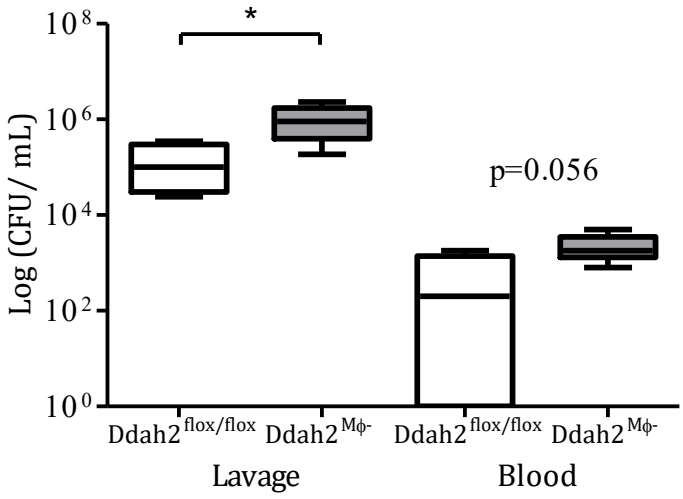

Figure 108: Whole blood and peritoneal washout bacterial loads in macrophage specific DDAH2 knockout mice and controls six hours after the onset of sepsis.

Serial dilutions of blood and peritoneal fluid collected from macrophage specific DDAH2 knockout mice and their litter mate controls collected six hours after the onset of sepsis were plated on Agar and the appropriate dilution counted for assessment of bacterial load at 24 hours. DDAH2 knockout mice ($Ddah2^{M\Phi-}$) had significantly higher peritoneal (p=0.03) and a trend towards higher blood (p=0.056) bacterial loads compared to floxed type litter mate controls ($Ddah2^{flox/flox}$). Data presented as Log_{10} colony forming units (CFU)/ml fluid.

6.3 Discussion

This series of experiments provides confirmation for the first time that the functional role of DDAH2 in macrophages observed previously translates to a meaningful pathophysiological impact in robust animal models of sepsis.

DDAH1 and DDAH2 have differing tissue distributions and chromosomal locations[23, 24]. This has led investigators to postulate that they play different roles in the maintenance of homeostasis and also the response to pathophysiological stress. The position of the DDAH2 gene in the MHC region of chromosome 6, coupled with human small scale human SNP association studies led us to explore the role of DDAH2 in sepsis.

6.3.1 The baseline physiology of DDAH2 knockout mice

6.3.1.1 Cardiovascular function

Our previous work has shown that knockout or pharmacological inhibition of DDAH1 results in a mouse or rat with a hypertensive phenotype, which arises as a consequence of elevated tissue ADMA concentrations and leads to inhibition of NO synthesis in vascular endothelial cells following pro-inflammatory stress. This modulates increased systemic vascular resistance and as a consequence, systemic blood pressure[47, 365]. these observations provide a potential mechanism for studies in humans that have associated plasma ADMA concentrations and SNP of DDAH1 with the presence of hypertension[33]. In sepsis, this elevation of systemic vascular resistance is one mechanism by which DDAH1 inhibition or knockout is protective in mouse and rat models of sepsis[213, 223]. In addition to improving survival, these studies showed that DDAH1 inhibition preserves organ perfusion and function as well as reducing the requirement for noradrenaline therapy to maintain blood pressure in rodent septic shock.

This contrasts starkly with the observations made in these studies of the role of DDAH2 in physiology and disease. The studies here show that under normal physiological conditions, global knockout of DDAH2 results in a developmentally normal mouse with a very subtle phenotype of increased blood pressure, only clearly demonstrated on secondary analysis when animals are at their most active. This validates the finding observed elsewhere that overexpression of DDAH2 generates resistance to the hypertensive phenotype caused by ADMA infusion[59]. Consistent with the finding that haemodynamics were minimally affected by deletion of DDAH2, we saw in *ex vivo* analysis of vascular responsiveness statistically significant but relatively small differences in reactivity following treatment with phenylephrine, acetylcholine and sodium nitroprusside. The modest impact of knockout on responsiveness is consistent with the degree of abnormal response seen in the *in vivo* testing. The decreased response to SNP, a NO donor was perhaps the most surprising *ex vivo* finding and at present is difficult to understand from the known mechanism of action of DDAH2.

6.3.1.2 Methylarginine handling

The pattern of methylarginine handling in the control mice is an interesting one. It is perhaps unsurprising that the pattern of MA concentrations in different tissues is variable between organs. There are multiple mechanisms that determine MA levels and these include PRMT expression and transport and the expression of DDAH1 which may compensate for the absence of DDAH2 to some degree in those tissues where they are co-expressed. Also, in the kidney and liver AGXT2 may play a role in regulating the MA bioavailability[21] and this may be altered in the absence of DDAH2. The action of AGXT2 may also explain the apparent increase in SDMA clearance seen in the urine of global DDAH2 knockout mice. Increased ADMA and L-NMMA reaching the kidney may compete with SDMA at the AGXT2 active site leading to reduced SDMA metabolism and a greater quantity reaching the collecting duct.

However, as might be expected, ADMA was elevated in both renal and cardiac tissues. The apparent increase in L-NMMA but not ADMA in the plasma may suggest differential handling by the tissues resulting in changes in the plasma 'pool' of MAs, however it may also point towards a role for DDAH2 in handling L-NMMA in preference to ADMA intracellularly, although this hypothesis requires further elucidation.

6.3.2 The septic response in the global knockout mice

A more apparent contrast to the actions of DDAH1 is the observation that in sepsis, mice display the opposite response to infection to that seen in DDAH1 knockout. It has been shown that DDAH2 knockout in macrophages using two different transgenic techniques leads to a pattern of significantly impaired cellular function, mediated by elevated ADMA concentrations and reduced NO synthesis by the cells in response to inflammatory cytokines. These effects result in impaired *in vitro* phagocytic ability and motility of knockout macrophages compared to appropriate controls[30]. The studies presented here addressed the question of how this apparent impairment of function at a cellular level contributed to modulating the pathophysiology and outcome from sepsis in the whole animal.

There are many potential models of sepsis in rodents, and here we chose a clinically relevant model of polymicrobial sepsis, analogous to human peritonitis, with a moderate to severe disease severity producing a rate of death of around 50% in control animals. Mechanisms for modifying the severity of this model include changing the size of bowel perforation, adding fluid resuscitation and/or antibiotic agents. We found that the optimum model included the administration of regular fluid resuscitation – which improved survival and also reduced suffering, regular long acting opioid analgesia with buprenorphine administered on a regular basis and two perforations of the ligated caecum with a 21Gauge needle. This achieved the desired illness severity for these studies coupled with a high degree of reproducibility.

6.3.2.1 Mortality

The impact of this model on DDAH2 global knockout mice with sepsis was profound. Exaggerated mortality of more than 30% was seen in the knockout mice, with all of the excess death arising in the first 24 hours after the induction of sepsis.

By using temperature as an additional surrogate endpoint, we were able to observe that the shock state developed earlier in global knockout mice and also that at the time of termination, a similar degree of hypothermia was present in both control and knockout populations, validating the blinded observation of severity as a tool for the assessment of severity in sepsis.

6.3.2.2 Cardiovascular function in sepsis

The cardiovascular impact of the global knockout of DDAH2 reflected the severity of the disease from which the septic mice were suffering. The early mortality of the Ddah2$^{-/-}$ mice prevented a direct comparison of the cardiovascular course of sepsis in the two groups over the whole of the disease, however it was possible to examine the terminal phase of disease – the last 24 hours – in both groups. Interrogation of the data set in this way showed that whilst at the start of the last day of life and also at termination, both groups were in a similar haemodynamic condition, knockout mice deteriorated earlier and displayed a shocked state for longer prior to reaching the severity end point than their wild type litter mates. Of note is that the subtle differences in aortic vascular responsiveness observed in control animals where completely overwhelmed in the septic mice. Interestingly, the only significant difference observed in the septic models was an exaggerated response to SNP administration in DDAH2 knockouts consistent with chronic NO deprivation in these mice. The consistent patterns of vascular responsiveness suggest that the hypotension seen in the DDAH2 deficient mice is not mediated by intrinsic vascular dysfunction but rather an indirect action on the vasculature.

6.3.2.3 The regulation of nitric oxide synthesis

Consistent with both previous animal[213] and human models[300] of sepsis, systemic levels of MAs are globally increased. This study shows however that in the absence of DDAH2, L-NMMA and ADMA are both significantly elevated over control animals. This may – as expected - reflect changes in intracellular tissue MA handling, with plasma measurement reflecting the net result of changes in MAs across the tissues. However it is important to note that greater illness severity at the time of collection may contribute to the observed differences and that given the differential impact of DDAH2 knockout on distinct tissues seen at baseline, interpretation of the changes seen in the plasma as reflective of specific tissue concentrations must be undertaken with caution.

6.3.3 Macrophage specific DDAH2 knockout in sepsis

The demonstration that excess mortality in DDAH2 deficient animals with sepsis arose during the first 24 hours of infection and was not mediated by vascular dysfunction, led to the suggestion that an impaired innate immune response was responsible. We therefore used the LoxP Cre recombinase mediated macrophage DDAH2 deficient mice in our sepsis model to explore this hypothesis.

6.3.3.1 Mortality

The knockout of DDAH2 in macrophages and granulocytes resulted in a near identical pattern of exaggerated early mortality to that seen in the global knockout mice. The degree of illness severity was similar in the $Ddah2^{M\Phi-}$ mice to that seen in the $Ddah2^{-/-}$ mice when temperature was measured at 18 hours after the onset of sepsis, consistent with a similar pattern of early deterioration in the knockout mice of both groups. At termination, temperatures were similar suggesting consistent illness severity at the threshold for experimental cessation. The similarities in response across the two transgenic models suggest that it is innate immune cell macrophage DDAH2 that plays a critical role in the regulation of the innate immune response and that this has a significant impact on the systemic response to infection.

6.3.3.2 Cardiovascular function in sepsis

Assessing the cardiovascular impact of macrophage specific knockout of DDAH2 in septic mice proved challenging. The attempt to undertake *in vivo* radiotelemetry in $Ddah2^{M\Phi-}$ and $Ddah2^{flox/flox}$ controls proved impossible when both knockout and control groups developed features of proximal gastrointestinal tract ischaemia making continuing with the experiment impossible. The mechanism for this apparent ischaemic complication was not immediately clear. Given that the finding arose in both groups of mice, it did not appear likely that this was DDAH2 mediated, instead it was suggested that a LoxP mediated phenomenon common to both groups might be responsible. The Cre LoxP model has been associated with a number of off target genetic and developmental effects [366, 367], and whilst unreported in the literature, a vascular malformation impairing mesenteric blood supply which only became apparent when the great vessel circulation was disrupted is a possible mechanism for this and may arise as a consequence of unidentified genetic variability introduced following breeding between floxed and Cre mice.

Instead of *in vivo* monitoring, measurement of anaesthetised blood pressure using the Millar catheter was considered the best alternative approach. These experiments revealed no significant differences at six hours after the onset of sepsis in systolic or diastolic blood pressure between the knockout and control groups. This method is limited by the single time point employed and the requirement for anaesthesia to facilitate catheter insertion. The use of volatile anaesthesia in sepsis mandated an early time point for assessment of haemodynamics as the volatile anaesthetic agents used in maintaining the sedation cause systemic vasodilatation. This both increases the risk of death causes by catastrophic hypotension and also reduces the sensitivity of the system to detect subtle differences in blood pressure between knockout and control groups. This contributes to the significant hypotension and also the similarities between the groups when tested.

6.3.3.3 Methylarginine handling

Plasma methylarginines in the macrophage specific knockout mice and their floxed controls were similarly elevated to the level seen in the global knockout models. No significant differences were observed in systemic concentrations of NO or methylarginines between Ddah2$^{M\Phi-}$ and the relevant controls. The absence of differences between these two models in the systemic concentrations does not necessarily reflect changes concentrations of MAs and local NO synthesis in macrophages. This is because whilst effects of DDAH2 knockout in macrophages at a cellular level may have a significant impact, the contribution that they make to the 'pool' of MAs and NO found in the plasma is relatively modest. This is in contrast to the impact of global knockout where multiple tissues are contributing additional MAs to the plasma.

6.3.4 Strengths and limitations

These studies explore, for the first time, the impact of DDAH2 knockout on the whole organism response to severe infection. The strengths of this study include the use of two different transgenic approaches. Both of which are associated with their own challenges, however the consistency of the response to sepsis across them makes the finding that DDAH2 is critical in regulating the systemic innate response to sepsis robust.

Corroborating this finding with the observations that bacterial load is significantly elevated in the abdominal cavity and also the blood in both knockout models suggests that the impacts of DDAH2 knockout on monocyte function observed previously lead to impaired bactericidal activity *in vivo.*

This, coupled with the observation that both at rest and in both models of sepsis, there are minor differences only between vascular function in knockout mice and their controls suggests that the hypotension seen in the knockout models is likely to be mediated by an exaggerated inflammatory state caused by an inability to eradicate bacteria rather than intrinsic dysfunction of vascular activity.

The inability to undertake *in vivo* monitoring of haemodynamics in the macrophage specific knockout mice and their controls is a limitation of this study. Had this been possible, it would have been valuable to observe whether the hypotension seen in the global knockout mice was also seen in the Ddah2$^{M\Phi-}$ mice. Had it been present, this would have confirmed the observation that intrinsic vascular dysfunction did not play a role in the sepsis induced hypotension seen in DDAH2 global knockout mice.

An additional limitation includes the use of only male mice in this study. It has been reported that female mice display quantitatively different responses to the septic insult[368]. It is not clear how this would affect the findings presented here but is the subject of further exploration.

6.3.5 Future work

In addition to understanding the role of sex hormones in DDAH2 knockout models of sepsis, it would also be interesting to study the impact of sepsis on the only other tissue that expresses DDAH2 exclusively – the heart. The development of a cardiac specific DDAH2 knockout mouse would provide valuable insights in to the role of DDAH2 in regulating the cardiac stress response.

Whilst understanding the mechanisms of mortality provides potential diagnostic, risk stratification and therapeutic insights, none of the studies undertaken here explore the impact of knockout on survivors from sepsis. With increasing interest in the survivor syndrome of sepsis and the long term consequences of the disease, a 'sepsis survivor' model, developed for use in the DDAH1 and DDAH2 knockout rats that the group is currently developing will provide great insights into the mechanisms of recovery from severe infections.

6.3.6 Summary statement

- Global knockout of DDAH2 in mice results in a developmentally normal mouse with a subtle hypertensive phenotype associated with exertion
- Global DDAH2 knockout results in systemic and organ specific dysregulation of methylarginine concentrations, with increased clearance of both L-NMMA and ADMA in the urine
- Global knockout of DDAH2 causes hypotension, impaired bactericidal activity and excess early mortality in a caecal ligation and puncture model of septic shock.
- In sepsis, global DDAH2 knockout is associated with systemic derangement of methylarginines
- Macrophage specific knockout of DDAH2 recapitulates the impaired bactericidal activity and early mortality from sepsis of global knockout suggesting the macrophage DDAH2 is a critical player in the innate immune response.

7 Endogenous inhibitors of nitric oxide synthesis and their regulators in human sepsis

7.1 Introduction

The work reported here, in conjunction with that undertaken previously presents strong evidence from animal experimentation that DDAH1 and DDAH2 both play important roles in the response to sepsis. It appears that in rodent models, DDAH1 inhibition or knockout leads to a protective effect based upon improvement in vascular tone and preservation of organ perfusion[47, 213, 223]. In contrast, knockout of DDAH2 results in significant impairment of the immune response which results in reduced ability to eradicate bacteria. This in turn leads to excess mortality in rodent models of sepsis[30].

These observations provide mechanistic insight into the role of each DDAH isoform in regulating NO synthesis in their respective tissue distributions. Understanding the relevance of these observations in human disease requires an alternative approach. Building upon small studies in the area to date, this chapter focuses on the largest observational study of methylarginines and their regulators ever undertaken in patients with septic shock.

7.1.1 Human sepsis

As described in the introductory chapter, septic shock is a syndrome characterised by catastrophic organ dysfunction and in around 30% of patients, death within 30 days of admission to hospital [86, 369-374]. A burgeoning number of patients are admitted to intensive care with sepsis each year with over 1million admissions per year in the USA[84], 120,000 annually in the UK[86] and countless others who are never admitted to hospital or go unreported in the developing world. The immediate costs of managing the care of these patients are huge, in the region of $20 billion annually in the US alone[13]. However this grossly underestimates the long term costs associated with what was once thought to be a transient insult leaving survivors relatively unscathed after discharge. There is now a growing body of evidence suggesting that sepsis leaves its mark on survivors with patients displaying an increased risk of premature death[90], long term functional[93] and cognitive[99] impairment and progressive chronic kidney disease[96].

In summary, sepsis confers acute distress coupled with a significant medical, social and health economic burden on survivors and their families in the long term.

7.1.2 Human studies of methylarginines and DDAH in sepsis

7.1.2.1 Methylarginines in sepsis

As described in the introduction, human studies in this area have been limited to small observational studies that have included less than thirty patients with septic shock. These studies have associated derangement of methylarginine levels with other indices of inflammatory stress. Two studies exploring an association of polymorphisms of DDAH2 with ADMA concentrations and clinical outcomes have included small numbers of patients making robust inferences from those data challenging.

The only study to focus entirely on ADMA in sepsis patients collected a group of 47 admissions to hospital with severe sepsis and septic shock[40]. Of these patients, who had a median SOFA score of 7 in survivors and 9 in non survivors (n=14), they found that ADMA was elevated in sepsis patients as a whole (median(IQR) 0.89(0.57-1.09)μM on day 1 and 1.05(0.71-1.32)μM on day 7) compared to a group of ten healthy volunteers (0.63(0.57-0.71), $p<0.01$. They did not detect a difference in ADMA concentrations between survivors and non-survivors at either day 1 or day 7, however they did observe positive correlations between ADMA levels and indices of illness severity such as plasma lactate, SOFA score and vasopressor requirement. Interestingly on Day 1 only 13(34%) of patients required a vasopressor infusion suggesting that septic shock by the conventional definition was present in only one third of patients.

A 2012 study by Brenner compared 60 septic patients to 30 healthy volunteers and 30 non-infected elective surgical patients[207]. Healthy volunteers had a median(IQR) plasma ADMA concentration of 0.43(0.37-0.51)μM. Whilst the average plasma concentrations of the septic patients were not reported, the paper states that they were significantly elevated throughout the 28 day period of observation over controls. No differences were observed between plasma ADMA concentrations based on survival, acute renal failure or the presence of adult respiratory distress syndrome (ARDS). The authors did observe an association with acute liver dysfunction, where ADMA levels were significantly higher throughout the study period compared to those in whom liver function remained normal. It is however impossible to determine if this is a reflection of illness severity or of an intrinsic difference in ADMA handling caused by liver dysfunction. Also of note is that only 15 patients in the septic group had deranged hepatic function making interpretation of these data difficult.

In 2011, Davis et al undertook a study examining 67 patients in a single centre with sepsis and septic shock[208]. The non-shock group were not severely unwell, with median SOFA scores of 2 and the septic shock group who numbered just 20 were also not at the high risk end of the spectrum (median SOFA score 6). This explains why only six patients overall and five in the septic shock group died. These observations make interpreting the finding of increased mortality risk in this study impossible. The group did note however that there was a trend towards elevated plasma ADMA in the sepsis cohort compared to healthy controls (median(IQR) 0.57(0.50-0.62)μM vs 0.52(0.39-0.65)μM respectively), p=0.10, and also that ADMA was higher in those six patients that did not survive compared to the other participants (p=0.01). They also observed a positive correlation between plasma ADMA and SOFA score. Furthermore it was reported that SDMA and serum creatinine were closely correlated and that the association of SDMA with outcome was lost when correction for renal function was undertaken.

Examining the association of SDMA with outcome, Kock et al in 2013[211] undertook a study including 160 patients with sepsis in a group of 247 admitted to critical care. They found that SDMA was highest in the septic group (median(IQR) 0.89(0.19-4.0)μM compared to 0.38(0.2-1.06)μM in healthy controls, p<0.01. Correlations at a univariate level were observed between SDMA and a range of makers of infection severity such as pro-calcitonin and also renal and hepatic dysfunction. Only the associations of SDMA with serum creatinine and pro-calcitonin survived multivariate correction. These observations led to the hypothesis that SDMA might independently predict outcome and the group showed that after multivariate Cox regression, SDMA remained positively associated with death both in the ICU (hazard ratio 1.379, p=0.042) and after discharge from hospital (hazard ratio 1.357, p=0.002).

It is of interest that in paediatric sepsis, an opposite finding has been observed[209]. Children with septic shock have been shown in a study of thirty patients with sepsis to have lower plasma ADMA concentrations (median(IQR) 0.38(0.30-0.56)μM) compared to healthy controls (0.60(0.54-0.67)μM, p<0.001. Interestingly the change in ADMA was inversely correlated with degree of inflammation measured by IL-6 and IL-8. Of note is that it was the septic patients with neutropenia (13/30) who had the lowest ADMA levels. Patients with sepsis and a normal white cell count did not have a significantly lower ADMA level. This suggests that immune cell regulation of ADMA may contribute more to the plasma pool of ADMA in paediatrics than impaired renal clearance does in adults. The finding of low ADMA in sepsis in paediatrics was confirmed by a separate study in children with malaria[210]. In that study both uncomplicated and severe malaria were associated with lower ADMA (median(IQR) 0.4(0.33-0.47)μM and 0.4(0.3-0.51)μM respectively) compared to 0.61(0.56-0.69)μM, p<0.001 for both. Plasma ADMA remained significantly reduced in both groups at 28days compared to healthy volunteers.

7.1.2.2 Dimethylarginine Dimethylaminohydrolase 2

The chromosomal location of the DDAH2 gene within the MHCIII region of chromosome six coupled with its tissue distribution had led to the hypothesis that SNPs of DDAH2 might be associated with outcome in humans with sepsis. Two studies have explored this association, although neither has had the power to make definitive inferences. In the study reported above, O'Dwyer et al examined one DDAH2 SNP(rs805305) in 47 patients to determine if there was an association with outcome[40]. The SNP rs805305 is found in the promoter region of DDAH2 and has been associated with a functional role in determining ADMA concentrations and the presence of hypertension[38, 375]. They found no relationship between it and any of the clinical outcomes. However they did observe that one allelic variant was associated with increased ADMA concentrations on day 1 of intensive care admission.

In a follow up to their paediatric ADMA study, Weiss et al associated the rs805305 polymorphism with lower plasma ADMA concentrations and within that group a greater incidence of 'cold shock' defined by sepsis with a low cardiac output state was observed[39]. This study involved only 27 participants and so interpreting these data remains challenging.

In summary, the literature exploring ADMA, DDAH2 and their association with sepsis have been largely small, single centre observational studies. They raised interesting hypotheses regarding a relationship between ADMA and surrogate outcomes in sepsis, however to date there is no definitive study exploring robust clinical endpoints and endogenous inhibitors of NO synthesis. Furthermore, no study has had the power to detect differences in either plasma methylarginines or clinical outcomes associated with SNPs of methylarginine regulating genes. No human studies have explored the role of DDAH1 polymorphisms in sepsis.

7.2 Study design

7.2.1.1 The Genetics Of sepsis and Septic shock in Europe (GenOSept) and Genome wide Association in Sepsis (GAinS) Studies

The GenOSept and GAinS studies were conducted in seventeen countries across Europe between 2005 and 2011. The GenOSept study recruited 1525 patients with severe sepsis and septic shock in 143 hospitals across sixteen countries. Patients included in this study were suffering from sepsis as a consequence of either community acquired pneumonia (CAP) (n=794) or faecal peritonitis (FP) (n=731). This study was completed in 2009 at which time the GAinS study started to recruit patients with CAP (n=241) in the UK [248]. GenOSept samples were analysed using the Affymetrix 500k SNP chip and GAinS using the Illumina 1M SNP chip. The directly measured SNPs are distributed evenly across the 4.5million documented SNPs to allow imputation of changes in other unmeasured SNPs through their linkage disequilibrium with them.

In our study, we drew on our previous work showing that in animal models, knockout of DDAH1 and DDAH2 both have significant – and opposite – impacts on outcome in septic shock[30, 213]. We interrogated the GAinS and GenOSept cohorts with the specific hypothesis that SNPs of DDAH1 and DDAH2 are associated with outcome in human sepsis.

Analysis of directly measured SNPs and those known to be in linkage disequilibrium with the measured polymorphisms was undertaken based on our hypothesis. 601 SNPs of the DDAH1 gene and 36 for DDAH2 were examined using this technique. Explored SNPs are published in Appendix 1.

7.2.2 VAsopressin versus Noradrenaline as Initial therapy in Septic sHock (VANISH) study

The VANISH study was undertaken between 2013 and 2015 and was a randomised controlled trial in a 2x2 format of vasopressin vs noradrenaline, with or without the addition of corticosteroids in patients with septic shock. This study recruited 412 participants with vasopressor dependent septic shock from eighteen intensive care units in the UK. The full protocol for this study has been published[250].

The primary endpoint of the study was the number of renal failure free days, with secondary end points including 28 day mortality and length of hospital and ICU stay. The study included the collection of an extensive amount of data including routinely collected clinical information and detailed assessment of illness severity (SOFA score[251]), degree of shock and level of organ support required during the ICU stay. In a subpopulation of patients recruited to three of the study centres, regular blood sampling was undertaken during the first seven days of admission to the critical care unit.

Samples were collected at admission to the ICU prior to the commencement of the intervention and on study day 3, 5 and 7 after enrolment. In 215 patients, plasma and buffy coat samples were collected by centrifugation of whole blood at the collection centre immediately following collection. In a further 75 patients, whole blood was collected in EDTA tubes and stored for subsequent analysis(Figure 12).

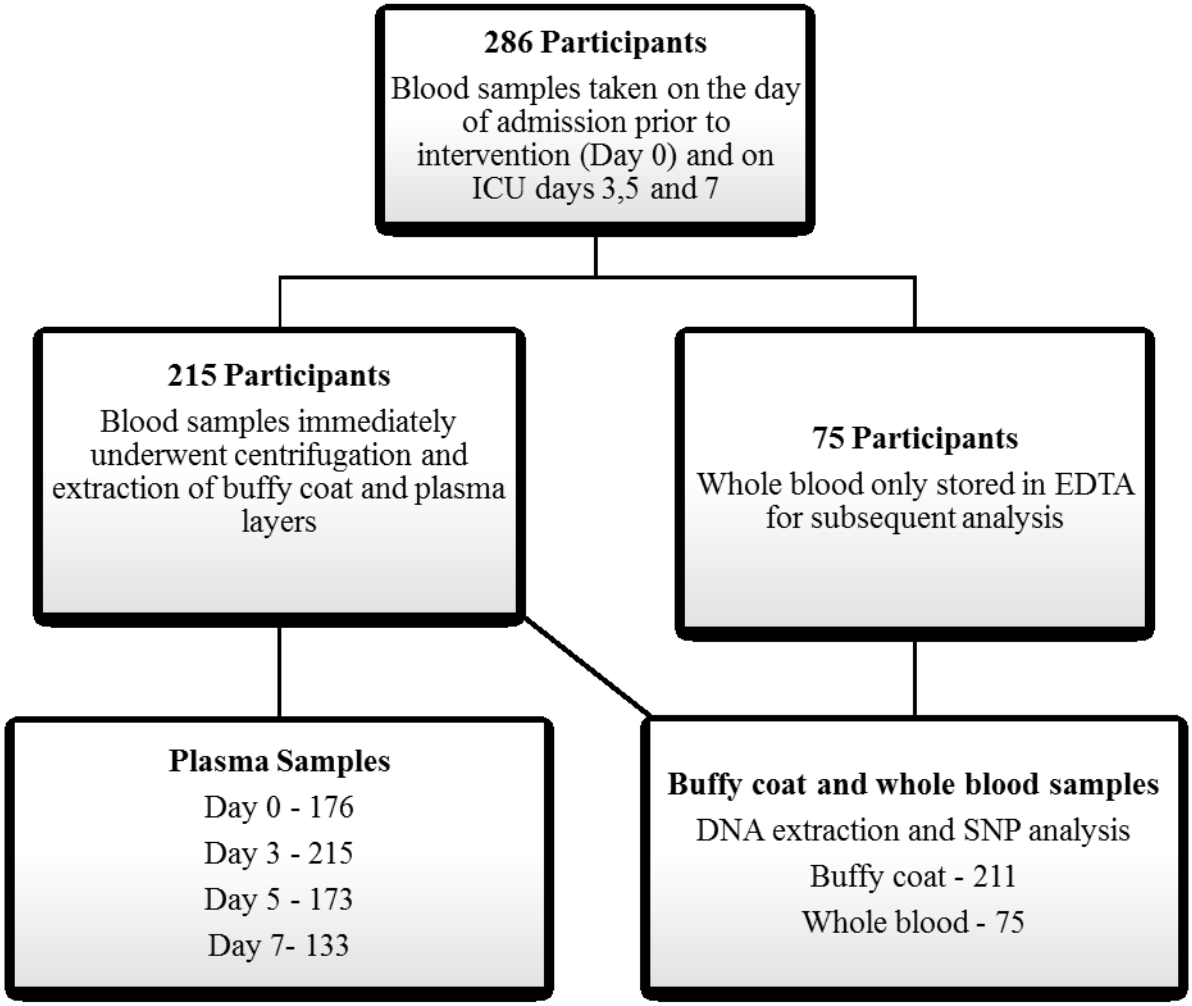

Figure 109: Schematic representation of sample handling of blood and plasma collected from patients in the VANISH trial

The following analyses were undertaken of the association between the following biochemical indices, 28day mortality and the SNPs that were identified:

Biochemical measures
Plasma Nitrate + Nitrite
Plasma ADMA
Plasma SDMA
Plasma L-Arginine

Table 26: Clinical outcomes and biochemical indices measured in the patients recruited into the VANISH study and for whom plasma was available.

Samples underwent extraction and analysis prior to release of the clinical outcomes associated with each patient. Treatment group allocation was labelled A, B, C or D in a blinded fashion. Analysis was undertaken of the relationship between the biochemical values and outcome as above. Prior to end point comparison, samples were analysed for group allocation, age and sex.

DNA extraction and analysis of SNPs was undertaken by the external contract research organisation LGCgroup plc(UK).

7.3 Results

7.3.1 GenOSept database interrogation

Analysis of polymorphisms of DDAH1, DDAH2 and their association with mortality was undertaken using data collected and stored in the GenOSept database by Dr Anna Rautanen of the Wellcome Trust Centre for Human Genetics, Oxford, UK. An initial screen of SNPs of DDAH1 and DDAH2 that have previously been associated with disease outcomes or risk factors revealed no significant associations with mortality in severe sepsis and septic shock (Table 27).

SNP	GENE	Genotyped/Imputed	p (GenOSept+GAinS)
rs233112	DDAH1	genotyped	0.81688
rs233128	DDAH1	imputed	0.82937
rs17384213	DDAH1	imputed	0.24033
rs7521189	DDAH1	genotyped	0.37867
rs11161614	DDAH1	imputed	0.5505
rs669173	DDAH1	imputed	0.099602
rs1146381	DDAH1	imputed	0.60201
rs7555486	DDAH1	imputed	0.33726
rs13373844	DDAH1	imputed	0.32798
rs37369	AGXT2	genotyped	0.3049
rs805305	DDAH2	genotyped	0.35586
rs9267551	DDAH2	imputed	0.87771
rs805304	DDAH2	genotyped	0.4557
rs2272592	DDAH2	imputed	0.94835
rs3131383	DDAH2	imputed	0.18412
rs707916	DDAH2	genotyped	0.3926

Table 27: SNPs of DDAH1 and DDAH2 that have previously been associated with disease and the probability that they were associated with mortality in severe sepsis and septic shock.

An interrogation of the dataset formulated by combination of the GAinS and GenOSept databases was undertaken. No positive associations with mortality were found in any of the published genes. Analysis undertaken by Dr Anna Rautanen

In the light of these findings, the interrogation was widened to include all remaining SNPs of DDAH1(n=601) and DDAH2(n=36). Exploration of this data set identified a series of 8 SNPs of DDAH1 that were associated with mortality (Table 28) after adjustment for multiple comparisons. Aside from these SNPs, of the remaining DDAH1 and DDAH2 SNPs interrogated, none were strongly associated with outcome (Appendix 1).

SNP	CHR	BP	p value	adjusted OR	maf cases	maf controls	Location
rs1524001	1	86017485	9.44E-05	1.976821	0.12583	0.090348	intronic
rs7531068	1	86016103	9.90E-05	1.97792833	0.12547	0.09016	intronic
rs10782552	1	86015715	0.000102	1.97662333	0.12536	0.090175	intronic
rs897255	1	86018583	0.00012	1.97581308	0.12224	0.087754	intronic
rs72726326	1	86040708	0.000225	1.92317987	0.11944	0.087453	intronic
rs6576775	1	86030595	0.000337	1.88357205	0.11959	0.088026	intronic
rs1378226	1	86038738	0.000434	1.84675492	0.12326	0.091876	intronic
rs6682848	1	86038476	0.000437	1.8463856	0.12323	0.091872	intronic

Table 28: DDAH1 SNPs associated with an increased odds ratio of death in sepsis.

SNP: Single nucleotide polymorphism, CHR: Chromosome, BP Base pair, OR: Odds ratio, maf: Minor allele frequency cases(sepsis population), controls (healthy cohorts for comparison). (Analysis by Dr Anna Rautanen)

Figure 110 represents the position of these SNPs in the first intron of DDAH1and describes the degree of linkage disequilibrium between the top SNP and the other SNPs in the region.

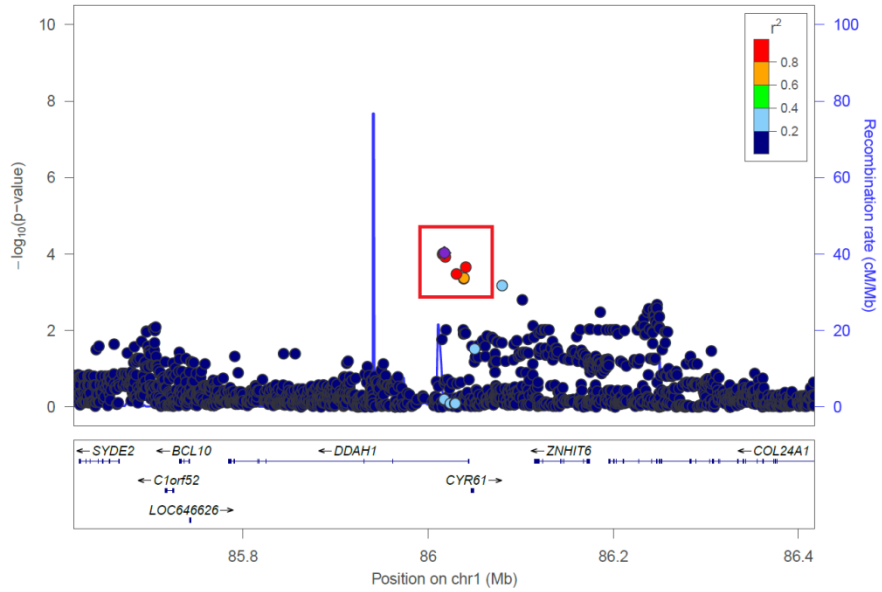

Figure 110: Association plot of the SNPs significantly associated with mortality in sepsis.

SNP associations in GenOSept/GAinS and the linkage disequilibrium structure in the region (each dot represents a SNP, y-axis shows the p-value and x-axis the chromosomal location; colour coding of each dot represents the linkage disequilibrium (LD) between the top associated SNP (purple dot) and other SNPs in the region). Red box highlights the seven SNPs associated with outcome. Blue spike represents a recombination hotspot in Intron 1 of the DDAH1 gene. (Analysis by Dr Anna Rautanen)

7.3.2 VANISH study findings

7.3.2.1 Demographic and treatment group analysis

Plasma ADMA concentrations in study participants were analysed based on age, sex and treatment group allocation. Correlations with age were undertaken for each time point and peak ADMA and revealed no significant associations (Table 29, representative Figure 111)

Time point	r^2	p value
Admission	0.0003	0.84
Day 3	0.0002	0.81
Day 5	0.021	0.07
Day 7	0.018	0.15
Peak	0.0024	0.44

Table 29: Linear regression (r^2) and p value for plasma ADMA concentration against age for each time point studied and peak value over the first seven days of ICU admission in patients with septic shock.

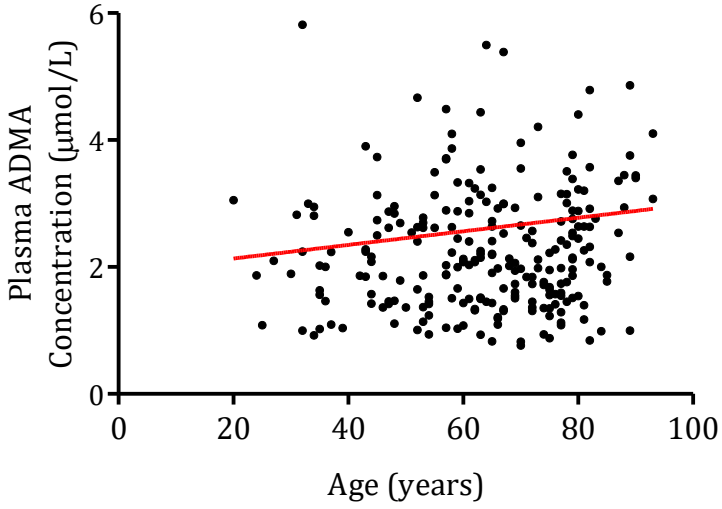

Figure 111: Relationship between peak plasma ADMA concentration over the course of the first seven days of admission to ICU with septic shock and age.

There was an association between sex and peak ADMA value, with men displaying higher (median(IQR) peak ADMA concentrations (2.26(1.64-2.99)µM) compared to women (1.97(1.42-2.73)µM), p=0.011(figure).

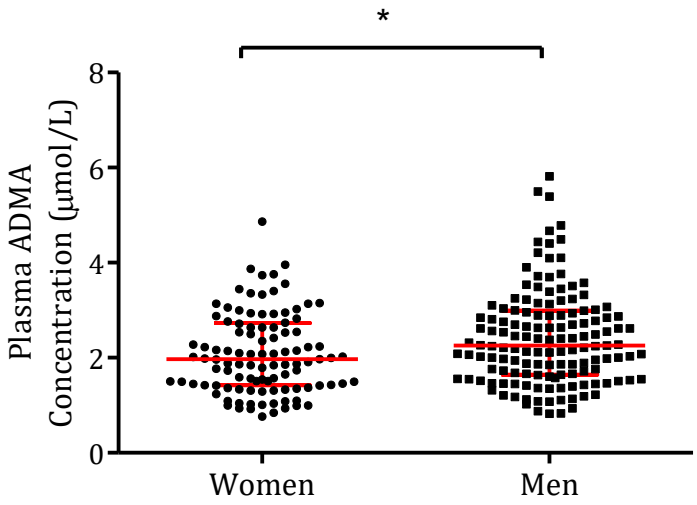

Figure 112: Peak plasma ADMA concentration in women and men over the first seven days of admission to the ICU with septic shock.

Plasma methylarginine concentration was measured using the mass spectrometric technique described above. Each point represents a single patient result, red bar represents median value and interquartile range. Men displayed a higher median peak plasma ADMA concentration than women (p=0.01).

Peak plasma ADMA concentration was analysed using one way ANOVA and was similar in all four treatment groups studied (p=0.73) as was ADMA concentration at each time point examined (day 3: p= 0.98, day 5: p=0.94 and day 7: p=0.18) Representative image, Figure 113.

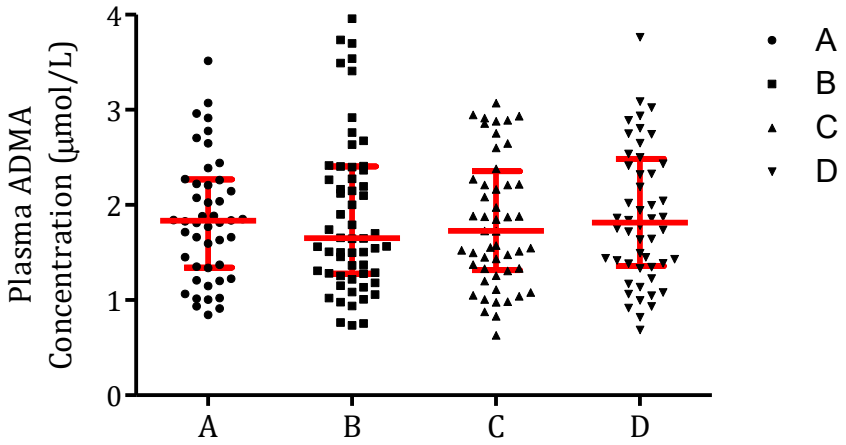

Figure 113: Peak plasma ADMA concentration over the course of the first seven days of ICU admission presented by treatment group allocation.

Plasma methylarginine concentration was measured using the mass spectrometric technique described above. Each point represents a single patient result, red bar represents median value and interquartile range. No differences were observed in median peak plasma ADMA concentration across the treatment groups (p=0.73). Treatment groups were given a blinded categorical value A-D.

7.3.2.2 Plasma nitric oxide in human septic shock

Plasma NOx was significantly elevated in patients with septic shock compared to normal values seen in healthy volunteers. Median(IQR) NOx was 101(63-148)µM on admission, 92(54-153)µM on day 3, 100(51-149)µM on day 5 and 81(45-120)µM on day 7. A trend towards change in NOx concentration was observed by one way ANOVA, p=0.052. When compared directly using non-parametric analysis, a significant reduction in NOx was seen between admission and day 7 of ICU stay (p<0.01)(Figure 114).

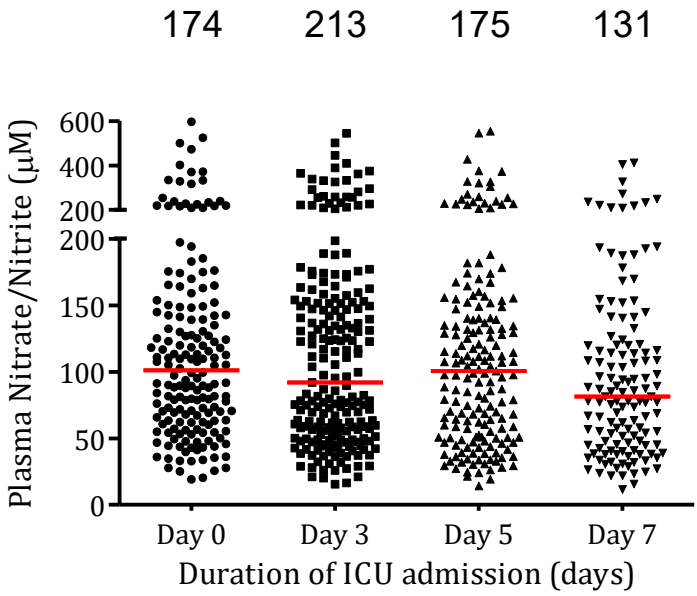

Figure 114: Plasma nitrate+nitrite over the first seven days of ICU admission in patients with septic shock.

Plasma nitrate+nitrite was measured using a chemiluminescent technique as described previously. The number of samples analysed for each study day is represented above each time point. Each point represents a single patient result, red bar represents median value.

7.3.2.3 Methylarginines and L-arginine in human septic shock

Plasma ADMA concentration rose over the course of admission to intensive care. Median(IQR) was 1.59(1.17-2.2)µM at admission, 1.8(1.3-2.4)µM on day 3, 2.0(1.6-2.7)µM on day 5 and 2.2(1.6-2.8)µM at day 7, p=0.08 (1 way ANOVA), p<0.001 if day 0 and 7 are compared by Mann Whitney analysis(Figure 115).

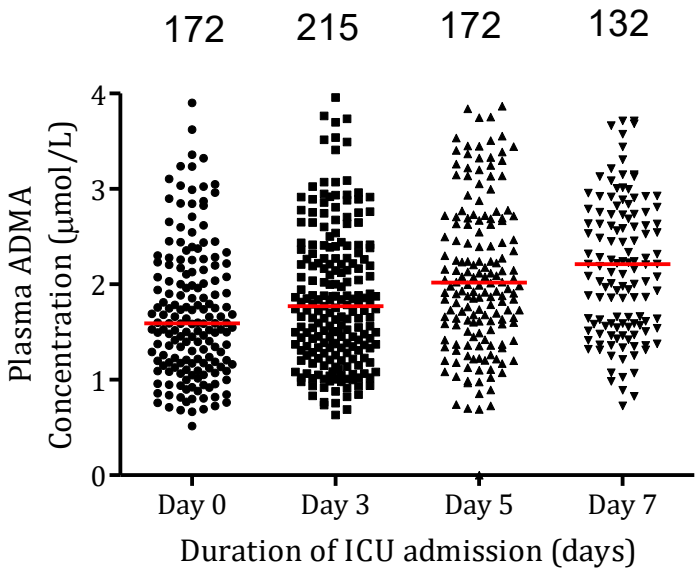

Figure 115: Plasma ADMA concentrations over the course of the first 7 days of admission to ICU with septic shock.

Plasma methylarginine concentration was measured using the mass spectrometric technique described above. The number of samples analysed for each study day is represented above each time point. Each point represents a single patient result, red bar represents median value.

Plasma SDMA concentration displayed no significant change over the course of the seven days studied. At admission, median(IQR) concentration was 3.4(2.0-5.2)µM, 3.4(1.8-5.3)µM on day 3, 3.4(2.0-5.2)µM on day 5 and 3.1(1.7-4.8)µM on day 7, p=0.31 by one way ANOVA, p=0.11 by comparison of admission to day 7 plasma values by Mann Whitney (Figure 116).

L-arginine concentration was significantly reduced compared to normal plasma concentrations from human volunteer studies presented here and the existing literature[376]. Median(IQR) plasma concentration was 25.3(17.2-35.1)µM at admission, 30.9(22.8-42.4)µM on day 3, 32.6(25.2-47.5)µM on day 5 and 32.9(24.2-47.3)µM on day 7, one way ANOVA revealed a significant rise over the course of the study period, p=0.009. Bonferroni's comparison revealed significant ($p<0.05$) differences between baseline values and days 5 and 7(Figure 117).

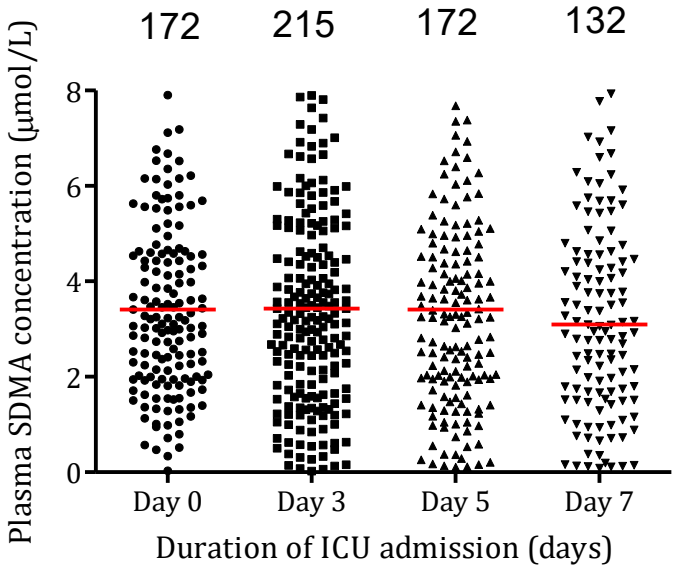

Figure 116: Plasma SDMA over the course of the first seven days of admission to ICU in patients with septic shock.

Plasma methylarginine concentration was measured using the mass spectrometric technique described above. The number of samples analysed for each study day is represented above each time point. Each point represents a single patient result, red bar represents median value.

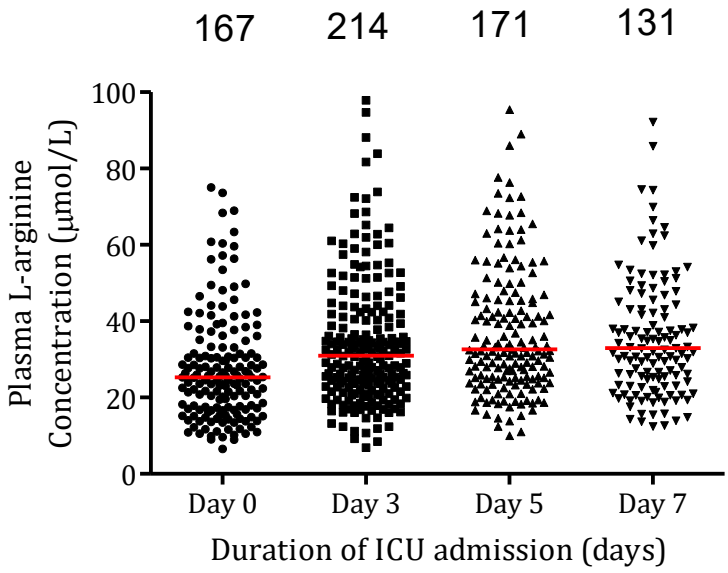

Figure 117: Plasma L-arginine concentrations over the course of the first seven days of admission to ICU in patients with septic shock.

Plasma L-arginine concentration was measured using the mass spectrometric technique described above. The number of samples analysed for each study day is represented above each time point. Each point represents a single patient result, red bar represents median value.

7.3.2.4 Correlations between methylarginines and nitric oxide synthesis

Correlation between plasma methylarginine concentrations and plasma NOx was undertaken using both Pearson's and Spearman's coefficients to search for both linear and non-linear correlations between the measured indices. Significant positive correlations were detected between plasma concentrations of ADMA and nitric oxide at admission and on days 3 and 5 of ICU stay (Table 30). SDMA was positively associated with plasma NOx at all four time points (Table 31). Arginine concentration was not associated with NOx at any time point (Table 32). ADMA and SDMA were positively correlated at all time points (Table 33)

Time point	Pearson's r	Pearson's p value	Spearman's r	Spearman's p value
Admission	0.1675	0.03	0.30	<0.001
Day 3	0.21	0.002	0.17	0.02
Day 5	0.38	<0.001	0.25	0.001
Day 7	0.001	0.67	0.27	0.003

Table 30: Correlation coefficients and p values for comparison of plasma ADMA and plasma NOx concentration over the first seven days of ICU admission with septic shock.

Time point	Pearson's r	Pearson's p value	Spearman's r	Spearman's p value
Admission	0.25	0.001	0.42	<0.001
Day 3	0.41	<0.001	0.40	<0.001
Day 5	0.54	<0.001	0.45	<0.001
Day 7	0.33	<0.001	0.40	<0.001

Table 31: Correlation coefficients and p values for comparison of plasma SDMA and plasma NOx concentration over the first seven days of ICU admission with septic shock.

Time point	Pearson's r	Pearson's p value	Spearman's r	Spearman's p value
Admission	-0.02	0.82	0.05	0.49
Day 3	-0.11	0.10	-0.11	0.11
Day 5	0.04	0.57	-0.05	0.53
Day 7	0.04	0.68	0.12	0.19

Table 32: Correlation coefficients and p values for comparison of plasma L-arginine and plasma NOx concentration over the first seven days of ICU admission with septic shock.

Time point	Pearson's r	Pearson's p value	Spearman's r	Spearman's p value
Admission	0.53	<0.001	0.56	<0.001
Day 3	0.50	<0.001	0.51	<0.001
Day 5	0.67	<0.001	0.51	<0.001
Day 7	0.22	0.01	0.46	<0.001

Table 33: Correlation coefficients and p values for comparison of plasma ADMA and SDMA concentration over the first seven days of ICU admission with septic shock.

7.3.2.5 Plasma nitric oxide and outcome in septic shock

Plasma NOx was measured and the relationship between these values and 28 day survival determined. Median(IQR) NOx concentrations of survivors and non-survivors were similar on admission (99.2(61.7-145.7)µM vs 100.1(70.3-160.2)µM, p=0.66) and on day 3 (90(51.5-155.7)µM vs 116.3(57.6-147.4)µM, p=0.92 (Figure 118). On day 5, plasma NOx was significantly higher in non-survivors (116.4(68.4-169.4)µM) compared to those that survived ICU admission (95.6(48.7-139.5)µM, p=0.04. This difference persisted at day 7, with survivors displaying a median(IQR) NOx of 77(43.2-116.2)µM and non-survivors (117.0(82.1-189.3)µM, p=0.01 (Figure 119).

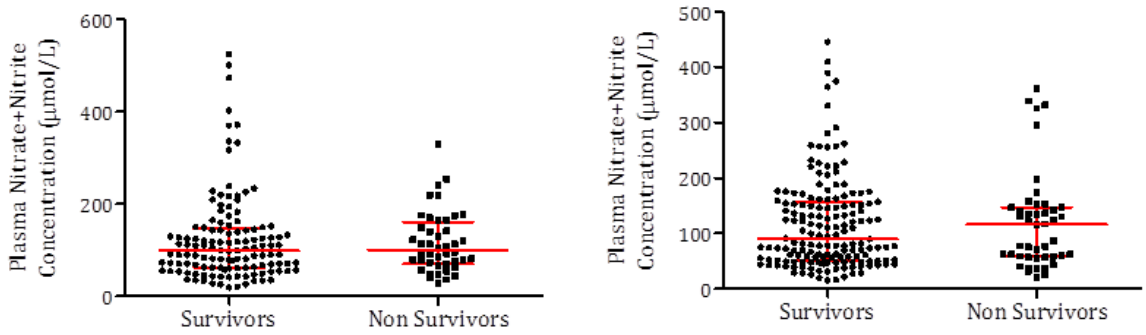

Figure 118: Plasma Nitrate+ Nitrite Concentrations on admission (Left panel) and day 3 (right panel) in survivors and non survivors of septic shock.

Plasma nitrate+nitrite was measured using a chemiluminescent technique as described previously. Samples analysed and were categorised by survival at 28 days after ICU admission. Each point represents a single patient value at the respective time point. The red bars represent median and interquartile range.

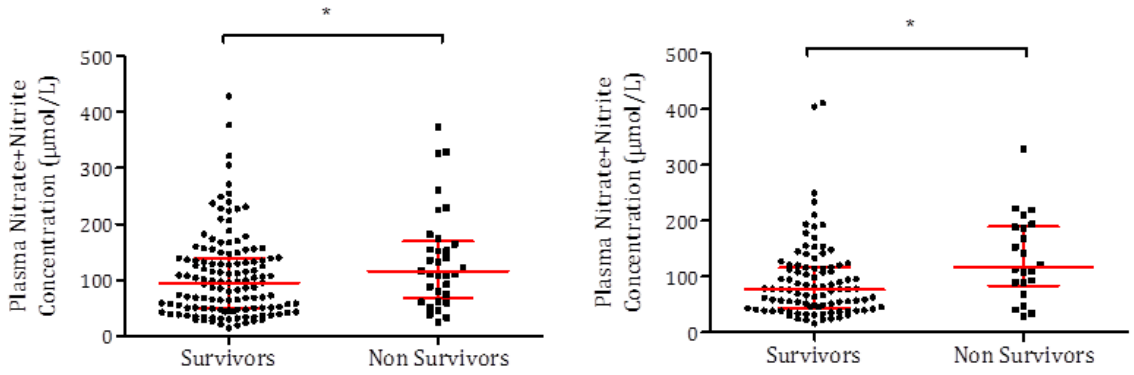

Figure 119: Plasma Nitrate+ Nitrite Concentrations on day 5 (Left panel) and day 7 (right panel) in survivors and non survivors of septic shock.

Plasma nitrate+nitrite was measured using a chemiluminescent technique as described previously. Samples analysed and were categorised by survival at 28 days after ICU admission. Each point represents a single patient value at the respective time point. The red bars represent median and interquartile range. *= p<0.05 (Mann Whitney analysis).

Analysis of survival by quartile of plasma NOx revealed no significant differences between outcomes, log rank test, p=0.91(Figure 120).

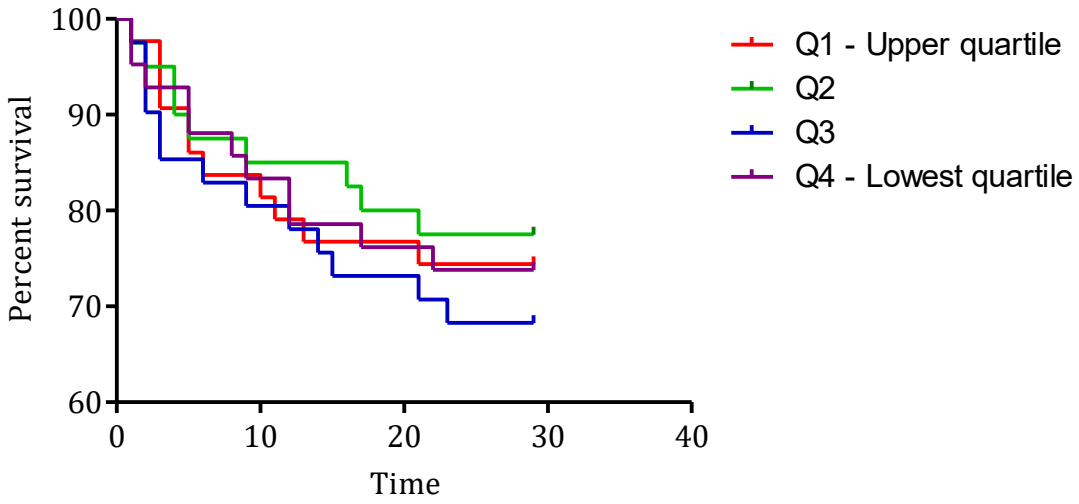

Figure 120: Kaplan Meier curves of peak plasma NOx concentrations during the first seven days of ICU admission with septic shock divided by quartiles and their relationship with 28 day mortality.

Kaplan Meier survival curves representing the four quartiles of plasma nitrate+nitrite concentrations. Highest quartile red, second green, third blue, fourth (the lowest) purple. P=0.91.

7.3.2.6 Association between ADMA and outcome in septic shock

Elevated plasma ADMA concentration was associated with mortality at 28days in samples taken at admission, day 3 (Figure 121), day 5 and day 7 (Figure 122) (Table 34), all p values <0.001. When plasma ADMA values were dichotomised, a value in the upper 50% of values was associated with a hazard ratio for death at 28days of 3.3(95% Confidence Interval: 2.0-5.4), p<0.01.

Time point	Survivors		Non-survivors	
	Median(µM)	Interquartile range(µM)	Median(µM)	Inter quartile range(µM)
Admission	1.49	1.11-1.96	2.08	1.50-2.78
Day 3	1.66	1.28-2.20	2.33	1.53-2.92
Day 5	1.92	1.43-2.61	2.63	2.08-3.30
Day 7	2.08	1.49-2.71	2.67	2.22-3.57

Table 34: Median(IQR) plasma ADMA concentrations of survivors and non-survivors of septic shock at admission and on days 3, 5 and 7 of ICU admission.

Plasma methylarginines were measured using the established mass spectrometry technique. Plasma concentrations (median(IQR)µM) are reported in survivors and non-survivors at 28days after ICU admission.

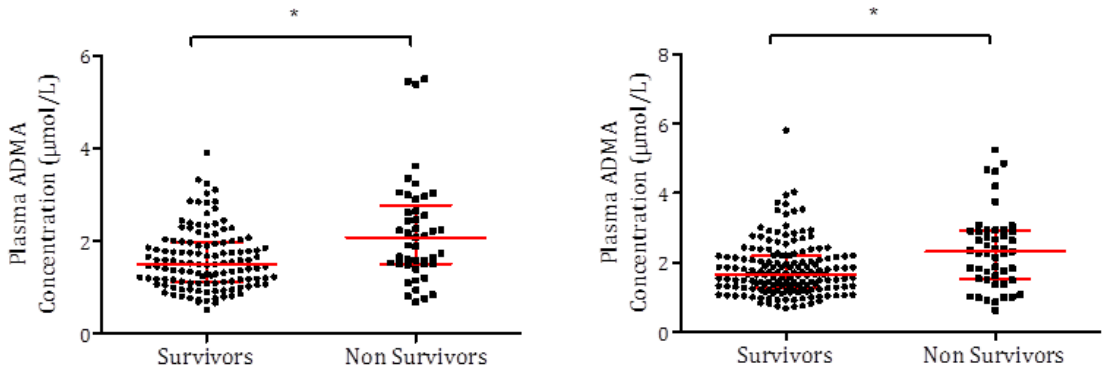

Figure 121: Plasma ADMA concentrations on admission (Left panel) and day 3 (right panel) in survivors and non survivors of septic shock.

Plasma methylarginines were measured using a mass spectrometry technique as described previously. Samples analysed and were categorised by survival at 28 days after ICU admission. Each point represents a single patient value at the respective time point. The red bars represent median and interquartile range. *=p<0.05

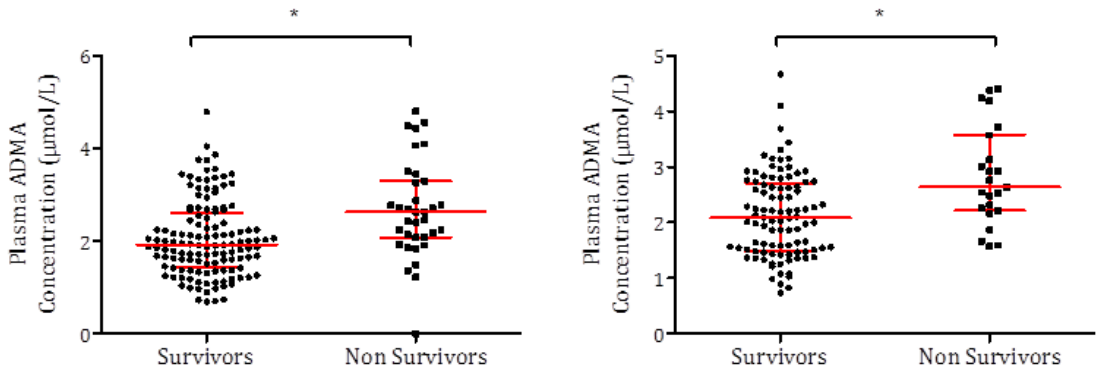

Figure 122: Plasma ADMA concentrations on day 5 (Left panel) and day 7 (right panel) in survivors and non survivors of septic shock.

Plasma methylarginines were measured using a mass spectrometry technique as described previously. Samples analysed and were categorised by survival at 28 days after ICU admission. Each point represents a single patient value at the respective time point. The red bars represent median and interquartile range. *=p<0.05

Peak plasma ADMA concentrations over the course of the study period were sorted by quartiles and revealed a significantly elevated mortality between the upper and lower two quartiles with a log rank test p value of <0.001 (Figure 123).

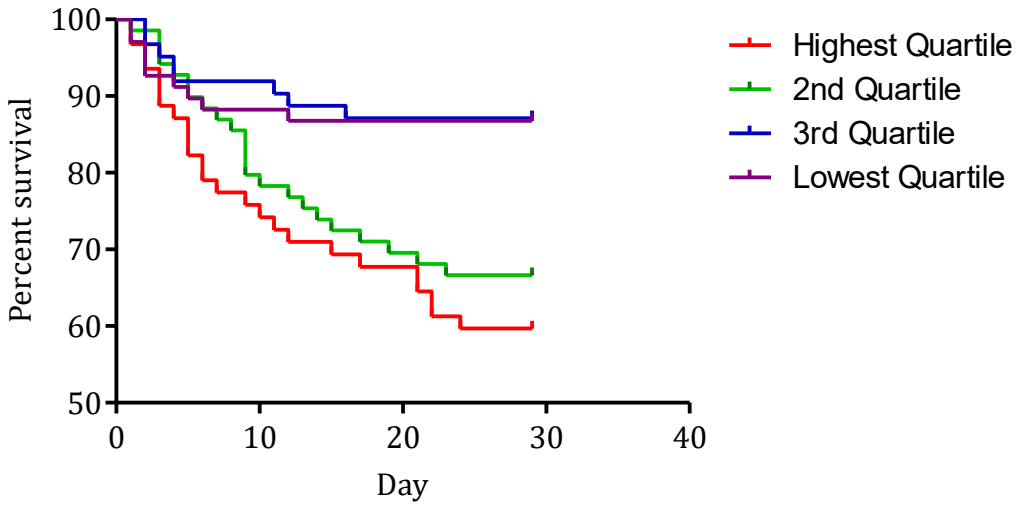

Figure 123: Kaplan Meier curves of peak plasma ADMA concentrations during the first seven days of ICU admission with septic shock and 28 day mortality.

Kaplan Meier survival curves representing the four quartiles of peak plasma ADMA concentrations. Highest quartile red, second green, third blue, fourth (the lowest) purple. p<0.001.

7.3.2.7 Plasma SDMA and outcome in septic shock

Plasma SDMA was also associated with a trend towards elevated mortality on admission (p=0.08) and significantly increased in non-survivors at day 3(p=0.01), day 5(p=0.008) and day 7(p=0.01) (Table 35), (Figure 124, Figure 125). When plasma SDMA values were dichotomised, a concentration in the upper 50% of values was associated with a hazard ratio for death at 28days of 2.25(95% Confidence Interval: 1.35-3.74), p<0.01.

Time point	Survivors		Non-survivors	
	Median(µM)	Interquartile range(µM)	Median(µM)	Inter quartile range(µM)
Admission	3.15	2.10-4.63	4.43	1.81-6.77
Day 3	3.32	1.73-5.03	4.47	2.66-6.89
Day 5	3.24	1.95-4.96	5.52	3.15-7.13
Day 7	2.85	1.67-4.42	4.63	2.46-6.05

Table 35: Median(IQR) plasma SDMA concentrations of survivors and non-survivors of septic shock at admission and on days 3, 5 and 7 of ICU admission.

Plasma methylarginines were measured using the established mass spectrometry technique. Plasma concentrations (median(IQR)µM) are reported in survivors and non-survivors at 28days after ICU admission.

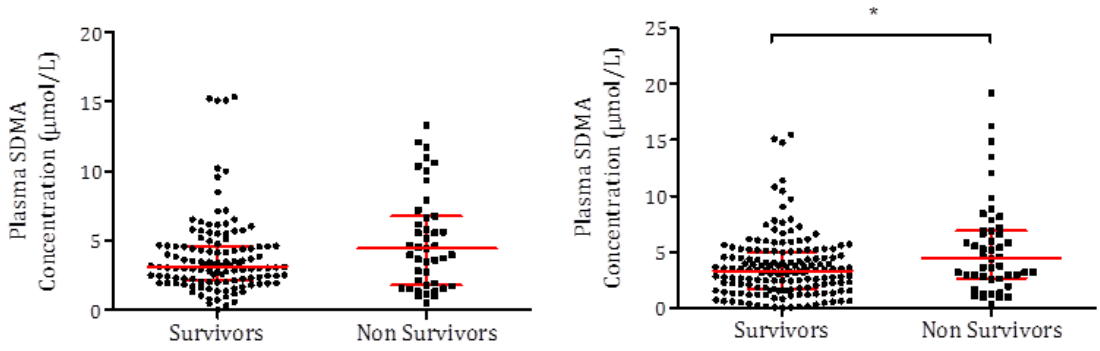

Figure 124: Plasma SDMA concentrations on admission (Left panel) and day 3 (right panel) in survivors and non survivors of septic shock.

Plasma methylarginines were measured using a mass spectrometry technique as described previously. Samples were analysed and categorised by survival at 28 days after ICU admission. Each point represents a single patient value at the respective time point. The red bars represent median and interquartile range. *=p<0.05

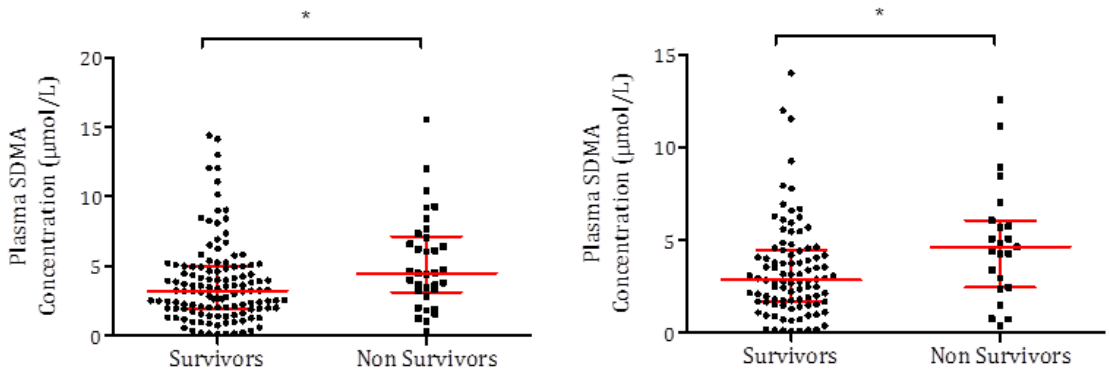

Figure 125: Plasma SDMA concentrations on day 5 (left panel) and day 7 (right panel) in survivors and non survivors of septic shock.

Plasma methylarginines were measured using a mass spectrometry technique as described previously. Samples analysed and were categorised by survival at 28 days after ICU admission. Each point represents a single patient value at the respective time point. The red bars represent median and interquartile range. *=p<0.05

Peak plasma SDMA concentrations over the course of the study period were sorted by quartiles and revealed a significantly elevated mortality between the quartiles with a log rank p value of 0.002 (Figure 126).

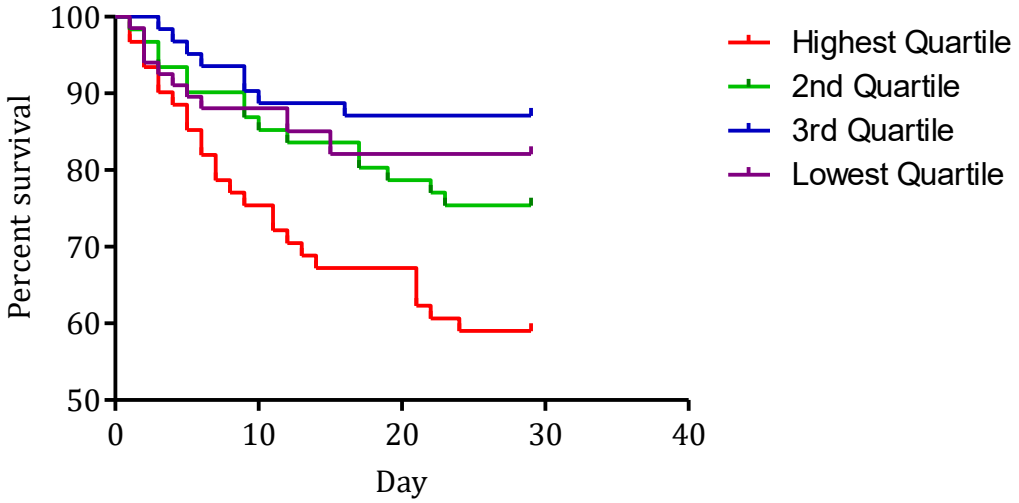

Figure 126: Kaplan Meier curves of peak plasma SDMA concentrations during the first seven days of ICU admission with septic shock and 28 day mortality.

Kaplan Meier survival curves representing the four quartiles of peak plasma SDMA concentrations. Highest quartile red, second green, third blue, fourth (the lowest) purple. P=0.002.

7.3.2.8 Plasma L-arginine concentration and outcome in septic shock

L-arginine concentrations were lower in both survivors and non-survivors compared to normal values as described above. No differences were observed between survivors and non-survivors at admission(p=0.19) or day 3(p=0.64). A trend was observed to higher L-arginine concentrations in non-survivors at day 5(p=0.06) and L-arginine was significantly higher in non-survivors at day 7(p=0.035, Table 36), (Figure 127). Dichotomised L-arginine concentrations revealed no significant differences in mortality associated. Hazard ratio(95% confidence interval)for death at 28 days, 1.32(0.79-2.17) when the upper 50% of values was compared to the lower half (Figure 128).

Time point	Survivors		Non-survivors	
	Median(μM)	Interquartile range(μM)	Median(μM)	Inter quartile range(μM)
Admission	24.8	17.2-30.6	27.3	16.8-43.9
Day 3	30.7	22.5-42.4	32.1	23.0-42.6
Day 5	32.1	24.7-46.1	38.1	29.5-57.6
Day 7	32.3	23.0-44.9	38.3	26.1-74.5

Table 36: Median(IQR) plasma L-arginine concentrations of survivors and non-survivors of septic shock at admission and on days 3, 5 and 7 of ICU admission.

Plasma L-arginine was measured using the established mass spectrometry technique. Plasma concentrations (median(IQR)μM) are reported in survivors and non-survivors at 28days after ICU admission.

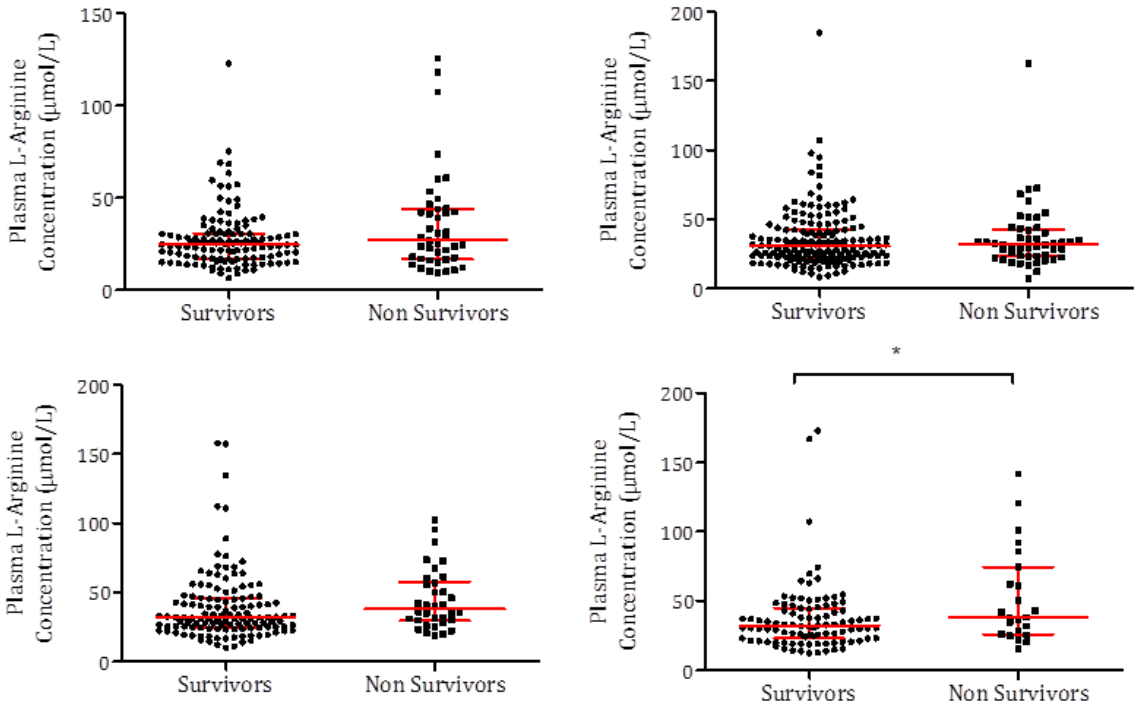

Figure 127: Plasma L-arginine concentrations on admission (top left panel), day 3(top right panel), day 5 (bottom left panel) and day 7 (bottom right panel) in survivors and non survivors of septic shock.

Plasma L-arginine was measured using a mass spectrometry technique as described previously. Samples analysed and were categorised by survival at 28 days after ICU admission. Each point represents a single patient value at the respective time point. The red bars represent median and interquartile range. *=p<0.05

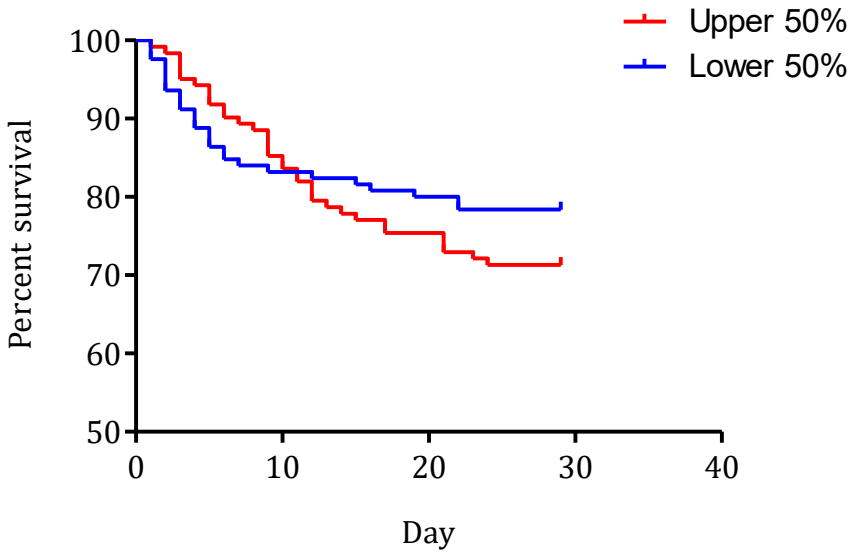

Figure 128: Kaplan Meier curves of peak plasma L-arginine concentrations during the first seven days of ICU admission with septic shock and 28 day mortality.

Kaplan Meier survival curves representing the upper and lower halves of patients' peak plasma L-arginine concentrations. Highest 50% red, lower 50% blue. P=0.34.

7.3.2.9 Plasma ADMA:SDMA ratio and outcome in septic shock

The plasma ADMA concentration is determined by methylarginine synthesis in the tissues, metabolism by DDAH isoforms and clearance via the kidney. SDMA can be employed to correct for non-DDAH effects on the ADMA concentration. SDMA is not metabolised by DDAH isoforms but is cleared by the kidney via the same mechanism. Therefore, correcting the ADMA concentration for the paired SDMA concentration will provide an index of the DDAH mediated ADMA flux. When corrected for SDMA, no difference was observed in ADMA concentrations between survivors and non-survivors at the four time points (Table 37), (Figure 129). However potting of survival curves revealed a significantly reduced mortality in the group with the higher ADMA:SDMA ratios(Figure 130), p=0.03. When dichotomised, patients in the higher 50% of ADMA:SDMA ratios displayed a reduced hazard ratio(95%CI) for death 0.63(0.37-1.0), p=0.03.

Time point	Survivors		Non-survivors		
	Median	Interquartile range	Median	Inter quartile range	p value
Admission	0.47	0.33-0.66	0.48	0.34-0.71	0.81
Day 3	0.56	0.37-0.80	0.51	0.38-0.78	0.62
Day 5	0.66	0.42-0.95	0.56	0.41-0.79	0.32
Day 7	0.81	0.50-1.13	0.56	0.46-0.84	0.18

Table 37: Median(IQR) plasma ADMA concentrations corrected for paired plasma SDMA concentrations of survivors and non-survivors of septic shock at admission and on days 3, 5 and 7 of ICU admission.

Plasma ADMA:SDMA ratios were measured using the established mass spectrometry technique. Plasma concentrations (median(IQR)) are reported in survivors and non-survivors at 28days after ICU admission.

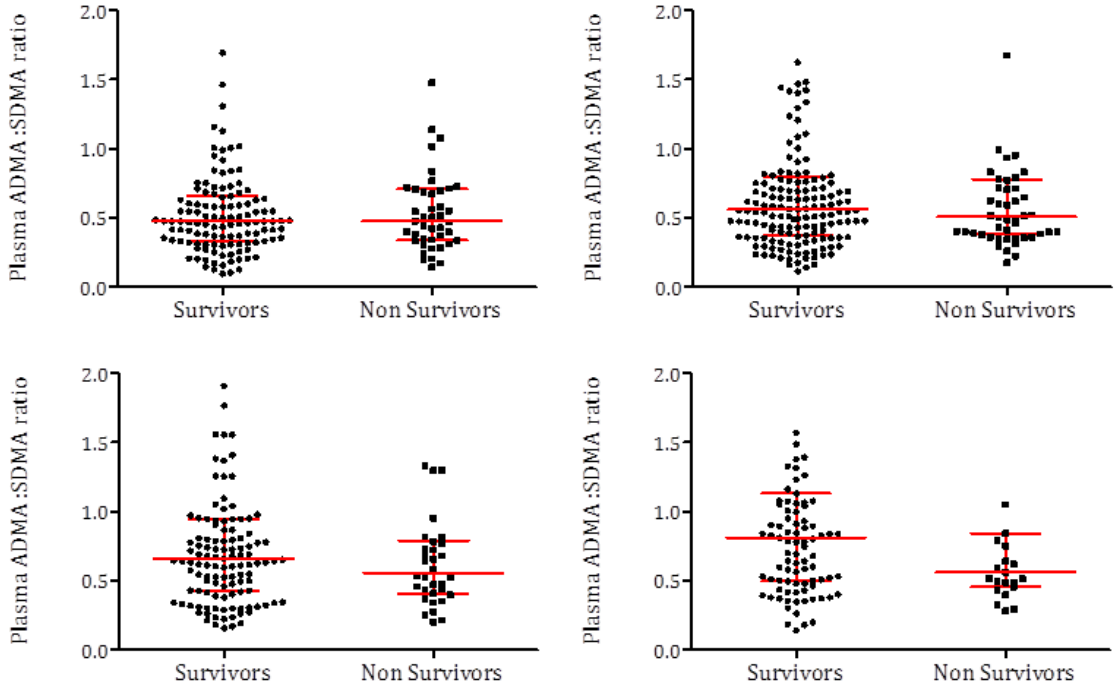

Figure 129: Plasma ADMA concentrations corrected for plasma SDMA concentration on admission (top left panel), day 3(top right panel), day 5 (bottom left panel) and day 7 (bottom right panel) in survivors and non survivors of septic shock.

Plasma ADMA:SDMA ratios were measured using a mass spectrometry technique as described previously. Samples analysed and were categorised by survival at 28 days after ICU admission. Each point represents a single patient value at the respective time point. The red bars represent median and interquartile range.

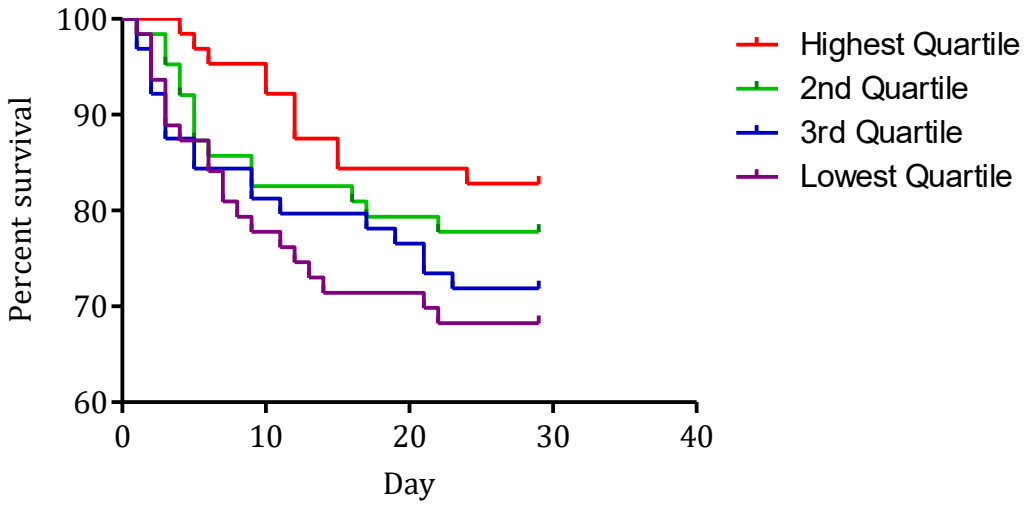

Figure 130: Kaplan Meier curves of peak plasma ADMA concentration corrected for plasma SDMA concentration during the first seven days of ICU admission with septic shock and 28 day mortality.

Kaplan Meier survival curves representing the four quartiles of peak plasma ADMA:SDMA ratios. Highest quartile red, second green, third blue, fourth (the lowest) purple, p=0.03.

7.3.2.10 Plasma ADMA:L-arginine ratio and outcome in septic shock

Plasma ADMA:L-arginine ratio was assessed to determine whether the relationship between the endogenous inhibitor and agonist in the plasma was associated with outcome. No difference in ADMA:L-arginine ratio was observed between survivors or non-survivors on admission or days 5 or 7, however on day 3 there was a significant association between plasma ratios and outcome (Table 38, Figure 131). Peak ADMA:L-arginine concentration was also associated with survival, (median(IQR) 0.069(0.047-0.091) in survivors vs 0.084(0.056-0.12), p=0.002. When dichotomised a trend towards increased mortality was seen in patients in the upper 50% of ratios, hazard ratio(95% CI) for death at 28days was 1.56(0.95-2.6), p=0.08.

Time point	Survivors		Non-survivors		
	Median	Interquartile range	Median	Inter quartile range	p value
Admission	0.062	0.012-0.088	0.061	0.048-0.098	0.63
Day 3	0.058	0.039-0.075	0.073	0.052-0.093	0.004
Day 5	0.058	0.040-0.081	0.068	0.048-0.091	0.20
Day 7	0.062	0.045-0.086	0.072	0.046-0.085	0.48

Table 38: Median(IQR) plasma ADMA concentrations corrected for paired plasma L-arginine concentrations of survivors and non-survivors of septic shock at admission and on days 3, 5 and 7 of ICU admission.

Plasma ADMA:L-arginine ratios were measured using the established mass spectrometry technique. Plasma concentrations (median(IQR)) are reported in survivors and non-survivors at 28days after ICU admission.

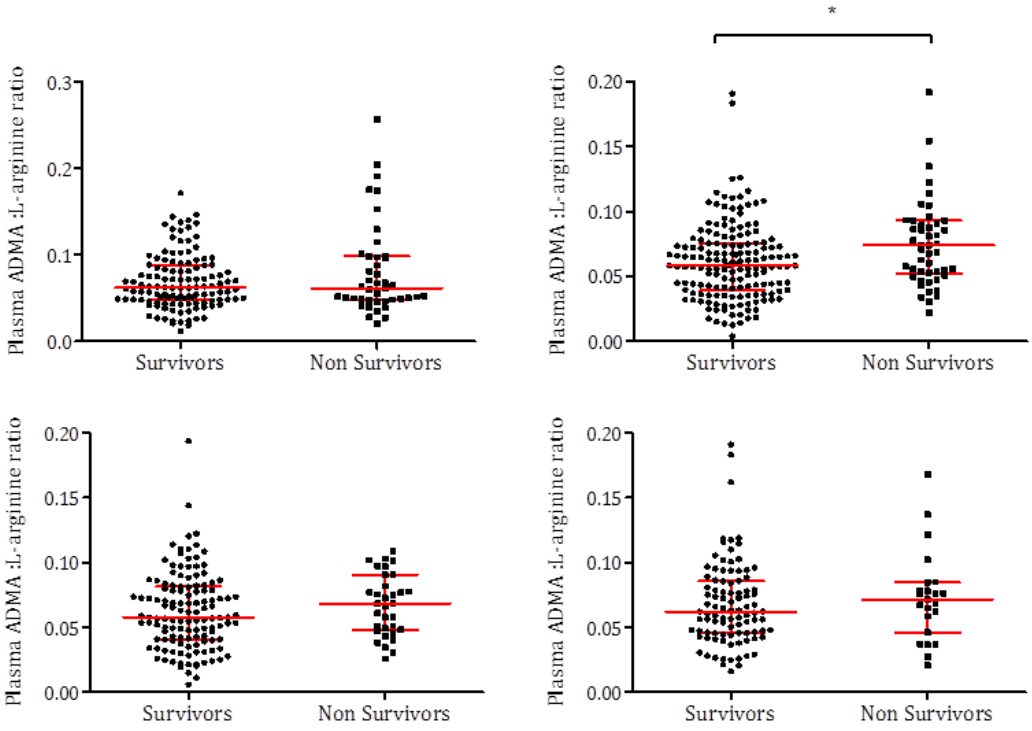

Figure 131: Plasma ADMA concentrations corrected for plasma L-arginine concentration on admission (top left panel), day 3(top right panel), day 5 (bottom left panel) and day 7 (bottom right panel) in survivors and non survivors of septic shock.

Plasma ADMA:L-arginine ratios were measured using a mass spectrometry technique as described previously. Samples analysed and were categorised by survival at 28 days after ICU admission. Each point represents a single patient value at the respective time point. The red bars represent median and interquartile range. * p<0.05

Kaplan Meier analysis of the ADMA:L-arginine ratio by quartile revealed a significant association with mortality, p<0.01(Figure 132).

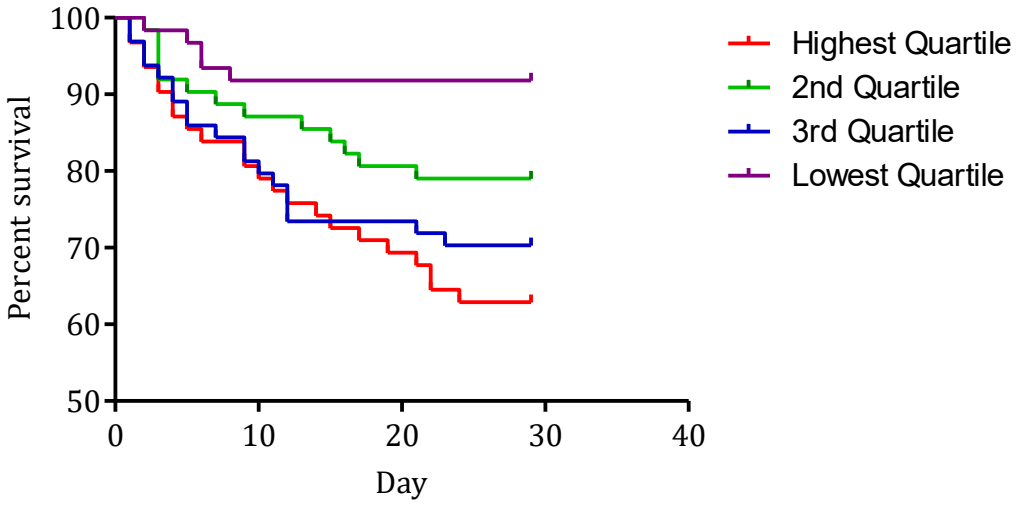

Figure 132: Kaplan Meier curves of peak plasma ADMA concentration corrected for plasma L-arginine concentration during the first seven days of ICU admission with septic shock and 28 day mortality.

Kaplan Meier survival curves representing the four quartiles of peak plasma ADMA:L-arginine ratios. Highest quartile red, second green, third blue, fourth (the lowest) purple, p<0.01.

7.3.3 Single nucleotide polymorphisms of DDAH genes, methylarginines and outcome in human septic shock

7.3.3.1 SNP Genotype and 28day mortality in septic shock

Buffy coat and whole blood samples were collected as described above from 286 patients with septic shock(75 whole blood and 211 buffy coat). DNA was extracted from these samples and analysis of nine pre-defined SNPs undertaken by the external research organisation (LGC Sciences ltd). Analysis of the SNPs was possible in 96.8% of samples. The eight SNPs of DDAH1 that had been identified by imputation in the GenOSept analysis were directly analysed. In addition, one SNP of DDAH2, rs805305 which had been identified in previous studies as being associated with plasma ADMA concentrations in sepsis was also determined.

As expected, the eight SNPs of DDAH1 were all in linkage disequilibrium with >90% concordance between genotypes of the polymorphisms. Allele frequencies were consistent with the incidence of the polymorphisms observed in the GenOSept cohort (Table 39). Of the SNP of the DDAH2 gene analysed, heterozygotes were more common that either the major or minor allele homozygote(Table 39)

SNP ID	rs1524001	n(%)	rs7531068	n(%)	rs10782552	n(%)
Major Allele	G:G	245(86.6)	A:A	245(86.6)	A:A	249(86.7)
Heterozygote	G:A	34(12.0)	A:C	34(12.2)	A:T	34(11.8)
Minor allele homozygote	A:A	4(1.4)	C:C	4(1.4)	TT	4(1.4)
Missing (n)		3		3		0
SNP ID	rs897255	n(%)	rs72726326	n(%)	rs6576775	n(%)
Major Allele	C:C	250(88.3)	A:A	238(89.1)	T:T	242(87.7)
Heterozygote	C:T	29(10.25)	G:A	27(10.1)	T:C	31(11.3)
Minor allele homozygote	T:T	4(1.4)	G:G	2(0.7)	C:C	3(1.1)
Missing (n)		5		19		10
SNP ID	rs1378226	n(%)	rs6682848	n(%)	rs805305	n(%)
Major Allele	G:G	249(87.1)	C:C	248(87.6)	C:G	128(44.7)
Heterozygote	G:A	33(11.5)	C:A	31(11.0)	C:C	112 (39.1)
Minor allele homozygote	A:A	4(1.4)	A:A	4(1.4)	G:G	40(13.9)
Missing (n)		0		4		8

Table 39: SNP ID and allele frequencies eight DDAH1 and one DDAH2 SNP of 286 patients with septic shock.

286 patients included in the VANISH study had DNA extracted from whole blood or buffy coat samples and analysis of SNPs undertaken. Eight SNPs of DDAH1 and one of DDAH2 (rs80305) were analysed. Data presented includes allele frequencies and number of data points that could not be collected.

The association with mortality of each of the SNPs of DDAH1 was determined. No association with survival at 28 days any of the SNPs of DDAH1 could be identified, odds ratios: 0.84-1.4, all p values non-significant using Fisher's exact test (Table 40). The SNP of DDAH2, rs805305 displayed increased mortality when heterozygotes and G:G homozygotes were considered together with an odds ratio for death in the most common C:C genotype of 2.0(95% CI 1.1-3.6) (p=0.03).

SNP ID	rs1524001	rs7531068	rs10782552
Odds Ratio	0.842	1.126	1.14
95% CI	0.38-1.84	0.52-2.45	0.52-2.48
p value	0.682	0.839	0.839
SNP ID	rs897255	rs72726326	rs6576775
Odds Ratio	1.23	1.21	0.976
95% CI	0.56-2.69	0.51-2.90	0.42-2.27
p value	0.678	0.65	1
SNP ID	rs1378226	rs6682848	rs805305
Odds Ratio	1.4	1.11	2.04
95% CI	0.88-1.36	0.49-2.50	1.1-3.9
p value	0.41	0.83	0.03

Table 40: Relationship between eight intronic SNPs of DDAH1 and one SNP of DDAH2 with mortality in septic shock.

Eight SNPs were of DDAH1 examined for an association with mortality in septic shock having previously been shown to be associated with mortality in genome wide association studies. No significant association was observed between any of the SNPs and 28 day mortality. Increased mortality was observed in heterozygotes and minor allele homozygotes of the DDAH2 SNP rs805305(p=0.03).

A representative Kaplan Meier plot of the DDAH1 SNP most strongly associated with mortality in the GenOSept study demonstrated no significant differences between the most common G:G genotype and the less common A:A and G:A genotypes in combination, hazard ratio 0.86 (95% CI 0.42-1.72), p=0.67(Figure 133). The SNP of DDAH2, rs805305 remained strongly associated with increased risk of death through this analysis, with a log-rank p value of 0.01 (Figure 134).

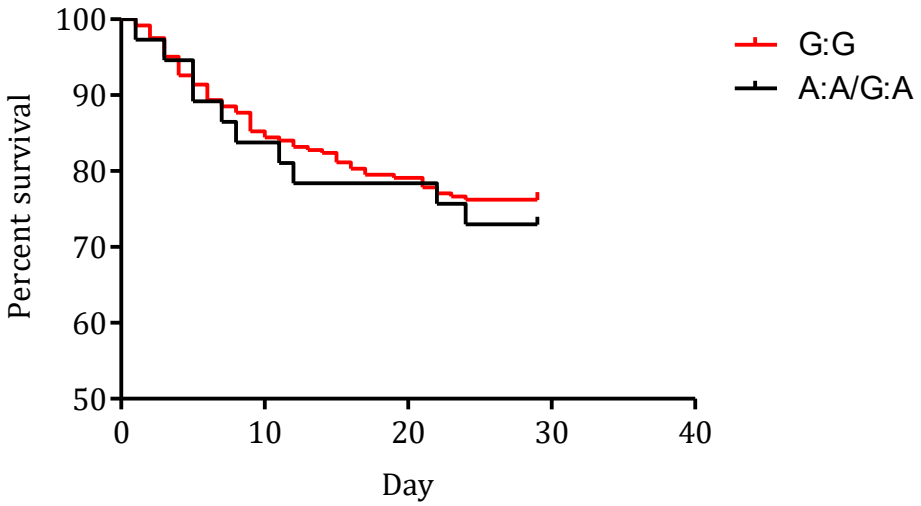

Figure 133: Kaplan Meier analysis of the impact of the rs1542001 SNP of DDAH1 on 28day mortality in sepsis.

Eight SNPs of DDAH1 were analysed and the relationship to mortality in septic shock determined. The most common G:G genotype was compared to the heterozygote and rare A:A homozygote. No difference in mortality was observed at 28 days, p=0.67. Similar patterns were observed in the seven other SNPs of DDAH1.

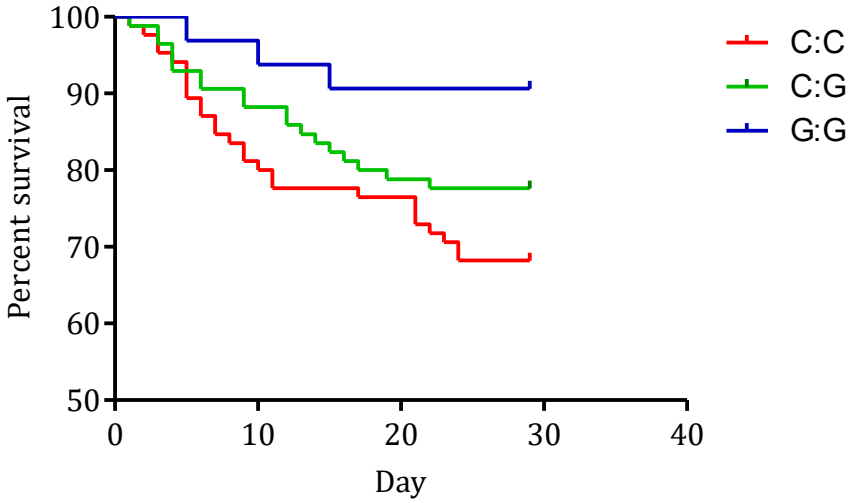

Figure 134: Kaplan Meier analysis of the impact of the rs805305 SNP of DDAH2 on 28day mortality in sepsis.

One SNP of DDAH2 was analysed and the relationship to mortality in septic shock determined. The most common C:C genotype was compared to the heterozygote and G:G homozygote. A significant difference in mortality was observed at 28 days, p=0.03 by Mantel-Cox analysis.

7.3.3.2 SNP Genotype and methylarginine concentrations in septic shock

The impact of SNPs of DDAH1 on plasma ADMA concentrations was explored. Given the linkage of each of the eight directly interrogated SNPs, the two with the most significant association with mortality were explored. Rs1542001 (Figure 135) and rs7531068(Figure 136) displayed no significant differences in peak plasma ADMA concentrations over the course of the first week of ICU admission in the septic shock cohort (p=0.35 and 0.36 respectively)(Table 41). ADMA:SDMA ratio revealed a trend to increase in the less common genotypes (A:A/G:A in the rs1542001), p=0.06 and (A:C/C:C in the rs7531068), p=0.11(Table 41). ADMA:L-arginine ratio was unchanged in both SNPs (rs1542001 p=0.57 and rs7531068 p=0.64)(Table 41).

Rs1542001	G:G Genotype		G:A and A:A Genotypes		
	Median	Interquartile range	Median	Inter quartile range	p value
Peak ADMA(μM)	2.24	1.55-3.02	1.97	1.57-2.92	0.35
ADMA:SDMA Ratio	0.69	0.44-1.04	0.83	0.54-1.38	0.06
ADMA:L-arginine ratio	0.07	0.05-0.097	0.06	0.05-0.10	0.57
Rs7361058	A:A Genotype		A:C and C:C Genotypes		
	Median	Interquartile range	Median	Inter quartile range	
Peak ADMA(μM)	2.16	1.54-2.95	1.87	1.51-2.69	0.36
ADMA:SDMA Ratio	0.68	0.44-1.00	0.83	0.57-1.65	0.11
ADMA:L-arginine ratio	0.07	0.05-0.10	0.07	0.05-1.00	0.64

Table 41: Impact of two DDAH1 SNPs on peak plasma ADMA, ADMA:SDMA and ADMA:L-arginine in septic shock.

The eight SNPs of DDAH1 associated with increased mortality in severe sepsis and septic shock were directly genotyped in a cohort of septic shock patients. Median(IQR) concentrations of ADMA, plasma ADMA:SDMA ratio and ADMA:L-arginine ratio were determined for each genotype. No significant genotype dependent differences were observed in peak plasma ADMA or ADMA:L-arginine ratios. A trend to increased ADMA:SDMA ratio was observed in both SNPs (p=0.06 and 0.11). Analysis by Mann Whitney test.

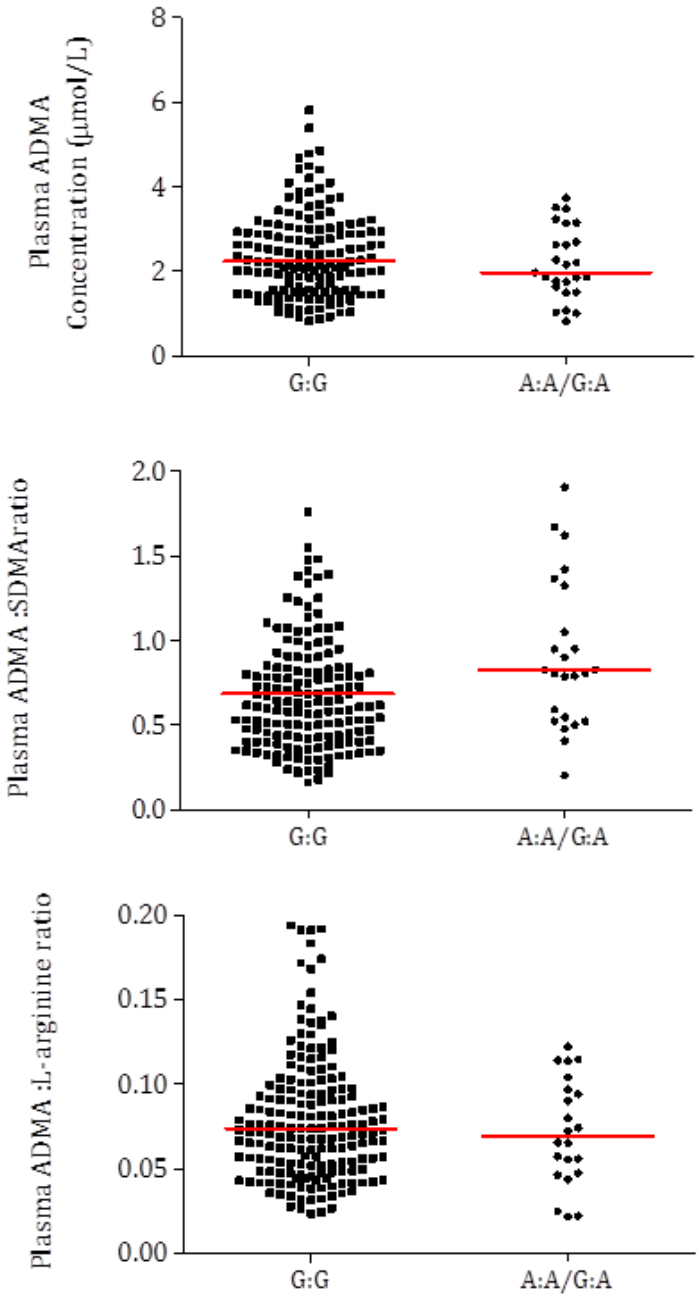

Figure 135: The impact of the DDAH1 SNP rs1524001 on peak plasma ADMA, ADMA:SDMA ratio and ADMA:L-arginine ratio in septic shock.

Plasma methylarginines and L-arginine concentrations were determined using the HPLC triple quad mass spectrometry technique as described previously. Peak plasma ADMA concentration over the course of the first week of ICU admission with septic shock was similar in both genotype groups. A trend to increase in ADMA:SDMA ratio was observed, p=0.06 and no difference was seen between ADMA:L-arginine ratios in the two groups, p=0.57. Red line represents median value

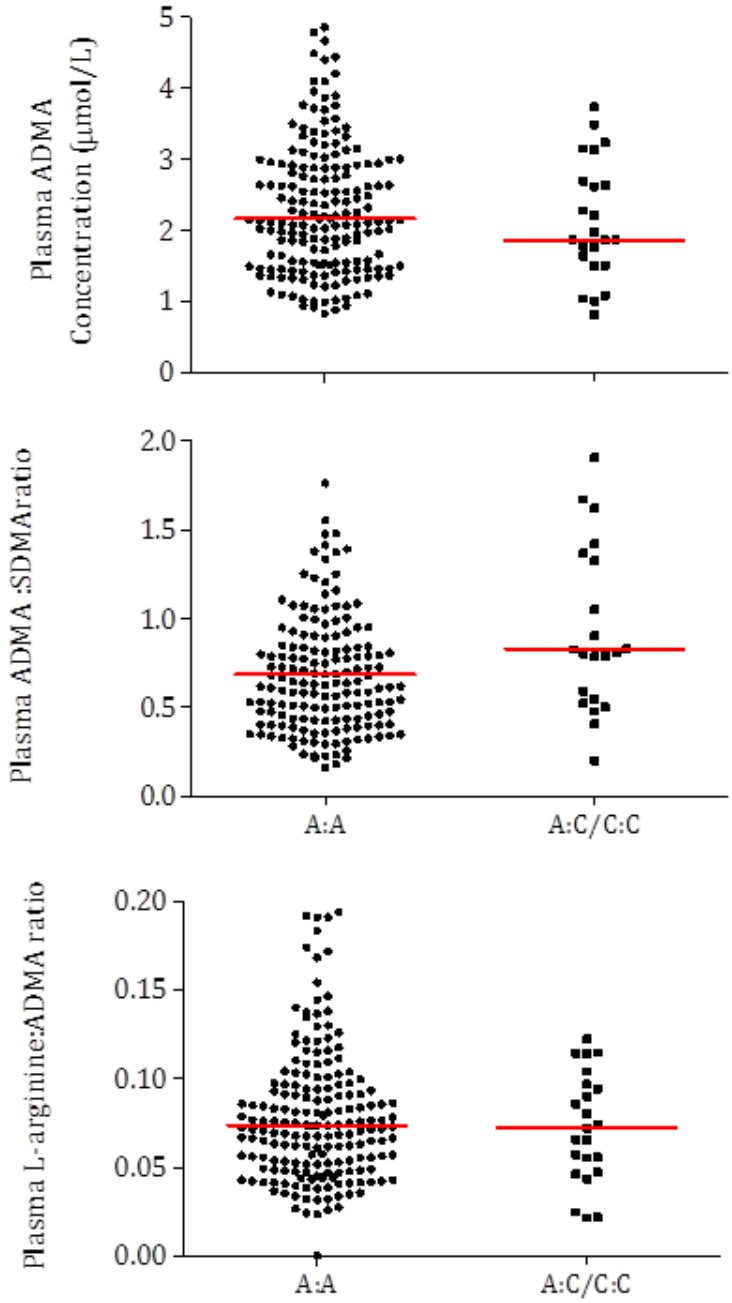

Figure 136:The impact of the DDAH1 SNP rs7531068 on peak plasma ADMA, ADMA:SDMA ratio and ADMA:L-arginine ratio in septic shock.

Plasma methylarginines and L-arginine concentrations were determined using the HPLC triple quad mass spectrometry technique as described previously. Peak plasma ADMA concentration over the course of the first week of ICU admission with septic shock was similar in both genotype groups(p=0.35).A trend to increase in ADMA:SDMA ratio was observed, p=0.09 and no difference was seen between ADMA:L-arginine ratios in the two groups, p=0.64. Red line represents median value

Plasma methylarginines were also compared to the rs805305 SNP of DDAH2 (Figure 137). Kruskall Wallis analysis was used to explore a relationship between the SNPs of rs805305 and methylarginines. Peak plasma ADMA was similar in all three genotypes (p=0.65), Peak ADMA:SDMA ratio was genotype dependent, p=0.004. Compared to the dominant C:C genotype, Dunn's multiple comparison test revealed that the less common G:G genotype was associated with an increased ADMA:SDMA ratio compared to the dominant C:C and heterozygote genotypes (Table 42). ADMA:L-arginine ratio was similar in all three groups(p=0.84)

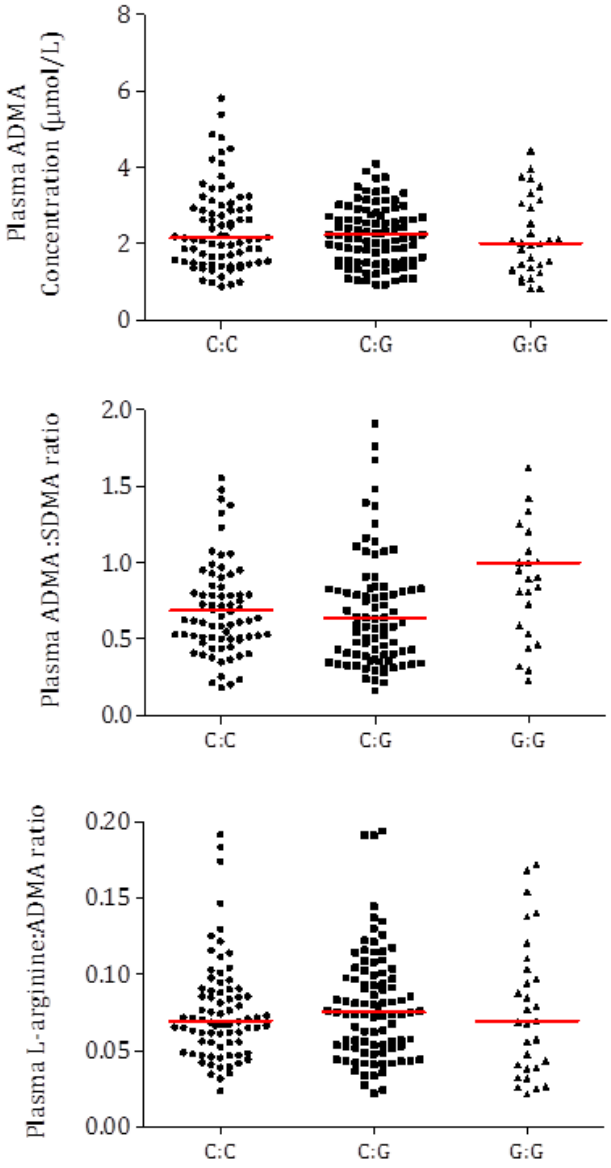

Figure 137: The impact of the DDAH2 SNP rs805305 on peak plasma ADMA, ADMA:SDMA ratio and ADMA:L-arginine ratio in septic shock.

Plasma methylarginines and L-arginine concentrations were determined using the HPLC triple quad mass spectrometry technique as described previously. Peak plasma ADMA concentration over the course of the first week of ICU admission with septic shock was similar in both genotype groups(p=0.65). Increased ADMA:SDMA ratio was observed, p=0.0043 and no difference was seen between ADMA:L-arginine ratios in the two groups, p=0.83. Red line represents median value. Analysis by Mann Whitney test.

rs805305	C:C Genotype		C:G Genotype		G:G Genotype		p value
	Median	Interquartile range	Median	Interquartile range	Median	Interquartile range	
Peak ADMA(μM)	2.16	1.53-3.05	2.24	1.55-2.78	2.02	1.36-3.13	0.65
ADMA:SDMA Ratio	0.69	0.51-0.95	0.64	0.40-0.91	1.0	0.69-1.96	0.0043
ADMA:L-arginine ratio	0.07	0.06-0.09	0.07	0.05-0.10	0.07	0.04-0.11	0.84

Table 42:Impact of the DDAH2 SNP rs805305 on peak plasma ADMA, ADMA:SDMA and ADMA:L-arginine in septic shock.

The SNP of DDAH2 rs805305 was directly genotyped in a cohort of septic shock patients. Median(IQR) concentrations of ADMA, plasma ADMA:SDMA ratio and ADMA:L-arginine ratio were determined for each genotype. No significant genotype dependent differences were observed in peak plasma ADMA or ADMA:L-arginine ratios. An increased ADMA:SDMA ratio was observed in the rs805305 SNP (p=0.0043). Analysis by Kruskall Wallis test.

7.4 Discussion

After a series of small studies that represent preliminary observations, the study presented here offers the most robust examination of plasma methylarginines, DDAH SNPs and their association with outcome in septic shock undertaken to date. By utilising a high quality randomised controlled trial to provide clinical data and samples, combined with a well-established method for analysing methylarginine and nitric oxide concentrations, this study answers a number of the existing questions and presents some new ones for future study.

7.4.1 Plasma nitric oxide in septic shock

To date, study has been adequately powered to explore the narrative pattern of plasma NO synthesis in early septic shock. The data reveal a pattern of significantly increased NO synthesis in patients with septic shock compared to healthy volunteers. The data is positively skewed as might be expected, however of interest is that there is a group of study participants that may be described as 'super-producers' of NO with plasma concentrations above 200μM. This group contains 25 patients of the admission group (14.7%), 31(14.6%) on day 3, 24(13.7%) on day 5 and 10(7.6%) on day 7. Of the patients in this group, 71% were consistently in this category. This suggests that there are a proportion of patients with septic shock who have a supranormal NOx level in the plasma. Whether this reflects increased synthesis or impaired clearance is not clear. Mortality in this group was 29%. This compares to 25% mortality in the study population as a whole, so whilst this group may not suffer excess mortality, they may have a mechanism of shock which is different to that seen in others.

Interestingly, plasma NO concentrations are similar in septic shock in both survivors and non survivors at admission to ICU. Only by day seven do we see a significant elevation in plasma NO in non-survivors compared to those who were alive at day 28. This may represent the failure of shock resolution in this population and may be a predictor of poor outcome in this group, a hypothesis that merits further exploration. Consistent with these findings is the observation that peak plasma NOx is not predictive of outcome in septic shock. The synthesis of NO is undoubtedly an important part of the pathophysiology of sepsis and is likely to play a role in those patients in whom shock is overwhelming and ultimately fatal - as shown here by the day 7 data. It may be the case however that measuring the plasma NO concentrations is not the best tool in this context since it is composite value made up of synthesis by different tissues, conversion to stable metabolites and clearance, all of which are dynamic and dysregulated in septic shock.

7.4.2 Plasma L-arginine and methylarginines in septic shock

This study offers the first robust narrative of the changes in plasma methylarginines observed over the first seven days of ICU admission with septic shock. Plasma ADMA is significantly elevated over the healthy controls that are studied elsewhere in this project, and indeed appear higher than values reported in the literature previously. The primary reason for this is that this population contains only those with vasopressor dependent septic shock, an inclusion criterion for this study. Studies by other groups have included the spectrum of severe sepsis and septic shock and often studied only a handful of patients with the more severe disease state and higher mortality. Hence this study contains a largely un-observed population in whom a higher plasma ADMA concentration is, based on animal and cell studies presented here entirely feasible. Secondly, all of the sepsis studies reported have used ELISA techniques to determine plasma ADMA concentrations. This study employs the gold standard technique of HPLC triple quad mass spectrometry and so is likely to present a more robust assessment of the true plasma MA concentrations. In addition, the inability to measure SDMA using ELISA techniques makes controlling for changes in methylarginine concentrations not mediated by DDAH impossible.

Consistent with previous studies in this area[207], ADMA appears to rise over the first week of ICU admission. In the context of the septic insult this is perhaps unexpected and may represent a change in ADMA flux. In the early stage of septic shock, impaired renal clearance coupled with endothelial and immune release of ADMA into the circulation may lead to higher values at presentation and in the early days of admission. By day 7 however, the shocked state has resolved in the majority of patients and so if this was the only mechanism for elevated ADMA, a reduction in plasma concentrations over time might be expected. In this patient group, protein catabolism, progressive critical illness polymyopathy and weakness is a common feature and it may be that increased ADMA release from muscle in part mediates the late increase in plasma concentrations seen in this study.

Plasma SDMA is also elevated in septic shock although in the population as a whole appears to be stable over the course of the first week of ICU stay. Given that it is not metabolised by DDAH isoforms and is largely cleared by the kidney with a small proportion metabolised by AGXT2, this increase is likely to represent a pattern of kidney injury in these patients. It would prove valuable to determine if this elevation resolves with improving renal function and whether it is a useful marker of kidney function in the context of acute kidney injury.

L-arginine concentrations are significantly reduced in the septic shock group compared to controls that have values in the 80-100μM range. The reduction seen in these studies is consistent with a recent meta-analysis of L-arginine concentrations in sepsis[377]. Of note is that this meta-analysis included 192 patients with sepsis, this makes the data presented here one of the biggest studies exploring L-arginine concentrations in critical illness of any aetiology.

It is of note that in initial analysis of associations between ADMA, SDMA and plasma NOx, positive correlations were observed at multiple time points between both methylarginines and plasma NOx. This may appear paradoxical as increased concentrations of ADMA might be expected to be associated with lower NO synthesis. This highlights an important observation that the relationship between plasma measures and intracellular bioavailability is not consistent. Whilst elevated ADMA intracellularly certainly reduces NO synthesis, the transport and clearance of the two is markedly different. In this case, correlations are likely because Nitrate, SDMA and ADMA are all cleared to some degree by the kidney and in the context of septic shock, all of these will experience some degree of reduced excretion. This will mediate the loose positive correlations between them. The choice of statistical test employed in this analysis is important. Whilst Spearman's coefficient is conventionally employed in parametric data sets and Pearson's employed for non-parametric, they can also be used to detect different kinds of associations. Whilst Spearman's searches for a linear relationship, Pearson's is better able to detect non-linear correlations between samples. In the study values presented, both tests reveal positive associations although the degree of linear correlation is less strong.

7.4.3 Methylarginines and outcome in septic shock

In addition to building understanding of the narrative pattern of NO and methylarginine expression in septic shock, a study of this size has the power to make robust inferences regarding the relationship of these important disease mediators with outcome in septic shock.

This study provides validation of the pilot data that had associated ADMA and SDMA with shock severity in sepsis. Interrogation of plasma ADMA concentrations in non-survivors at all time points studied revealed significantly elevated concentrations compared to those who were still alive at 28 days. This finding was borne out when peak ADMA concentration during the seven days studied was considered. Whether dichotomised or considered in quartiles, plasma ADMA concentration is strongly associated with increased 28 day mortality. Plasma SDMA, displays a similar association, with higher SDMA concentrations associated with non-survival on days 3, 5 and 7 as well as on Kaplan Meier analysis. When patients in the upper 50% of SDMA values were compared to the lower 50%, a hazard ratio of 2.25 is observed, consistent with the only previous study in this area with power to detect mortality differences[211]. These data suggest that both plasma ADMA and SDMA have the potential to act alone or in a panel as biomarkers predictive of poor outcome in sepsis. Receiver operator characteristic (ROC) analysis reveals an area under the curve(95% CI) of 0.71(0.63-0.78), $p<0.0001$ for peak ADMA concentration and 0.64(0.56-0.73), $p<0.001$ for peak SDMA level(Figure 138).

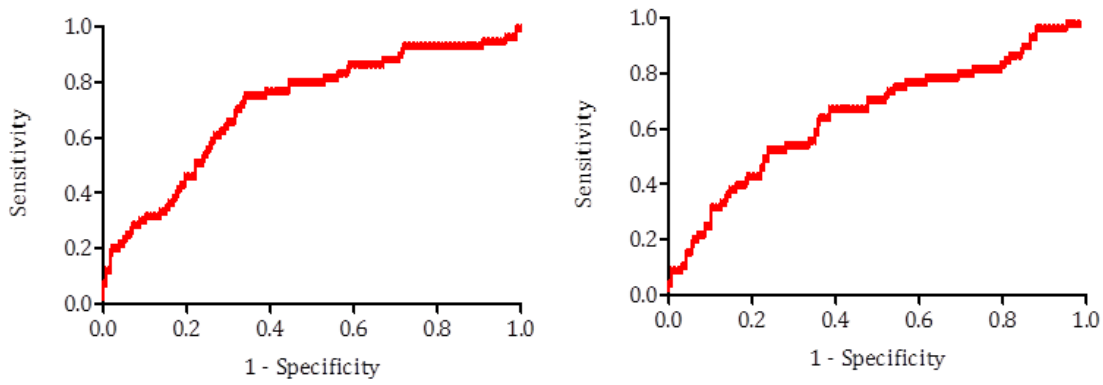

Figure 138: Receiver Operator Characteristic curves for peak plasma ADMA (Left) and SDMA (right) over the course of a seven day ICU admission with septic shock.

However, whilst both increased plasma ADMA and SDMA are in isolation associated with worsened outcome, their differing actions and metabolism means that they are unlikely to have similar mechanistic effects. Methylarginine clearance by the kidney is mediated by amino acid transporters removing the freely filtered amino acids and their derivatives from the tubular fluid. In the acute kidney injury that is typically seen in sepsis, as well as chronic kidney disease this process is impaired[12]. Since SDMA is not metabolised by DDAH and the kidney is the primary route of excretion and in small part metabolism by AGXT2, it may be that SDMA acts as a biomarker of renal dysfunction. This merits further exploration in itself, however in addition it can serve as an index of impaired MA clearance. Correcting for SDMA may therefore give an indication of the impact of ADMA flux on outcome that is independent of renal function.

When this secondary analysis is undertaken, ADMA appears to have an opposite effect on outcome, with improved survival when ADMA is corrected for impaired renal MA clearance. This observation may suggest that in sepsis, patients that are able to maintain higher intracellular concentrations of ADMA are able to control NO synthesis more effectively and have less severe shock. This increase may be reflected in plasma ADMA. In diseases where renal dysfunction is an important feature, this effect may not be readily seen due to competing factors determining the 'pool' of plasma MA concentrations. No previous study has been able to undertake the analysis of ADMA:SDMA ratio and so the observation has not previously been made. It is of interest that inhibition of DDAH1 and increase of intracellular ADMA within the vasculature is associated with improved outcomes in rodent models of sepsis[213]. It may be the case that ADMA, corrected for plasma SDMA concentrations demonstrates the physiological response that therapeutic inhibition takes advantage of. Circumstantial corroboration of this observation may be found in the apparently paradoxical observation that in paediatric sepsis, elevations in the plasma ADMA concentration are associated with less severe shock[209]. Clinically significant acute kidney injury is much less common in children on the ICU. This raises the possibility that the elevation in ADMA observed is mediated, at least in part, by increased intracellular concentrations rather than impaired renal clearance alone and therefore reflects the same pattern of protection observed when ADMA is corrected for SDMA in adults.

Given the consistent pattern of reduced L-arginine concentrations in septic shock observed here and the absence of survival impact on patients with differing L-arginine concentrations, the differences seen in the survival of patients with elevated ADMA:L-arginine ratios seem likely to reflect increases in ADMA rather than L-arginine mediated changes. This does raise the question of whether increases in the competitive inhibitor (ADMA) relative to the substrate at the NOS enzyme (L-arginine) are deleterious. However in the light of the observation that once corrected for renal clearance ADMA is protective, this would appear likely to be a similar pattern to that seen in uncorrected ADMA, reflecting largely the impact of renal failure on outcome in septic shock.

In summary, both plasma ADMA and SDMA concentrations are associated with increased mortality in septic shock, however when plasma ADMA is corrected for SDMA which may reflect renal clearance of methylarginines, increases in ADMA are associated with a protective effect in septic shock. Plasma nitrate+nitrite and L-arginine do not predict mortality in septic shock.

7.4.4 Genomic associations with outcome and methylarginines in septic shock

This study undertook two experiments exploring the role of SNPs of DDAH1 and DDAH2 in sepsis. The first was interrogation of the genome wide study cohort – the GenOSept study - which showed that a group of intronic DDAH1 SNPs were associated with mortality in severe sepsis and septic shock. This observation is of considerable interest since in the original study, only one SNP was associated at a genome wide level with mortality[248], however the tightly clustered group of SNPs within the first intron of DDAH1 almost reach genome wide significance and display a consistent pattern of increased odds ratio of death in sepsis. It is of interest that none of the DDAH2 polymorphisms identified in previous studies were associated with mortality in this study.

This observation was further explored by direct genotyping of the DDAH1 polymorphisms identified in the GenOSept study in a prospective cohort of septic shock patients in the VANISH study. This revealed that like the GenOSept study, the minor alleles were more common in septic patients (~12%) compared to matched healthy controls (~9%). This may suggest that these SNPs of DDAH1 may play a role in susceptibility to sepsis, perhaps mediating an increased metabolism of ADMA by the vasculature and predisposing those people to overproduction of NO and septic shock. It has previously been shown that regions of intron 1 of DDAH1 are associated with functional differences in the turnover of ADMA and it may be the case that these SNPs replicate that effect[378]. It is of interest that in a population of only septic shock patients, this difference in mortality is not observed. This may be due to power of the study, however given the findings of the GWAS study and the reasonable size of this phase of the project – 286 patients were analysed – an alternative explanation is more likely.

It may be the case that whilst polymorphisms of DDAH1 increase the susceptibility to septic shock in people with early infections or the transition from severe sepsis to the shock state, in patients who already have established septic shock, no difference in mortality is observed. This would explain the exaggerated mortality seen in the severe sepsis/septic shock group in the GenOSept study compared to the VANISH study. Another possible explanation for the apparent difference observed here is that in the GenOSept study, the patients were drawn only from community acquired pneumonia and faecal peritonitis cohorts. In the VANISH study, any cause of septic shock was an acceptable criteria for inclusion and whilst the majority of patients had either respiratory tract or abdominal sources of infection, differences in the underlying infective source may contribute to the differences observed between the studies. Of interest is the observation in a sub-group of 215 genotyped patients that no significant differences were observed between ADMA concentrations and genotype. This may suggest that in this context, the DDAH1 SNPs do not have a significant effect on plasma ADMA levels. A limitation of this study is that the number of available samples prohibited analysis of outcome or methylarginine concentrations in the rare homozygote populations of DDAH1 SNPs which arise in 1.4% of patients giving insufficient numbers to conduct robust analysis.

The second phase of the VANISH genotype interrogation was to determine whether the rs805305 SNP DDAH2, which had previously been associated with plasma ADMA levels and inflammatory state in sepsis was explored[40, 208, 209]. This study was able to show by direct genotyping that the SNP of DDAH2 was strongly associated with 28 day mortality, with the least common C:C genotype displaying significantly lower death than the C:G heterozygotes which in turn were relatively protected compared to the most prevalent G:G homozygote. A potential mechanism for this benefit is that plasma ADMA:SDMA ratio in the C:C homozygote was elevated, which was shown in the observational studies of sepsis to confer protection in septic shock. It is possible that this SNP has a functional impact on ADMA turnover which results in increased NOS inhibition and limits the exaggerated NO synthesis seen in septic shock. Of note is that the rs805305 SNP has been implicated through this mechanism in essential hypertension, offering corroboration of this hypothesis[38, 375].

7.4.5 Strengths and limitations

The key limitation of this study is that this work was undertaken in a subgroup of participants in a randomised controlled trial of vasopressin vs noradrenaline in septic shock. Hence this analysis was not the primary intention of the VANISH study. However, by building this series of experiments into the prospective study and confirming that no treatment group effect was observed, we have undertaken the largest study of this kind to date which would have been impossible through conventional observational study techniques. The size of this study means that associations detected are likely to be robust and that small groups, previously considered outlying values[379] and therefore ignored can be identified as potentially important groups of patients in whom specific therapeutic strategies may be appropriate.

By including only patients with septic shock in this study, one of the main limitations of most human sepsis trials has been eliminated. Because most studies in this area – even phase III studies – include patients with severe sepsis and septic shock, a broad spectrum of disease is included. This increases the number of patients that are eligible but, as seen in the studies undertaken previously in this area[40, 207, 208] reduces the ability of the studies to detect differences in survival in the patients most likely to die as a consequence of their infections.

The results presented here are a detailed assessment of the impact of septic shock on methylarginine concentrations during the first week of critical care admission. This makes it possible to detect narrative changes over the first week that may not have been apparent if only one or two samples had been taken. However, this study does not reveal the longer term narrative of MA regulation. A later analysis might help to identify patients with delayed or slow recovery, severity of polymyopathy and the persistence of kidney dysfunction after the recovery of gross clinical renal failure.

To date, only the outcome of association with mortality has been explored. This was only a secondary outcome of the original study, however this study included four groups of patients and therefore by considering the population as a whole and categorising the outcomes by survival status, we have sufficient power to make the presented observations. Further analysis of severity of organ failure, composite renal failure outcomes and biochemical indices of disease severity and their relationship to plasma MA levels will all contribute to the narrative observations made here.

By undertaking a hypothesis based interrogation of the GWAS data set in the GenOSept study, there is potential for identifying genes that do not achieve the required significance at the genome wide level. The typical threshold for genome wide statistical significance is a p value of at least 10^{-6}, in the observations presented here, a p value of 10^{-5} was detected in the two most closely related SNPs of DDAH1. This makes a spurious finding possible, however since the linkage between the SNPs and their allele frequencies was confirmed in the VANISH cohort, differences in the result due to the sampled population must be considered before ruling out a potentially important observation.

7.4.6 Future work

Building on the work presented here, further analysis of the existing data set will reveal associations between other indices of inflammation and organ dysfunction and methylarginines. Understanding these relationships will build a picture of how ADMA or SDMA may be employed as biomarkers in human sepsis.

It is clear that there is a disparity between plasma and intracellular indices of NOS inhibition. Future work will look to determine from monocytes extracted from whole blood how intracellular methylarginine concentrations change in sepsis. Also, following patients over a longer time course will give insights into the changes in MA seen in the recovery phase and how they relate to longer term outcomes such as chronic renal, cognitive and functional impairment in survivors of sepsis.

Finally, the evidence presented here that ADMA may have a protective role in septic shock provides further evidence that DDAH1 inhibition may be a therapeutically advantageous approach to improve vascular tone in sepsis. The translation of the compound L-257 into clinical practice is underway and will constitute a major portion of forthcoming work in this area.

7.4.7 Summary statement

- Presented here are the first results from the largest ever study of methylarginines and nitric oxide synthesis in septic shock, exploring the relationship between these, polymorphisms of ADMA regulating genes and 28 day mortality.
- High plasma ADMA and SDMA concentrations are associated with an increased risk of death in patients with septic shock
- When corrected for renal clearance of methylarginines however, ADMA has a protective effect in patients with septic shock.
- Plasma NO concentrations do not associate with outcome, although a group of patients who are 'super-producers' of NO have been identified in the first study of this size to explore plasma nitrate+nitrite concentrations in sepsis.
- SNPs within the intron of DDAH1 are associated with an increased risk of death in severe sepsis and septic shock; however in septic shock alone no significant association was detected.
- The DDAH2 SNP rs805305 is associated with reduced mortality in septic shock and mediates an increased ADMA:SDMA ratio, a potential mechanism for this protective effect.

8 General discussion

Each chapter of results presented here contains a detailed discussion of the methodology, implications, strengths and limitations of the work contained within it. This chapter offers a brief summary of the context for the work, the background data upon which this project was built and a narrative description of the findings of each group of experiments. This is followed by discussion of the immediate clinical implications of this work, future projects in this area and concluding remarks.

8.1 Clinical context

Sepsis is a disease that poses challenges for patients, clinicians and researchers.

For patients and their families, sepsis is an alien and poorly understood syndrome. Whilst most people have heard of 'septicaemia', this does not translate well into understanding of the impact of sepsis as a disease. Unlike other specialties, who have managed to effectively educate the public about illnesses such as myocardial infarction, stroke and cancer; sepsis, which kills more people in this country than bowel and breast cancer combined has limited penetration of the public consciousness. When exposed to sepsis therefore, patients and their families are poorly equipped to cope with the high risk of early mortality in the days after diagnosis. Because of the nature of the illness, there is minimal time to prepare people for the experience of prolonged intensive care admission, ventilation, haemofiltration and profound weakness that will arise as a consequence of something as ostensibly simple as a chest infection. In addition, even as intensivists we are not good at explaining the longer term sequelae of critical illness, in part because this work has only come to fore in recent years. Patients and families do not leave hospital prepared for what may be long periods of rehabilitation, significant long term cognitive, functional and organ impairment all of which will have significant healthcare and economic impacts long after the patient is discharged from the ICU[93, 96, 99].

For clinicians, sepsis remains a challenging disease. Improvements in outcome from critical care as a whole have been mediated by simple measures to limit iatrogenic injury that leads to increased mortality. Examples of treatments of this kind include, regulating fluid balance[69], less injurious ventilation strategies[380], improved infection control and central line care[381]. This has led to a trend towards improved survival in critical care as a whole and to some degree in sepsis, where mortality has fallen from 30-40% fifteen years ago to 20-30% now. These improvements must have a plateau point however and to date, no specific therapy for sepsis has been shown to improve survival since the introduction of antibiotics. The reasons for this are varied and certainly include poor selection of animal models, incorrect endpoints in early trials and poor drug design with limited understanding of the mechanisms involved. Moving forward, maintaining engagement with clinicians in sepsis research is a critical part of academic activity in this area.

For academics, sepsis has proven difficult to study in a robust fashion. It presents suddenly with limited prodrome, is followed by rapid clinical deterioration and the requirement for immediate therapy. This makes is difficult to recruit patients for studies using traditional models of informed consent and so interventional studies in this area tend to be smaller than those of other specialties in spite of the large number of patients we encounter. In addition, sepsis is a broad church of disease aetiologies and severity. The pathophysiology of a gram negative infection of the urinary tract is certainly different from that of hospital acquired multi-resistant gram positive chest infection or post-operative peritonitis due to anastomotic leak, however all of these infections may lead to a physiological response that is of sufficient magnitude to merit the diagnosis of severe sepsis or septic shock and therefore be included in the same study of sepsis patients. These heterogeneous groups have common features, the study of which is valuable, however it is critical to understand that in undertaking large phase III interventional trials based on existing diagnostic criteria, we risk missing specific populations of patients who would benefit from a treatment amidst the 'noise' of the heterogeneous patient sample.

8.2 Methylarginine regulation

8.3 ADMA, DDAH and NO in sepsis

8.3.1 Global NOS inhibition in sepsis

The field of NO regulation provides one of the best examples of a therapy that was based on incomplete understanding of the physiology, limited understanding of the differences between animal and human sepsis and hurried progression to phase III. This is global NOS inhibition in sepsis and caused significant harm to the field of NO research in this area.

Synthetic L-NMMA (546C88) was developed when it was determined that elevations in NO synthesis were associated with vascular dysfunction in shock states[191, 196]. L-NMMA was shown to be protective in animal models of septic shock and in healthy volunteers to cause a rise in blood pressure mediated by reduced NO availability and increased systemic vascular resistance[382, 383]. When trialled in sepsis, L-NMMA did indeed inhibit NOS, and in doing so improved blood pressure significantly[200]. However it was also associated with significantly increased mortality[384] and so was withdrawn from use, one of a tranche of drugs trialled between 1995 and 2010 which were not effective. In fact, L-NMMA delivered exactly the profile of response we might expect given the understanding we now how of NOS, ADMA and NO in sepsis. As a pan-NOS inhibitor, L-NMMA reduced NO synthesis not just in the vasculature but also in the heart and immune cells, both of which are essential parts of the normal septic response. As a result, L-NAME treated patients displayed impaired immune and cardiac function in spite of their improved blood pressure. The net result of these effects was increased mortality. Animal models had failed to predict this effect because rodents, whilst employing near identical genetic and signalling pathways, are able to produce more NO in response to sepsis, therefore reducing their NOS activity does not have the same deleterious effects that were seen in humans. Only as work has continued in this area have we shown that the tissue specificity of the NO response to infection is critical and modulating it must be done with insight into the tissues to be targeted.

8.3.2 ADMA and DDAH in sepsis

Sepsis models have been used in DDAH research since its discovery as a tool to explore the physiology of NOS regulation by ADMA and in turn by DDAH[47]. A modest amount of work has described limited associations between ADMA and surrogate endpoints of inflammatory state in human sepsis [40, 207, 208]and in a handful of patients SNPs of DDAH2 have also been related to both plasma ADMA and shock severity in sepsis[39, 40].

In animals, it has been clearly demonstrated that knockout or pharmacological inhibition of DDAH1, the predominant isoform in the vasculature leads to improved vascular tone without harmful impacts on immune cell or cardiac function because of the absence of the isoform in these tissues[213]. Pilot work in isolated primary macrophages of Ddah2 knockout mice has shown that when exposed to inflammatory stimulus, cells deficient in DDAH2 display impaired motility, phagocytosis and bactericidal ability compared to controls[30].

The studies presented here explore the role of DDAH2 in sepsis in three ways. The first goal of this work was to understand how DDAH2 expression changes in response to stimuli commonly experienced in a septic or critically ill patient. Second this study aimed to determine the impact of global and tissue specific DDAH2 knockout on a whole animal model of sepsis. Thirdly this project observed for the first time in a robust fashion the relationship between septic shock, methylarginine concentrations, SNPs of DDAH genes and outcome in humans.

8.4 Summary of results

8.4.1 Regulation of DDAH2 by hypoxia

DDAH2 is found in the immune cells of both humans and mice, it is highly conserved and regulates ADMA concentrations within the cell. Reductions in intracellular ADMA lead to an increase in L-arginine binding to NOS isoforms and result in increased NO synthesis. In the studies presented here, it was shown that hypoxia is able to increase expression of DDAH2 in murine primary peritoneal macrophages. An increase in DDAH2 mediates reduced competitive inhibition by ADMA with L-arginine at the active site of NOS which in turn results in increased NO synthesis by macrophages. This finding was recapitulated in a human study of normobaric hypoxia, deomonstrating that hypoxia mediated induction of DDAH2 expression is preserved across species.

Changes in DDAH2 expression may be one of the mechanisms by which NO synthesis is increased in response to pathophysiological stress. This is particularly important in hypoxia where one of the essential co-factors for NOS, oxygen has limited availability. In conditions such as critical illness where oxygen availability is impaired, reducing competitive inhibition of NOS is a further mechanism for increasing immune cell NO production.

8.4.2 Regulation of DDAH2 expression by Interferon-γ

In this series of studies, the regulation of NO synthesis by ADMA and its regulators was explored using the immortalised murine macrophage cell line RAW264.7. The expression of DDAH2 was shown to be determined by IFN-γ, and activated, like a number of other genes within the MHC region of chromosome 6 by the canonical JAK/STAT signalling pathway. This results in reductions in ADMA concentrations within the cell and increased NO synthesis by macrophages. In contrast, TNF-α and LPS have no effect on DDAH2 expression or ADMA mediated inhibition of NO synthesis.

In a study of macrophage specific Ddah2 knockout mice and controls, differential synthesis of IFN-γ was observed in response to polyinosinic polycytidylic acid, a viral mimic and TLR3 stimulus. This suggests a regulatory role for DDAH2 in the viral response that may differ to that observed in bacterial infection.

8.4.3 Impact of Ddah2 knockout on outcome in murine septic shock

This study explored the role of DDAH2 in the systemic response to infection. The model chosen was the caecal ligation and puncture technique which, coupled with regular analgesia and fluid resuscitation produced a clinically relevant model with 50% mortality in control animals. Two kinds of transgenic animals were used in these studies. The first were global Ddah2 knockout mice developed using a high throughput gene trapping strategy which were compared to wild type litter mate controls. The second were macrophage and granulocyte specific Ddah2 knockouts, which were made using the LoxP Cre recombinase technique. These mice were compared to their floxed litter mate controls.

Studies in global knockout mice showed that sepsis led to early mortality compared to controls associated with significant hypotension observed up to twelve hours prior to death. *Ex vivo* analysis revealed that this phenomenon was unlikely to be mediated by intrinsic vascular dysfunction. Follow up studies in macrophage and granulocyte specific knockout mice revealed a similar pattern of early mortality suggesting that immune cell DDAH2 is an important mediator of the response to sepsis. The preliminary finding of *in vitro* innate immune cell dysfunction was corroborated by the observation that bacterial loads were higher in knockout mice than controls.

This study suggests that in contrast to DDAH1, DDAH2 has limited activity under normal conditions but when exposed to a pro-inflammatory stress such as sepsis, plays a critical role in regulating the innate immune response.

8.4.4 Methylarginines and NO in human septic shock

In the light of pilot work suggesting that ADMA concentrations in the plasma are increased and that this was associated with the inflammatory state of patients with sepsis, we undertook the definitive study of early methylarginine and NO levels in human septic shock[40, 207, 377].

This study used serial plasma samples from patients from a subgroup of 215 patients in the VANISH trial, a randomised controlled study exploring vasopressor choice in sepsis. By analysing the plasma concentrations of NO, ADMA, SDMA and L-arginine this study built the first complete picture of the relationship between NO, its substrate and its endogenous inhibitors over the first seven days of admission to the ICU with septic shock.

Plasma NO, ADMA and SDMA are all significantly elevated over normal plasma concentrations throughout the first seven days of ICU admission and plasma L-arginine is significantly depressed. ADMA appears to rise throughout the first week, even though shock resolves in these patients around day 4. This implies that more than one mechanism may be responsible for this persistent elevation. Analysis of the relationships between these indices showed that plasma ADMA, SDMA and NO(nitrate+nitrite) are all positively correlated, suggesting that clearance of all three may be impaired by sepsis associated acute kidney injury or other common metabolic pathways.

Whilst plasma NO and L-arginine concentrations are not strongly associated with mortality, patients in the top half of plasma concentrations of ADMA and SDMA display a 2-3 fold increase in the hazard ratio for mortality at 28 days compared to those with lower values. This suggests that both ADMA and SDMA may have a role as biomarkers of illness severity in septic shock. However, when the clearance of methylarginines by the kidney and changes in rate of synthesis are accounted for it appears that ADMA may exert a protective effect in sepsis. This challenges the hypothesis that measuring plasma ADMA concentrations is a simple surrogate for intracellular levels in dynamic disease states such as sepsis and merits further investigation as a potential therapeutic target. Changes in SDMA, not mediated by DDAH may reflect the illness severity of patients with sepsis such that the relationship between them serves as a useful control in studies of the role of ADMA in dynamic diseases such as sepsis.

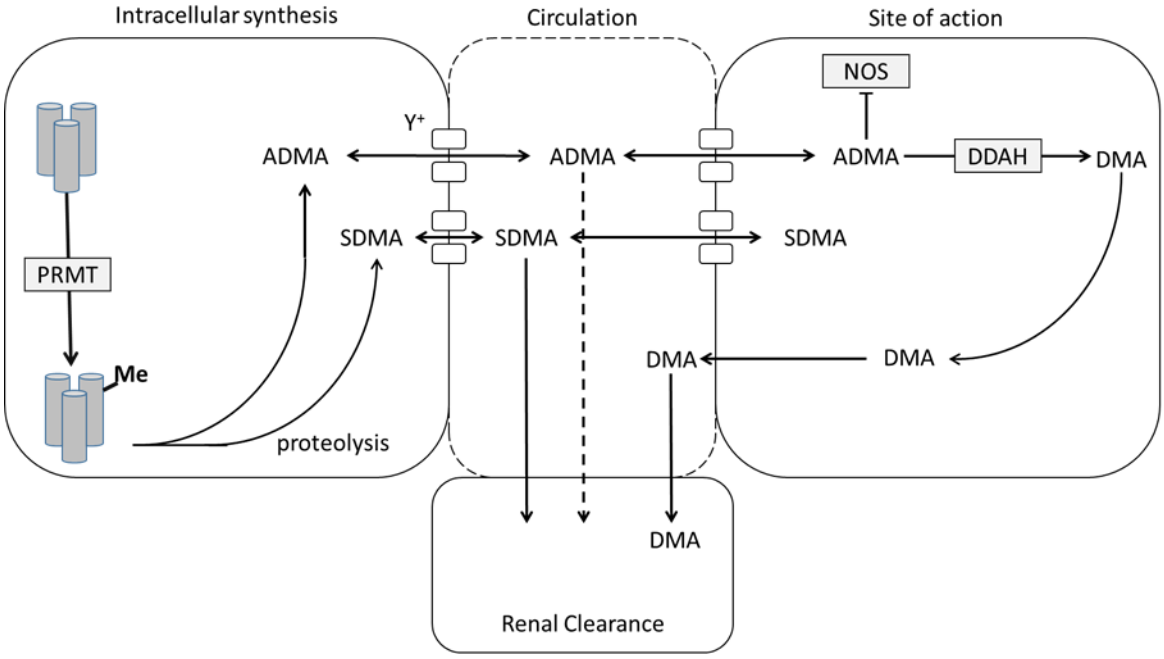

Figure 139: Representative image of the synthesis and regulation of ADMA and SDMA in sepsis.

Protein Arginine Methyl Transferases (PRMT) catalyse the methylation of arginine containing protein residues to ADMA and SDMA which are released upon proteolysis. ADMA and SDMA are transported via the y^+ cationic amino acid transporter into and out of the circulation. SDMA is not metabolised in most cells whereas ADMA is metabolised by the two isoforms of dimethylarginine dimethylaminohydrolase (DDAH) in diffuse tissues. ADMA acts intracellularly to inhibit nitric oxide synthase (NOS), SDMA has no action on NOS isoforms. SDMA is cleared by the kidney largely unchanged and in small part through metabolism by AGXT2(not shown). ADMA is largely metabolised by DDAH to dimethylamine (DMA), a small amount by AGXT2 and a proportion is cleared unchanged through the kidney. In sepsis, the synthesis of ADMA and SDMA may be increased through high protein turnover by patients in a catabolic state, clearance by the tubule and AGXT2 are impaired by acute kidney injury. Differences in the concentrations of these methylarginines may be related to the metabolism by DDAH isoforms which only metabolises ADMA. nb. L-NMMA (monomethylarginine) is considered to have the same synthetic pathway, activity, metabolism and clearance as ADMA but is present in only 10% of the concentration. Not shown for clarity.

8.4.5 Polymorphisms of the DDAH genes in human sepsis

This study has offered insights into the role of SNPs of both DDAH1 and DDAH2 in human severe sepsis and septic shock. In a large cohort of severe sepsis and septic shock patients, a number of SNPs within the first intron of DDAH1 are associated with mortality. However in a second cohort of septic shock patients, this association is not seen. Both cohorts have similar incidences of the SNPs, which are higher than the general population and the direct analysis of the VANISH cohort confirms the high degree of linkage between the SNPs. This suggests that the difference may lie in the nature of the study cohorts. In the GWAS study, severe sepsis and septic shock patients were considered together, this is significantly different from the VANISH population who were already in established septic shock at the time of recruitment. This suggests that the role of the SNPs of DDAH1 in determining mortality may be in making the transition to septic shock more likely. Once the patient is in vasopressor dependent shock however the risk of death is determined by other factors. This may explain the difference between the observed results.

DDAH2 SNPs are not associated with mortality in the GenOSept cohort as a whole, however when a septic shock only population is considered, a strong association with mortality is observed. It is also the case that in the least common G:G homozygote, the ADMA:SDMA ratio is increased, recapitulating the observation that ADMA:SDMA ratio predicts outcome in septic shock and offering a potential mechanism for this effect. It is an interesting contrast that whilst DDAH1 SNPs may be associated with the risk of transition from severe sepsis to septic shock, the SNP of the DDAH2 promoter that we studied is shown to have its effect when septic shock has become established.

It is also important to observe that in mouse models of septic shock, knockout of DDAH2 from monocytes or in the whole animal leads to an increased mortality, however when a SNP of DDAH2 which appears to reduce DDAH2 activity is considered in humans, it appears to offer a protective effect. This may seem to be a contrast in effect; however the knockout of a gene leads to a number of effects such as adaptive responses and a maximal effect size that would not be seen with a SNP. The animal models studied here provide strong evidence for a mechanistic role for DDAH2 in sepsis. The human studies, undertaken in the challenging clinical and scientific environment of critical illness, corroborate this observation that DDAH2 is an important mediator of outcome across species.

8.5 Clinical implications

8.5.1.1 Understanding methylarginines in sepsis

This study answers a number of questions about the role of ADMA in sepsis. Changes in ADMA concentrations have an impact on immune cell function that not only impairs NO synthesis but has a functional impact on immune cells that limits their ability to mount essential innate responses. Conditions which elevate intracellular ADMA therefore may well be associated with impaired immune function.

In addition to this, it is clear that as a biomarker of critical illness, ADMA and SDMA concentration in the plasma may play a role as part of a panel of tools that may allow us to better predict which of our patients will not benefit from prolonged critical care. However this study also shows that understanding the role of ADMA is more complex than simply measuring plasma methylarginine concentrations. It is important to recognise that the plasma reflects the net result of MA movement, synthesis and clearance and that within the cell, different concentrations are likely to be found. In fact it may well be the case that the ability to increase ADMA availability within the cell offers a protective mechanism in septic shock. By competing with L-arginine, ADMA may limit the exaggerated NO synthesis seen in septic shock and prevent the associated vascular dysfunction, organ failure and death.

8.5.1.2 DDAH genes and sepsis outcomes

This study has significant implications for our understanding of sepsis and its progression as a disease. By considering populations with only septic shock, for the first time a DDAH SNP has been found in an adequately powered study which is associated with 28 day mortality in septic shock. In addition, a group of intronic SNPs have been associated with the progression of severe sepsis to septic shock. Both of these findings have profound implications both for our knowledge of the mechanisms that underlie the pathogenesis of sepsis but also in stratifying the risk of disease progression or death in patients admitted to hospital with sepsis.

8.5.1.3 Therapeutic modulation of DDAH isoforms

Modulating the function of the isoforms of DDAH1 and DDAH2 is an area of considerable interest. This study presents further evidence that there may be a place for both of these therapeutic strategies.

DDAH1 inhibition using a highly specific inhibitor has been shown to increase vascular tone and improve mortality in animal models of sepsis[212, 213]. These studies show that unlike global NOS inhibition that has an impact on all tissues, inhibition solely of DDAH1 eliminates the potentially deleterious effects seen when Ddah2 is knocked out in immune cells. It may also be the case that DDAH1 inhibition plays a protective role in the kidney[8], making it an ideal target for patients with sepsis.

In contrast, inhibiting DDAH2 in sepsis – whilst not yet possible – would be associated with significant immune dysfunction and possibly poor outcomes in sepsis. This is consistent with a number of studies that have attempted to modulate the exaggerated immune response in sepsis and have been shown to be ineffective or in some cases harmful[385]. However, there are a large number of chronic disease states in which inflammation is a persistent and pathological component. Diseases such as arthritis, inflammatory bowel disease, connective tissue disorders and even atherosclerosis all exhibit significant chronic inflammatory components which may be amenable to modification of DDAH2 activity as a therapeutic target. Of note is that because the actions of DDAH2 on NO synthesis are indirect, knockout does not result in complete abolition of NO production by immune cells. This means that inhibition of DDAH2 may provide a more tolerable means of limiting the immune response in these chronic conditions.

8.6 Future projects

8.6.1 Animal studies

The studies presented here have shown that animal studies can provide valuable mechanistic insights into the role of DDAH2 in determining mortality in sepsis. Future studies will focus on understanding better the role of DDAH isoforms in regulating the recovery from sepsis. The development of Ddah1 and Ddah2 knockout rats using the CRISPR Cas9 technique means that it is now possible to develop a more clinically relevant model of sepsis and understand not just how DDAH isoform knockout affects mortality but also what the impact is on organ function, muscle catabolism and cognition in survivors of a septic insult.

In parallel to this work is a better understanding of how different types of infection modulate the septic response and explore whether inhibition of DDAH1 may be more effective in some disease states that others and whether DDAH2 plays a more significant immune role in viral than bacterial infection.

8.6.2 Human studies

Human studies moving forward can be divided into interventional and observational studies. The translation of L-257 into human trials forms a major part of the work to be undertaken over the next two years. Building a package of IP and evidence of efficacy in a number of models will herald engagement with potential funders and ultimately phase I studies in humans. If successful, phase IIa and IIb studies will be undertaken to fully understand the role of L-257 as a modulator of haemodynamics in sepsis.

In addition to the drug development work, observational studies, built around randomised controlled trials that are currently underway will explore the intracellular regulation of ADMA. By taking whole blood samples and extracting mononuclear cells from patients with sepsis, it will be possible to understand how the intracellular expression of DDAH2 varies, how this affects cellular ADMA concentrations and how this relates to both outcome and plasma indices of methylarginine concentrations. Genotyping of a further cohort of septic shock patients will deliver definitive confirmation that DDAH1 SNPs play a role in the transition from severe sepsis to septic shock and that rs805305 predicts mortality in patients in established shock.

A second observational arm will examine patients admitted to critical care and focus on those who have survived critical illness. By taking serial samples over the course of ICU admission, it will be possible to understand how methylarginine turnover and the regulation of NO synthesis predict and possibly regulate the recovery phase of critical illness. Work within the group has already shown a role for these enzymes in blood brain barrier, mitochondrial, renal and cardiac function. All of these may be important in patients who have suffered the inflammatory stress of sepsis and survived.

8.7 Conclusions

- Dimethylarginine dimethylaminohydrolase 2 is the only DDAH isoform expressed in immune cells. It is present in both human and murine cells and metabolises ADMA. ADMA is a competitive inhibitor of L-arginine, the substrate for nitric oxide synthase.
- DDAH2 expression is upregulated in hypoxia in both mice and human immune cells. This leads to the increased metabolism of ADMA and reduced inhibition of nitric oxide synthase. This in turn leads to increased systemic and intracellular nitric oxide concentrations
- Interferon-γ regulates DDAH2 expression via the JAK/STAT pathway, directly stimulating two postulated transcription factor binding sites on the human DDAH2 promoter. In contrast, lipopolysaccharide and tumour necrosis factor have no impact on DDAH2 expression or ADMA regulation.
- Global and macrophage specific Ddah2 knockout mice display exaggerated early mortality in a caecal ligation and puncture model of septic shock. This is mediated by impaired innate immune function and ability to eradicate bacteria. Cardiovascular collapse does not arise as a result of intrinsic vascular dysfunction; instead it appears to result from an overwhelming infectious insult.
- In human septic shock, ADMA, SDMA and NO levels in the plasma are elevated over controls. Positive correlations between them suggest that impaired clearance plays an important role in determining plasma methylarginine and nitrate concentrations in sepsis.
- High plasma ADMA and SDMA are both associated with an increased risk of death in septic shock and may offer promise as biomarkers of disease outcome. The biology of ADMA is more complex and correction for impaired clearance suggests that ADMA may have a protective role in sepsis. Future work will elucidate the relationship of intracellular ADMA concentrations to outcome in sepsis.
- SNPs of the first intron of DDAH1 are associated with increased risk of death in severe sepsis and septic shock cohorts and may play an important role in the progression to septic shock.
- The DDAH2 promoter SNP rs805305 is associated with mortality in septic shock and also an increased ADMA:SDMA ratio.

9 Bibliography

1. Palmer, R.M.J., A.G. Ferrige, and S. Moncada, *Nitric oxide release accounts for the biological activity of endothelium-derived relaxing factor.* Nature, 1987. **327**(6122): p. 524-526.

2. Moncada, S., R.M. Palmer, and E.A. Higgs, *Nitric oxide: physiology, pathophysiology, and pharmacology.* Pharmacol Rev, 1991. **43**(2): p. 109-42.

3. Denninger, J.W. and M.A. Marletta, *Guanylate cyclase and the ·NO/cGMP signaling pathway.* Biochimica et Biophysica Acta (BBA) - Bioenergetics, 1999. **1411**(2–3): p. 334-350.

4. Hakim, T.S., et al., *Half-life of nitric oxide in aqueous solutions with and without haemoglobin.* Physiol Meas, 1996. **17**(4): p. 267-77.

5. Kelm, M., *Nitric oxide metabolism and breakdown.* Biochimica et Biophysica Acta (BBA) - Bioenergetics, 1999. **1411**(2–3): p. 273-289.

6. Knowles, R.G. and S. Moncada, *Nitric oxide synthases in mammals.* Biochemical Journal, 1994. **298**(Pt 2): p. 249-258.

7. Shaul, P.W., *REGULATION OF ENDOTHELIAL NITRIC OXIDE SYNTHASE: Location, Location, Location.* Annual Review of Physiology, 2002. **64**(1): p. 749-774.

8. Tomlinson, J.A.P., et al., *Reduced Renal Methylarginine Metabolism Protects against Progressive Kidney Damage.* Journal of the American Society of Nephrology, 2015.

9. Pekarova, M., et al., *Asymmetric dimethylarginine regulates the lipopolysaccharide-induced nitric oxide production in macrophages by suppressing the activation of NF-kappaB and iNOS expression.* European Journal of Pharmacology, 2013. **713**(1–3): p. 68-77.

10. Lowenstein, C.J. and E. Padalko, *iNOS (NOS2) at a glance.* Journal of cell science, 2004. **117**(14): p. 2865-2867.

11. Nathan, C. and Q.W. Xie, *Regulation of biosynthesis of nitric oxide.* J Biol Chem, 1994. **269**(19): p. 13725-8.

12. Leone, A., et al., *Accumulation of an endogenous inhibitor of nitric oxide synthesis in chronic renal failure.* The Lancet, 1992. **339**(8793): p. 572-575.

13. McBride, A.E. and P.A. Silver, *State of the Arg: Protein Methylation at Arginine Comes of Age.* Cell, 2001. **106**(1): p. 5-8.

14. Verrey, F., et al., *CATs and HATs: the SLC7 family of amino acid transporters.* Pflugers Arch, 2004. **447**(5): p. 532-42.

15. Closs, E.I., et al., *Interference of L-arginine analogues with L-arginine transport mediated by the y+ carrier hCAT-2B.* Nitric Oxide, 1997. **1**(1): p. 65-73.

16. Davids, M., et al., *Role of dimethylarginine dimethylaminohydrolase activity in regulation of tissue and plasma concentrations of asymmetric dimethylarginine in an animal model of prolonged critical illness.* Metabolism, 2012. **61**(4): p. 482-490.

17. Davids, M. and T. Teerlink, *Plasma concentrations of arginine and asymmetric dimethylarginine do not reflect their intracellular concentrations in peripheral blood mononuclear cells.* Metabolism, 2013. **62**(0): p. 1455-61.

18. Meier, J., N. Richter, and M. Hecker, *High-performance liquid chromatographic determination of nitric oxide synthase-related arginine derivatives in vitro and in vivo.* Anal Biochem, 1997. **247**(1): p. 11-6.

19. Schepers, E., et al., *Role of symmetric dimethylarginine in vascular damage by increasing ROS via store-operated calcium influx in monocytes.* Nephrology Dialysis Transplantation, 2009. **24**(5): p. 1429-1435.

20. Tran, C.T.L., J.M. Leiper, and P. Vallance, *The DDAH/ADMA/NOS pathway.* Atherosclerosis Supplements, 2003. **4**(4): p. 33-40.

21. Caplin, B., et al., *Alanine-Glyoxylate Aminotransferase-2 Metabolizes Endogenous Methylarginines, Regulates NO, and Controls Blood Pressure.* Arteriosclerosis, Thrombosis, and Vascular Biology, 2012. **32**(12): p. 2892-2900.

22. Ogawa, T., M. Kimoto, and K. Sasaoka, *Dimethylarginine:pyruvate aminotransferase in rats. Purification, properties, and identity with alanine:glyoxylate aminotransferase 2.* J Biol Chem, 1990. **265**(34): p. 20938-45.

23. Tran, C.T., et al., *Chromosomal localization, gene structure, and expression pattern of DDAH1: comparison with DDAH2 and implications for evolutionary origins.* Genomics, 2000. **68**(1): p. 101-5.

24. Leiper, J.M., *Identification of two human dimethylarginine dimethylaminohydrolases with distinct tissue distributions and homology with microbial arginine deiminases.* . Biochem.J., 1999. **343**(1): p. 209-214.

25. Lucio Iannone, L.Z., Olivier Dubois, Lucie Duluc, Christopher J. Rhodes, John Wharton, Martin R. Wilkins, James Leiper, Beata Wojciak-Stothard and *miR-21/DDAH1 pathway regulates pulmonary vascular responses to hypoxia.* Biochemical Journal, 2014. **462**: p. 103-112.

26. Anderssohn, M., et al., *Severely decreased activity of placental dimethylarginine dimethylaminohydrolase in pre-eclampsia.* Eur J Obstet Gynecol Reprod Biol, 2012. **161**(2): p. 152-6.

27. Forbes, S.P., et al., *Mechanism of 4-HNE Mediated Inhibition of hDDAH-1: Implications in No Regulation†.* Biochemistry, 2008. **47**(6): p. 1819-1826.

28. Hong, L. and W. Fast, *Inhibition of Human Dimethylarginine Dimethylaminohydrolase-1 by S-Nitroso-L-homocysteine and Hydrogen Peroxide: ANALYSIS, QUANTIFICATION, AND IMPLICATIONS FOR HYPERHOMOCYSTEINEMIA.* Journal of Biological Chemistry, 2007. **282**(48): p. 34684-34692.

29. Pope, A.J., et al., *Role of Dimethylarginine Dimethylaminohydrolases in the Regulation of Endothelial Nitric Oxide Production.* Journal of Biological Chemistry, 2009. **284**(51): p. 35338-35347.

30. Lambden, S., et al., *Dimethylarginine Dimethylaminohydrolase 2 Regulates Nitric Oxide Synthesis and Hemodynamics and Determines Outcome in Polymicrobial Sepsis.* Arteriosclerosis, Thrombosis, and Vascular Biology, 2015. **35**: p. 1382-92.

31. Leiper, J. and M. Nandi, *The therapeutic potential of targeting endogenous inhibitors of nitric oxide synthesis.* Nat Rev Drug Discov, 2011. **10**(4): p. 277-291.

32. Dimitroulas, T., et al., *Relationship between dimethylarginine dimethylaminohydrolase gene variants and asymmetric dimethylarginine in patients with rheumatoid arthritis.* Atherosclerosis, 2014. **237**(1): p. 38-44.

33. Caplin, B., et al., *Circulating methylarginine levels and the decline in renal function in patients with chronic kidney disease are modulated by DDAH1 polymorphisms.* Kidney Int, 2009. **77**(5): p. 459-467.

34. Lu, T.M., et al., *The association of dimethylarginine dimethylaminohydrolase 1 gene polymorphism with type 2 diabetes: a cohort study.* Cardiovasc Diabetol, 2011. **10**: p. 16.

35. Anderssohn, M., et al., *Genetic and Environmental Determinants of Dimethylarginines and Association With Cardiovascular Disease in Patients With Type 2 Diabetes.* Diabetes Care, 2014. **37**(3): p. 846-854.

36. Marra, M., et al., *Chronic renal impairment and DDAH2-1151 A/C polymorphism determine ADMA levels in type 2 diabetic subjects.* Nephrology Dialysis Transplantation, 2013. **28**(4): p. 964-971.

37. Pérez-Hernández, N., et al., *Protective role of DDAH2 (rs805304) gene polymorphism in patients with myocardial infarction.* Experimental and Molecular Pathology, 2014. **97**(3): p. 393-398.

38. Bai, Y., et al., *Common genetic variation in DDAH2 is associated with intracerebral haemorrhage in a Chinese population: a multi-centre case-control study in China.* Clinical Science, 2009. **117**(7): p. 273-279.

39. Weiss, S.L., et al., *Pilot Study of the Association of the DDAH2 -449G Polymorphism with Asymmetric Dimethylarginine and Hemodynamic Shock in Pediatric Sepsis.* PLoS ONE, 2012. **7**(3): p. e33355.

40. O'Dwyer, M., et al., *Septic shock is correlated with asymmetrical dimethyl arginine levels, which may be influenced by a polymorphism in the dimethylarginine dimethylaminohydrolase II gene: a prospective observational study.* Critical Care, 2006. **10**(5): p. R139.

41. Ryan, R., et al., *Gene Polymorphism and Requirement for Vasopressor Infusion After Cardiac Surgery.* The Annals of Thoracic Surgery, 2006. **82**(3): p. 895-901.

42. Jones, L.C., et al., *Common genetic variation in a basal promoter element alters DDAH2 expression in endothelial cells.* Biochemical and Biophysical Research Communications, 2003. **310**(3): p. 836-843.

43. Andreozzi, F., et al., *A Functional Variant of the Dimethylarginine Dimethylaminohydrolase-2 Gene Is Associated with Insulin Sensitivity.* PLoS ONE, 2012. **7**(4): p. e36224.

44. Sesti, G., et al., *A functional variant of the dimethylarginine dimethylaminohydrolase-2 gene is associated with chronic kidney disease.* Atherosclerosis, 2013. **231**(1): p. 141-144.

45. Seppala, I., et al., *Genome-wide association study on dimethylarginines reveals novel AGXT2 variants associated with heart rate variability but not with overall mortality.* Eur Heart J, 2014. **35**(8): p. 524-31.

46. Seok, J., et al., *Genomic responses in mouse models poorly mimic human inflammatory diseases.* Proceedings of the National Academy of Sciences of the United States of America, 2013. **110**(9): p. 3507-3512.

47. Leiper, J., et al., *Disruption of methylarginine metabolism impairs vascular homeostasis.* Nat Med, 2007. **13**(2): p. 198-203.

48. Hu, X., et al., *Global DDAH1 gene deficient mice reveal that DDAH1 is the critical enzyme for degrading the cardiovascular risk factor ADMA.* Arteriosclerosis, thrombosis, and vascular biology, 2011. **31**(7): p. 1540-1546.

49. Pullamsetti, S.S., et al., *The role of dimethylarginine dimethylaminohydrolase in idiopathic pulmonary fibrosis.* Sci Transl Med, 2011. **3**(87): p. 87ra53.

50. Dowsett, L., et al., *Endothelial Dimethylarginine Dimethylaminohydrolase 1 Is an Important Regulator of Angiogenesis but Does Not Regulate Vascular Reactivity or Hemodynamic Homeostasis.* Circulation, 2015. **131**(25): p. 2217-2225.

51. Hu, X., et al., *Vascular Endothelial-Specific Dimethylarginine Dimethylaminohydrolase-1–Deficient Mice Reveal That Vascular Endothelium Plays an Important Role in Removing Asymmetric Dimethylarginine.* Circulation, 2009. **120**(22): p. 2222-2229.

52. Dowsett, L.B., et al., *Abstract 600: Asymmetric Dimethylarginine is a Novel Regulator of mTOR Expression in Adipocytes.* Arteriosclerosis, Thrombosis, and Vascular Biology, 2014. **34**(Suppl 1): p. A600.

53. Hu, X., et al., *Dimethylarginine dimethylaminohydrolase-1 is the critical enzyme for degrading the cardiovascular risk factor asymmetrical dimethylarginine.* Arterioscler Thromb Vasc Biol, 2011. **31**(7): p. 1540-6.

54. Wang, D., et al., *Isoform-specific regulation by N(G),N(G)-dimethylarginine dimethylaminohydrolase of rat serum asymmetric dimethylarginine and vascular endothelium-derived relaxing factor/NO.* Circ Res, 2007. **101**(6): p. 627-35.

55. Dayoub, H., et al., *Dimethylarginine dimethylaminohydrolase regulates nitric oxide synthesis: genetic and physiological evidence.* Circulation, 2003. **108**(24): p. 3042-7.

56. Matsuguma, K., et al., *Molecular mechanism for elevation of asymmetric dimethylarginine and its role for hypertension in chronic kidney disease.* J Am Soc Nephrol, 2006. **17**(8): p. 2176-83.

57. D'Mello, R., et al., *Dimethylarginine dimethylaminohydrolase 1 is involved in spinal nociceptive plasticity.* Pain, 2015. **156**(10): p. 2052-60.

58. Dunser, M., et al., *Association of arterial blood pressure and vasopressor load with septic shock mortality: a post hoc analysis of a multicenter trial.* Critical Care, 2009. **13**(6): p. R181.

59. Hasegawa, K., et al., *Role of asymmetric dimethylarginine in vascular injury in transgenic mice overexpressing dimethylarginie dimethylaminohydrolase 2.* Circ Res, 2007. **101**(2): p. e2-10.

60. Feng, M., et al., *Improvement of endothelial dysfunction in atherosclerotic rabbit aortas by ex vivo gene transferring of dimethylarginine dimethylaminohydrolase-2.* Int J Cardiol, 2010. **144**(2): p. 180-6.

61. Bone, R.C., et al., *DEfinitions for sepsis and organ failure and guidelines for the use of innovative therapies in sepsis. the accp/sccm consensus conference committee. american college of chest physicians/society of critical care medicine.* Chest, 1992. **101**(6): p. 1644-1655.

62. Jaimes, F., et al., *The systemic inflammatory response syndrome (SIRS) to identify infected patients in the emergency room.* Intensive Care Medicine, 2003. **29**(8): p. 1368-1371.

63. Lever, A. and I. Mackenzie, *Sepsis: definition, epidemiology, and diagnosis.* BMJ, 2007. **335**(7625): p. 879-883.

64. Dellinger, R.P., et al., *Surviving Sepsis Campaign: International Guidelines for Management of Severe Sepsis and Septic Shock: 2012.* Critical Care Medicine, 2013. **41**(2): p. 580-637 10.1097/CCM.0b013e31827e83af.

65. Opal, S.M., et al., *The Next Generation of Sepsis Clinical Trial Designs: What Is Next After the Demise of Recombinant Human Activated Protein C?* Crit Care Med, 2014.

66. Ranieri, V.M., et al., *Drotrecogin Alfa (Activated) in Adults with Septic Shock.* New England Journal of Medicine, 2012. **366**(22): p. 2055-2064.

67. Cross, A.S. and S. Opal, *Minireview: Therapeutic intervention in sepsis with antibody to endotoxin: is there a future?* Journal of Endotoxin Research, 1994. **1**(1): p. 57-69.

68. Dellinger, R., et al., *Surviving Sepsis Campaign: international guidelines for management of severe sepsis and septic shock, 2012.* Intensive Care Med, 2013. **39**: p. 165 - 228.

69. group, T.A., *Comparison of Two Fluid-Management Strategies in Acute Lung Injury.* New England Journal of Medicine, 2006. **354**(24): p. 2564-2575.

70. Myburgh, J.A., et al., *Hydroxyethyl Starch or Saline for Fluid Resuscitation in Intensive Care.* New England Journal of Medicine, 2012. **367**(20): p. 1901-1911.

71. Perner, A., et al., *Hydroxyethyl Starch 130/0.42 versus Ringer's Acetate in Severe Sepsis.* New England Journal of Medicine, 2012. **367**(2): p. 124-134.

72. D., S.A., et al., *Association between intravenous chloride load during resuscitation and in-hospital mortality among patients with SIRS.* Intensive Care Medicine, 2014. **40**(12): p. 1897-1905.

73. Helmerhorst, H.J., et al., *Association Between Arterial Hyperoxia and Outcome in Subsets of Critical Illness: A Systematic Review, Meta-Analysis, and Meta-Regression of Cohort Studies.* Crit Care Med, 2015. **43**(7): p. 1508-19.

74. Altemeier, W.A. and S.E. Sinclair, *Hyperoxia in the intensive care unit: why more is not always better.* Current Opinion in Critical Care, 2007. **13**(1): p. 73-78.

75. Asfar, P., et al., *High versus Low Blood-Pressure Target in Patients with Septic Shock.* New England Journal of Medicine, 2014. **370**(17): p. 1583-1593.

76. Russell, J.A., et al., *Vasopressin versus Norepinephrine Infusion in Patients with Septic Shock.* New England Journal of Medicine, 2008. **358**(9): p. 877-887.

77. Singer, M., *Catecholamine treatment for shock—equally good or bad?* The Lancet. **370**(9588): p. 636-637.

78. De Backer, D., et al., *Comparison of dopamine and norepinephrine in the treatment of shock.* New England Journal of Medicine, 2010. **362**(9): p. 779-789.

79. Zhou, F., et al., *Vasopressors in septic shock: a systematic review and network meta-analysis.* Therapeutics and Clinical Risk Management, 2015. **11**: p. 1047-1059.

80. Andrea Morelli, C.E.M.W.S.R.T.K.S.L.A.O.A.D.E.F.D.I.C.R.M.V.F.G., *Effect of Heart Rate Control With Esmolol on Hemodynamic and Clinical Outcomes in Patients With Septic Shock. A Randomized Clinical Trial.* 2013. **310**(16): p. 1683-1691.

81. Gordon, A., *Evidence about inotropes: when is enough, enough?* Intensive Care Medicine, 2015: p. 1-3.

82. Kaukonen, K., et al., *MOrtality related to severe sepsis and septic shock among critically ill patients in australia and new zealand, 2000-2012.* JAMA, 2014. **311**(13): p. 1308-1316.

83. Leentjens, J., et al., *Immunotherapy for the Adjunctive Treatment of Sepsis: From Immunosuppression to Immunostimulation. Time for a Paradigm Change?* American Journal of Respiratory and Critical Care Medicine, 2013. **187**(12): p. 1287-1293.

84. Hall MJ, W.S., DeFrances CJ, Golosinskiy A, *Inpatient care for septicemia or sepsis: A challenge for patients and hospitals.* . 2011: NCHS data brief Hyattsville, MD: National Center for Health Statistics.

85. Seymour, C.W., et al., *Severe Sepsis in Pre-Hospital Emergency Care.* American Journal of Respiratory and Critical Care Medicine, 2012. **186**(12): p. 1264-1271.

86. Padkin, A., et al., *Epidemiology of severe sepsis occurring in the first 24 hrs in intensive care units in England, Wales, and Northern Ireland.* Critical Care Medicine, 2003. **31**(9): p. 2332-2338 10.1097/01.CCM.0000085141.75513.2B.

87. Yeh, R.W., et al., *Population Trends in the Incidence and Outcomes of Acute Myocardial Infarction.* New England Journal of Medicine, 2010. **362**(23): p. 2155-2165.

88. Liu, V., et al., *HOspital deaths in patients with sepsis from 2 independent cohorts.* JAMA, 2014. **312**(1): p. 90-92.

89. Henriksen, D.P., et al., *Incidence Rate of Community-Acquired Sepsis Among Hospitalized Acute Medical Patients—A Population-Based Survey*.* Critical Care Medicine, 2015. **43**(1): p. 13-21.

90. Iwashyna, T.J., et al., *Identifying Patients With Severe Sepsis Using Administrative Claims: Patient-Level Validation of the Angus Implementation of the International Consensus Conference Definition of Severe Sepsis.* Medical Care, 2014. **52**(6): p. e39-e43.

91. Torio CM, A.R., *National Inpatient Hospital Costs: The Most Expensive Conditions by Payer, 2011: Statistical Brief #160. In: Healthcare Cost and Utilization Project (HCUP) Statistical Briefs [Internet] Rockville (MD)*, A.f.H.C.P.a.R. (US), Editor. 2006-2013.

92. Lozano, R., et al., *Global and regional mortality from 235 causes of death for 20 age groups in 1990 and 2010: a systematic analysis for the Global Burden of Disease Study 2010.* The Lancet. **380**(9859): p. 2095-2128.

93. Iwashyna, T.J., et al., *LOng-term cognitive impairment and functional disability among survivors of severe sepsis.* JAMA, 2010. **304**(16): p. 1787-1794.

94. Singbartl, K. and J.A. Kellum, *AKI in the ICU: definition, epidemiology, risk stratification, and outcomes.* Kidney Int, 2012. **81**(9): p. 819-825.

95. Ostermann, M. and R.W.S. Chang, *Acute kidney injury in the intensive care unit according to RIFLE*.* Critical Care Medicine, 2007. **35**(8): p. 1837-1843.

96. Lo, L.J., et al., *Dialysis-requiring acute renal failure increases the risk of progressive chronic kidney disease.* Kidney international, 2009. **76**(8): p. 893-899.

97. Kirwan, C.J., et al., *Critically Ill Patients Requiring Acute Renal Replacement Therapy Are at an Increased Risk of Long-Term Renal Dysfunction, but Rarely Receive Specialist Nephrology Follow-Up.* Nephron, 2015. **129**(3): p. 164-170.

98. Quasim, T., J. Brown, and J. Kinsella, *Employment, social dependency and return to work after intensive care.* Journal of the Intensive Care Society, 2015. **16**(1): p. 31-36.

99. Pandharipande, P.P., et al., *Long-Term Cognitive Impairment after Critical Illness.* New England Journal of Medicine, 2013. **369**(14): p. 1306-1316.

100. Alberts B, J.A., Lewis J, et al., *Molecular Biology of the Cell*

2002, Garland Science: New York.

101. Charles A. Janeway, J.a. and R. Medzhitov, *INNATE IMMUNE RECOGNITION.* Annual Review of Immunology, 2002. **20**(1): p. 197-216.

102. Schroder, K. and J. Tschopp, *The inflammasomes.* Cell, 2010. **140**(6): p. 821-32.

103. Wiersinga, W.J., et al., *Host innate immune responses to sepsis.* Virulence, 2014. **5**(1): p. 36-44.

104. Lamkanfi, M., *Emerging inflammasome effector mechanisms.* Nat Rev Immunol, 2011. **11**(3): p. 213-20.

105. Lemaitre, B., et al., *The dorsoventral regulatory gene cassette spatzle/Toll/cactus controls the potent antifungal response in Drosophila adults.* Cell, 1996. **86**(6): p. 973-83.

106. King, E.G., et al., *Pathophysiologic mechanisms in septic shock.* Lab Invest, 2014. **94**(1): p. 4-12.

107. Boomer, J.S., et al., *IMmunosuppression in patients who die of sepsis and multiple organ failure.* JAMA, 2011. **306**(23): p. 2594-2605.

108. Lacy, P. and J.L. Stow, *Cytokine release from innate immune cells: association with diverse membrane trafficking pathways.* Blood, 2011. **118**(1): p. 9-18.

109. Dinarello, C.A., *Historical Review of Cytokines.* European journal of immunology, 2007. **37**(Suppl 1): p. S34-S45.

110. Cavaillon, J.M., *Pro- versus anti-inflammatory cytokines: myth or reality.* Cell Mol Biol (Noisy-le-grand), 2001. **47**(4): p. 695-702.

111. Gogos, C.A., et al., *Pro- versus Anti-inflammatory Cytokine Profile in Patients with Severe Sepsis: A Marker for Prognosis and Future Therapeutic Options.* Journal of Infectious Diseases, 2000. **181**(1): p. 176-180.

112. Belardelli, F., *Role of interferons and other cytokines in the regulation of the immune response.* APMIS, 1995. **103**(1-6): p. 161-179.

113. Alfano, M. and G. Poli, *Role of cytokines and chemokines in the regulation of innate immunity and HIV infection.* Mol Immunol, 2005. **42**(2): p. 161-82.

114. Mirantes, C., E. Passegue, and E.M. Pietras, *Pro-inflammatory cytokines: emerging players regulating HSC function in normal and diseased hematopoiesis.* Exp Cell Res, 2014. **329**(2): p. 248-54.

115. Tecchio, C. and M.A. Cassatella, *Neutrophil-derived cytokines involved in physiological and pathological angiogenesis.* Chem Immunol Allergy, 2014. **99**: p. 123-37.

116. Grunnet, L.G., et al., *Proinflammatory cytokines activate the intrinsic apoptotic pathway in beta-cells.* Diabetes, 2009. **58**(8): p. 1807-15.

117. Goya, T., T. Morisaki, and M. Torisu, *Immunologic assessment of host defense impairment in patients with septic multiple organ failure: relationship between complement activation and changes in neutrophil function.* Surgery, 1994. **115**(2): p. 145-55.

118. Solomkin, J.S., et al., *Neutrophil dysfunction in sepsis. II. Evidence for the role of complement activation products in cellular deactivation.* Surgery, 1981. **90**(2): p. 319-27.

119. Ward, P.A., *The Harmful Role of C5a on Innate Immunity in Sepsis.* Journal of Innate Immunity, 2010. **2**(5): p. 439-445.

120. van der Poll, T. and H. Herwald, *The coagulation system and its function in early immune defense.* Thromb Haemost, 2014. **112**(4): p. 640-8.

121. Chu, A.J., *Tissue factor mediates inflammation.* Archives of biochemistry and biophysics, 2005. **440**(2): p. 123-132.

122. van den Berg, Y.W., et al., *Alternatively spliced tissue factor induces angiogenesis through integrin ligation.* Proceedings of the National Academy of Sciences, 2009. **106**(46): p. 19497-19502.

123. Kirschenbaum, L.A., et al., *Importance of platelets and fibrinogen in neutrophil-endothelial cell interactions in septic shock.* Critical Care Medicine, 2004. **32**(9): p. 1904-1909.

124. Tang, Y.-Q., M.R. Yeaman, and M.E. Selsted, *Antimicrobial Peptides from Human Platelets.* Infection and Immunity, 2002. **70**(12): p. 6524-6533.

125. Oehmcke, S., et al., *A Novel Role for Pro-Coagulant Microvesicles in the Early Host Defense against <italic>Streptococcus pyogenes</italic>.* PLoS Pathog, 2013. **9**(8): p. e1003529.

126. Kumpf, O. and R.R. Schumann, *Genetic variation in innate immunity pathways and their potential contribution to the SIRS/CARS debate: evidence from human studies and animal models.* J Innate Immun, 2010. **2**(5): p. 381-94.

127. Xiao, W., et al., *A genomic storm in critically injured humans.* J Exp Med, 2011. **208**(13): p. 2581-90.

128. Liew, F.Y., et al., *Negative regulation of toll-like receptor-mediated immune responses.* Nat Rev Immunol, 2005. **5**(6): p. 446-58.

129. Ward, P.A., *SEPSIS, APOPTOSIS AND COMPLEMENT.* Biochemical pharmacology, 2008. **76**(11): p. 1383-1388.

130. Dahdah, A., et al., *Mast cells aggravate sepsis by inhibiting peritoneal macrophage phagocytosis.* The Journal of Clinical Investigation, 2014. **124**(10): p. 4577-4589.

131. Cole, J., et al., *Chapter Four - The Role of Macrophages in the Innate Immune Response to Streptococcus pneumoniae and Staphylococcus aureus: Mechanisms and Contrasts*, in *Advances in Microbial Physiology*, K.P. Robert, Editor. 2014, Academic Press. p. 125-202.

132. Buchmeier, N.A. and R.D. Schreiber, *Requirement of endogenous interferon-gamma production for resolution of Listeria monocytogenes infection.* Proceedings of the National Academy of Sciences, 1985. **82**(21): p. 7404-7408.

133. BoseDasgupta, S. and J. Pieters, *Inflammatory Stimuli Reprogram Macrophage Phagocytosis to Macropinocytosis for the Rapid Elimination of Pathogens.* PLoS Pathog, 2014. **10**(1): p. e1003879.

134. Mosser, D.M. and E. Handman, *Treatment of murine macrophages with interferon-γ inhibits their ability to bind leishmania promastigotes.* Journal of Leukocyte Biology, 1992. **52**(4): p. 369-376.

135. Hesse, M., et al., *Differential Regulation of Nitric Oxide Synthase-2 and Arginase-1 by Type 1/Type 2 Cytokines In Vivo: Granulomatous Pathology Is Shaped by the Pattern of l-Arginine Metabolism.* The Journal of Immunology, 2001. **167**(11): p. 6533-6544.

136. Mosser, D.M. and J.P. Edwards, *Exploring the full spectrum of macrophage activation.* Nat Rev Immunol, 2008. **8**(12): p. 958-969.

137. Ali, F., et al., *Streptococcus pneumoniae–Associated Human Macrophage Apoptosis after Bacterial Internalization via Complement and Fcγ Receptors Correlates with Intracellular Bacterial Load.* Journal of Infectious Diseases, 2003. **188**(8): p. 1119-1131.

138. Minakami, R. and H. Sumimoto, *Phagocytosis-Coupled Activation of the Superoxide-Producing Phagocyte Oxidase, a Member of the NADPH Oxidase (Nox) Family.* International Journal of Hematology, 2006. **84**(3): p. 193-198.

139. Slauch, J.M., *How does the oxidative burst of macrophages kill bacteria? Still an open question.* Molecular Microbiology, 2011. **80**(3): p. 580-583.

140. Lehrer, R.I., A.K. Lichtenstein, and T. Ganz, *Defensins: antimicrobial and cytotoxic peptides of mammalian cells.* Annu Rev Immunol, 1993. **11**: p. 105-28.

141. Jin, M., et al., *Proteome Comparison of Alveolar Macrophages with Monocytes Reveals Distinct Protein Characteristics.* American Journal of Respiratory Cell and Molecular Biology, 2004. **31**(3): p. 322-329.

142. Huynh, K.K. and S. Grinstein, *Regulation of Vacuolar pH and Its Modulation by Some Microbial Species.* Microbiology and Molecular Biology Reviews, 2007. **71**(3): p. 452-462.

143. Bermudez, L.E., *Differential mechanisms of intracellular killing of Mycobacterium avium and Listeria monocytogenes by activated human and murine macrophages. The role of nitric oxide.* Clin Exp Immunol, 1993. **91**(2): p. 277-81.

144. Schneemann, M., et al., *Nitric oxide synthase is not a constituent of the antimicrobial armature of human mononuclear phagocytes.* J Infect Dis, 1993. **167**(6): p. 1358-63.

145. Marriott, H.M., et al., *Contrasting roles for reactive oxygen species and nitric oxide in the innate response to pulmonary infection with Streptococcus pneumoniae.* Vaccine, 2007. **25**(13): p. 2485-2490.

146. Nicholson, S., et al., *Inducible nitric oxide synthase in pulmonary alveolar macrophages from patients with tuberculosis.* The Journal of Experimental Medicine, 1996. **183**(5): p. 2293-2302.

147. Jourd'heuil, D., et al., *The oxidative and nitrosative chemistry of the nitric oxide/superoxide reaction in the presence of bicarbonate.* Arch Biochem Biophys, 1999. **365**(1): p. 92-100.

148. Abu-Soud, H.M. and S.L. Hazen, *Nitric oxide is a physiological substrate for mammalian peroxidases.* J Biol Chem, 2000. **275**(48): p. 37524-32.

149. Wink, D.A., et al., *Nitric oxide and redox mechanisms in the immune response.* Journal of Leukocyte Biology, 2011. **89**(6): p. 873-891.

150. Pacelli, R., et al., *Nitric oxide potentiates hydrogen peroxide-induced killing of Escherichia coli.* J Exp Med, 1995. **182**(5): p. 1469-79.

151. Gregory, S.H., et al., *Reactive nitrogen intermediates suppress the primary immunologic response to Listeria.* J Immunol, 1993. **150**(7): p. 2901-9.

152. Rockett, K.A., et al., *Killing of Plasmodium falciparum in vitro by nitric oxide derivatives.* Infect Immun, 1991. **59**(9): p. 3280-3.

153. Kun, J.F., et al., *Nitric oxide synthase 2(Lambarene) (G-954C), increased nitric oxide production, and protection against malaria.* J Infect Dis, 2001. **184**(3): p. 330-6.

154. Zell, R., et al., *Nitric oxide donors inhibit the coxsackievirus B3 proteinases 2A and 3C in vitro, virus production in cells, and signs of myocarditis in virus-infected mice.* Med Microbiol Immunol, 2004. **193**(2-3): p. 91-100.

155. Chaturvedi, U.C. and R. Nagar, *Nitric oxide in dengue and dengue haemorrhagic fever: necessity or nuisance?* FEMS Immunol Med Microbiol, 2009. **56**(1): p. 9-24.

156. Turpaev, K., et al., *Variation in gene expression profiles of human monocytic U937 cells exposed to various fluxes of nitric oxide.* Free Radic Biol Med, 2010. **48**(2): p. 298-305.

157. Zhang, Z., et al., *Activation of tumor necrosis factor-alpha-converting enzyme-mediated ectodomain shedding by nitric oxide.* J Biol Chem, 2000. **275**(21): p. 15839-44.

158. Connelly, L., et al., *Biphasic regulation of NF-kappa B activity underlies the pro- and anti-inflammatory actions of nitric oxide.* J Immunol, 2001. **166**(6): p. 3873-81.

159. Endres, S., et al., *Cyclic nucleotides differentially regulate the synthesis of tumour necrosis factor-alpha and interleukin-1 beta by human mononuclear cells.* Immunology, 1991. **72**(1): p. 56-60.

160. Tsertsvadze, A., P. Royle, and N. McCarthy, *Community-onset sepsis and its public health burden: protocol of a systematic review.* Syst Rev, 2015. **4**(1): p. 119.

161. Donelli, G., *Vascular catheter-related infection and sepsis.* Surg Infect (Larchmt), 2006. **7 Suppl 2**: p. S25-7.

162. Reigle, B.S. and M.J. Dienger, *Sepsis and treatment-induced immunosuppression in the patient with cancer.* Crit Care Nurs Clin North Am, 2003. **15**(1): p. 109-18.

163. van der Poll, T. and S.M. Opal, *Host–pathogen interactions in sepsis.* The Lancet Infectious Diseases, 2008. **8**(1): p. 32-43.

164. Rice, T.W., et al., *A randomized, double-blind, placebo-controlled trial of TAK-242 for the treatment of severe sepsis*.* Critical Care Medicine, 2010. **38**(8): p. 1685-1694 10.1097/CCM.0b013e3181e7c5c9.

165. Phillip Dellinger, R., et al., *Efficacy and safety of a phospholipid emulsion (GR270773) in Gram-negative severe sepsis: Results of a phase II multicenter, randomized, placebo-controlled, dose-finding clinical trial.* Critical Care Medicine, 2009. **37**(11): p. 2929-2938 10.1097/CCM.0b013e3181b0266c.

166. Tidswell, M., et al., *Phase 2 trial of eritoran tetrasodium (E5564), a Toll-like receptor 4 antagonist, in patients with severe sepsis*.* Critical Care Medicine, 2010. **38**(1): p. 72-83 10.1097/CCM.0b013e3181b07b78.

167. Albertson, T.E., et al., *Multicenter evaluation of a human monoclonal antibody to Entero-bacteriaceae common antigen in patients with Gram-negative sepsis.* Critical Care Medicine, 2003. **31**(2): p. 419-427 10.1097/01.CCM.0000045564.51812.3F.

168. Abraham, E., et al., *Lenercept (p55 tumor necrosis factor receptor fusion protein) in severe sepsis and early septic shock: A randomized, double-blind, placebo-controlled, multicenter phase III trial with 1,342 patients.* Critical Care Medicine, 2001. **29**(3): p. 503-510.

169. Reinhart, K., et al., *Randomized, placebo-controlled trial of the anti-tumor necrosis factor antibody fragment afelimomab in hyperinflammatory response during severe sepsis: The RAMSES Study.* Critical Care Medicine, 2001. **29**(4): p. 765-769.

170. Sunden-Cullberg, J., et al., *Persistent elevation of high mobility group box-1 protein (HMGB1) in patients with severe sepsis and septic shock.* Crit Care Med, 2005. **33**(3): p. 564-73.

171. Bozza, F.A., et al., *Macrophage migration inhibitory factor levels correlate with fatal outcome in sepsis.* Shock, 2004. **22**(4): p. 309-13.

172. Rigato, O. and R. Salomao, *Impaired production of interferon-gamma and tumor necrosis factor-alpha but not of interleukin 10 in whole blood of patients with sepsis.* Shock, 2003. **19**(2): p. 113-6.

173. Gressner, O.A., et al., *High C5a levels are associated with increased mortality in sepsis patients--no enhancing effect by actin-free Gc-globulin.* Clin Biochem, 2008. **41**(12): p. 974-80.

174. Conway Morris, A., et al., *C5a mediates peripheral blood neutrophil dysfunction in critically ill patients.* Am J Respir Crit Care Med, 2009. **180**(1): p. 19-28.

175. Czermak, B.J., et al., *Protective effects of C5a blockade in sepsis.* Nat Med, 1999. **5**(7): p. 788-92.

176. Ward, P.A., R.-F. Guo, and N.C. Riedemann, *Manipulation of the Complement System for Benefit in Sepsis.* Critical Care Research and Practice, 2012. **2012**: p. 8.

177. Rittirsch, D., et al., *Functional roles for C5a receptors in sepsis.* Nat Med, 2008. **14**(5): p. 551-7.

178. Osterud, B. and T. Flaegstad, *Increased tissue thromboplastin activity in monocytes of patients with meningococcal infection: related to an unfavourable prognosis.* Thromb Haemost, 1983. **49**(1): p. 5-7.

179. Vallet, B., *Microthrombosis in sepsis.* Minerva Anestesiol, 2001. **67**(4): p. 298-301.

180. Warren, B.L., et al., *High-dose antithrombin iii in severe sepsis: A randomized controlled trial.* JAMA, 2001. **286**(15): p. 1869-1878.

181. Jaimes, F., et al., *Unfractioned heparin for treatment of sepsis: A randomized clinical trial (The HETRASE Study)*.* Critical Care Medicine, 2009. **37**(4): p. 1185-1196 10.1097/CCM.0b013e31819c06bc.

182. Bernard, G.R., et al., *Efficacy and Safety of Recombinant Human Activated Protein C for Severe Sepsis.* New England Journal of Medicine, 2001. **344**(10): p. 699-709.

183. Abraham, E., et al., *Drotrecogin Alfa (Activated) for Adults with Severe Sepsis and a Low Risk of Death.* New England Journal of Medicine, 2005. **353**(13): p. 1332-1341.

184. Brealey, D., et al., *Association between mitochondrial dysfunction and severity and outcome of septic shock.* Lancet, 2002. **360**: p. 219 - 223.

185. Brealey, D., et al., *Mitochondrial dysfunction in a long-term rodent model of sepsis and organ failure.* Am J Physiol Regul Integr Comp Physiol, 2004. **286**: p. R491 - R497.

186. Boomer, J.S., et al., *Immunosuppression in patients who die of sepsis and multiple organ failure.* JAMA, 2011. **306**(23): p. 2594-605.

187. Conway Morris, A., et al., *Combined dysfunctions of immune cells predict nosocomial infection in critically ill patients.* Br J Anaesth, 2013. **111**(5): p. 778-87.

188. Hotchkiss, R.S., et al., *Role of apoptosis in Pseudomonas aeruginosa pneumonia.* Science, 2001. **294**(5548): p. 1783.

189. Hotchkiss, R.S., et al., *Apoptotic cell death in patients with sepsis, shock, and multiple organ dysfunction.* Crit Care Med, 1999. **27**(7): p. 1230-51.

190. Meisel, C., et al., *Granulocyte-macrophage colony-stimulating factor to reverse sepsis-associated immunosuppression: a double-blind, randomized, placebo-controlled multicenter trial.* Am J Respir Crit Care Med, 2009. **180**(7): p. 640-8.

191. Thiemermann, C., et al., *Vascular hyporeactivity to vasoconstrictor agents and hemodynamic decompensation in hemorrhagic shock is mediated by nitric oxide.* Proceedings of the National Academy of Sciences of the United States of America, 1993. **90**(1): p. 267-271.

192. Titheradge, M.A., *Nitric oxide in septic shock.* Biochimica et Biophysica Acta (BBA) - Bioenergetics, 1999. **1411**(2–3): p. 437-455.

193. Taylor, B.S. and D.A. Geller, *Molecular regulation of the human inducible nitric oxide synthase (iNOS) gene.* Shock, 2000. **13**(6): p. 413-424.

194. Ikeda, U., et al., *Adenosine stimulates nitric oxide synthesis in vascular smooth muscle cells.* Cardiovascular Research, 1997. **35**(1): p. 168-174.

195. Landry, D.W. and J.A. Oliver, *The Pathogenesis of Vasodilatory Shock.* New England Journal of Medicine, 2001. **345**(8): p. 588-595.

196. Ochoa, J.B., et al., *Nitrogen oxide levels in patients after trauma and during sepsis.* Annals of Surgery, 1991. **214**(5): p. 621-626.

197. Wei, X.-q., et al., *Altered immune responses in mice lacking inducible nitric oxide synthase.* Nature, 1995. **375**(6530): p. 408-411.

198. Kilbourn, R., *Nitric oxide synthase inhibitors - A mechanism-based treatment of septic shock.* Critical Care Medicine, 1999. **27**(5): p. 857-858.

199. Fink, M.P., *Modulating the L-arginine-nitric oxide pathway in septic shock: Choosing the proper point of attack.* Critical Care Medicine, 1999. **27**(9): p. 2019-2022.

200. Bakker, J., et al., *Administration of the nitric oxide synthase inhibitor NG-methyl-L-arginine hydrochloride (546C88) by intravenous infusion for up to 72 hours can promote the resolution of shock in patients with severe sepsis: results of a randomized, double-blind, placebo-controlled multicenter study (study no. 144-002).* Crit Care Med, 2004. **32**(1): p. 1-12.

201. Bolotina, V.M., et al., *Nitric oxide directly activates calcium-dependent potassium channels in vascular smooth muscle.* Nature, 1994. **368**(6474): p. 850-853.

202. Archer, S.L., et al., *Nitric oxide and cGMP cause vasorelaxation by activation of a charybdotoxin-sensitive K channel by cGMP-dependent protein kinase.* Proceedings of the National Academy of Sciences of the United States of America, 1994. **91**(16): p. 7583-7587.

203. Quayle, J.M., M.T. Nelson, and N.B. Standen, *ATP-sensitive and inwardly rectifying potassium channels in smooth muscle.* Physiological Reviews, 1997. **77**(4): p. 1165-1232.

204. Murphy, M.E. and J.E. Brayden, *Nitric oxide hyperpolarizes rabbit mesenteric arteries via ATP-sensitive potassium channels.* The Journal of Physiology, 1995. **486**(1): p. 47-58.

205. Jaggar, J.H., et al., *Calcium sparks in smooth muscle.* American Journal of Physiology - Cell Physiology, 2000. **278**(2): p. C235-C256.

206. Ince, C., *The microcirculation is the motor of sepsis.* Critical Care, 2005. **9**(Suppl 4): p. S13 - S19.

207. Brenner, T.e.a., *L-Arginine and Asymmetric Dimethylarginine Are Early Predictors for Survival in Septic Patients with Acute Liver Failure.* Mediators of Inflammation, 2012. **2012**: p. 11.

208. Davis, J.S., et al., *Asymmetric Dimethylarginine, Endothelial Nitric Oxide Bioavailability and Mortality in Sepsis.* PLoS ONE, 2011. **6**(2): p. e17260.

209. Weiss, S.L., et al., *Evaluation of Asymmetric Dimethylarginine, Arginine, and Carnitine Metabolism in Pediatric Sepsis.* Pediatric Critical Care Medicine, 2012. **13**(4): p. e210-e218.

210. Chertow, J.H., et al., *Plasmodium Infection Is Associated with Impaired Hepatic Dimethylarginine Dimethylaminohydrolase Activity and Disruption of Nitric Oxide Synthase Inhibitor/Substrate Homeostasis.* PLoS Pathogens, 2015. **11**(9): p. e1005119.

211. Koch, A., et al., *Regulation and Prognostic Relevance of Symmetric Dimethylarginine Serum Concentrations in Critical Illness and Sepsis.* Mediators of Inflammation, 2013. **2013**: p. 413826.

212. Nandi, M., et al., *Genetic and Pharmacological Inhibition of Dimethylarginine Dimethylaminohydrolase 1 Is Protective in Endotoxic Shock.* Arteriosclerosis, Thrombosis, and Vascular Biology, 2012. **32**(11): p. 2589-2597.

213. Zhen Wang, S.L., Valerie Taylor, Elizabeth Sujkovic, Manasi Nandi, James Tomlinson, Alex Dyson, Neil McDonald, Stephen Caddick, Mervyn Singer and James Leiper, *Pharmacological inhibition of DDAH1 improves survival, hemodynamics and organ function in experimental septic shock.* Biochemical Journal, 2014. **460**: p. 309-316.

214. Raschke, W.C., et al., *Functional macrophage cell lines transformed by abelson leukemia virus.* Cell, 1978. **15**(1): p. 261-267.

215. Hartley, J., et al., *Expression of infectious murine leukemia viruses by RAW264.7 cells, a potential complication for studies with a widely used mouse macrophage cell line.* Retrovirology, 2008. **5**(1): p. 1.

216. Denlinger, L.C., et al., *Regulation of Inducible Nitric Oxide Synthase Expression by Macrophage Purinoreceptors and Calcium.* Journal of Biological Chemistry, 1996. **271**(1): p. 337-342.

217. Taylor, M.F., et al., *In Vitro Efficacy of Morpholino-modified Antisense Oligomers Directed against Tumor Necrosis Factor-Î± mRNA.* Journal of Biological Chemistry, 1996. **271**(29): p. 17445-17452.

218. Hambleton, J., et al., *Activation of c-Jun N-terminal kinase in bacterial lipopolysaccharide-stimulated macrophages.* Proceedings of the National Academy of Sciences, 1996. **93**(7): p. 2774-2778.

219. Bradford, M.M., *A rapid and sensitive method for the quantitation of microgram quantities of protein utilizing the principle of protein-dye binding.* Analytical Biochemistry, 1976. **72**(1): p. 248-254.

220. Peng, Y.-L., et al., *Inducible nitric oxide synthase is involved in the modulation of depressive behaviors induced by unpredictable chronic mild stress.* Journal of Neuroinflammation, 2012. **9**: p. 75-75.

221. Yip, K.H., et al., *Induction of nitric oxide synthases in primary human cultured mast cells by IgE and proinflammatory cytokines.* International Immunopharmacology, 2008. **8**(5): p. 764-768.

222. Wojciak-Stothard, B., et al., *The ADMA/DDAH pathway is a critical regulator of endothelial cell motility.* Journal of Cell Science, 2007. **120**(6): p. 929-942.

223. Wang, Z., et al., *A novel DDAH-1 inhibitor improved cardiovascular function in a short-term anesthetized rat model of sepsis.* Critical Care, 2011. **15**(Suppl 3): p. P30.

224. Ho C, L.H., Chan M, Cheung R et al, *Electrospray ionisation mass spectrometry: Prinicples and clinical applications.* Clinical Biochemistry reviews, 2003. **24**(1): p. 3-12.

225. Pitt, J., *Principles and Applications of Liquid Chromatography-*

Mass Spectrometry in Clinical Biochemistry. Clinical Biochemistry reviews, 2009. **30**(1): p. 19-34.

226. Achan, V., et al., *all-trans-Retinoic Acid Increases Nitric Oxide Synthesis by Endothelial Cells: A Role for the Induction of Dimethylarginine Dimethylaminohydrolase.* Circulation Research, 2002. **90**(7): p. 764-769.

227. Verdon, C.P., B.A. Burton, and R.L. Prior, *Sample Pretreatment with Nitrate Reductase and Glucose-6-Phosphate Dehydrogenase Quantitatively Reduces Nitrate While Avoiding Interference by NADP+ When the Griess Reaction Is Used to Assay for Nitrite.* Analytical Biochemistry, 1995. **224**(2): p. 502-508.

228. Ding, A.H., C.F. Nathan, and D.J. Stuehr, *Release of reactive nitrogen intermediates and reactive oxygen intermediates from mouse peritoneal macrophages. Comparison of activating cytokines and evidence for independent production.* The Journal of Immunology, 1988. **141**(7): p. 2407-12.

229. Green, L.C., et al., *Analysis of nitrate, nitrite, and [15N]nitrate in biological fluids.* Analytical Biochemistry, 1982. **126**(1): p. 131-138.

230. Mehta, K., P. Claringbold, and G. Lopez-Berestein, *Suppression of macrophage cytostatic activation by serum retinoids: a possible role for transglutaminase.* The Journal of Immunology, 1987. **138**(11): p. 3902-6.

231. Aggarwal, B.B., K. Mehta, and P. Lester, *[15] Determination and regulation of nitric oxide production from macrophages by lipopolysaccharides, cytokines, and retinoids*, in *Methods in Enzymology*. 1996, Academic Press. p. 166-171.

232. Bryan, N.S. and M.B. Grisham, *Methods to detect nitric oxide and its metabolites in biological samples.* Free Radical Biology and Medicine, 2007. **43**(5): p. 645-657.

233. Zambrowicz, B.P., et al., *Disruption and sequence identification of 2,000 genes in mouse embryonic stem cells.* Nature, 1998. **392**(6676): p. 608-611.

234. Clausen, B.E., et al., *Conditional gene targeting in macrophages and granulocytes using LysMcre mice.* Transgenic Research, 1999. **8**(4): p. 265-277.

235. Kaindl, A.M., et al., *Activation of microglial N-methyl-D-aspartate receptors triggers inflammation and neuronal cell death in the developing and mature brain.* Annals of Neurology, 2012. **72**(4): p. 536-549.

236. Ebong, S., et al., *Immunopathologic Alterations in Murine Models of Sepsis of Increasing Severity.* Infection and Immunity, 1999. **67**(12): p. 6603-6610.

237. Rittirsch, D., et al., *Immunodesign of experimental sepsis by cecal ligation and puncture.* Nat. Protocols, 2008. **4**(1): p. 31-36.

238. Rosner, B., *Fundamentals of Biostatistics*. 2010, Canada: Brooks/Cole.

239. Cunningham, C., et al., *The sickness behaviour and CNS inflammatory mediator profile induced by systemic challenge of mice with synthetic double-stranded RNA (poly I:C).* Brain, Behavior, and Immunity, 2007. **21**(4): p. 490-502.

240. Eeftinck Schattenkerk, D.W., et al., *Nexfin Noninvasive Continuous Blood Pressure Validated Against Riva-Rocci/Korotkoff.* American Journal of Hypertension, 2009. **22**(4): p. 378-383.

241. Broch, O., et al., *A comparison of the Nexfin® and transcardiopulmonary thermodilution to estimate cardiac output during coronary artery surgery.* Anaesthesia, 2012. **67**(4): p. 377-383.

242. Chen, G., et al., *Comparison of noninvasive cardiac output measurements using the Nexfin monitoring device and the esophageal Doppler.* Journal of Clinical Anesthesia, 2012. **24**(4): p. 275-283.

243. *Lake Louise consensus on definition and quantification of altitude illness*, in *Hypoxia: Mountain Medicine.*, C.G. Sutton JR, Houston CS, Editor. 1992, Queen City Press: Burlington, Vermont.

244. Savourey, G., et al., *Evaluation of the Lake Louise acute mountain sickness scoring system in a hypobaric chamber.* Aviation, space, and environmental medicine, 1995.

245. Maggiorini, M., et al., *Assessment of acute mountain sickness by different score protocols in the Swiss Alps.* Aviation, space, and environmental medicine, 1998. **69**(12): p. 1186-1192.

246. McCarthy, M.I., et al., *Genome-wide association studies for complex traits: consensus, uncertainty and challenges.* Nat Rev Genet, 2008. **9**(5): p. 356-369.

247. Bodmer, W. and C. Bonilla, *Common and rare variants in multifactorial susceptibility to common diseases.* Nat Genet, 2008. **40**(6): p. 695-701.

248. Rautanen, A., et al., *Genome-wide association study of survival from sepsis due to pneumonia: an observational cohort study.* The Lancet Respiratory Medicine, 2015. **3**(1): p. 53-60.

249. Dhainaut, J.-F., et al., *Drotrecogin alfa (activated) in the treatment of severe sepsis patients with multiple-organ dysfunction: data from the PROWESS trial.* Intensive Care Medicine, 2003. **29**(6): p. 894-903.

250. Gordon, A.C., et al., *Protocol for a randomised controlled trial of VAsopressin versus Noradrenaline as Initial therapy in Septic sHock (VANISH).* BMJ Open, 2014. **4**(7).

251. Vincent, J.L., et al., *The SOFA (Sepsis-related Organ Failure Assessment) score to describe organ dysfunction/failure. On behalf of the Working Group on Sepsis-Related Problems of the European Society of Intensive Care Medicine.* Intensive Care Med, 1996. **22**(7): p. 707-10.

252. Ferreira, F., et al., *SErial evaluation of the sofa score to predict outcome in critically ill patients.* JAMA, 2001. **286**(14): p. 1754-1758.

253. Nizet, V. and R.S. Johnson, *Interdependence of hypoxic and innate immune responses.* Nat Rev Immunol, 2009. **9**(9): p. 609-617.

254. Vogelberg, K.H. and M. König, *Hypoxia of diabetic feet with abnormal arterial blood flow.* The clinical investigator, 1993. **71**(6): p. 466-470.

255. Arnold, F., D. West, and S. Kumar, *Wound healing: the effect of macrophage and tumour derived angiogenesis factors on skin graft vascularization.* Br J Exp Pathol, 1987. **68**(4): p. 569-74.

256. Negus, R.P., et al., *Quantitative assessment of the leukocyte infiltrate in ovarian cancer and its relationship to the expression of C-C chemokines.* Am J Pathol, 1997. **150**(5): p. 1723-34.

257. Semenza, G.L. and G.L. Wang, *A nuclear factor induced by hypoxia via de novo protein synthesis binds to the human erythropoietin gene enhancer at a site required for transcriptional activation.* Mol Cell Biol, 1992. **12**(12): p. 5447-54.

258. Wang, G.L., et al., *Hypoxia-inducible factor 1 is a basic-helix-loop-helix-PAS heterodimer regulated by cellular O2 tension.* Proc Natl Acad Sci U S A, 1995. **92**(12): p. 5510-4.

259. Weidemann, A. and R.S. Johnson, *Biology of HIF-1alpha.* Cell Death Differ, 2008. **15**(4): p. 621-7.

260. Fukuda, R., et al., *HIF-1 regulates cytochrome oxidase subunits to optimize efficiency of respiration in hypoxic cells.* Cell, 2007. **129**(1): p. 111-22.

261. Semenza, G.L., et al., *Transcriptional regulation of genes encoding glycolytic enzymes by hypoxia-inducible factor 1.* J Biol Chem, 1994. **269**(38): p. 23757-63.

262. Shimoda, L.A., et al., *HIF-1 regulates hypoxic induction of NHE1 expression and alkalinization of intracellular pH in pulmonary arterial myocytes.* American Journal of Physiology - Lung Cellular and Molecular Physiology, 2006. **291**(5): p. L941-L949.

263. Jaakkola, P., et al., *Targeting of HIF-alpha to the von Hippel-Lindau ubiquitylation complex by O2-regulated prolyl hydroxylation.* Science, 2001. **292**(5516): p. 468-72.

264. Lando, D., et al., *FIH-1 is an asparaginyl hydroxylase enzyme that regulates the transcriptional activity of hypoxia-inducible factor.* Genes Dev, 2002. **16**(12): p. 1466-71.

265. Cramer, T., et al., *HIF-1alpha is essential for myeloid cell-mediated inflammation.* Cell, 2003. **112**(5): p. 645-57.

266. Peyssonnaux, C., et al., *HIF-1alpha expression regulates the bactericidal capacity of phagocytes.* J Clin Invest, 2005. **115**(7): p. 1806-15.

267. Jantsch, J., et al., *Hypoxia and hypoxia-inducible factor-1 alpha modulate lipopolysaccharide-induced dendritic cell activation and function.* J Immunol, 2008. **180**(7): p. 4697-705.

268. Peyssonnaux, C., et al., *Cutting edge: Essential role of hypoxia inducible factor-1alpha in development of lipopolysaccharide-induced sepsis.* J Immunol, 2007. **178**(12): p. 7516-9.

269. Walmsley, S.R., et al., *Hypoxia-induced neutrophil survival is mediated by HIF-1alpha-dependent NF-kappaB activity.* J Exp Med, 2005. **201**(1): p. 105-15.

270. Strieter, R.M., *Mastering innate immunity.* Nat Med, 2003. **9**(5): p. 512-513.

271. Fang, H.Y., et al., *Hypoxia-inducible factors 1 and 2 are important transcriptional effectors in primary macrophages experiencing hypoxia.* Blood, 2009. **114**(4): p. 844-59.

272. Murdoch, C., M. Muthana, and C.E. Lewis, *Hypoxia Regulates Macrophage Functions in Inflammation.* The Journal of Immunology, 2005. **175**(10): p. 6257-6263.

273. Knowles, R.G. and S. Moncada, *Nitric oxide synthases in mammals.* Biochem J, 1994. **298 (Pt 2)**: p. 249-58.

274. Daniliuc, S., et al., *Hypoxia Inactivates Inducible Nitric Oxide Synthase in Mouse Macrophages by Disrupting Its Interaction with α-Actinin 4.* The Journal of Immunology, 2003. **171**(6): p. 3225-3232.

275. Mi, Z., et al., *Synergystic induction of HIF-1alpha transcriptional activity by hypoxia and lipopolysaccharide in macrophages.* Cell Cycle, 2008. **7**(2): p. 232-41.

276. Melillo, G., et al., *Regulation of inducible nitric oxide synthase expression in IFN-gamma-treated murine macrophages cultured under hypoxic conditions.* The Journal of Immunology, 1996. **157**(6): p. 2638-44.

277. Grocott, M.P., et al., *Arterial blood gases and oxygen content in climbers on Mount Everest.* N Engl J Med, 2009. **360**(2): p. 140-9.

278. Levett, D.Z., et al., *Design and conduct of Caudwell Xtreme Everest: an observational cohort study of variation in human adaptation to progressive environmental hypoxia.* BMC Med Res Methodol, 2010. **10**: p. 98.

279. Bailey, D.M. and B. Davies, *Physiological implications of altitude training for endurance performance at sea level: a review.* British Journal of Sports Medicine, 1997. **31**(3): p. 183-190.

280. Martin, D.S., et al., *Changes in sublingual microcirculatory flow index and vessel density on ascent to altitude.* Exp Physiol, 2010. **95**(8): p. 880-91.

281. Martin, D.S., et al., *Reduced coagulation at high altitude identified by thromboelastography.* Thromb Haemost, 2012. **107**(6): p. 1066-71.

282. Levett, D.Z., et al., *Acclimatization of skeletal muscle mitochondria to high-altitude hypoxia during an ascent of Everest.* FASEB J, 2012. **26**(4): p. 1431-41.

283. Coppel, J., et al., *The physiological effects of hypobaric hypoxia versus normobaric hypoxia: a systematic review of crossover trials.* Extrem Physiol Med, 2015. **4**: p. 2.

284. Dufour, S.P., et al., *Exercise training in normobaric hypoxia in endurance runners. I. Improvement in aerobic performance capacity.* Journal of Applied Physiology, 2006. **100**(4): p. 1238-1248.

285. Wiesner, S., et al., *Influences of normobaric hypoxia training on physical fitness and metabolic risk markers in overweight to obese subjects.* Obesity (Silver Spring), 2010. **18**(1): p. 116-20.

286. Miyagawa, K., et al., *Reduced hyperthermia-induced cutaneous vasodilation and enhanced exercise-induced plasma water loss at simulated high altitude (3,200 m) in humans.* J Appl Physiol (1985), 2011. **110**(1): p. 157-65.

287. Roach, R.C., J.A. Loeppky, and M.V. Icenogle, *Acute mountain sickness: increased severity during simulated altitude compared with normobaric hypoxia.* J Appl Physiol (1985), 1996. **81**(5): p. 1908-10.

288. Savourey, G., et al., *Normo- and hypobaric hypoxia: are there any physiological differences?* Eur J Appl Physiol, 2003. **89**(2): p. 122-6.

289. Savourey, G., et al., *Normo or hypobaric hypoxic tests: propositions for the determination of the individual susceptibility to altitude illnesses.* Eur J Appl Physiol, 2007. **100**(2): p. 193-205.

290. Tucker, A., et al., *Cardiopulmonary response to acute altitude exposure: water loading and denitrogenation.* Respir Physiol, 1983. **54**(3): p. 363-80.

291. Phelan, M.W. and D.V. Faller, *Hypoxia decreases constitutive nitric oxide synthase transcript and protein in cultured endothelial cells.* Journal of cellular physiology, 1996. **167**(3): p. 469-476.

292. Jung, F., et al., *Hypoxic Regulation of Inducible Nitric Oxide Synthase via Hypoxia Inducible Factor-1 in Cardiac Myocytes.* Circulation Research, 2000. **86**(3): p. 319-325.

293. Di Gangi, I.M., et al., *Online trapping and enrichment ultra performance liquid chromatography-tandem mass spectrometry method for sensitive measurement of "arginine-asymmetric dimethylarginine cycle" biomarkers in human exhaled breath condensate.* Anal Chim Acta, 2012. **754**: p. 67-74.

294. Scott, J.A., et al., *Asymmetric dimethylarginine is increased in asthma.* Am J Respir Crit Care Med, 2011. **184**(7): p. 779-85.

295. Pekarova, M., et al., *Asymmetric dimethyl arginine induces pulmonary vascular dysfunction via activation of signal transducer and activator of transcription 3 and stabilization of hypoxia-inducible factor 1-alpha.* Vascul Pharmacol, 2015. **73**: p. 138-48.

296. Tannheimer, M., et al., *Decrease of asymmetric dimethylarginine predicts acute mountain sickness.* J Travel Med, 2012. **19**(6): p. 338-43.

297. Mizuno, S., et al., *Endogenous Asymmetric Dimethylarginine Pathway in High Altitude Adapted Yaks.* Biomed Res Int, 2015. **2015**: p. 196904.

298. Arrigoni, F.I., et al., *Metabolism of asymmetric dimethylarginines is regulated in the lung developmentally and with pulmonary hypertension induced by hypobaric hypoxia.* Circulation, 2003. **107**(8): p. 1195-201.

299. Millatt, L.J., et al., *Evidence for dysregulation of dimethylarginine dimethylaminohydrolase I in chronic hypoxia-induced pulmonary hypertension.* Circulation, 2003. **108**(12): p. 1493-8.

300. O'Dwyer, M.J., et al., *Septic shock is correlated with asymmetrical dimethyl arginine levels, which may be influenced by a polymorphism in the dimethylarginine dimethylaminohydrolase II gene: a prospective observational study.* Crit Care, 2006. **10**(5): p. R139.

301. Nagai, H., et al., *Pulmonary Macrophages Attenuate Hypoxic Pulmonary Vasoconstriction via β(3)AR/iNOS Pathway in Rats Exposed to Chronic Intermittent Hypoxia.* PLoS ONE, 2015. **10**(7): p. e0131923.

302. Ho, J.J.D., H.S.J. Man, and P. Marsden, *Nitric oxide signaling in hypoxia.* Journal of Molecular Medicine, 2012. **90**(3): p. 217-231.

303. Jung, J.-Y., et al., *The Intracellular Environment of Human Macrophages That Produce Nitric Oxide Promotes Growth of Mycobacteria.* Infection and Immunity, 2013. **81**(9): p. 3198-3209.

304. Kimura, H., et al., *Identification of Hypoxia-inducible Factor 1 Ancillary Sequence and Its Function in Vascular Endothelial Growth Factor Gene Induction by Hypoxia and Nitric Oxide.* Journal of Biological Chemistry, 2001. **276**(3): p. 2292-2298.

305. Goto, H., et al., *Up-regulation of iNOS mRNA expression and increased production of NO in human monoblast cell line, U937 transfected by HTLV-1 tax gene.* Immunobiology, 1997. **197**(5): p. 513-521.

306. Cox, G.W., et al., *Heterogeneity of Hematopoietic Cells Immortalized by v-myc/v-raf Recombinant Retrovirus Infection of Bone Marrow or Fetal Liver.* Journal of the National Cancer Institute, 1989. **81**(19): p. 1492-1496.

307. Miyamoto, A., et al., *Establishment and characterization of an immortal macrophage-like cell line inducible to differentiate to osteoclasts.* Biochem Biophys Res Commun, 1998. **242**(3): p. 703-9.

308. Yang, C.-S., et al., *TLR3-Triggered Reactive Oxygen Species Contribute to Inflammatory Responses by Activating Signal Transducer and Activator of Transcription-1.* The Journal of Immunology, 2013.

309. Crnic, L.S. and M.A. Segall, *Behavioral effects of mouse interferons-alpha and -gamma and human interferon-alpha in mice.* Brain Res, 1992. **590**(1-2): p. 277-84.

310. Sen, G.C. and S.N. Sarkar, *Transcriptional signaling by double-stranded RNA: role of TLR3.* Cytokine & Growth Factor Reviews, 2005. **16**(1): p. 1-14.

311. Ichinohe, T., et al., *Intranasal immunization with H5N1 vaccine plus Poly I:Poly C12U, a Toll-like receptor agonist, protects mice against homologous and heterologous virus challenge.* Microbes and Infection, 2007. **9**(11): p. 1333-1340.

312. Suhadolnik, R.J., et al., *Changes in the 2-5A synthetase/RNase L antiviral pathway in a controlled clinical trial with poly(I)-poly(C12U) in chronic fatigue syndrome.* In Vivo, 1994. **8**(4): p. 599-604.

313. Thompson, J.E., et al., *Photochemical preparation of a pyridone containing tetracycle: A jak protein kinase inhibitor.* Bioorganic & Medicinal Chemistry Letters, 2002. **12**(8): p. 1219-1223.

314. Obrig, T.G., et al., *The Mechanism by which Cycloheximide and Related Glutarimide Antibiotics Inhibit Peptide Synthesis on Reticulocyte Ribosomes.* Journal of Biological Chemistry, 1971. **246**(1): p. 174-181.

315. Cartharius K, F.K., Grote K, Klocke B, Haltmeier M, Klingenhoff A, Frisch M, Bayerlein M, Werner T, *MatInspector and beyond: promoter analysis based on transcription factor binding sites* Bioinformatics, 2005. **21**: p. 2933-42.

316. Lange, M., et al., *Time course of nitric oxide synthases, nitrosative stress, and poly(ADP ribosylation) in an ovine sepsis model.* Crit Care, 2010. **14**(4): p. R129.

317. Ziegler, E.J., et al., *Treatment of Gram-Negative Bacteremia and Septic Shock with HA-1A Human Monoclonal Antibody against Endotoxin.* New England Journal of Medicine, 1991. **324**(7): p. 429-436.

318. Fang, F.C. and A. Vazquez-Torres, *Nitric oxide production by human macrophages: there's NO doubt about it.* American Journal of Physiology - Lung Cellular and Molecular Physiology, 2002. **282**(5): p. L941-L943.

319. Dorman, S.E., et al., *Viral infections in interferon-gamma receptor deficiency.* J Pediatr, 1999. **135**(5): p. 640-3.

320. Lee, J.Y., et al., *Interferon-gamma polymorphisms in systemic lupus erythematosus.* Genes Immun, 2001. **2**(5): p. 254-7.

321. Panitch, H.S., et al., *Exacerbations of multiple sclerosis in patients treated with gamma interferon.* Lancet, 1987. **1**(8538): p. 893-5.

322. Sarvetnick, N., et al., *Insulin-dependent diabetes mellitus induced in transgenic mice by ectopic expression of class II MHC and interferon-gamma.* Cell, 1988. **52**(5): p. 773-82.

323. Isaacs, A. and J. Lindenmann, *Virus interference. I. The interferon.* Proc R Soc Lond B Biol Sci, 1957. **147**(927): p. 258-67.

324. Schroder, K., et al., *Interferon-γ: an overview of signals, mechanisms and functions.* Journal of Leukocyte Biology, 2004. **75**(2): p. 163-189.

325. Paludan, S.R., *Interleukin-4 and interferon-gamma: the quintessence of a mutual antagonistic relationship.* Scand J Immunol, 1998. **48**(5): p. 459-68.

326. Golab, J., et al., *Direct stimulation of macrophages by IL-12 and IL-18--a bridge too far?* Immunol Lett, 2000. **72**(3): p. 153-7.

327. Greenlund, A.C., et al., *Stat recruitment by tyrosine-phosphorylated cytokine receptors: an ordered reversible affinity-driven process.* Immunity, 1995. **2**(6): p. 677-87.

328. Schindler, C. and J.E. Darnell, Jr., *Transcriptional responses to polypeptide ligands: the JAK-STAT pathway.* Annu Rev Biochem, 1995. **64**: p. 621-51.

329. MacMicking, J., Q.W. Xie, and C. Nathan, *Nitric oxide and macrophage function.* Annu Rev Immunol, 1997. **15**: p. 323-50.

330. Xaus, J., et al., *Interferon gamma induces the expression of p21waf-1 and arrests macrophage cell cycle, preventing induction of apoptosis.* Immunity, 1999. **11**(1): p. 103-13.

331. Decker, T., et al., *IFNs and STATs in innate immunity to microorganisms.* J Clin Invest, 2002. **109**(10): p. 1271-7.

332. Mouktaroudi, M., et al., *Interferon-gamma reverses sepsis-induced immunoparalysis of monocytes in vitro.* Critical Care, 2010. **14**(Suppl 1): p. P17-P17.

333. Fink, M.P., *Animal models of sepsis.* Virulence, 2014. **5**(1): p. 143-153.

334. Deitch, E.A., *Animal Models of Sepsis and Shock: A Review and Lessons Learned.* Shock, 1998. **9**(1): p. 1-11.

335. The Lancet Infectious, D., *For sepsis, the drugs don't work.* The Lancet Infectious Diseases, 2012. **12**(2): p. 89.

336. Weinberg, J., et al., *Human mononuclear phagocyte inducible nitric oxide synthase (iNOS): analysis of iNOS mRNA, iNOS protein, biopterin, and nitric oxide production by blood monocytes and peritoneal macrophages.* Blood, 1995. **86**(3): p. 1184-1195.

337. Munford, R.S., *Detoxifying endotoxin: time, place and person.* J Endotoxin Res, 2005. **11**(2): p. 69-84.

338. Kamisoglu, K., et al., *Human metabolic response to systemic inflammation: assessment of the concordance between experimental endotoxemia and clinical cases of sepsis/SIRS.* Critical Care, 2015. **19**(1): p. 71.

339. Wang, P.F., et al., *Polyinosinic-polycytidylic acid has therapeutic effects against cerebral ischemia/reperfusion injury through the downregulation of TLR4 signaling via TLR3.* J Immunol, 2014. **192**(10): p. 4783-94.

340. Zhou, C.X., et al., *Resiquimod and polyinosinic-polycytidylic acid formulation with aluminum hydroxide as an adjuvant for foot-and-mouth disease vaccine.* BMC Vet Res, 2014. **10**: p. 2.

341. Ammi, R., et al., *Poly(I:C) as cancer vaccine adjuvant: Knocking on the door of medical breakthroughs.* Pharmacology & Therapeutics, 2015. **146**: p. 120-131.

342. Volman, T.J., T. Hendriks, and R.J. Goris, *Zymosan-induced generalized inflammation: experimental studies into mechanisms leading to multiple organ dysfunction syndrome.* Shock, 2005. **23**(4): p. 291-7.

343. Goris, R.J., et al., *Multiple-organ failure and sepsis without bacteria. An experimental model.* Arch Surg, 1986. **121**(8): p. 897-901.

344. Minnaard, R., et al., *Ubiquitin-proteasome-dependent proteolytic activity remains elevated after zymosan-induced sepsis in rats while muscle mass recovers.* Int J Biochem Cell Biol, 2005. **37**(10): p. 2217-25.

345. Hill, N.E., et al., *Detailed Characterization of a Long-Term Rodent Model of Critical Illness and Recovery.* Critical Care Medicine, 2015. **43**(3): p. e84-e96.

346. Wichterman, K.A., A.E. Baue, and I.H. Chaudry, *Sepsis and septic shock--a review of laboratory models and a proposal.* J Surg Res, 1980. **29**(2): p. 189-201.

347. Harvill, E.T., et al., *Multiple Roles for BordetellaLipopolysaccharide Molecules during Respiratory Tract Infection.* Infection and Immunity, 2000. **68**(12): p. 6720-6728.

348. Boucher, J.C., et al., *Mucoid Pseudomonas aeruginosa in cystic fibrosis: characterization of muc mutations in clinical isolates and analysis of clearance in a mouse model of respiratory infection.* Infection and Immunity, 1997. **65**(9): p. 3838-46.

349. Traeger, T., et al., *Colon ascendens stent peritonitis (CASP)--a standardized model for polymicrobial abdominal sepsis.* J Vis Exp, 2010(46).

350. Natanson, C., et al., *Gram-negative bacteremia produces both severe systolic and diastolic cardiac dysfunction in a canine model that simulates human septic shock.* J Clin Invest, 1986. **78**(1): p. 259-70.

351. Cross, A.S., et al., *Choice of bacteria in animal models of sepsis.* Infect Immun, 1993. **61**(7): p. 2741-7.

352. Feng, M., et al., *Genetic analysis of blood pressure in 8 mouse intercross populations.* Hypertension, 2009. **54**(4): p. 802-9.

353. Doevendans, P.A., et al., *Cardiovascular phenotyping in mice.* Cardiovasc Res, 1998. **39**(1): p. 34-49.

354. Hart, C.Y., J.C. Burnett, Jr., and M.M. Redfield, *Effects of avertin versus xylazine-ketamine anesthesia on cardiac function in normal mice.* Am J Physiol Heart Circ Physiol, 2001. **281**(5): p. H1938-45.

355. Lorenz, J.N., *A practical guide to evaluating cardiovascular, renal, and pulmonary function in mice.* Am J Physiol Regul Integr Comp Physiol, 2002. **282**(6): p. R1565-82.

356. Mattson, D.L., *Long-term measurement of arterial blood pressure in conscious mice.* Am J Physiol, 1998. **274**(2 Pt 2): p. R564-70.

357. Zhao, X., et al., *Arterial Pressure Monitoring in Mice.* Current protocols in mouse biology, 2011. **1**: p. 105-122.

358. Huet, O., et al., *Ensuring animal welfare while meeting scientific aims using a murine pneumonia model of septic shock.* Shock, 2013. **39**(6): p. 488-94.

359. Shrum, B., et al., *A robust scoring system to evaluate sepsis severity in an animal model.* BMC Research Notes, 2014. **7**(1): p. 233.

360. Davis, G.S., et al., *Intermingled Klebsiella pneumoniae Populations Between Retail Meats and Human Urinary Tract Infections.* Clinical Infectious Diseases, 2015.

361. Johnson, J.R., et al., *Virulence of Escherichia coli Clinical Isolates in a Murine Sepsis Model in Relation to Sequence Type ST131 Status, Fluoroquinolone Resistance, and Virulence Genotype.* Infection and Immunity, 2012. **80**(4): p. 1554-1562.

362. Brealey, D., et al., *Mitochondrial dysfunction in a long-term rodent model of sepsis and organ failure.* Am J Physiol Regul Integr Comp Physiol, 2004. **286**(3): p. R491-7.

363. Vlach, K.D., J.W. Boles, and B.G. Stiles, *Telemetric Evaluation of Body Temperature and Physical Activity as Predictors of Mortality in a Murine Model of Staphylococcal Enterotoxic Shock.* Comparative Medicine, 2000. **50**(2): p. 160-166.

364. Soothill, J.S., D.B. Morton, and A. Ahmad, *The HID50 (hypothermia-inducing dose 50): an alternative to the LD50 for measurement of bacterial virulence.* Int J Exp Pathol, 1992. **73**(1): p. 95-8.

365. Torondel, B., et al., *Adenoviral-mediated overexpression of DDAH improves vascular tone regulation.* Vasc Med, 2010. **15**(3): p. 205-13.

366. Schmidt, E.E., et al., *Illegitimate Cre-dependent chromosome rearrangements in transgenic mouse spermatids.* Proceedings of the National Academy of Sciences, 2000. **97**(25): p. 13702-13707.

367. Loonstra, A., et al., *Growth inhibition and DNA damage induced by Cre recombinase in mammalian cells.* Proceedings of the National Academy of Sciences, 2001. **98**(16): p. 9209-9214.

368. Zellweger, R., et al., *Females in proestrus state maintain splenic immune functions and tolerate sepsis better than males.* Crit Care Med, 1997. **25**(1): p. 106-10.

369. Wang, H.E., et al., *National estimates of severe sepsis in United States emergency departments.* Critical care medicine, 2007. **35**(8): p. 1928-1936.

370. Melamed, A. and F.J. Sorvillo, *The burden of sepsis-associated mortality in the United States from 1999 to 2005: an analysis of multiple-cause-of-death data.* Critical Care, 2009. **13**(1): p. R28.

371. Dombrovskiy, V.Y., et al., *Rapid increase in hospitalization and mortality rates for severe sepsis in the United States: A trend analysis from 1993 to 2003*.* Critical care medicine, 2007. **35**(5): p. 1244-1250.

372. Dombrovskiy, V.Y., et al., *Facing the challenge: Decreasing case fatality rates in severe sepsis despite increasing hospitalizations*.* Critical care medicine, 2005. **33**(11): p. 2555-2562.

373. Angus, D.C., et al., *Epidemiology of severe sepsis in the United States: analysis of incidence, outcome, and associated costs of care.* Critical care medicine, 2001. **29**(7): p. 1303-1310.

374. Lagu, T., et al., *What is the best method for estimating the burden of severe sepsis in the United States?* Journal of Critical Care, 2012. **27**(4): p. 414.e1-414.e9.

375. Maas, R., et al., *Polymorphisms in the promoter region of the dimethylarginine dimethylaminohydrolase 2 gene are associated with prevalence of hypertension.* Pharmacological Research, 2009. **60**(6): p. 488-493.

376. Rector, T.S., et al., *Randomized, Double-Blind, Placebo-Controlled Study of Supplemental Oral l-Arginine in Patients With Heart Failure.* Circulation, 1996. **93**(12): p. 2135-2141.

377. Davis, J.S. and N.M. Anstey, *Is plasma arginine concentration decreased in patients with sepsis? A systematic review and meta-analysis*.* Critical Care Medicine, 2011. **39**(2): p. 380-385.

378. Hu, T., et al., *Farnesoid X Receptor Agonist Reduces Serum Asymmetric Dimethylarginine Levels through Hepatic Dimethylarginine Dimethylaminohydrolase-1 Gene Regulation.* Journal of Biological Chemistry, 2006. **281**(52): p. 39831-39838.

379. Neilly, I.J., et al., *Plasma nitrate concentrations in neutropenic and non-neutropenic patients with suspected septicaemia.* British Journal of Haematology, 1995. **89**(1): p. 199-202.

380. Stewart, T.E., et al., *Evaluation of a Ventilation Strategy to Prevent Barotrauma in Patients at High Risk for Acute Respiratory Distress Syndrome.* New England Journal of Medicine, 1998. **338**(6): p. 355-361.

381. Bion, J., et al., *'Matching Michigan': a 2-year stepped interventional programme to minimise central venous catheter-blood stream infections in intensive care units in England.* BMJ Qual Saf, 2013. **22**(2): p. 110-23.

382. Grover, R., et al., *An open-label dose escalation study of the nitric oxide synthase inhibitor, N(G)-methyl-L-arginine hydrochloride (546C88), in patients with septic shock. Glaxo Wellcome International Septic Shock Study Group.* Crit Care Med, 1999. **27**(5): p. 913-22.

383. Haynes, W.G., et al., *Inhibition of nitric oxide synthesis increases blood pressure in healthy humans.* Journal of Hypertension, 1993. **11**(12): p. 1375-1380.

384. Lopez, A., et al., *Multiple-center, randomized, placebo-controlled, double-blind study of the nitric oxide synthase inhibitor 546C88: effect on survival in patients with septic shock.* Crit Care Med, 2004. **32**(1): p. 21-30.

385. Angus, D.C., *The search for effective therapy for sepsis: Back to the drawing board?* JAMA, 2011. **306**(23): p. 2614-2615.

Appendix – SNPs interrogated in the GenOSept and GAinS analysis

A.DDAH1 SNPs interrogated in the GenOSept and GAinS analysis

SNP	CHR	BP	P	adjusted OR	maf cases	maf controls
rs233104	1	85775186	0.79663	0.95954698	0.090988	0.09389
rs35240561	1	85775217	0.51037	0.92796803	0.19034	0.20426
rs12047189	1	85775448	0.62643	1.06058856	0.17501	0.16185
rs12122154	1	85775865	0.79522	1.05726671	0.05216	0.049756
rs4949897	1	85776121	0.61489	1.06272036	0.17538	0.16179
rs11161595	1	85776360	0.63919	1.10862444	0.050102	0.045393
rs34642410	1	85776712	0.60207	1.13718965	0.038796	0.034037
rs34561661	1	85777250	0.46196	0.92010269	0.1914	0.20674
rs6669293	1	85777524	0.66058	0.95695874	0.27908	0.28301
rs72722663	1	85777534	0.62093	1.0615414	0.1751	0.16159
rs4949889	1	85778344	0.62406	1.06094073	0.17495	0.16149
rs79095356	1	85778440	0.61715	0.91100946	0.059631	0.065878
rs233105	1	85778531	0.17849	0.69105214	0.023174	0.033029
rs1874807	1	85779393	0.58234	1.05156444	0.47786	0.493
rs72722664	1	85779606	0.36632	1.2188405	0.055093	0.044129
rs11590830	1	85779863	0.60817	1.11899392	0.050432	0.045285
rs72722665	1	85780781	0.39693	1.13808839	0.10601	0.095618
rs12042780	1	85780903	0.75529	1.03807496	0.17472	0.16398
rs233108	1	85781720	0.71897	0.9669205	0.36752	0.37207
rs10489510	1	85782571	0.75802	1.03755917	0.17454	0.16377
rs233109	1	85783101	0.76541	0.97277156	0.38424	0.38738
rs12138621	1	85783970	0.39494	0.90900562	0.19313	0.2102
rs11161597	1	85784936	0.39711	0.90943386	0.19313	0.21016
rs233111	1	85785655	0.68217	0.95984641	0.28049	0.2799
rs233112	1	85785751	0.7627	0.97247005	0.38415	0.38734
rs3813600	1	85786166	0.31748	1.16581452	0.10616	0.093909
rs233113	1	85786299	0.71149	0.96606805	0.3673	0.37202
rs233114	1	85786957	0.71153	0.96607288	0.3673	0.37202
rs233115	1	85786977	0.71686	0.9667223	0.3673	0.37169
rs3087894	1	85787118	0.71778	0.96681511	0.36722	0.37132
rs1498375	1	85787323	0.71776	0.96681318	0.36722	0.37132
rs1498374	1	85787334	0.40683	0.91121264	0.19314	0.20969
rs233117	1	85787682	0.67742	0.92567877	0.074639	0.073609
rs233118	1	85787967	0.7628	0.97248172	0.38415	0.38734

rs233119	1	85788052	0.71146	0.96606515	0.3673	0.37202
rs233120	1	85788490	0.68837	0.96338997	0.36885	0.3746
rs2300633	1	85788826	0.65831	1.05457095	0.17407	0.16114
rs17590006	1	85789270	0.54277	0.93673205	0.2271	0.23303
rs12140272	1	85789757	0.38895	0.90795905	0.19315	0.21089
rs233121	1	85789913	0.71049	0.96594923	0.3673	0.37205
rs1498373	1	85790633	0.71369	0.96631733	0.36722	0.37166
rs72722671	1	85791003	0.047917	1.77652641	0.040444	0.028898
rs2300634	1	85791257	0.72038	0.96711197	0.36745	0.37171
rs233124	1	85791658	0.75895	0.97202476	0.38415	0.38769
rs233125	1	85792056	0.85147	0.94975616	0.027951	0.029141
rs2284797	1	85792383	0.46985	0.91766489	0.17969	0.19336
rs12122816	1	85792384	0.46985	0.91766489	0.17969	0.19336
rs2268667	1	85793746	0.72066	0.96714485	0.36686	0.37129
rs233127	1	85793801	0.68897	0.96332927	0.367	0.3726
rs233128	1	85794413	0.68981	0.96073468	0.28377	0.28453
rs72722672	1	85794568	0.85769	0.96667397	0.060037	0.062969
rs143314690	1	85794729	0.12964	0.65890231	0.020899	0.031354
rs18582	1	85794819	0.60694	0.95311663	0.36432	0.37301
rs233130	1	85795112	0.69274	0.96377347	0.36688	0.37239
rs233131	1	85795259	0.69274	0.96377347	0.36688	0.37239
rs731194	1	85795951	0.68585	1.04982029	0.17345	0.16121
rs11161599	1	85795965	0.4035	0.91068702	0.19335	0.21043
rs423105	1	85796427	0.69286	0.96378793	0.36688	0.37239
rs233132	1	85796545	0.69286	0.96378793	0.36688	0.37239
rs233133	1	85796557	0.74445	0.97029804	0.38373	0.38769
rs761601	1	85797298	0.69899	0.96452069	0.3668	0.37168
rs2389913	1	85798075	0.39656	0.87184816	0.093293	0.088915
rs12121675	1	85798484	0.69333	0.96370408	0.36444	0.36967
rs233055	1	85798486	0.6841	0.9628304	0.38213	0.38806
rs78193202	1	85798617	0.76526	1.06428584	0.052726	0.049576
rs233057	1	85798855	0.69299	0.96380431	0.36688	0.37239
rs233058	1	85798865	0.69299	0.96380431	0.36688	0.37239
rs233059	1	85798936	0.69299	0.96380431	0.36688	0.37239
rs233060	1	85798943	0.69299	0.96380431	0.36688	0.37239
rs233061	1	85799282	0.74454	0.97030774	0.38373	0.38769
rs72722676	1	85799538	0.85419	0.95063414	0.027919	0.029125
rs72722677	1	85800179	0.48274	1.11024421	0.11017	0.10174
rs233062	1	85800385	0.69303	0.96380913	0.36692	0.37244
rs3768227	1	85804087	0.69923	0.96455059	0.3668	0.37167
rs173026	1	85804249	0.69321	0.9638313	0.36689	0.37239
rs190804399	1	85804743	0.87085	0.97879701	0.14964	0.14768
rs74599242	1	85804747	0.9355	0.99180467	0.28377	0.28045
rs12035116	1	85804837	0.66517	1.05336837	0.17321	0.16066

rs233066	1	85804930	0.70215	0.96490947	0.36689	0.37167
rs233067	1	85804978	0.69255	0.96375227	0.36689	0.3724
rs233068	1	85805355	0.74415	0.97026214	0.38373	0.3877
rs233069	1	85805466	0.69266	0.9637648	0.36689	0.3724
rs233071	1	85806005	0.69274	0.9637754	0.36689	0.3724
rs233072	1	85807695	0.74386	0.97022915	0.38373	0.38771
rs12717763	1	85808164	0.37286	0.90531801	0.1936	0.21106
rs3768226	1	85808325	0.4923	0.92916309	0.22711	0.23435
rs233074	1	85809065	0.79044	0.97538892	0.36716	0.3688
rs233075	1	85809124	0.39921	0.87253719	0.09323	0.088917
rs3768224	1	85809173	0.55249	1.13866896	0.051201	0.045349
rs3768223	1	85809183	0.39152	0.90862755	0.1936	0.21089
rs12120551	1	85810903	0.39074	0.90847855	0.19357	0.21089
rs12124170	1	85811182	0.69741	0.96432684	0.36678	0.37171
rs4949898	1	85811652	0.66594	1.05323249	0.17321	0.16067
rs36166679	1	85812626	0.42354	1.19042454	0.049503	0.043243
rs140553832	1	85813467	0.27831	0.70992922	0.016622	0.024378
rs56373808	1	85813622	0.30324	0.85028814	0.080817	0.094059
rs233080	1	85814552	0.70501	0.96278322	0.28111	0.28112
rs2284798	1	85814578	0.69131	1.08631692	0.053799	0.049893
rs233081	1	85814973	0.41788	0.87734937	0.093374	0.08944
rs61769484	1	85815240	0.53747	0.93580608	0.22719	0.23342
rs2284800	1	85815610	0.36579	1.14508629	0.10823	0.097255
rs10158674	1	85816134	0.39894	0.9099533	0.19353	0.21054
rs2076699	1	85817295	0.36815	0.90378842	0.19214	0.20997
rs233087	1	85821000	0.19479	0.86046701	0.20171	0.18647
rs2300637	1	85822772	0.69631	0.96419666	0.36668	0.37159
rs233091	1	85823044	0.69055	0.9635104	0.36677	0.37229
rs233093	1	85823120	0.66369	0.96011712	0.36539	0.37157
rs2300639	1	85823676	0.3973	0.90962941	0.19346	0.21056
rs2300640	1	85823795	0.39664	0.90950844	0.19346	0.21058
rs2235990	1	85823902	0.69096	1.08640491	0.053878	0.04995
rs233095	1	85824816	0.69829	0.96443967	0.36675	0.37161
rs233097	1	85825473	0.74018	0.96979167	0.38358	0.38762
rs72954638	1	85826140	0.35285	0.8676039	0.088209	0.10177
rs233099	1	85826194	0.68946	0.96337455	0.36674	0.37231
rs2474123	1	85827452	0.83824	0.98174861	0.43677	0.43801
rs7520993	1	85828090	0.43232	1.12458041	0.11014	0.10031
rs36062892	1	85828626	0.70345	0.96227116	0.26872	0.27114
rs12130145	1	85828970	0.39339	0.90885928	0.1933	0.2106
rs233046	1	85829405	0.6488	0.9555454	0.28866	0.28809
rs111820059	1	85830429	0.79177	0.96497026	0.13064	0.12822
rs113752360	1	85830446	0.3206	0.85867051	0.087075	0.1011
rs233047	1	85830570	0.67488	0.96155838	0.36635	0.37252

rs4949890	1	85830632	0.7025	0.96485254	0.36555	0.37028
rs66811655	1	85831544	0.6688	0.96066166	0.36389	0.37001
rs12038426	1	85831790	0.68523	1.04986754	0.17324	0.16101
rs71652696	1	85831792	0.35434	0.89981148	0.18586	0.20498
rs72722689	1	85832808	0.92156	0.97328046	0.029229	0.029901
rs12136295	1	85833730	0.68949	1.08644294	0.054462	0.050372
rs75481609	1	85834202	0.33421	1.37847801	0.028053	0.020907
rs12758768	1	85835206	0.41877	0.91405549	0.19728	0.21527
rs72722690	1	85835362	0.26686	0.84088531	0.082471	0.09646
rs72722691	1	85835439	0.68929	1.04916961	0.17325	0.16108
rs79695640	1	85836073	0.43217	0.91638106	0.19793	0.21561
rs986639	1	85836392	0.54335	0.92379601	0.15478	0.16554
rs1498377	1	85836436	0.85987	0.98273576	0.31496	0.3127
rs4475804	1	85836466	0.86105	0.98217675	0.26661	0.26752
rs79594869	1	85836755	0.82688	1.0489	0.048334	0.045668
rs72722692	1	85837169	0.78701	0.96416774	0.1306	0.12827
rs233050	1	85837793	0.76624	0.97269958	0.37068	0.3758
rs4949899	1	85838237	0.63209	1.05915773	0.17364	0.16071
rs233051	1	85838413	0.75825	0.96983532	0.28659	0.28686
rs140056707	1	85838505	0.34603	1.36712501	0.027991	0.020983
rs233053	1	85839507	0.79985	0.9768824	0.38738	0.39196
rs233054	1	85840191	0.76207	0.97221044	0.37059	0.37587
rs1391556	1	85841056	0.63277	1.05903276	0.17365	0.16072
rs2012683	1	85841485	0.70843	0.96575896	0.37055	0.37744
rs12139958	1	85842112	0.37771	0.906648	0.19681	0.21603
rs76842501	1	85842370	0.752	1.06718143	0.052866	0.049822
rs10873700	1	85842824	0.83489	1.04428245	0.051459	0.049386
rs78200919	1	85843395	0.27332	1.16976164	0.15224	0.13676
rs75140285	1	85843762	0.68145	1.08627455	0.057575	0.053669
rs72722697	1	85843863	0.04095	1.99164315	0.029965	0.01963
rs2064510	1	85844330	0.63308	1.05897769	0.17366	0.16073
rs729655	1	85844617	0.8832	0.98668247	0.41755	0.42011
rs2011825	1	85844671	0.72025	0.96699012	0.36704	0.37385
rs4512701	1	85844835	0.633	1.05899146	0.17366	0.16073
rs4631749	1	85844852	0.633	1.05899146	0.17366	0.16073
rs997251	1	85845367	0.71344	0.96635695	0.37053	0.37678
rs35092233	1	85845821	0.89267	0.9865917	0.27443	0.27215
rs1884139	1	85845998	0.76481	0.97242337	0.37428	0.37901
rs12044537	1	85846385	0.73554	0.96927976	0.38686	0.3928
rs67611930	1	85846592	0.70576	0.96543935	0.37053	0.37749
rs11161604	1	85847260	0.49448	1.19298671	0.038688	0.032724
rs2207368	1	85847683	0.68594	0.96299024	0.36965	0.37706
rs7553530	1	85848566	0.81058	1.05064367	0.051796	0.049333
rs12568573	1	85848821	0.43374	1.12390587	0.10823	0.099037

rs12047422	1	85848830	0.71165	0.96614244	0.37052	0.37682
rs3920521	1	85848866	0.7794	0.97498226	0.42517	0.42964
rs79817777	1	85848923	0.82717	1.04595882	0.051799	0.050026
rs11588128	1	85848998	0.43369	1.12391711	0.10823	0.099037
rs72724604	1	85849182	0.82351	0.94030875	0.027771	0.029207
rs72724605	1	85849188	0.29502	0.84960818	0.083558	0.096749
rs12140103	1	85849489	0.77693	0.97388602	0.37025	0.37564
rs12140170	1	85849723	0.37493	0.90614404	0.19676	0.21608
rs72724606	1	85850246	0.70383	0.96520574	0.37051	0.37752
rs761602	1	85851308	0.43196	0.88155314	0.094787	0.090385
rs61769490	1	85851370	0.92327	0.99040186	0.27431	0.27107
rs72724608	1	85852755	0.46792	1.09081705	0.18251	0.16584
rs36110608	1	85852936	0.38194	0.90735274	0.19805	0.21704
rs12116463	1	85853705	0.74592	1.06887319	0.052938	0.049816
rs11161606	1	85853902	0.8121	0.97871088	0.42343	0.42758
rs10782548	1	85855098	0.77448	0.97182357	0.28564	0.28638
rs10489513	1	85855622	0.70063	0.96513432	0.38564	0.39284
rs12140935	1	85855716	0.36547	0.90439416	0.19666	0.21627
rs11161607	1	85855855	0.69096	0.9635104	0.36817	0.37524
rs72724610	1	85856396	0.041355	1.98780298	0.03	0.019669
rs1342323	1	85857574	0.61617	0.94148299	0.17379	0.16065
rs12022248	1	85857681	0.53934	0.93661122	0.25014	0.25176
rs77529889	1	85857838	0.69182	0.93262695	0.081635	0.08287
rs12033483	1	85858123	0.61983	1.06150637	0.17369	0.16064
rs6576761	1	85858274	0.72434	1.03249273	0.42157	0.42826
rs6671599	1	85858857	0.68161	1.0389764	0.37043	0.37794
rs35193119	1	85859265	0.34684	0.90080182	0.19665	0.21661
rs6659486	1	85859372	0.92155	0.99017815	0.2742	0.271
rs6576763	1	85859376	0.72837	1.03260527	0.3872	0.39327
rs7515261	1	85859804	0.62538	0.94302074	0.17378	0.16134
rs10747318	1	85859910	0.60881	0.94021002	0.17349	0.16085
rs12140457	1	85860170	0.33776	0.8982831	0.19439	0.21472
rs10873701	1	85860374	0.62538	0.94302074	0.17378	0.16134
rs35876501	1	85860624	0.92116	0.99012855	0.27419	0.271
rs35294786	1	85860743	0.92106	0.99011706	0.27419	0.271
rs34750524	1	85860778	0.58174	1.14034403	0.040784	0.036191
rs4949900	1	85861034	0.67875	1.0393505	0.37043	0.37796
rs4428939	1	85861564	0.62552	0.94303677	0.17376	0.16132
rs2177461	1	85861976	0.67756	1.03950434	0.37043	0.378
rs12564698	1	85862711	0.42076	1.12857977	0.1077	0.098301
rs11161609	1	85862736	0.99746	1.00029428	0.47653	0.47881
rs3949301	1	85863383	0.67511	1.03982975	0.37043	0.37804
rs61769518	1	85864246	0.34591	1.16959788	0.091277	0.086126
rs12034249	1	85864391	0.61283	1.06279794	0.17369	0.16049

rs12118950	1	85864519	0.34217	0.89989247	0.19665	0.21667
rs12402128	1	85864711	0.92093	0.99010023	0.27419	0.27102
rs11161610	1	85865896	0.40522	1.08194571	0.38948	0.40528
rs2892888	1	85866147	0.82677	1.02061154	0.36941	0.37311
rs6576764	1	85866411	0.67318	1.0400783	0.37043	0.37805
rs12125557	1	85867406	0.76253	1.02864561	0.38276	0.38649
rs6704103	1	85868657	0.67734	1.03958334	0.36987	0.37753
rs11161611	1	85868679	0.66771	1.04082847	0.37066	0.37845
rs111933205	1	85868702	0.59174	1.14141646	0.038248	0.03362
rs1357635	1	85868798	0.50789	0.92389209	0.17874	0.16415
rs1357636	1	85869042	0.61645	0.94152724	0.17377	0.16064
rs61769519	1	85870024	0.42553	1.13762186	0.093305	0.089139
rs12758237	1	85870783	0.33774	0.89902899	0.19665	0.21675
rs6576765	1	85871012	0.71806	1.03390718	0.3872	0.3934
rs2037594	1	85871618	0.58406	0.93864588	0.19055	0.17663
rs17387935	1	85871701	0.76147	0.9676537	0.22793	0.22824
rs12133722	1	85873237	0.33524	0.89853466	0.19663	0.21681
rs66924115	1	85873751	0.29217	0.84850441	0.08364	0.097064
rs12123722	1	85873950	0.78953	1.05645398	0.051927	0.049234
rs12564550	1	85874205	0.43903	1.12241207	0.10822	0.099116
rs6657732	1	85874495	0.91307	0.9901133	0.49542	0.4929
rs6657817	1	85874614	0.66611	1.04100855	0.37043	0.37817
rs80164976	1	85874960	0.78898	1.05660929	0.05193	0.049231
rs4949902	1	85875488	0.40877	1.14190737	0.094843	0.090237
rs6673833	1	85875622	0.94324	0.99279359	0.26871	0.26496
rs6576766	1	85876218	0.85886	1.01654843	0.39296	0.39472
rs6576767	1	85876316	0.70827	1.03553997	0.36915	0.37597
rs17127199	1	85876355	0.43869	1.12250186	0.10823	0.099113
rs1554597	1	85877098	0.64454	1.04390136	0.37043	0.37829
rs17127201	1	85877498	0.78763	1.05698763	0.051933	0.04922
rs12138852	1	85878208	0.32459	0.89638972	0.19646	0.21692
rs1001604	1	85879524	0.65701	1.04219806	0.38109	0.38952
rs12132677	1	85879613	0.32276	0.89600436	0.19639	0.21692
rs78773881	1	85880460	0.78586	1.0574803	0.051936	0.049205
rs7532508	1	85880468	0.73039	1.0350037	0.28525	0.28529
rs76032550	1	85880540	0.72486	1.07491222	0.053043	0.04969
rs10493764	1	85880663	0.92331	0.99039285	0.27411	0.2709
rs76711495	1	85880859	0.7243	1.07507347	0.053044	0.049686
rs7554669	1	85880933	0.82008	0.9737643	0.17593	0.18542
rs7546931	1	85880976	0.51644	0.93166125	0.22718	0.21105
rs17127231	1	85881185	0.72377	1.07522829	0.053044	0.04968
rs10782549	1	85881278	0.6092	0.9403821	0.17419	0.16138
rs12062903	1	85881594	0.26836	0.840776	0.082573	0.096495
rs56215900	1	85881759	0.43792	1.12273761	0.10825	0.099155

rs2016104	1	85882871	0.5943	0.93796185	0.17458	0.16144
rs1975755	1	85882905	0.5061	0.9300518	0.22755	0.21126
rs1006988	1	85883320	0.49063	0.92930712	0.24335	0.22589
rs1006989	1	85883456	0.52209	0.92839592	0.19174	0.17657
rs7539738	1	85884024	0.55217	0.9335031	0.19144	0.17676
rs7525786	1	85884076	0.88582	1.01305853	0.44233	0.44416
rs7547571	1	85884091	0.78201	1.02535511	0.42328	0.42792
rs10873702	1	85884101	0.50398	0.92970588	0.22753	0.21107
rs61783046	1	85884365	0.99823	0.9997779	0.28169	0.27597
rs2124139	1	85884370	0.58777	1.06744613	0.17452	0.16075
rs17384213	1	85884621	0.5874	1.06751445	0.17453	0.16076
rs12123745	1	85884772	0.30644	0.89256138	0.19574	0.21688
rs1965876	1	85885178	0.59077	0.93738893	0.17468	0.16146
rs1608537	1	85885731	0.58993	0.93725302	0.1747	0.16146
rs1608536	1	85885836	0.30128	0.89143746	0.19628	0.21741
rs2840319	1	85886224	0.78109	1.02546483	0.42328	0.42796
rs11161613	1	85886678	0.73587	1.07166231	0.052872	0.049751
rs12064909	1	85886681	0.27036	0.84125538	0.082619	0.096492
rs72724630	1	85886964	0.27374	0.84218127	0.08261	0.096205
rs35479962	1	85887753	0.62413	1.12437801	0.040306	0.036215
rs6697083	1	85887775	0.79201	1.02432412	0.43381	0.43782
rs6420965	1	85888480	0.59967	0.938202	0.1725	0.15998
rs1523995	1	85888986	0.58827	0.93699625	0.17484	0.16162
rs7555670	1	85889080	0.5383	0.93123651	0.19181	0.17679
rs7521189	1	85889596	0.81759	0.97940308	0.44994	0.45505
rs12135333	1	85890494	0.30057	0.89130375	0.19548	0.21693
rs1523994	1	85890726	0.4973	0.92866984	0.22779	0.21109
rs12128907	1	85891385	0.29664	0.89049303	0.1954	0.21702
rs6672870	1	85891457	0.6077	0.94049401	0.17702	0.16431
rs12129013	1	85891709	0.47948	0.93165286	0.26495	0.28179
rs12126355	1	85891874	0.54848	1.13805424	0.051172	0.045442
rs2389948	1	85892383	0.57207	0.93442492	0.17531	0.16164
rs72724632	1	85892717	0.43013	1.12499658	0.10842	0.099114
rs7540393	1	85893728	0.96965	0.9962375	0.28406	0.27888
rs12131926	1	85893955	0.34877	0.90342697	0.21234	0.23235
rs12029221	1	85893977	0.53324	1.07765674	0.17661	0.16174
rs1146374	1	85894027	0.46542	0.92350968	0.22955	0.21225
rs561614	1	85894864	0.85801	1.02062481	0.23325	0.23223
rs561422	1	85894932	0.43134	0.91752817	0.23382	0.21527
rs1146377	1	85895609	0.44267	0.91279314	0.21529	0.19757
rs12125900	1	85895781	0.29432	0.8899411	0.19521	0.21699
rs1146378	1	85895820	0.36908	0.89920881	0.21417	0.19437
rs1146379	1	85896551	0.61325	1.04854239	0.39568	0.40532
rs17127399	1	85897168	0.75913	1.06380276	0.05273	0.049252

rs12743049	1	85897386	0.29643	0.89040399	0.19526	0.21698
rs138155098	1	85897526	0.32361	0.72667932	0.01654	0.022933
rs17384381	1	85897570	0.29063	0.88910495	0.19272	0.21396
rs11582061	1	85897781	0.45096	1.11857997	0.10823	0.099444
rs17388521	1	85897904	0.31943	0.8949835	0.19426	0.21606
rs551140	1	85898042	0.22573	0.82087043	0.073877	0.089287
rs11161614	1	85898160	0.42101	0.9164892	0.21257	0.23102
rs553257	1	85898330	0.74387	0.96225287	0.16875	0.18003
rs35956189	1	85898461	0.97709	0.99716104	0.28389	0.27875
rs990916	1	85898508	0.57466	1.06982384	0.1749	0.16067
rs1523993	1	85899128	0.86801	0.98347211	0.27287	0.27121
rs506082	1	85899215	0.87776	1.01432361	0.38988	0.39307
rs669173	1	85899428	0.52559	0.9428661	0.40782	0.41595
rs12129502	1	85900727	0.37732	0.90635157	0.19921	0.21857
rs12130380	1	85901309	0.41667	0.9155164	0.21623	0.23452
rs12736004	1	85901367	0.38452	0.90772573	0.19993	0.21895
rs570121	1	85901598	0.26164	0.88675194	0.31375	0.28571
rs3851268	1	85901887	0.60181	1.06483728	0.17605	0.16245
rs12131258	1	85901913	0.59261	1.09417866	0.086834	0.079845
rs76807140	1	85901919	0.61384	0.9515843	0.49113	0.4805
rs593728	1	85902045	0.5691	0.90690371	0.081628	0.074446
rs76046560	1	85903135	0.58828	1.12660648	0.04753	0.042389
rs539714	1	85904338	0.58874	0.93683978	0.1733	0.16016
rs17127565	1	85904962	0.62975	1.11454918	0.044207	0.039774
rs12130591	1	85904985	0.38663	0.90945478	0.20274	0.22111
rs591917	1	85905136	0.63126	1.04937841	0.28339	0.28138
rs17388696	1	85905427	0.71258	1.04560221	0.16942	0.15857
rs604974	1	85905705	0.59791	0.9382902	0.17291	0.16
rs12724823	1	85906385	0.43591	0.91767682	0.20387	0.22058
rs11161615	1	85906816	0.62996	0.95247064	0.26372	0.27538
rs11161616	1	85907625	0.45634	0.92309604	0.21951	0.23574
rs499869	1	85907851	0.59577	0.93776678	0.17265	0.15933
rs28816748	1	85908182	0.62718	1.11547464	0.044288	0.039748
rs141311774	1	85908251	0.70288	1.08893374	0.044523	0.040751
rs1261681	1	85908282	0.60666	0.93955962	0.17499	0.16232
rs138821189	1	85908433	0.62166	1.11597672	0.047174	0.042505
rs1240939	1	85908649	0.95249	1.00545704	0.44786	0.44661
rs4949903	1	85908724	0.17404	1.25341271	0.10067	0.089876
rs10782550	1	85908784	0.41748	0.913288	0.21116	0.22879
rs80091879	1	85909013	0.70308	1.0858347	0.048402	0.04411
rs147156346	1	85909169	0.62763	1.11524041	0.04441	0.039849
rs661686	1	85909210	0.93057	0.99211555	0.44391	0.44002
rs4949904	1	85909275	0.16521	1.17362823	0.20623	0.18977
rs149476073	1	85909708	0.16881	1.17212694	0.20666	0.19026

rs61783053	1	85910700	0.28988	1.18525744	0.097133	0.090098
rs12034839	1	85910777	0.87641	0.98508633	0.32594	0.33341
rs12049529	1	85910893	0.46084	0.92368331	0.2195	0.23565
rs28529751	1	85910951	0.45092	0.92012753	0.20401	0.22032
rs1146381	1	85911290	0.76947	0.9734761	0.49675	0.49088
rs2124140	1	85912143	0.072552	1.66066811	0.041179	0.029583
rs600098	1	85912584	0.57098	0.93280696	0.16833	0.15561
rs17388780	1	85912729	0.51154	0.93332948	0.2338	0.23982
rs17127623	1	85913005	0.30076	1.18333888	0.095384	0.088981
rs17127637	1	85913412	0.23915	1.21627146	0.09296	0.085449
rs530006	1	85913508	0.61876	0.95567632	0.45236	0.46339
rs11161617	1	85913538	0.46223	0.92385052	0.21945	0.23572
rs72724639	1	85913632	0.064446	1.78446741	0.03182	0.021327
rs631817	1	85913740	0.58276	0.93477633	0.16826	0.15578
rs648216	1	85915057	0.59186	1.05526192	0.28381	0.28099
rs648310	1	85915134	0.34189	0.91501118	0.40593	0.4189
rs659070	1	85915149	0.58301	0.9348427	0.16799	0.15564
rs11587876	1	85915183	0.16541	1.17283043	0.20565	0.1895
rs61783054	1	85915221	0.29237	1.18412014	0.096498	0.089635
rs74098835	1	85915373	0.43073	0.91080815	0.18475	0.20078
rs11801146	1	85915374	0.43073	0.91080815	0.18475	0.20078
rs11161618	1	85915402	0.24015	0.90000946	0.4375	0.45967
rs2935	1	85917563	0.48115	1.11086612	0.10754	0.099875
rs17127710	1	85918009	0.19951	1.16031324	0.20286	0.18893
rs1146382	1	85918101	0.92913	0.99189552	0.43937	0.43634
rs1146383	1	85918329	0.57413	0.93550293	0.18381	0.17103
rs35761966	1	85918357	0.46789	0.92221214	0.204	0.21991
rs56216312	1	85918454	0.51708	1.11678051	0.088488	0.08129
rs7555486	1	85918970	0.61987	0.95149866	0.2725	0.27587
rs1146384	1	85919710	0.57829	1.05832768	0.30848	0.30281
rs13373844	1	85919759	0.64557	0.95490827	0.27371	0.27668
rs12717764	1	85920219	0.76541	0.97151653	0.32401	0.32338
rs67644506	1	85920734	0.4781	1.11268944	0.10857	0.10087
rs12143626	1	85921219	0.71258	1.08608556	0.045205	0.041294
rs3738111	1	85921557	0.17599	1.24554103	0.099988	0.089932
rs506733	1	85922661	0.93944	0.99226983	0.37261	0.37101
rs36104818	1	85923472	0.99065	1.00120112	0.26678	0.2615
rs877041	1	85923920	0.73311	1.0327798	0.37928	0.36822
rs582145	1	85923999	0.70491	0.96501368	0.39673	0.38492
rs12568675	1	85924464	0.56623	1.08961345	0.11068	0.10451
rs597168	1	85925028	0.98459	0.99804791	0.28518	0.27929
rs974874	1	85925108	0.82475	0.97756353	0.30039	0.30742
rs17389112	1	85925235	0.96015	0.99490473	0.2672	0.26274
rs1523991	1	85925978	0.72716	1.03355881	0.37933	0.36804

rs6658151	1	85926281	0.53144	1.09799523	0.11234	0.10532
rs61783057	1	85926726	0.86662	0.98302965	0.26818	0.2657
rs56154783	1	85926818	0.57488	1.08717436	0.11103	0.10487
rs485928	1	85926904	0.90313	0.98844725	0.30593	0.30946
rs12032315	1	85927407	0.77738	0.96358941	0.1342	0.13303
rs480414	1	85927463	0.86306	0.98369538	0.30488	0.30946
rs1146386	1	85927482	0.8538	1.01870376	0.31877	0.32535
rs1241321	1	85927879	0.51859	0.93889747	0.31149	0.31998
rs1241320	1	85928237	0.94737	0.99334733	0.28628	0.27934
rs4949905	1	85928564	0.81556	0.96820736	0.12328	0.12168
rs11161619	1	85928811	0.49343	0.86749112	0.049769	0.057296
rs529582	1	85929008	0.94083	0.99252349	0.28645	0.27934
rs527762	1	85929214	0.95832	0.99473461	0.28685	0.28004
rs12044882	1	85931014	0.69819	0.95079576	0.14358	0.14362
rs61783058	1	85931756	0.14093	1.27979512	0.095965	0.085695
rs61223539	1	85931843	0.9892	1.00138035	0.26832	0.26275
rs55639236	1	85932800	0.6464	1.06995972	0.11296	0.10804
rs4949906	1	85933598	0.22422	1.21481281	0.10264	0.09469
rs1403956	1	85933638	0.87661	1.01355606	0.48933	0.48609
rs149635670	1	85934276	0.78484	1.03058747	0.24044	0.22885
rs539750	1	85934458	0.089127	0.5741469	0.014998	0.023825
rs665091	1	85935422	0.5579	0.93303273	0.18277	0.19351
rs542109	1	85935933	0.1483	0.79209812	0.082851	0.10003
rs535723	1	85936622	0.57666	0.93829395	0.20089	0.211
rs1403953	1	85936774	0.8594	1.01590211	0.4959	0.49202
rs11161621	1	85936912	0.47958	0.93516715	0.50796	0.49005
rs587843	1	85937641	0.8884	0.98615868	0.30872	0.30838
rs12079811	1	85937647	0.31976	0.81176045	0.049737	0.060289
rs7539880	1	85938435	0.4828	1.10713987	0.11842	0.11014
rs7547650	1	85938436	0.48116	1.10757174	0.11842	0.11009
rs12060713	1	85938487	0.63614	0.95598027	0.46048	0.46192
rs2210073	1	85938561	0.99448	0.99910761	0.15122	0.1504
rs79401519	1	85938569	0.20677	1.23228479	0.10033	0.092087
rs12735541	1	85938605	0.87579	0.96125361	0.035322	0.036415
rs12038062	1	85938724	0.42482	0.91390103	0.20438	0.21381
rs72724648	1	85938729	0.43106	0.79621184	0.025122	0.030898
rs7540169	1	85938736	0.36185	1.16820689	0.093349	0.083458
rs12134668	1	85938882	0.75085	0.96686829	0.28645	0.29453
rs76145780	1	85938894	0.20352	1.23446787	0.10027	0.091929
rs12134672	1	85938901	0.75069	0.96684315	0.28643	0.29451
rs10157640	1	85939177	0.54112	1.06372511	0.38131	0.37815
rs10157643	1	85939250	0.7645	1.02928872	0.48287	0.48479
rs10782551	1	85939275	0.27768	0.80734839	0.059762	0.071463
rs150926317	1	85939316	0.36403	1.29480486	0.035474	0.031346

rs7538364	1	85939350	0.79676	1.02503627	0.48493	0.48628
rs10158333	1	85939476	0.70199	0.96006432	0.2848	0.29385
rs61785160	1	85939827	0.1988	1.23817683	0.1003	0.091801
rs10157511	1	85939854	0.7165	0.96202196	0.28544	0.29442
rs975880	1	85939935	0.48855	1.10507809	0.1189	0.11022
rs1403955	1	85940105	0.61266	0.95165472	0.41289	0.42063
rs1403954	1	85940157	0.63893	0.95499517	0.41363	0.42048
rs1403951	1	85940249	0.82301	1.02210477	0.48878	0.48908
rs72724659	1	85942181	0.15471	0.85911714	0.24041	0.26048
rs512298	1	85942879	0.20681	1.13467924	0.41051	0.39222
rs17127783	1	85943006	0.94678	1.0087199	0.15317	0.15278
rs68072919	1	85943635	0.20784	0.87435396	0.22492	0.24231
rs2168199	1	85943856	0.25693	1.11859116	0.42838	0.41178
rs596520	1	85944749	0.24902	1.12046077	0.42894	0.4119
rs1241338	1	85945151	0.26999	0.89677526	0.42909	0.41335
rs1774666	1	85945246	0.30239	1.27207573	0.037886	0.046667
rs1755314	1	85945249	0.24684	1.12076333	0.42835	0.41122
rs1146390	1	85945508	0.27207	1.11402546	0.4282	0.41224
rs10493766	1	85945660	0.23033	0.88092746	0.22095	0.23725
rs1146393	1	85946445	0.38413	1.0890971	0.48197	0.4707
rs1146394	1	85947200	0.33349	1.09925096	0.45632	0.44192
rs478496	1	85948630	0.6293	1.05593011	0.19268	0.20256
rs55940591	1	85948694	0.85374	1.02391652	0.14535	0.1434
rs114275915	1	85949338	0.5522	1.21763445	0.023611	0.021297
rs685176	1	85949388	0.10978	1.15534615	0.4269	0.45483
rs76002294	1	85949535	0.76546	0.91769701	0.028634	0.030642
rs17391765	1	85949883	0.93955	1.00966198	0.14635	0.14596
rs17127802	1	85950320	0.23539	0.88195874	0.22176	0.23769
rs17391800	1	85951222	0.90688	1.01494558	0.14634	0.14545
rs17127805	1	85951495	0.25894	0.88718655	0.2233	0.23871
rs1146395	1	85951597	0.074835	1.19439526	0.28055	0.30799
rs57794103	1	85951899	0.47322	0.84801242	0.041328	0.045465
rs17127806	1	85953046	0.24698	0.88453783	0.22355	0.23937
rs6661365	1	85953366	0.93484	1.0104381	0.14614	0.1455
rs534004	1	85953405	0.23079	1.13541702	0.22266	0.23936
rs562080	1	85954113	0.15145	1.13724651	0.43445	0.45932
rs6665825	1	85955261	0.83286	0.97467909	0.15701	0.15821
rs17099243	1	85955709	0.26448	0.88735513	0.2266	0.24173
rs11161622	1	85956591	0.269	0.89629113	0.39196	0.40542
rs11161623	1	85956663	0.2795	0.89711609	0.37917	0.39033
rs17392043	1	85957134	0.9578	1.00682619	0.14469	0.14423
rs72724671	1	85957652	0.93369	1.01076351	0.14557	0.14485
rs551379	1	85958322	0.36847	1.1008075	0.31404	0.3017
rs1952642	1	85959459	0.29128	0.89933471	0.37917	0.38962

rs2222515	1	85959529	0.3174	0.89399062	0.21677	0.22678
rs1361714	1	85960156	0.29028	0.89898404	0.37843	0.38892
rs1361715	1	85960392	0.26832	0.89592372	0.39214	0.4052
rs6661976	1	85960515	0.29458	0.89992847	0.37917	0.38943
rs7535386	1	85962610	0.27563	0.89714301	0.40248	0.41657
rs12745559	1	85962958	0.30577	0.90175718	0.38245	0.39271
rs12745805	1	85962970	0.37053	0.91402258	0.38683	0.39478
rs61785165	1	85964405	0.98725	0.99793384	0.14401	0.14458
rs61785166	1	85964429	0.98688	0.99787546	0.14401	0.14458
rs113037091	1	85964512	0.68621	1.06635362	0.11467	0.11239
rs61785167	1	85964519	0.98611	0.99774914	0.144	0.14459
rs12085736	1	85964708	0.20949	0.87368096	0.24286	0.25764
rs636379	1	85965127	0.197	1.13593943	0.43858	0.42093
rs78560891	1	85965679	0.97366	0.99572656	0.14389	0.14474
rs1240764	1	85965759	0.23877	1.1264375	0.41697	0.40044
rs1241375	1	85965780	0.20318	1.13429351	0.43428	0.41623
rs6576769	1	85967092	0.81316	0.97146892	0.16997	0.17487
rs563199	1	85967270	0.16627	1.14697725	0.44436	0.42575
rs12060378	1	85967977	0.28971	0.9024518	0.41632	0.43019
rs72724680	1	85968486	0.87561	0.98378195	0.32008	0.31927
rs572245	1	85968572	0.82806	1.02483539	0.2868	0.29225
rs72724681	1	85969709	0.99279	0.99907116	0.36443	0.35884
rs2066357	1	85971357	0.32004	1.11498394	0.29711	0.28475
rs17392306	1	85971852	0.63097	0.94449961	0.21499	0.22365
rs10493768	1	85972024	0.58339	0.94514682	0.36806	0.36137
rs61785199	1	85972286	0.57251	0.93503156	0.21284	0.2232
rs10493769	1	85972426	0.85712	1.0176703	0.32927	0.32093
rs55866846	1	85973274	0.99053	0.99870774	0.29146	0.28916
rs12024511	1	85974666	0.90058	0.98629774	0.30098	0.30071
rs1240759	1	85977428	0.43627	0.90784556	0.17827	0.1881
rs138273116	1	85978094	0.78297	1.08035317	0.035965	0.034483
rs11806789	1	85979832	0.48049	0.91607137	0.17817	0.18719
rs150418406	1	85981896	0.95917	1.01415626	0.032362	0.033047
rs71654706	1	85983660	0.93889	1.01244682	0.10845	0.1067
rs671020	1	85987130	0.80458	1.04962609	0.066983	0.068945
rs567401	1	85988158	0.63901	0.93866183	0.1481	0.15384
rs481582	1	85994163	0.50739	1.12405198	0.079763	0.086007
rs549660	1	85994419	0.58332	0.92710171	0.13969	0.14667
rs683146	1	85995684	0.57569	1.10158715	0.085987	0.09065
rs144024662	1	86004523	0.71194	1.10465051	0.0323	0.030437
rs17099678	1	86006208	0.93243	1.02241451	0.032012	0.032095
rs1813203	1	86006583	0.63645	1.06846923	0.12511	0.11981
rs79068413	1	86006771	0.62466	0.9004866	0.048259	0.052979
rs6679477	1	86007419	0.55047	0.88137684	0.048905	0.054152

rs6666916	1	86007429	0.82266	1.06053553	0.033116	0.031694
rs6667327	1	86007799	0.82189	1.06080388	0.033133	0.031702
rs34181267	1	86008146	0.67199	1.06076675	0.12516	0.12059
rs35560539	1	86008280	0.67961	1.05917044	0.12517	0.12095
rs17099679	1	86008398	0.61236	1.07299628	0.12652	0.12065
rs12734233	1	86008536	0.63981	1.06742051	0.125	0.11996
rs11161635	1	86008940	0.22223	0.87296484	0.20272	0.21683
rs12738255	1	86008978	0.65053	1.06553924	0.1248	0.12004
rs972674	1	86009218	0.63479	1.06949973	0.12602	0.12077
rs11161636	1	86010248	0.58691	1.05069726	0.37652	0.38282
rs1524004	1	86011057	0.2859	0.90045058	0.28811	0.30529
rs1524002	1	86011289	0.98627	1.00230956	0.15418	0.15114
rs7536438	1	86014249	0.73545	1.03273332	0.40458	0.3933
rs17390740	1	86014981	0.017282	0.7256264	0.12529	0.15959
rs71654708	1	86015302	0.98309	1.00519083	0.038477	0.036428
rs10782552	1	86015715	0.00010192	0.50591328	0.12536	0.090175
rs7531068	1	86016103	9.90E-05	0.50557949	0.12547	0.09016
rs79073958	1	86017258	0.22358	0.82640526	0.081207	0.09183
rs1880209	1	86017278	0.70116	1.04197401	0.24642	0.24279
rs1880208	1	86017307	0.62824	0.94732695	0.24914	0.24879
rs1524001	1	86017485	9.44E-05	0.5058627	0.12583	0.090348
rs138985640	1	86017838	0.23045	0.68260426	0.018892	0.025349
rs74723550	1	86018184	0.24346	0.72052152	0.020515	0.027813
rs17127877	1	86018324	0.20394	0.82041087	0.080752	0.092109
rs897255	1	86018583	0.0001204	0.50612075	0.12224	0.087754
rs80322172	1	86018861	0.2039	0.82059959	0.080761	0.09214
rs17390886	1	86019123	0.60518	1.06849274	0.14857	0.13556
rs17127878	1	86019307	0.0095136	0.70235943	0.1143	0.14969
rs11161637	1	86021169	0.55007	1.05665895	0.4436	0.42594
rs17127881	1	86021214	0.1945	0.81790425	0.080793	0.092837
rs71654710	1	86022361	0.91898	0.97614123	0.039448	0.038777
rs76548961	1	86023016	0.33169	0.81510365	0.051183	0.059785
rs10747322	1	86023841	0.81905	0.97429709	0.23277	0.23527
rs6656373	1	86025642	0.84778	1.01923567	0.2925	0.2895
rs12070993	1	86025987	0.23638	0.83255999	0.083039	0.093348
rs79594399	1	86026159	0.23981	0.83362635	0.082918	0.093086
rs11161638	1	86026583	0.94097	0.99168159	0.22719	0.2292
rs1378227	1	86028530	0.81147	0.97326586	0.23409	0.23632
rs7522274	1	86029244	0.81153	0.97327559	0.23409	0.23631
rs138722718	1	86030422	0.58751	0.9064413	0.063459	0.065419
rs6576775	1	86030595	0.00033732	0.53090616	0.11959	0.088026
rs7528000	1	86030624	0.89888	1.0143865	0.23885	0.23716
rs12090959	1	86031235	0.24609	0.83543728	0.083011	0.092989
rs9970631	1	86031501	0.66483	1.04142503	0.43336	0.42022

rs12734039	1	86031531	0.98903	1.00139267	0.27855	0.27899
rs12409518	1	86031687	0.71481	1.03479879	0.43242	0.42208
rs61783713	1	86033462	0.6225	1.06579074	0.14717	0.13521
rs10493770	1	86034864	0.22761	0.85371318	0.12738	0.13807
rs10493771	1	86035403	0.83466	1.02041867	0.37594	0.37132
rs10493772	1	86035513	0.50889	1.08115942	0.22299	0.2121
rs1378228	1	86036573	0.6985	0.96093261	0.35058	0.35074
rs2297138	1	86037931	0.009494	0.73677701	0.1686	0.21035
rs2297139	1	86038234	0.012123	0.74591025	0.17192	0.21236
rs6682848	1	86038476	0.00043678	0.54159868	0.12323	0.091872
rs1378226	1	86038738	0.0004342	0.54149037	0.12326	0.091876
rs721471	1	86039011	0.54214	1.07461773	0.2219	0.21222
rs75408726	1	86039973	0.011756	0.74538084	0.17223	0.21288
rs12086058	1	86040054	0.91605	0.99036838	0.43942	0.43781
rs12034319	1	86040107	0.53095	1.07676589	0.22177	0.21162
rs74399770	1	86040370	0.011738	0.74545538	0.17231	0.21292
rs112584068	1	86040637	0.6531	1.06051538	0.14736	0.13664
rs72726326	1	86040708	0.00022467	1.92317987	0.11944	0.087453
rs61783714	1	86041612	0.47822	1.20835508	0.039127	0.034241
rs71654711	1	86042392	0.42772	0.83627314	0.040064	0.044359
rs116261635	1	86044028	0.18976	1.4718204	0.036454	0.029707
rs954353	1	86044651	0.81294	0.97816002	0.43496	0.43768
rs3753795	1	86045104	0.87106	1.01812938	0.25821	0.2526
rs3753794	1	86045642	0.60789	1.06271717	0.21586	0.2072
rs3753793	1	86045888	0.97514	0.99654887	0.25322	0.25064
rs2297140	1	86046561	0.96405	1.00418594	0.49765	0.4979
rs2297141	1	86046924	0.72718	1.03338312	0.41875	0.41419
rs9658584	1	86047311	0.02576	0.78201606	0.1807	0.21602
rs35234617	1	86049527	0.58709	0.86413178	0.026774	0.030365
rs7543409	1	86049823	0.065943	0.84697	0.52095	0.48913
rs6576776	1	86050077	0.030868	0.79534444	0.29118	0.26054
rs1329961	1	86050700	0.95773	0.99460421	0.26873	0.26795
rs1571549	1	86050965	0.050018	0.83761225	0.52472	0.49042
rs9658595	1	86051247	0.78254	1.0304535	0.24965	0.24462
rs7549783	1	86051951	0.36466	1.1284782	0.16451	0.15362
rs12734475	1	86052701	0.37019	0.76886491	0.018352	0.02411
rs12756618	1	86052888	0.69045	0.92353738	0.052529	0.054328
rs4370804	1	86052985	0.76636	1.03281181	0.25008	0.2446
rs55750909	1	86053765	0.025115	0.76844215	0.15527	0.18836

B. DDAH2 SNPs analysed in the GAinS and GenOSept cohorts

SNP	CHR	BP	P	adjusted OR	maf cases	maf controls
rs116821080	6	31684843	0.20892	1.366223	0.041288	0.032022
rs115090578	6	31684844	0.28731	1.32293136	0.036642	0.029503
rs116588512	6	31685654	0.70545	1.050754	0.14065	0.14843
rs114767747	6	31685945	0.19207	0.80233424	0.065572	0.08209
rs114217246	6	31686497	0.21075	1.14346143	0.23793	0.21224
rs114330570	6	31686726	0.3568	1.29898086	0.031412	0.02073
rs115777364	6	31687008	0.2193	1.14099421	0.23786	0.21238
rs115138428	6	31688200	0.26616	0.82647964	0.064024	0.077538
rs116316082	6	31688217	0.1826	1.14220431	0.3782	0.34483
rs115268511	6	31688388	0.075507	0.67973654	0.039479	0.053368
rs115395274	6	31688518	0.31194	0.90753876	0.51887	0.49316
rs116799208	6	31688799	0.2109	1.36424341	0.04123	0.032001
rs114316669	6	31690009	0.2212	1.13936376	0.23933	0.21384
rs115871250	6	31690876	0.029103	1.36819178	0.13265	0.10317
rs116739740	6	31691657	0.17943	0.79741503	0.065691	0.082816
rs116193838	6	31692163	0.18366	1.14193021	0.37836	0.34476
rs114777003	6	31692386	0.46315	1.15150525	0.064242	0.058322
rs114860403	6	31692970	0.48883	1.20858469	0.03197	0.022529
rs114397592	6	31695368	0.17328	0.69769028	0.027078	0.038006
rs116485062	6	31695590	0.43362	1.15638643	0.071424	0.064719
rs116512138	6	31697387	0.15753	1.15230006	0.37766	0.34299
rs116109728	6	31697558	0.17451	1.14524662	0.37896	0.34501
rs115034626	6	31697957	0.36898	1.13792906	0.10333	0.11423
rs114585169	6	31698088	0.23453	1.12587442	0.38017	0.34861
rs115643301	6	31698352	0.69867	1.05195885	0.14061	0.14871
rs115943095	6	31699573	0.70387	1.12095388	0.025451	0.02296

rs144489798	6	31700657	0.31292	0.84090213	0.065104	0.07756
rs115490753	6	31702710	0.43162	0.87594673	0.070245	0.080317
rs3131383	6	31704294	0.52579	0.87230164	0.097561	0.098403
rs28366163	6	31704804	0.52788	1.12618971	0.068309	0.062695
rs378538	6	31704934	0.32446	0.84441601	0.065265	0.077455
rs148749314	6	31705183	0.21626	1.36938263	0.039651	0.025881
rs3101018	6	31705864	0.52601	0.87237142	0.097561	0.098401
rs28381344	6	31707526	0.56263	1.16694591	0.032412	0.030846
rs3131382	6	31707730	0.62803	1.09786787	0.065738	0.069661
rs409558	6	31708147	0.02917	1.31679401	0.17534	0.1378
rs2075789	6	31708328	0.038974	1.39280542	0.10595	0.081143